



Backbone decoration of imidazol-2-ylidene ligands with amino groups and their application in palladium catalyzed arylation amination reaction

Yin Zhang

► To cite this version:

Yin Zhang. Backbone decoration of imidazol-2-ylidene ligands with amino groups and their application in palladium catalyzed arylation amination reaction. Catalysis. Université Paul Sabatier - Toulouse III, 2015. English. NNT : 2015TOU30109 . tel-01383825

HAL Id: tel-01383825

<https://theses.hal.science/tel-01383825>

Submitted on 19 Oct 2016

HAL is a multi-disciplinary open access archive for the deposit and dissemination of scientific research documents, whether they are published or not. The documents may come from teaching and research institutions in France or abroad, or from public or private research centers.

L'archive ouverte pluridisciplinaire **HAL**, est destinée au dépôt et à la diffusion de documents scientifiques de niveau recherche, publiés ou non, émanant des établissements d'enseignement et de recherche français ou étrangers, des laboratoires publics ou privés.



Université
de Toulouse

THÈSE

En vue de l'obtention du

DOCTORAT DE L'UNIVERSITÉ DE TOULOUSE

Délivré par :

Université Toulouse 3 Paul Sabatier (UT3 Paul Sabatier)

Présentée et soutenue par :

Yin ZHANG

Le mardi 15 septembre 2015

Titre :

Backbone decoration of imidazol-2-ylidene ligands with amino groups and their application in palladium catalyzed arylation reaction

ED SDM : Chimie moléculaire - CO 046

Unité de recherche :

Laboratoire de Chimie de Coordination du CNRS

Directeur(s) de Thèse :

Dr. Vincent César et Dr. Guy Lavigne

Rapporteurs :

Prof. Christophe Darcel, Université de Rennes 1, Rennes
Dr. Vincent Ritleng, Université de Strasbourg, Strasbourg

Autre(s) membre(s) du jury :

Examineur: Prof. Montserrat Gómez, Université Toulouse 3 Paul Sabatier, Toulouse
Directeur de thèse: Dr. Vincent César, LCC, Toulouse

Acknowledgements

How time flies, and finally it comes to the last moment of my three years' PhD studying in LCC as well as my colorful life in Toulouse. It seems more difficult than I thought to come up with a list of everyone who has influenced or helped me in some way during these three years.

First of all, I would like to thank my supervisor Dr. Guy Lavigne for accepting my PhD studying in team A of Laboratoire de Chimie de Coordination du CNRS. His profound knowledge of chemistry as well as his great passion for chemistry largely encouraged and influenced me, giving me day to day progress. Unfortunately, he passed away in a sudden five months ago. In that moment, I could hardly accept this bad news coming from his family. I was in a fully painful sadness and until now I often recall all the unforgettable time passed with him in LCC. I wish that Guy, in the other side of the world, would be gratified to see the finishing of my PhD studying.

Equally, I'm also grateful for the mentoring of Dr. Vincent César through my three years' thesis research. His endless offerings of knowledge and insightful suggestions have been extremely supportive. Not only has my knowledge of organometallic chemistry been enriched, but the development of my independent understanding of how to plan, execute, and thinking of the research results is something essential for my future career. This thesis would not have been possible without the guidance of my both supervisors.

I would like also to thank my thesis committee Prof. Montserrat Gómez, Prof. Christophe Darcel and Dr. Vincent Ritleng for judging my thesis and also for the helpful discussion and suggestions.

I would like to express my gratitude to group leader Dr. Noël Lugan for all the administrative supports and all the X-Ray diffraction analyses of the complexes in my thesis. I appreciate all the other permanent staffs Dr. Stéphanie Bastin, Dr. Dmitry Valyaev, Cécile Barthes for all their generous advices during my research.

Of course, it has been a great pleasure to work with all my colleagues in the team. Thanks to all their solid supports, my studying in LCC and the life in Toulouse has become much facilitated. Specially, thank rémy for picking me up in the airport in the

first day I arrived in Toulouse and all his suggestions for working in the lab and French; Ludovik for encouraging me and inviting me several times for enjoying the nice French traditional dinners at his home; Mirko, in the same office with me for almost two years, for his dozens of helpful ideas and discussion in all the parts; Jérémy and other Master students Marie, Matthiew working together for a short time.

I would also like to thank all the permeant staffs; PhD students and post-docs in our neighbor team G for all their discussions and advices during each seminar. Many thanks to the director of team G Prof. Rinaldo Poli for his kind helps of scientific advice, supports and enthusiasm.

My results in thesis would not have been achieved without all the assistances of technical services in LCC, hereby I would equally thanks to all the technicians for their attentive working.

Besides, I won't forget the nice moment when I played tennis with all my partners of LCC in almost every Thursday afternoon.

Finally, I would like to thank my parents and Lin for their love and support for giving me enough confidence to start a totally new studying period and life in Toulouse.

-Content-

Chapter 1	Introduction	1
Chapitre 2	4-(dimethylamino)-imidazol-2-ylidene and 4,5-bis(dimethylamino)-imidazol-2-ylidene: Synthesis, complexation and catalytic properties in Pd-catalyzed arylative amination	33
Chapitre 3	Amination of (hetero)aryl tosylates catalysed by the Pd-PEPPSI-IPr ^{(NMe₂)₂} pre-catalyst	75
Chapitre 4	Further skeleton derivatization of imidazol-2-ylidene ligands	93
General Conclusion		129
Chapitre 5	Experimental section	133

-Chapitre 1-

1. Introduction	3
2. N-heterocyclic carbenes (NHCs): Generalities	4
2.1. Definition of N-Heterocyclic Carbenes	4
2.2. General properties of NHCs.....	5
2.3. Coordination of NHCs to transition metals	6
2.3.1. Historical aspects	6
2.3.2. Electronic properties	7
2.3.3. Steric properties	9
2.4. Application in homogeneous catalysis.....	10
3. Electronic and steric tuning of NHCs and its impact on metal catalysts	11
3.1. Steric modification.....	11
3.2. Backbone functionalization	16
4. Application of NHC ligands in palladium-catalyzed Buchwald-Hartwig Amination.....	21
4.1. Introduction.....	21
4.2. <i>In situ</i> generated Pd-NHC catalysts	22
4.3. Well-defined Pd-NHC catalysts.....	24
4.4. Conclusion	29
5. Thesis Overview.....	30

Chapter 1: Introduction

1. Introduction

Catalysis has become an extremely important synthetic tool in modern organic chemistry, since a judicious choice of the catalysts enables the activation of poor or even unreactive substrates under standard conditions and a subtle control of the selectivity of the transformation. Hence, it revolutionized the way of thinking the disconnections for the synthesis of complex and/or natural products. Among the many catalytic reactions available, transition-metal-catalyzed reactions have proved to be one of the most important and promising routes to the economical and straightforward formation of complex organic frameworks. The ancillary ligands in the transition metal catalysts play a significant role in determining the activity, selectivity, generality and stability of the resulting catalysts which represent the main factors characterizing their catalytic efficiency.¹

Over the two last decades, *N*-heterocyclic carbenes (NHCs) have gained considerable significance in modern chemistry.² These species indeed show spectacular aptitudes to stabilize transition-metal centers or polyatomic main-group allotropes, and to give highly robust and efficient organometallic-and organo-catalysts. Obviously, the stereoelectronic properties of the NHCs greatly depend on the nature, the size and the substitution pattern of the carbenic heterocycle, as well as on the nature of the “arms”, the denticity of the ligand and its three-dimensional arrangement. Especially, our group has been engaged in the development of new classes of backbone-functionalized NHCs since 2008. In line with these research interests, this thesis aims at developing new NHC families obtained by the formal substitution of the carbenic heterocycle by amino groups in the series of the imidazol-2-ylidenes and at studying the influence of this decoration in homogeneous organometallic catalysis, focusing on the well-known Pd-catalyzed Buchwald-Hartwig amination as model reaction.

This chapter will firstly introduce the definition and the general properties of NHCs. Then, the main examples of modification of NHCs and its benefits in transition metal-catalyzed

¹ (a) *Applied Homogeneous Catalysis with Organometallic Compounds*, (Eds.: B. Cornils; W. A. Herrmann), 2nd edition, Wiley-VCH, Weinheim, **2002**; (b) *Transitions Metals for Organic Chemistry*, (Eds.: M. Beller, C. Bolm), 2nd edition, Wiley-VCH, Weinheim, **2004**.

² For a recent overview, see: M. N. Hopkinson, C. Richter, M. Schedler, F. Glorius, *Nature* **2014**, *510*, 485.

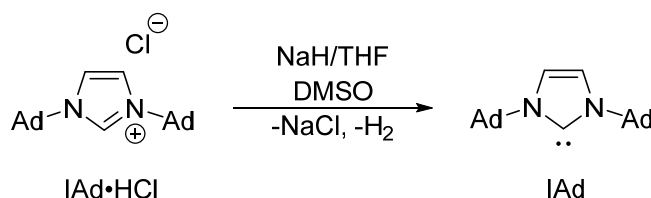
organic reactions in the literature will be presented. Finally, the developing path of Pd-NHC catalyzed Buchwald-Hartwig amination will be described in details.

2. *N*-heterocyclic carbenes (NHCs): Generalities

Since a number of reviews and books have well described the chemistry of *N*-heterocyclic carbenes (NHCs) in all its aspects,^{3,4} this part will give a simplified summary of the general definition of NHCs, their electronic and steric properties and their applications in homogenous transition metal catalysis. Moreover, while different types of NHCs exist in the literature, we will focus this thesis on the NHCs limited to imidazol-2-ylidene or imidazolin-2-ylidene derivatives.

2.1. Definition of *N*-Heterocyclic Carbenes

The *N*-heterocyclic carbenes (NHCs) are defined as heterocyclic compounds containing a divalent carbon atom surrounded by at least one nitrogen atom and possessing six valence electrons. The first free and stable NHC was successfully isolated by Arduengo and coll. in 1991 by exposing the corresponding imidazolium salt **IAd·HCl** to NaH and a catalytic amount of DMSO in THF (Scheme 1.2.1).⁵ This seminal discovery led to an explosion of experimental and theoretical studies with libraries of novel NHCs being synthesized, analyzed and used as ligands and organocatalysts.



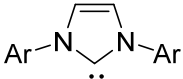
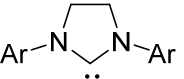
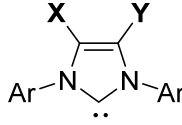
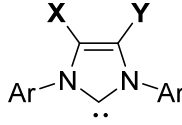
Scheme 1.2.1: Arduengo's first example of isolation of the stable free IAd carbene.

In order to clarify and simplify the name of NHCs, we will use throughout this thesis the abbreviations of the NHCs listed in Scheme 1.2.2.

³ For the selective reviews about NHCs: (a) D. Bourissou, O. Guerret, F. Gabbai, G. Bertrand, *Chem. Rev.* **2000**, *100*, 39; (b) S. Díez-González, S. P. Nolan, *Coord. Chem. Rev.* **2007**, *251*, 874.

⁴ For monographs, see: a) S. Díez-González (Ed.), *N-Heterocyclic Carbenes*; RSC: Cambridge, UK; **2011**; b) C. S. J. Cazin, *N-Heterocyclic Carbenes in Transition Metal Catalysis and Organocatalysis*. In *Catalysis by metal complexes*; Springer: Berlin; Germany; **2011**; Vol. 32; c) F. Glorius (Ed.), *N-Heterocyclic Carbenes in Transition Metal Catalysis*. In *Top. Organomet. Chem.*; Springer: Berlin; Germany; **2007**, Vol. 21; d) S. P. Nolan (Ed.), in *N-Heterocyclic Carbenes in Synthesis*; Wiley-VCH: Weinheim; Germany; **2007**.

⁵ A. J. Arduengo III, R. L. Harlow, M. Kline, *J. Am. Chem. Soc.* **1991**, *113*, 361.

				
IAr	Ar	SIAr	Ar	
IMes	Mesityl	SIMes	Mesityl	 IAr^{XY}
IPr	2,6-diisopropylphenyl	SIPr	2,6-diisopropylphenyl	
IAd	Adamantyl			
IPent	2,6-di(3-pentyl)phenyl			
IPr*	2,6-di(diphenylmethyl)phenyl			

Scheme 1.2.2 : Abbreviations of NHCs used in this thesis.

2.2. General properties of NHCs

The NHCs have a stable singlet ground-state electronic configuration. The benefit of remarkable stability of the carbene centre C2 can be explained by the overall electronic and steric effects of these structural features (Figure 1.2.1). The adjacent nitrogen atoms directly linked to the centre carbenic carbon play a crucial role in the stabilization of the carbene. In one hand, the negative inductive effect lowers the relative energy of the non-bonding σ orbital, while this effect essentially does not change the level of the p_π orbital. In the other hand, nitrogen atoms as mesomerically π donors donate electron density into the empty p_π orbital, which raises the relative energy of π^* orbital of NHC. In addition, the cyclic nature of NHCs also helps to favor the singlet state by forcing the carbenic carbon into a bent, more sp^2 -like arrangement. Finally, the aromatic π -conjugation more or less further increases the stabilization.⁵

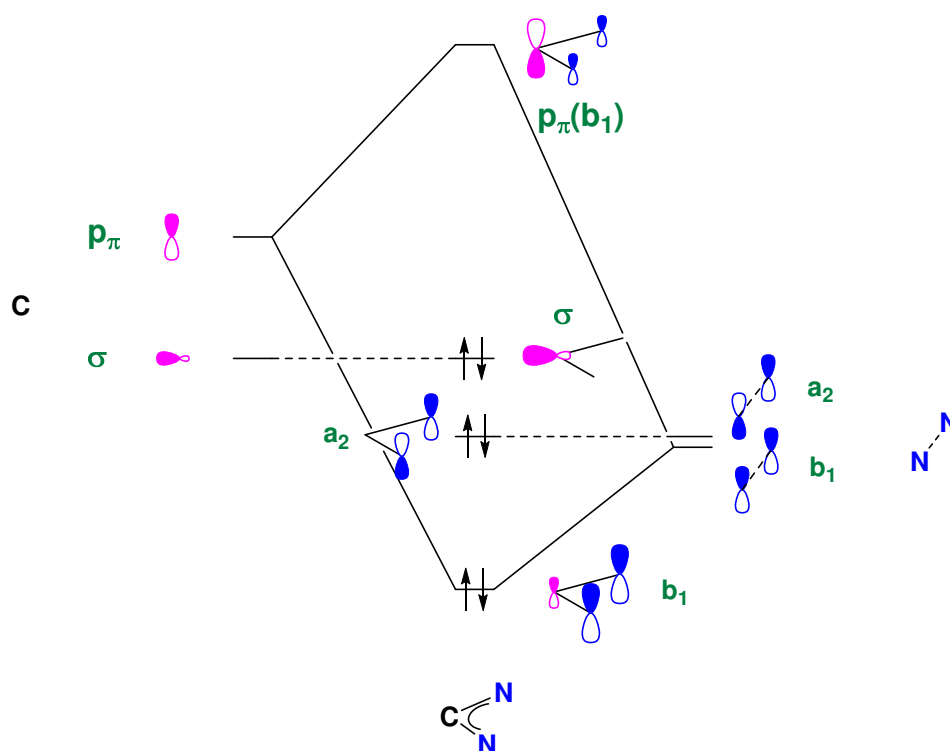
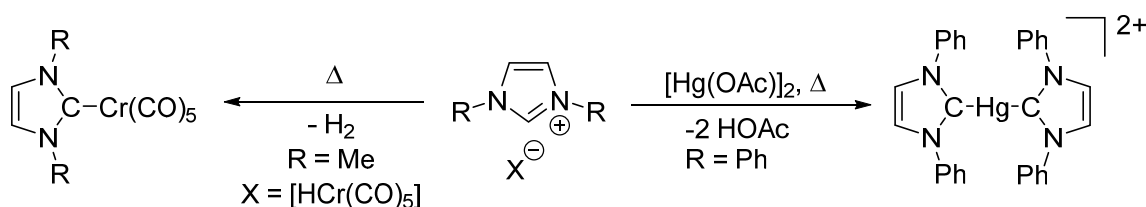


Figure 1.2.1: Perturbation orbital diagrams of NHC.

2.3. Coordination of NHCs to transition metals

2.3.1. Historical aspects

The above mentioned unique properties make NHCs suitable ligands for transition metal complexes. Surprisingly, the first examples of NHC-metal complexes were reported over 20 years before the isolation by Arduengo of a free NHC with the independent works of Wanzlick⁶ and Öfele,⁷ who synthesized imidazol-2-ylidene coordinated to mercury (II) and chromium(0) respectively in 1968 (Scheme 1.2.3). Detail studies before the isolation of IAd by Arduengo were followed by Lappert and co-workers during the 1970's and the 1980's.⁸



Scheme 1.2.3: First examples of NHC-metal complexes reported by Wanzlick and Öfele groups.

⁶ H.-W. Wanzlick, H.-J. Schönherr, *Angew. Chem. Int. Ed.* **1968**, 7, 141.

⁷ K. Öfele, *J. Organomet. Chem.* **1968**, 12, 42.

⁸ (a) D. J. Cardin, B. Cetinkaya, M. F. Lappert, *Chem. Rev.* **1972**, 72, 545; (b) M. F. Lappert, *J. Organomet. Chem.* **1988**, 358, 185.

2.3.2. Electronic properties

The strong σ -donor and comparatively weak π -acceptor properties of NHCs make the NHC-metal bond even more stable (Figure 1.2.2).⁴ In order to well understand electronic properties of the corresponding NHC quantitatively, a wide range of metrics (including pKa measurements,⁹ NMR spectroscopic measurements,¹⁰ electrochemistry¹¹ etc ...) have been employed. Among the variety of methods, the Tolman electronic parameter (TEP)¹² is by far the most commonly-utilized method to investigate the electronic properties of phosphines and has been extended to measure NHCs.¹³

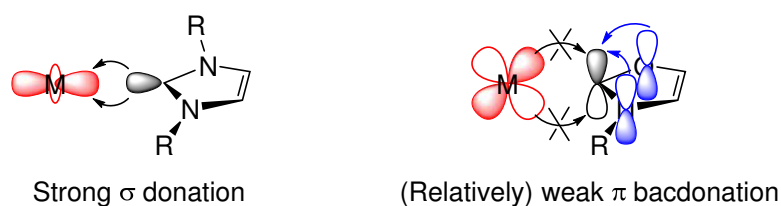


Figure 1.2.2 : Electronic properties of NHC-Metal bond.

The TEP value is determined by measuring the infrared-stretching frequencies of carbonyl ligands in model transition metal carbonyl complexes. Electron-rich ligands will increase the π donor ability of the metal centre, leading to donation into the π^*_{CO} antibonding orbital, which will weaken the C-O bond and decrease the CO stretching frequency (Figure 1.2.3).

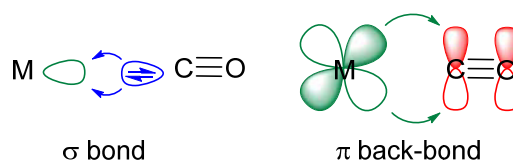


Figure 1.2.3: Schematic representation of the coordination mode of CO ligand.

The initially used complex was $[\text{Ni}(\text{NHC})(\text{CO})_3]$. However, due to the highly toxic $[\text{Ni}(\text{CO})_4]$ precursor, the less toxic complexes $[\text{Rh}(\text{NHC})\text{Cl}(\text{CO})_2]$ and $[\text{Ir}(\text{NHC})\text{Cl}(\text{CO})_2]$ were rapidly preferred (Figure 1.2.4). The different scales were found to be correlated by a

⁹ (a) Y. Chu, H. Deng, J. P. Cheng, *J. Org. Chem.*, **2007**, 72, 7790; (b) E. M. Higgins, J. A. Sherwood, A. G. Lindsay, J. Armstrong, R. S. Massey, R. W. Alder, A. C. O'Donoghue, *Chem. Commun.*, **2011**, 47, 1559.

¹⁰ (a) H. V. Huynh, Y. Han, R. Jothibasu, J. A. Yang, *Organometallics*, **2009**, 28, 5395.

¹¹ L. Perrin, E. Clot, O. Eisenstein, J. Loch, R. H. Crabtree, *Inorg. Chem.*, **2001**, 40, 5806.

¹² C. A. Tolman, *Chem. Rev.*, **1977**, 77, 313.

¹³ (a) T. Dröge, F. Glorius, *Angew. Chem. Int. Ed.* **2010**, 49, 6940; (b) D. J. Nelson, S. P. Nolan, *Chem. Soc. Rev.* **2013**, 42, 6723.

linear regression.¹⁴ The following equations permit to calculate the TEP value from the $\tilde{\nu}_{\text{CO}}$ values using the Ir(I) and Rh(I) carbonyl complexes:¹⁵

$$\text{Ir to Ni: TEP [cm}^{-1}\text{]} = 0.8475\tilde{\nu}_{\text{CO}} [\text{cm}^{-1}] + 336.2 [\text{cm}^{-1}]$$

$$\text{Rh to Ni : TEP [cm}^{-1}\text{]} = 0.8001\tilde{\nu}_{\text{CO}} [\text{cm}^{-1}] + 420.0 [\text{cm}^{-1}].^{15a}$$

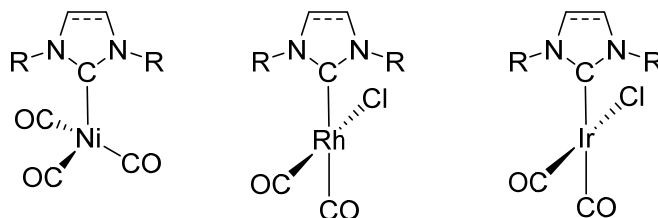


Figure 1.2.4: Model Systems used to determine TEP for NHCs.

However, recent studies have established that the contributions from π -backbonding originally considered as negligible cannot be ignored especially in certain cases.¹⁶ A significant influence of π -accepting ability of NHC on gold catalyzed cycloisomerization was reported by Fürstner and co-workers.¹⁷ During the last years, different types of NHCs bearing low level of π^* orbital have been achieved by changing the heterocyclic structure. This feature makes the π^* orbital more accessible, thus enhancing the interaction between NHC and coordinated metal or main elements through increase of π -backdonation.¹⁸

Two main methods have been developed these last years to quantify the π -acidity of NHCs: 1) By ^{31}P NMR spectroscopy on the phosphinidene adducts of type $\text{NHC}=\text{PPh}$, which are generated by reaction of free NHC with PPhCl_2 followed by reduction by KC_8 or Mg , and originally developed by Bertrand and co-workers¹⁹. 2) By ^{77}Se NMR spectroscopy on selenoureas of type $\text{NHC}=\text{Se}$ prepared by reacting the free carbene with elemental selenium, and first reported by Ganter,²⁰ and further studied by Nolan (Figure 1.2.5).²¹

¹⁴ (a) A. R. Chianese, X. Li, M. C. Janzen, J.W. Faller, R. H. Crabtree, *Organometallics* **2003**, 22, 1663; (b) S. Wolf, H. Plenio, *J. Organomet. Chem.* **2009**, 694, 1487.

¹⁵ For a comprehensive review on the stereoelectronic properties of NHCs, see: D. J. Nelson, S. P. Nolan, *Chem. Soc. Rev.* **2013**, 42, 6723.

¹⁶ (a) H. Jacobsen, A. Correa, C. Costabile, L. Cavallo, *J. Organomet. Chem.* **2006**, 691, 4350; (b) D. Nemcsok, K. Wichmann, G. Frenking, *Organometallics* **2004**, 23, 3640 ; (c) A. A. D. Tulloch, A. A. Danopoulos, S. Kleinhenz, M. E. Light, M. B. Hursthouse, G. Eastham, *Organometallics* **2001**, 20, 2027.

¹⁷ M. Alcarazo, T. Stork, A. Anoop, W. Thiel, A. Fürstner, *Angew. Chem. Int. Ed.* **2010**, 49, 2542.

¹⁸ (a) M. Braun, W. Frank, G. J. Reiss, C. Ganter, *Organometallics* **2010**, 29, 4418; (b) V. César, J.-C. Tourneux, N. Vujkovic, R. Brousses, N. Lugan, G. Lavigne, *Chem. Commun.* **2012**, 48, 2349; (c) J. P. Moerdyk, C. W. Bielawski, *Chem. Commun.* **2014**, 50, 4551.

¹⁹ O. Back, M. Henry-Ellinger, C. D. Martin, D. Martin, G. Bertrand, *Angew. Chem. Int. Ed.* **2013**, 52, 2939.

²⁰ A. Liske, K. Verlinden, H. Buhl, K. Schaper, C. Ganter, *Organometallics* **2013**, 32, 5269.

²¹ S. V. C. Vummaleti, D. J. Nelson, A. Poater, A. Gomez-Suarez, D. B. Cordes, A. M. Z. Slawin, S. P. Nolan, L. Cavallo, *Chem. Sci.* **2015**, 6, 1895.

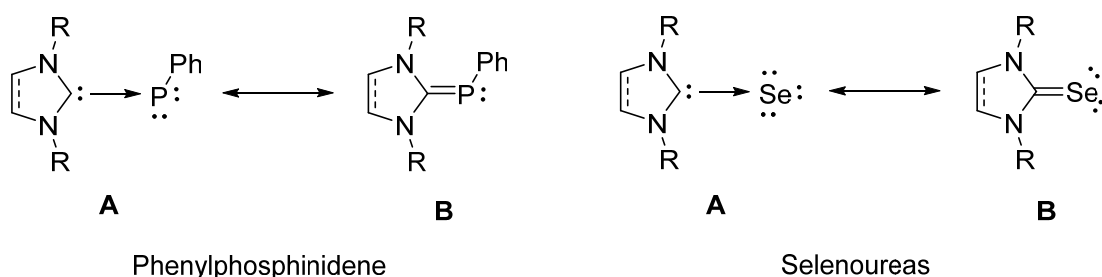


Figure 1.2.5: Canonical structures of phenylphosphinidene and selenoureas

The principle of these two scales is based on the relative propensities of the phosphorous (for the $\text{NHC}=\text{PPh}$) or of the selenium atom (in $\text{NHC}=\text{Se}$) to donate into the π^* -molecular orbital of the NHC. In the conventional Lewis representation, this is illustrated by the two limit resonance forms **A** and **B** (Figure 1.2.5). Whereas the adducts of the poor π -Lewis acidic NHCs such as the imidazol-2-ylidenes are better described by the forms **A**, the contribution of resonance form **B** increases when the π -electrophilicity of the NHC becomes non-negligible, such as in the case of the diamidocarbenes. This effect can be quantified by ^{31}P or ^{77}Se NMR spectroscopy, since the chemical shift of the phosphorus or selenium nucleus correlates with the relative contributions of forms **A** and **B**, being lower when the form **A** dominates and higher when the resonance form **B** becomes more important.^{19,21}

2.3.3. Steric properties

The Tolman cone angle is commonly used to quantify the steric hindrance of phosphines.²² However, it becomes inappropriate to measure the steric properties of NHC ligands due to their much difference in geometry. Consequently, the “percentage of buried volume” parameter ($\%V_{\text{bur}}$) was introduced by Nolan, Cavallo and co-workers as a reasonable means to quantify the steric bulkiness of NHCs as ligands in transition metal complexes.²³ The $\%V_{\text{bur}}$ corresponds to the percentage of the volume of a fixed 3 Å or 3.5 Å radius sphere (**r**) centred on a metal and occupied by the NHC ligand (Figure 1.2.6). For the sake of comparison, the metal-carbon bond distance (**d**) is always fixed to 2.0 Å and the same metal fragment should be used for comparison among all the NHCs. The data used for the calculation of the buried volume are taken from the crystallographic structure of the corresponding M-NHC complexes,

²² C. A. Tolman, *Chem. Rev.* 1977, 77, 313.

²³ A. C. Hillier, W. J. Sommer, B. S. Yong, J. L. Petersen, L. Cavallo, S. P. Nolan, *Organometallics* **2003**, 22, 4322.

and the calculation can be realized by using a simple Web-based software developed by Cavallo and co-workers^{24,25} Hydrogen atoms are usually excluded for the calculation.

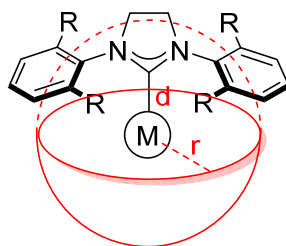


Figure 1.2.6: Schematic representation of the sphere for calculation of the % V_{bur} of NHC ligands.

2.4. Application in homogeneous catalysis

The unique and attractive features of NHCs led to their fruitful application as ligands in homogenous catalysis and/or organocatalysts. In 1995, the first example of NHC acting as supporting ligand in the Pd-catalyzed Mizoroki–Heck reaction was reported by Herrmann and co-workers.²⁶ Since then, the number of studies on the NHC-metal complexes catalyzed reactions has grown at an astonishing rate and is continuing to increase.²⁷ Especially, cross-couplings, cycloisomerizations and olefin metathesis employing NHC-Pd complexes²⁸ NHC-Au²⁹ and NHC-Ru complexes³⁰ as catalysts respectively have dominated in this greatly progressing field (Figure 1.2.7).

The benefits taken from the NHC ligand to the above described reactions are most attributed to the increase of catalyst stability resulting from strong σ -donation of NHCs that strengthens the metal-ligand bond and largely decreases the rate of catalyst decomposition during the reaction. Furthermore, the strong σ -electron donating and the steric bulkiness of the NHC ligands significantly improve both the activity and the efficiency. The most famous example is Grubbs(II) catalyst where one of two PCy_3 ligands is replaced by **SIMes** compared to its first generation (Figure 1.2.7), and this apparently simple change largely improves thermal stability and remains catalytically active for cross- and ring-closing metathesis, and

²⁴ URL of the SambVca program: <http://www.molnac.unisa.it/OMtools.php>.

²⁵ A. Poater, B. Cosenza, A. Correa, S. Giudice, F. Ragone, V. Scarano, L. Cavallo, *Eur. J. Inorg. Chem.*, **2009**, 1759.

²⁶ W. A. Herrmann, M. Elison, J. Fischer, C. Köcher, G. R. J. Artus, *Angew. Chem. Int. Ed.* **1995**, *34*, 2371.

²⁷ For the selected reviews in this part: (a) W. A. Herrmann, *Angew. Chem. Int. Ed.* **2002**, *41*, 1290 ; (b) S. Díez-González, N. Marion, S. P. Nolan, *Chem. Rev.* **2009**, *109*, 3612.

²⁸ (a) E. A. B. Kantchev, C. J. O'Brien, M. G. Organ, *Angew. Chem. Int. Ed.* **2007**, *46*, 2768; (b) G. C. Fortman, S. P. Nolan, *Chem. Soc. Rev.* **2011**, *40*, 5151; (c) S. Würtz, F. Glorius, *Acc. Chem. Res.* **2008**, *41*, 1523; (d) C. Valente, S. Çalimsiz, K. H. Hoi, D. Mallik, M. Sayah, M. G. Organ, *Angew. Chem. Int. Ed.* **2012**, *51*, 3314.

²⁹ N. Marion, S. P. Nolan, *Chem. Soc. Rev.* **2008**, *37*, 1776.

³⁰ (a) G. C. Vougioukalakis, R. H. Grubbs, *Chem. Rev.* **2010**, *110*, 1746; (b) C. Samojłowicz, M. Bieniek, K. Grela, *Chem. Rev.* **2009**, *109*, 3708; (c) *Olefin Metathesis: Theory and Practice.*, ed. K. Grela. Wiley-VCH.

ring-opening metathesis polymerization (ROMP) reactions at much lower catalyst loadings.³¹ Meanwhile, the series of palladium pre-catalysts introduced by Organ or Nolan and co-workers have received widespread attention and show high activities in a variety of benchmark cross-couplings, including the Negishi, Kumada, Suzuki-Miyaura and Buchwald–Hartwig reactions.^{28a,b}

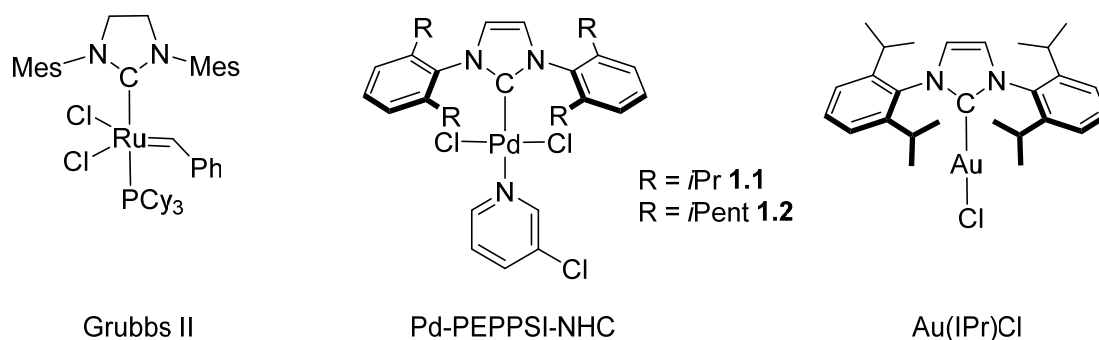


Figure 1.2.7: Widely studied NHC-catalysis during the last decade.

3. Electronic and steric tuning of NHCs and its impact on metal catalysts

Since the first application of NHCs in metal catalysed organic transformation reported by Herrmann and co-workers²⁶, a huge range of different NHC-metal complexes have been prepared and employed as highly active and robust catalysts in a multitude of different reactions. In most cases, imidazol-2-ylidenes and imidazolin-2-ylidenes remain the most studied, the typical NHCs such as **IMes**, **IPr** and **SIPr** being particularly widely applied and shown to be highly efficient supporting ligand in the corresponding metal catalysts. Thanks to the performances of these three NHC ligands, studies on the further optimization in terms of their electronic or steric properties have been carried out during last decades.^{28d} On contrary to phosphine ligands, the *N*-substituents of NHCs are not directly linked to the carbenic carbon coordinated to metal centre, thus making it capable to independently modify the steric and the electronic properties of the NHCs.

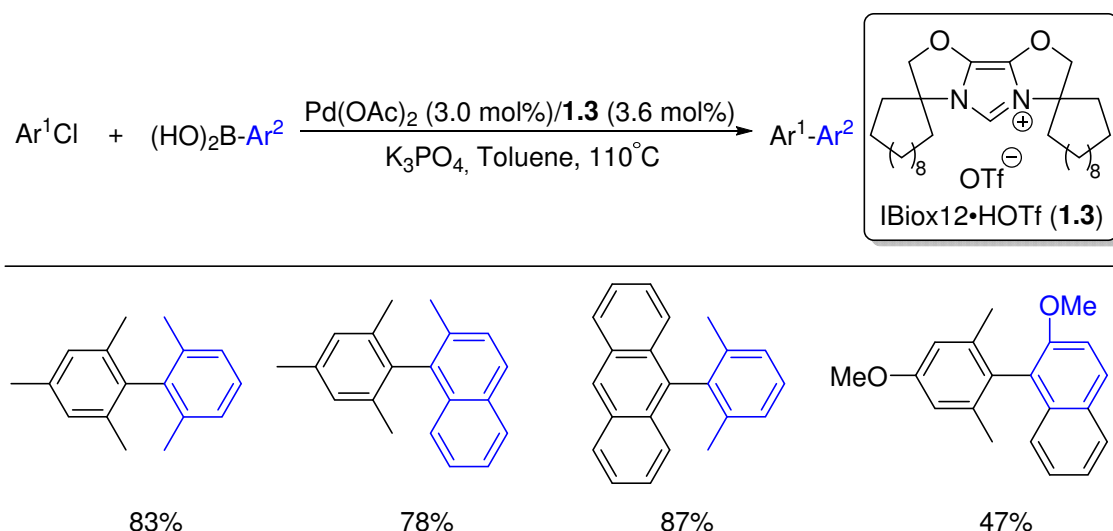
3.1. Steric modification

Usually, most examples of modification of the steric properties of imidazol-2-ylidenes were realized by changing the substituents on the nitrogen atoms of the imidazolyl ring. Noteworthy, the electronic density of the carbenic carbon is not much affected by these

³¹ M. S. Sanford, J. A. Love, R. H. Grubbs, *J. Am. Chem. Soc.* **2001**, 123, 6543.

modifications.³² The effect of steric modification of NHC ligands were mostly investigated in Pd-catalyzed cross-coupling reactions, especially in the formation of sterically hindered products, for which the reductive elimination step appears quite problematic. The most efficient strategy to increase the steric hindrance of NHC ligands was shown to introduce bulky substituents in the close proximity of the metal center.³³

In 2004, Glorius and co-workers successfully synthesized sterically demanding NHCs named IBiox, which were applied in the challenging palladium-catalyzed Suzuki-Miyaura cross-coupling of *tetra*-substituted biaryls from *ortho*-disubstituted aryl chlorides and boronic acids (Scheme 1.3.1).³⁴ The authors rationalized these outstanding catalytic performances to the highly bulky but flexible alkyl rings, which function as protecting “ears”.



Scheme 1.3.1: Suzuki-Miyaura cross-coupling with high sterically hindered substrates using ligand IBiox12 reported by Glorius.

In 2009, Organ and co-workers developed the second generation Pd-PEPPSI-IPent complex (**1.2**) in which the isopropyl groups on the *ortho*-positions of the 2,6-diisopropylphenyl substituents in the classical **IPr** were replaced by 3-pentyl groups. The reactivity of this palladium complex was investigated in the Suzuki-Miyaura reaction for the synthesis of *tetra*-substituted biaryls (Scheme 1.3.2).³⁵ The conditions used were much milder compared to the catalytic system of Glorius, and various difficult substrates including aryl chlorides and arylboronic acids were successfully coupled at 65°C. Interestingly, Pd-PEPPSI-

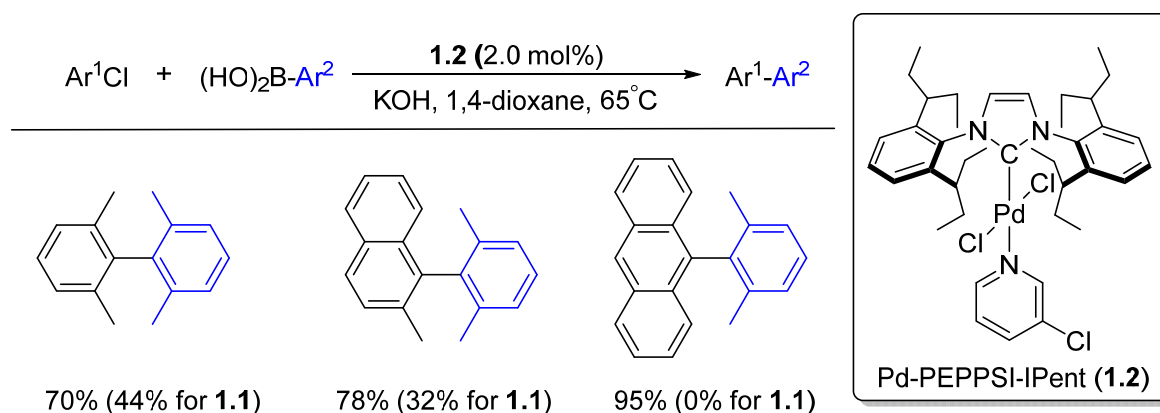
³² R. Dorta, E. D. Stevens, N. M. Scott, C. Costabile, L. Cavallo, C. D. Hoff, S. P. Nolan, *J. Am. Chem. Soc.* **2005**, *127*, 2485.

³³ For the review of relation between different *N*-substituents and catalytic properties in Pd catalyzed cross-coupling reactions: (a) E. A. B. Kantchev, C. J. O'Brien, M. G. Organ, *Aldrichim. Acta* **2006**, *39*, 97; (b) ref 27a.

³⁴ G. Altenhoff, R. Goddard, C. W. Lehmann, F. Glorius, *J. Am. Chem. Soc.* **2004**, *126*, 15195.

³⁵ S. Çalimsiz, M. Sayah, D. Mallik, M. G. Organ, *Angew. Chem. Int. Ed.* **2010**, *49*, 2014.

I \mathbf{Pr} (**1.1**) was shown to be much less efficient under the same conditions. A sterically demanding yet conformationally flexible environment is an essential requirement for the outcome of this catalysis.

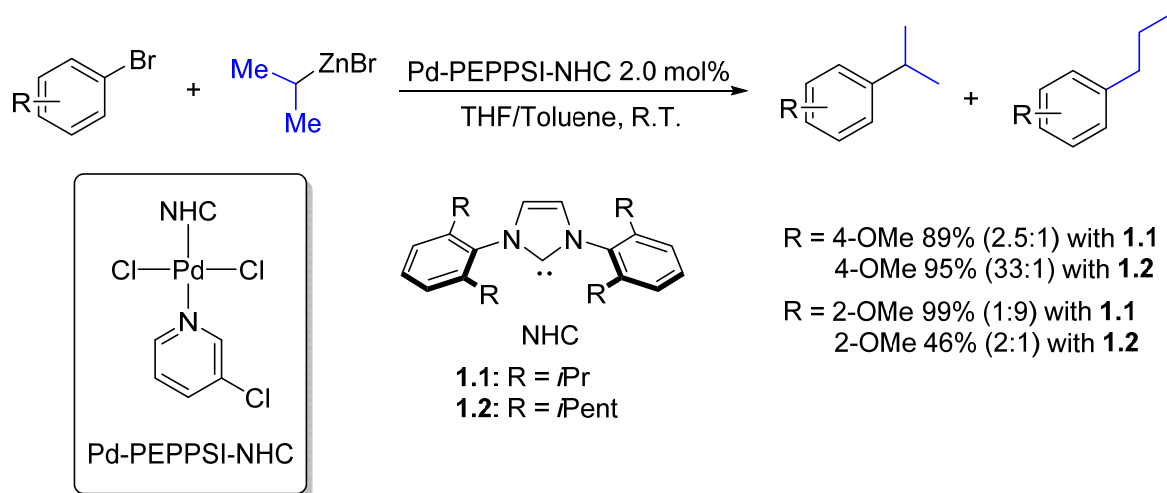


Scheme 1.3.2: Suzuki-Miyaura reactions for synthesis of tetra-*ortho*-substituted biaryls using IPent ligand reported by Organ.

Later, the benefit of this sterically modification was also found in Negishi cross-coupling reaction of secondary alkylzinc reagents with a wide range of (hetero)aryl halides as it resulted in a high selectivity in favor of the branched product compared to the isomerized linear ones, while the **I \mathbf{Pr}** analogue only exhibited poor branched/linear ratios (Scheme 1.3.3).³⁶ The key role of the **IPent** ligand in this reaction consisted in favoring the reductive elimination compared to the β -hydride elimination, which would lead to the isomerization of the alkyl chain. Finally, the stereoelectronic properties of **IPent** were quantified by Nolan and co-workers demonstrating that **IPent** is more flexible, bulkier than **I \mathbf{Pr}** while the electronic properties is only slightly increased.³⁷

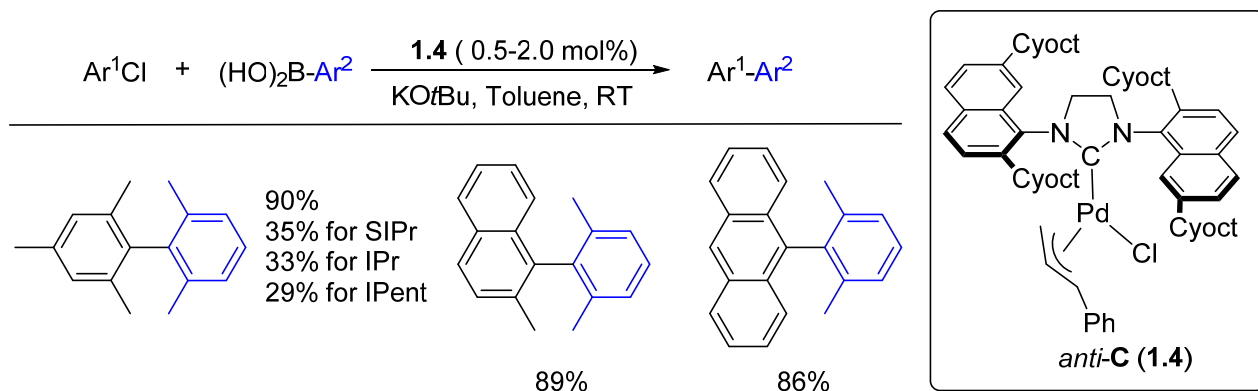
³⁶ S. Calimsiz, M. G. Organ, *Chem. Commun.* **2011**, 47, 5181.

³⁷ A. Collado, J. Balogh, S. Meiries, A. M. Z. Slawin, L. Falivene, L. Cavallo, S. P. Nolan, *Organometallics* **2013**, 32, 3249.



Scheme 1.3.3: Highly branch selective Negishi cross-coupling reaction with secondary alkylzinc using IPent ligand reported by Organ.

In 2008, Dorta and co-workers replaced 1,3-diisopropylphenyl groups of **SIPr** by 2,7-cyclooctylnaphth-1-yl groups and obtained the pre-catalyst **anti-C** (Scheme 1.3.4).³⁸ The latter was found to be especially efficient for the synthesis of tetra-*ortho*-substituted biaryls by Suzuki-Miyaura coupling at room temperature. The effect of the 2,7-bicyclooctylnaphthalyl substituents was calculated by DFT which showed that the special steric properties combined with its C_2 -symmetry facilitate the reductive elimination.³⁹



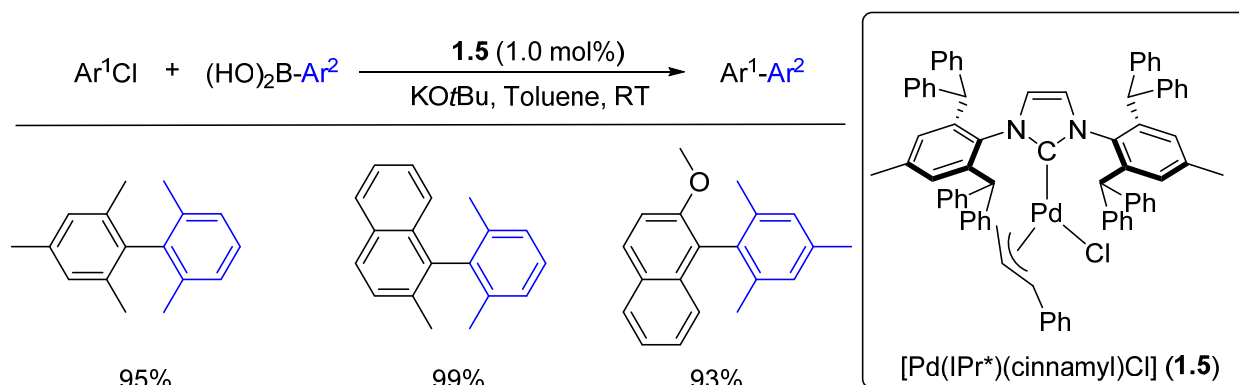
Scheme 1.3.4: Suzuki-Miyaura reactions for the synthesis of tetra-*ortho*-substituted biaryls reported by Dorta.

In 2009, Markó and co-workers developed a highly hindered *N*-heterocyclic carbene named **IPr*** where the *ortho* isopropyl groups are replaced by diphenylmethyl groups. This replacement has led to a great improvement of the steric properties of the corresponding metal

³⁸ X. Luan, R. Mariz, M. Gatti, C. Costabile, A. Poater, L. Cavallo, A. Linden, R. Dorta, *J. Am. Chem. Soc.* **2008**, *130*, 6848.

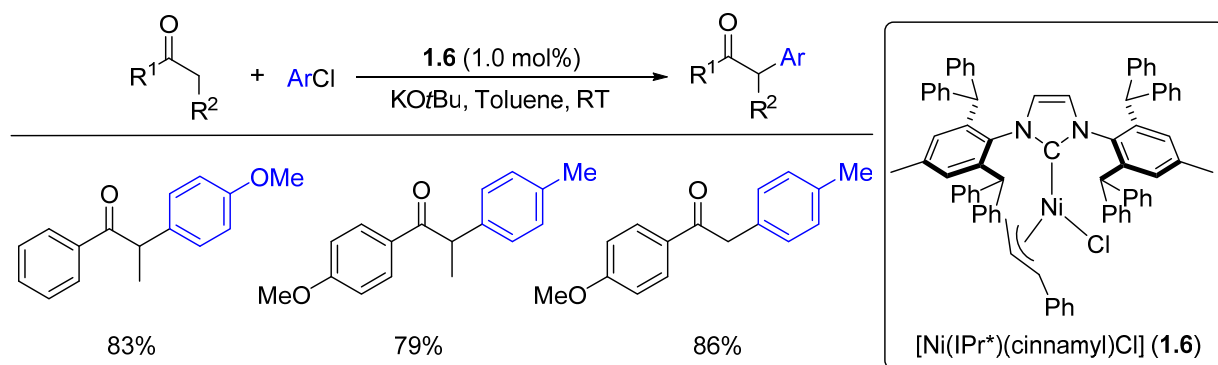
³⁹ L. Wu, E. Drinkel, F. Gaggia, S. Capolicchio, A. Linden, L. Falivene, L. Cavallo, R. Dorta, *Chem. Eur. J.* **2011**, *17*, 12886.

complexes.⁴⁰ Its influence in palladium-catalyzed reactions was investigated by Nolan and co-workers who demonstrated the high catalytic activity of the [Pd(IPr*)(cin)Cl] pre-catalyst (**1.5**) in Suzuki-Miyaura coupling for tetra-*ortho*-substituted biaryls at room temperature (Scheme 1.3.5).⁴¹



Scheme 1.3.5: Suzuki-Miyaura reactions for the synthesis of tetra-*ortho*-substituted biaryls using IPr* ligand reported by Nolan.

Very recently, the same group reported the α -arylation of ketones using a Ni(II) pre-catalyst (**1.6**) bearing the IPr* as ancillary ligand (Scheme 1.3.6). The high reactivity of the catalyst allowed a large variety of coupling partners to be employed in the reaction with good yields whereas the less sterically hindered NHC ligands such as IPr and SIPr are not capable to achieve satisfied results.⁴²



Scheme 1.3.6: Ni-catalyzed α -arylation of ketones using IPr* ligand reported by Nolan.

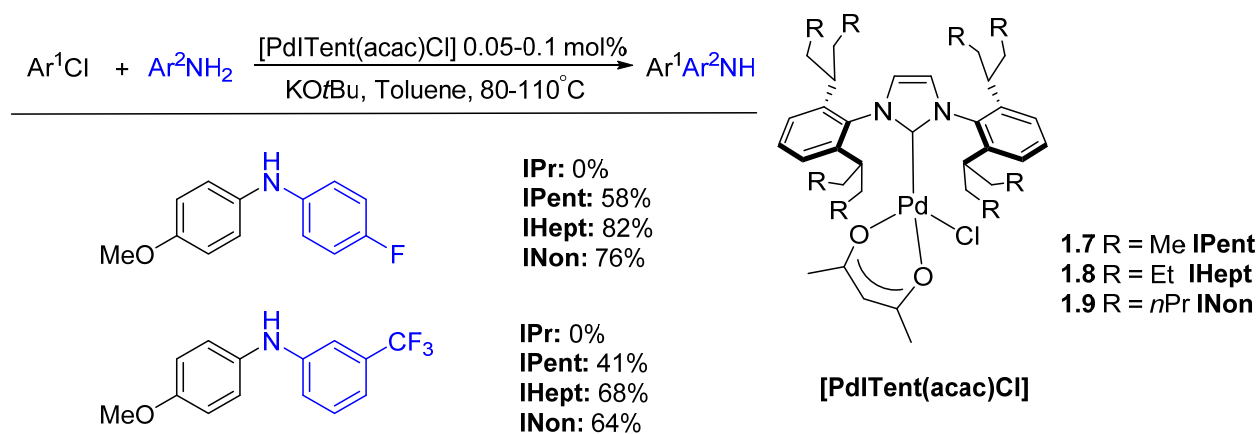
Based on the IPent ligand which was previously developed by Organ group, Nolan and co-workers further studied the effect of the length of the alkyl chains on the aryl substituents in palladium-catalyzed cross-coupling reactions. It was found that there was almost no difference in Suzuki-Miyaura reaction employing bulky substrates between IPent, and IHept,

⁴⁰ G. Berthon-Gelloz, M. A. Siegler, A. L. Spek, B. Tinant, J. N. H. Reek, I. E. Marko, *Dalton Trans.* **2010**, 39, 1444.

⁴¹ A. Chartoire, M. Lesieur, L. Falivene, A. M. Z. Slawin, L. Cavallo, C. S. J. Cazin, S. P. Nolan, *Chem. Eur. J.* **2012**, 18, 4517.

⁴² J. A. Fernández-Salas, E. Marelli, D. B. Cordes, A. M. Z. Slawin, S. P. Nolan, *Chem. Eur. J.* **2015**, 21, 3906.

INon who bear longer alkyl chains (Scheme 1.3.7). However, the positive effect on the reactivity was observed with **IHept** ligand when comparing the three ligands in amination with challenging anilines coupling partners at low catalyst loading.⁴³ It was shown that the catalytic properties were optimized using **IHept** ligand while no further improvement was observed by increasing the length of the alkyl chain to a 5-nonyl group (a small decrease was even noticed).



Scheme 1.3.7: Comparison in Pd-catalyzed amination using IPr, IPent, IHept and INon ligands reported by Nolan.

3.2. Backbone functionalization

An obvious difference between NHC and phosphine ligand structures consists in the ease of varying their steric and electronic properties. For the NHC ligands, the electronic properties are mainly imparted by the nature of heterocyclic moiety⁴⁴, thus making it possible to tune the electronic density of the carbenic carbon through modification of the heterocyclic backbone.

Backbone chlorinated **IPr** derivative **IPr^{Cl2}** was synthesized by Arduengo by addition of two equivalents of CCl₄ to a THF solution of **IPr**. **IPr^{Cl2}** is more stable compared to **IPr** and later this procedure was extended to its bromide derivative **IPr^{Br2}**. It was assumed that both the π -electron-releasing component of the chlorine lone pair and the σ -electron-withdrawal effects due to the higher electronegativity of chlorine atom are the main factors to stabilize the free carbene.⁴⁵

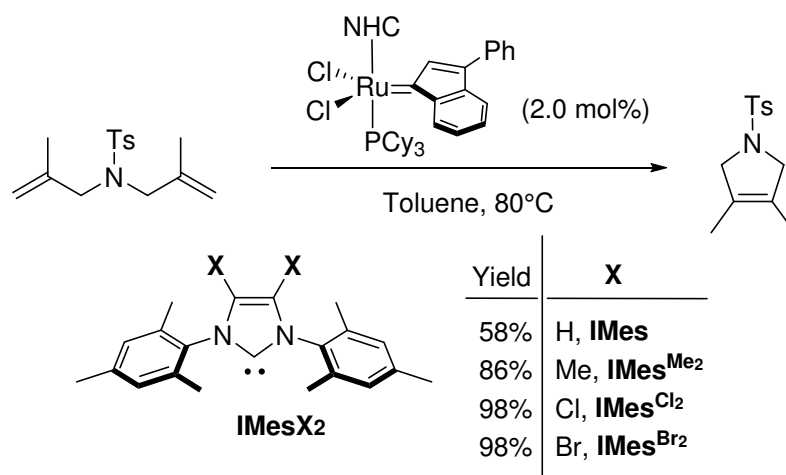
The influence of backbone halogenated **IMes^{Cl2}** and **IMes^{Br2}** was investigated in the Ru catalyzed metathesis. It was found that the Ru complexes bearing halogenated ligands were

⁴³ S. Meiries, G. Le Duc, A. Chartoine, A. Collado, K. Speck, K. S. A. Arachchige, A.M. Z. Slawin, S. P. Nolan, *Chem. Eur. J.* **2013**, *19*, 17358.

⁴⁴ W. A. Herrmann, J. Schütz, G. D. Frey, E. Herdtweck, *Organometallics* **2006**, *25*, 2437.

⁴⁵ (a) A. J. Arduengo, F. Davidson, H. V. R. Dias, J. R. Goerlich, D. Khasnis, W. J. Marshall, T. K. Prakasha, *J. Am. Chem. Soc.* **1997**, *119*, 12742; (b) M. L. Cole, C. Jones, P. C. Junk, *New J. Chem.* **2002**, *26*, 1296; (c) S. K. Furfari, M. R. Gyton, D. Twycross, M. L. Cole, *Chem. Commun.* **2015**, *51*, 74.

superior to the non-halogenated analogues when introducing tetra-substituted olefin (Scheme 1.3.8).⁴⁶ The higher catalytic properties were attributed to improved stability resulting from reduced catalyst initiation due to the relative poor electron donation of **IMes**^{X₂} compared to this of **IMes** (determined by measurement of TEP values).

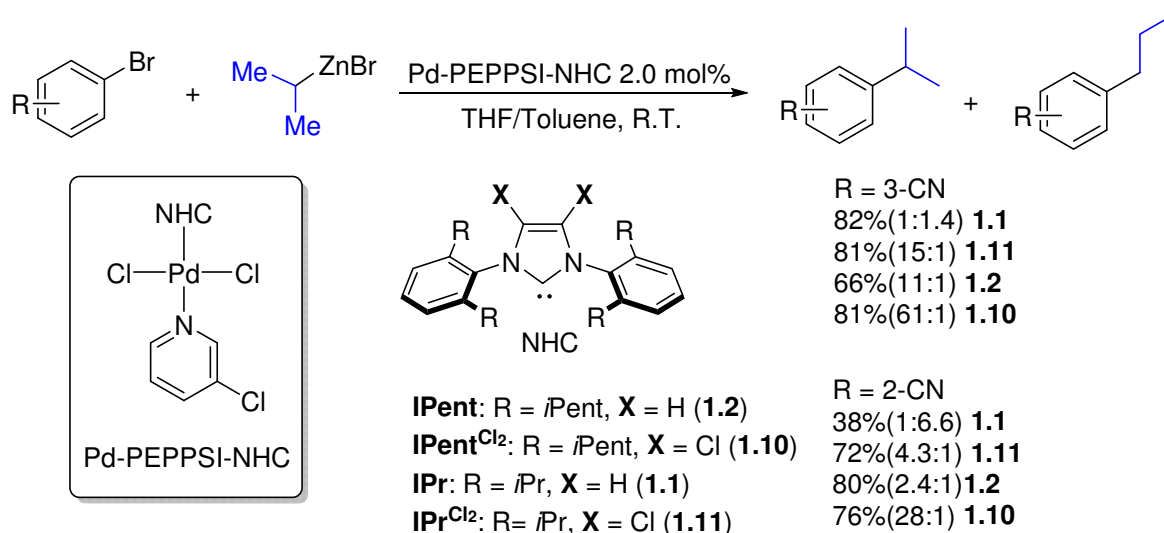


Scheme 1.3.8: Backbone effect of IMes investigated in Ru-catalyzed metathesis reported by Nolan.

The chlorinated NHCs **IPr**^{Cl₂} and **IPent**^{Cl₂} were later evaluated in the palladium-catalyzed Negishi cross-coupling of secondary alkylzinc halides by Organ and co-workers. An excellent selectivity of branched products *vs* linear products was observed when using **IPent**^{Cl₂} as ligand (Scheme 1.3.9). The increase of steric bulkiness around the metal and the reduction of the electronic density on metal are the two crucial factors which speed up the rate of reductive elimination (RE) and thus suppress the β -hydride elimination (BHE). Detailed theoretical studies were carried out to confirm this proposal which revealed a linear correlation between the size of the backbone substituents and the difference in energy ($\Delta\Delta E^\ddagger$) between the transition states of the RE and BHE, which determines the selectivity.⁴⁷

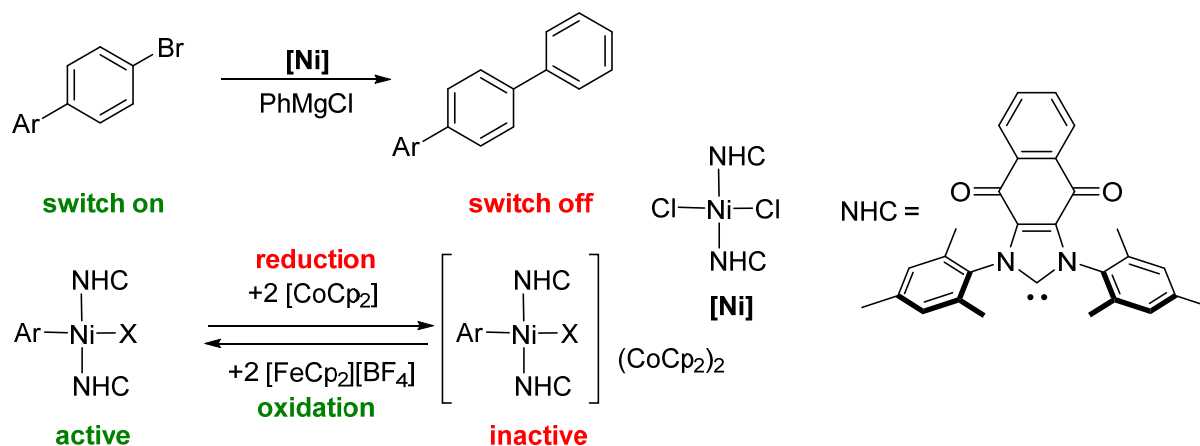
⁴⁶ C. A. Urbina-Blanco, X. Bantreil, H. Clavier, A. M. Z. Slawin, S. P. Nolan, *Beilstein J. Org. Chem.* **2010**, *6*, 1120.

⁴⁷ M. Pompeo, R. D. J. Froese, N. Hadei, M. G. Organ, *Angew. Chem. Int. Ed.* **2012**, *51*, 11354.



Scheme 1.3.9: Backbone-effect investigated in Pd-catalyzed branch selective Negishi reaction reported by Organ.

The extension of the aromatic π -system of imidazol-2-ylidene is also an effective way to modify the electronic properties of the carbenic center. An interesting example reported by Bielawski and co-workers has shown that simply grafting naphthoquinone motif onto the skeleton of **IMes** led to a redox-active NHC-catalytic system.⁴⁸ The redox-active naphthoquinone could be reduced by addition of cobaltocene CoCp_2 to “switch off” the reaction, and by simple oxidation with ferrocenium tetrafluoroborate $[\text{FcCp}_2][\text{BF}_4]$, the reaction could be “switched on” (Scheme 1.3.10).⁴⁹



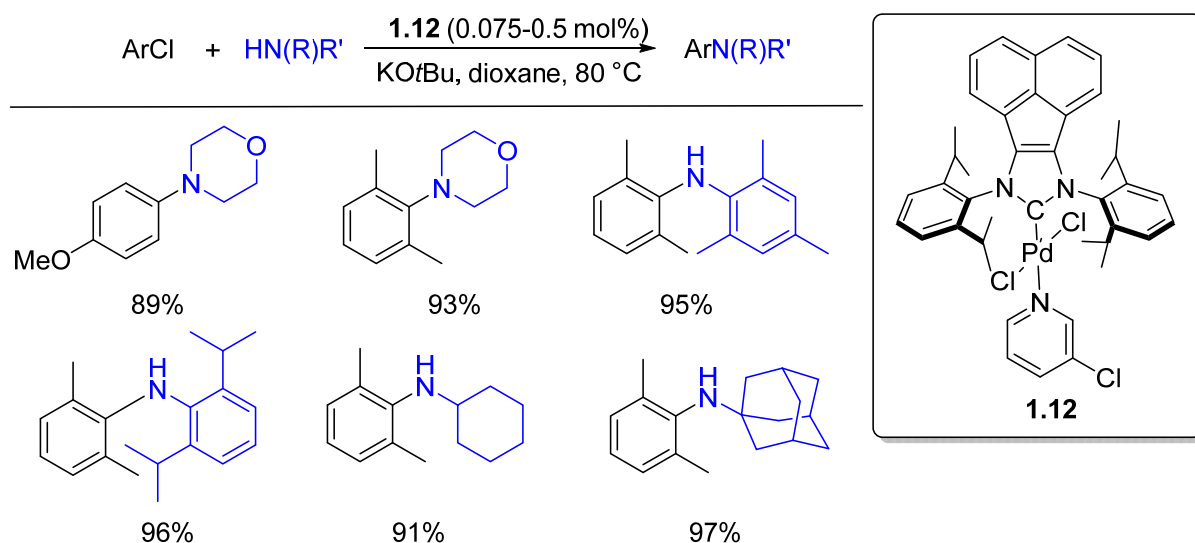
Scheme 1.3.10: Redox-active NHC in nickel-catalyzed Kumada reaction reported by Bielawski.

Fusion of acenaphtho and imidazolyliene units afforded an acenaphthoimidazolyliene which was developed by Tu and co-workers and whose catalytic studies were conducted in palladium-catalyzed Buchwald-Hartwig amination. Under the optimized conditions using the

⁴⁸ M. D. Sanderson, J. W. Kamplain, C. W. Bielawski, *J. Am. Chem. Soc.* **2006**, 128, 16514.

⁴⁹ A. G. Tennyson, V. M. Lynch, C. W. Bielawski, *J. Am. Chem. Soc.* **2010**, 132, 9420.

PEPPSI type palladium pre-catalyst (**1.12**) bearing the above NHC ligand, a large scope of amines as well as anilines were coupled with various aryl chlorides with a catalyst loading as low as 0.075 mol% (Scheme 1.3.11).⁵⁰



Scheme 1.3.11: The catalytic influence of π -extended NHC in Pd-catalyzed amination reaction reported by Tu.

Later, PEPPSI-type palladium complex **1.13** with pyracene-linked bis-imidazolyliene was developed by Peris and co-workers (Figure 1.3.1). The catalytic properties of this complex were tested in the acylation of aryl halides and Suzuki-Miyaura coupling and compared to the monometallic analogue bearing acenaphthoimidazolyliene. The results showed that the larger π -extension system of backbone had a slightly better outcome probably due to the interaction between the catalyst and aromatic substrates.⁵¹

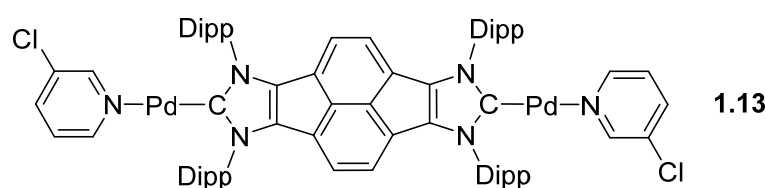


Figure 1.3.1: Bimetallic palladium complex linked by pyracene reported by Peris.

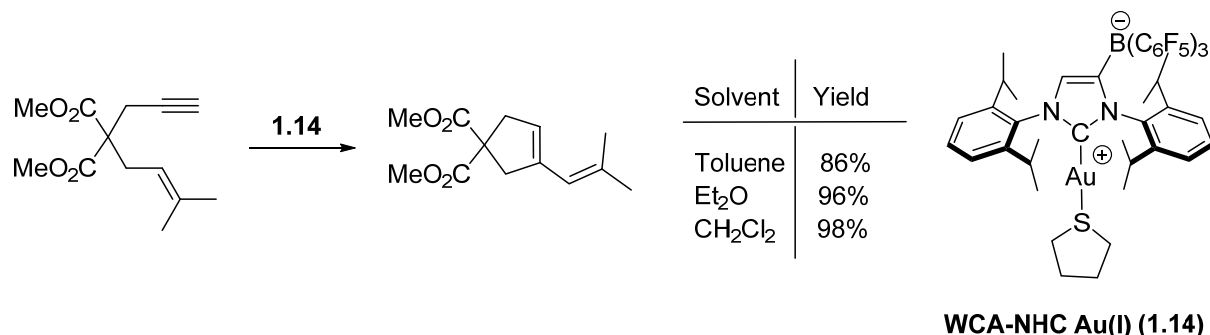
A Weakly-Coordinating Anion-*N*-Heterocyclic Carbene (WCA-NHC) bearing a borate anion was introduced by Tamm and co-workers through the substitution of the backbone of **IPr** by $\text{B}(\text{C}_6\text{F}_5)$ (Scheme 1.3.12).⁵² The benefit of this modification was found in the gold-catalyzed cycloisomerization revealing that the zwitterionic WCA-NHC gold(I) catalyst (**1.14**)

⁵⁰ T. Tu, W. Fang, J. Jiang, *Chem. Commun.* **2011**, 47,12358.

⁵¹ G. Guisado-Barrios, J. Hiller, E. Peris, *Chem. Eur. J.* **2013**, 19, 10405.

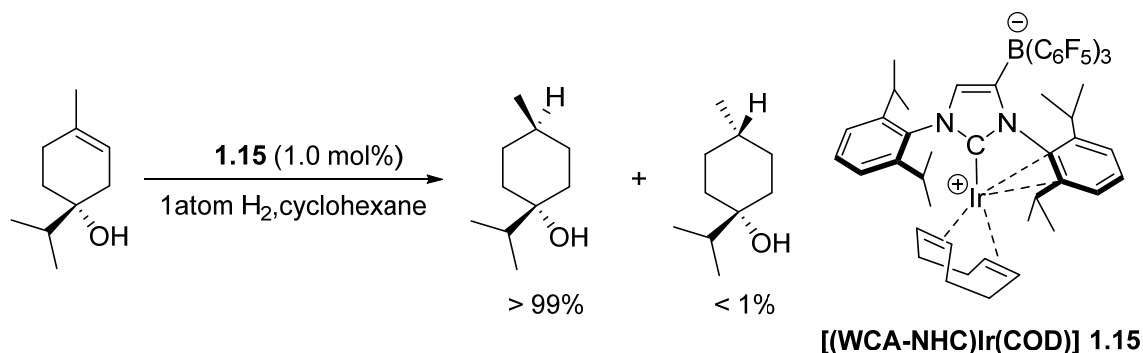
⁵² S.Kronig, E. Theuergarten, C. G. Daniliuc, P. G. Jones, M. Tamm, *Angew. Chem. Int. Ed.* **2012**, 51, 3240.

(WCA = weakly coordinating anions) performed well in this reaction even in less polar solvent without adding external silver salt to activate the pre-catalyst.



Scheme 1.3.12: The catalytic benefits of WCA-NHC ligand in Au(I)-catalyzed cycloisomerization reported by Tamm.

Later, zwitterionic Iridium complexes (**1.15**) bearing the same anionic borate NHC were synthesized and further investigated in the hydrogenation of alkenes.⁵³ High yields of products have been obtained under exceptional conditions of nonpolar solvent or even neat alkenes with very low catalyst loading (Scheme 1.3.13). The outstanding outcome of the catalytic properties inherent to this reaction is mostly attributed to the high solubility of the globally neutral catalyst in nonpolar solvent and the stabilization of the catalytically active electrophilic transition-metal complex by the anionic NHC ligand.



Scheme 1.3.13: (WCA-NHC)Ir(COD) catalyzed hydrogenation of alkenes reported by Tamm.

Even though several great achievements have been realized by apparently simple ways of decoration of backbone, the lack of the versatile synthetic transformations to the target NHC precursors is an obvious obstacle, which still limits the development of this strategy as an efficient way to introduce more powerful NHCs as ancillary in transition metal catalysts.⁵⁴

⁵³ E. L. Kolychev, S. Kronig, K. Brandhorst, M. Freytag, P. G. Jones, M. Tamm, *J. Am. Chem. Soc.* **2013**, *135*, 12448.

⁵⁴ L. Benhamou, E. Chardon, G. Lavigne, S. Bellemin-Laponnaz, V. César, *Chem. Rev.* **2011**, *111*, 2705.

4. Application of NHC ligands in palladium-catalyzed Buchwald-Hartwig Amination

4.1. Introduction

Palladium-catalyzed cross-couplings have attracted much attention of communes for the last decades and their importance was recognized in 2010 by the award of the Nobel Prize to Richard F. Heck, Ei-ichi Negishi and Akira Suzuki for their considerable contributions to the organic synthetic chemistry.⁵⁵ This powerful chemical tool has enabled organic chemists to directly combine C-C bonds of nucleophilic and electrophilic fragments under mild reaction conditions.⁵⁶ Meanwhile, another highly efficient Pd-catalyzed methodology of cross-coupling named Buchwald-Hartwig amination has increasingly become one of the most valuable synthetic methods for construction of the C-N bonds in contemporary organic synthesis, and still receives much interest from academic and industrial research groups^{57,58} where the nature of ancillary ligand on palladium metal center has a large influence on determining the outcome of this transformation.

Since the discovery of the first catalytic application in aryl amination reaction,⁵⁹ the optimization of reaction conditions inherent to the development of customized ligand architectures has resulted in an increased applicability of this transformation, taking also advantage of a better understanding of its mechanism and of its special requirements.⁶⁰ A simplified catalytic cycle implying a monodentate ligand is depicted in Figure 1.4.1. The active Pd(0) species is generated *in situ* from Pd(II) pre-catalyst (If a Pd(II) precursor is used). In the first step, the aryl halide (or pseudo-halide) undergoes oxidative addition to the Pd(0) center to give the unsaturated Pd(II) intermediate **A**; in a second step, coordination of the amine HNR^1R^2 generates the tetra-coordinated Pd(II) adduct **B**; Subsequently, deprotonation

⁵⁵ http://nobelprize.org/nobel_prizes/chemistry/laureates/2010/index.html.

⁵⁶ (a) J. F. Hartwig, in *Handbook of Organopalladium Chemistry for Organic Synthesis* (Ed.: E.-i. Negishi), Wiley, New York, **2002**, pp. 1051; b) L. Jiang, S. L. Buchwald, in *Metal-Catalyzed Cross-Coupling Reactions* (Eds.: A. de Meijere, F. Diederich), Wiley-VCH, Weinheim, **2004**, pp. 699.

⁵⁷ J. F. Hartwig, in *Modern Amination Methods* (Ed.: A. Ricci), Wiley-VCH, Weinheim, **2000**, pp. 195

⁵⁸ a) D. S. Surry, S. L. Buchwald, *Chem. Sci.* **2011**, 2, 27-50; b) J. F. Hartwig, *Acc. Chem. Res.* **2008**, 41, 1534-1544; c) D. S. Surry, S. L. Buchwald, *Angew. Chem. Int. Ed.* **2008**, 47, 6338-6361;

⁵⁹ M. Kosugi, M. Kameyama, T. Migita, *Chem. Lett.* **1983**, 927.

⁶⁰ Experimental and theoretical contributions: a) Y. Sunesson, E. Limé, S. O. N. Lill, R. E. Meadows, P.-O. Norrby, *J. Org. Chem.* **2014**, 79, 11961; b) K. H. Hoi, S. Çalimsiz, R. D. J. Froese, A. C. Hopkinson, M. G. Organ, *Chem. Eur. J.* **2012**, 18, 145-151; c) K. H. Hoi, S. Çalimsiz, R. D. J. Froese, A. C. Hopkinson, M. G. Organ, *Chem. Eur. J.* **2011**, 17, 3086-3090; d) C. L. McMullin, R. Bastian, M. Besora, G. A. Orpen, J. N. Harvey, N. Fey, *J. Mol. Catal. A: Chem.* **2010**, 324, 48-55; e) T. E. Barder, M. R. Biscoe, S. L. Buchwald, *Organometallics* **2007**, 26, 2183-2192; f) T. E. Barder, S. L. Buchwald, *J. Am. Chem. Soc.* **2007**, 129, 12003-12010; g) S. Shekhar, J. F. Hartwig, *Organometallics* **2007**, 26, 340-351.

of the latter with a base M^+B^- yields the anionic amido complex **C**, which further loses MX to liberate the tricoordinated complex **D**; Finally, reductive elimination from the latter produces the targeted amine $ArNR^1R^2$ with concomitant regeneration of the initial $Pd(0)$ species. It was shown that the rate of the oxidative addition is enhanced by an electron-rich metal center, while a sterically-hindered ancillary ligand facilitates the reductive elimination. Such findings have led to the advent of several powerful ligand classes of bulky, electron-rich phosphines.^{58b,c} In contrast, NHC-type ligands, although being stronger electron-donor ligands and even more sterically hindered than phosphines, were comparatively much less explored. The following section will present the important examples of NHC-Pd catalyzed amination reported in the literature.

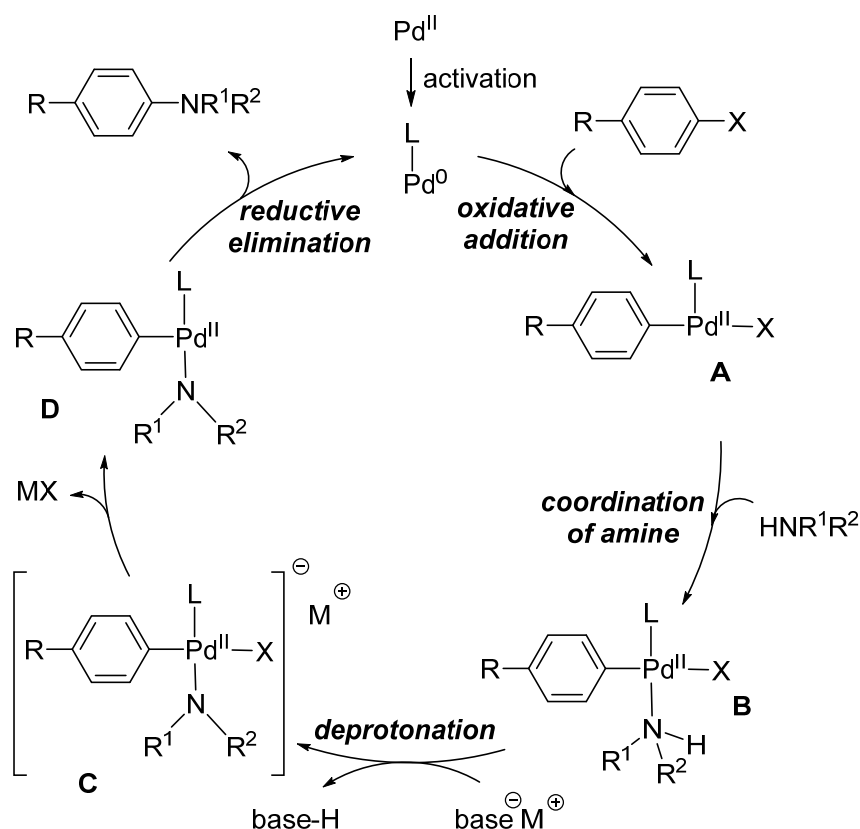
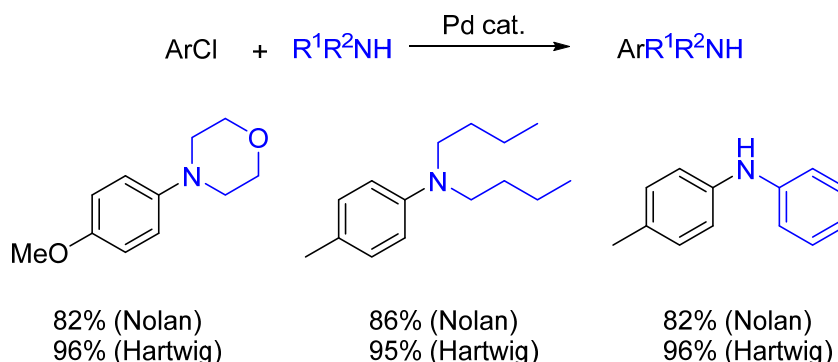


Figure 1.4.1: Catalytic cycle of the palladium catalysed aryl amination.

4.2. *In situ* generated Pd-NHC catalysts

After its first successful application in homogeneous catalysis,²⁶ NHC ligands were then widely investigated in the palladium catalyzed organic transformations.^{57,58} Pd-NHC catalysts prepared *in situ* from imidazolium salts and $Pd(0)$ precursor were commonly applied in the early stage of palladium catalyzed arylative amination. Such a system was firstly reported by Nolan and co-workers and consisted in the mixture of **IPr·HCl** with $Pd_2(dba)_3$, albeit heating

was necessary to obtain good results.⁶¹ Later, Hartwig and co-workers used **SIPr**·**HBf₄** as NHC ligand precursor and the same reaction resulted in good yields at room temperature (Scheme 1.4.1).⁶²

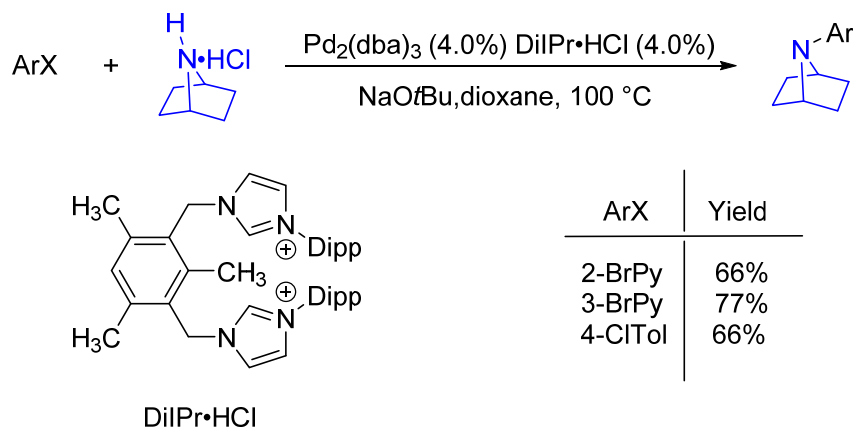


Nolan's protocol: Pd₂(dba)₃ (1.0 mol%), IPr·HCl (4.0mol%), KO^tBu, dioxane, 100°C

Hartwig's protocol: Pd(dba)₃ (1.0 mol%), SIPr·HCl (1.0mol%), NaO^tBu, DME, R.T.

Scheme 1.4.1: Comparison between Nolan's and Hartwig's protocols using NHC ligand in aryl amination.

Regarding to the more challenging amine substrates such as 7-azabicyclo[2.2.1]heptanes, Trudell and co-workers introduced a catalytic protocol using a bis(imidazolium) salt precursor with the suitable Pd source. Readily available (hetero)aryl halides (Cl, Br and I) were employed in the coupling (Scheme 1.4.2).⁶³



Scheme 1.4.2: Aryl amination with 7-azabicyclo[2.2.1]heptanes using DiIPr ligand reported by Trudell.

⁶¹ J. Huang, G. Grasa, S. P. Nolan, *Org. Lett.* **1999**, 1, 1307.

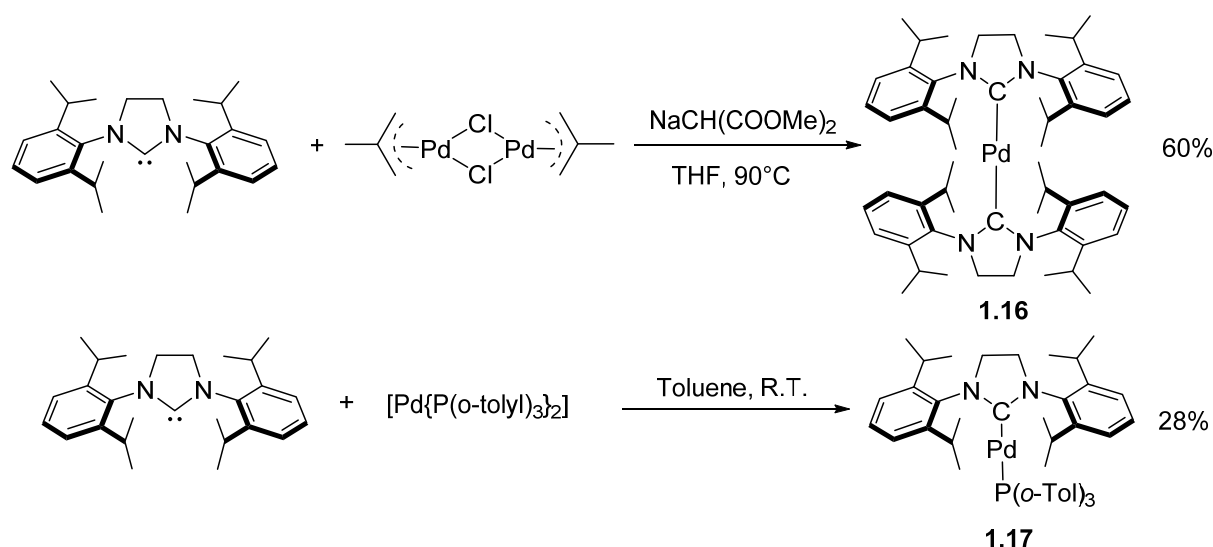
⁶² S. R. Stauffer, S. Lee, J. P. Stambuli, S. I. Hauck, J. F. Hartwig, *Org. Lett.* **2000**, 2, 1423.

⁶³ J. Chen, G. Grasa, M. L. Trudell, *Org. Lett.* **2001**, 3, 1371.

Several detailed works were published following the above original studies which enlarged the substrate scope in both amines and aryl halides.⁶⁴ However, this protocol is still suffering from several drawbacks such as long reaction times and a limited substrate scope.

4.3. Well-defined Pd-NHC catalysts

Significant improvement of Pd-NHC catalyzed Buchwald-Hartwig amination has been made by use of well-defined palladium catalysts which avoided the utilization of air and moisture sensitive palladium(0) precursors. Such efforts were first made by Caddick, Cloke and co-workers by employing complexes $[\text{Pd}(\text{SIPr})_2]$ (**1.16**) and $[\text{PdSIPr}\{\text{P}(o\text{-Tol})\}]$ (**1.17**) which were synthesized by complexation of free carbene with either Pd(II) or Pd (0) precursors Scheme 1.4.3.⁶⁵

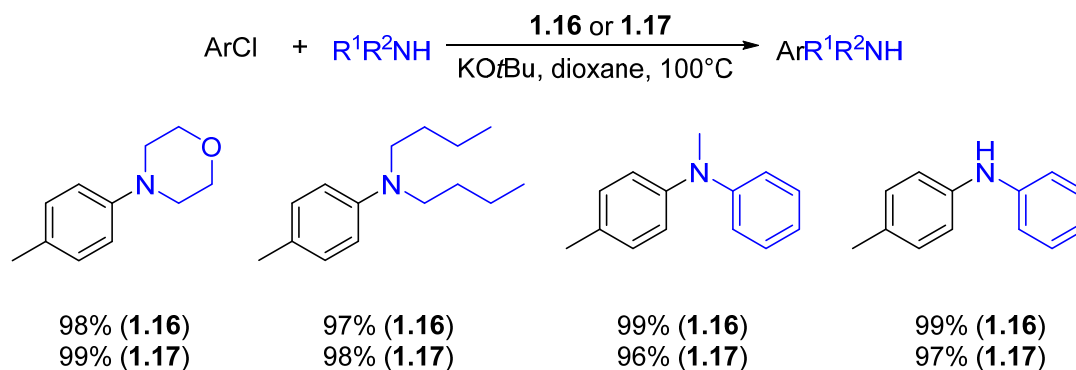


Scheme 1.4.3: Synthetic procedure of palladium-NHC catalysts **1.16** and **1.17**.

The evaluation of both complexes was carried out in the Buchwald-Hartwig amination of chloroarenes at a relatively higher temperature (100 °C) (Scheme 1.4.4). A number of *N*-mono and bis-substituted anilines were obtained in excellent yields in only 1 hour. They thus concluded that the simple dissociation of Pd-carbene bond could be the explanation of high efficiency of these two well-defined Pd(0) complexes.^{64b}

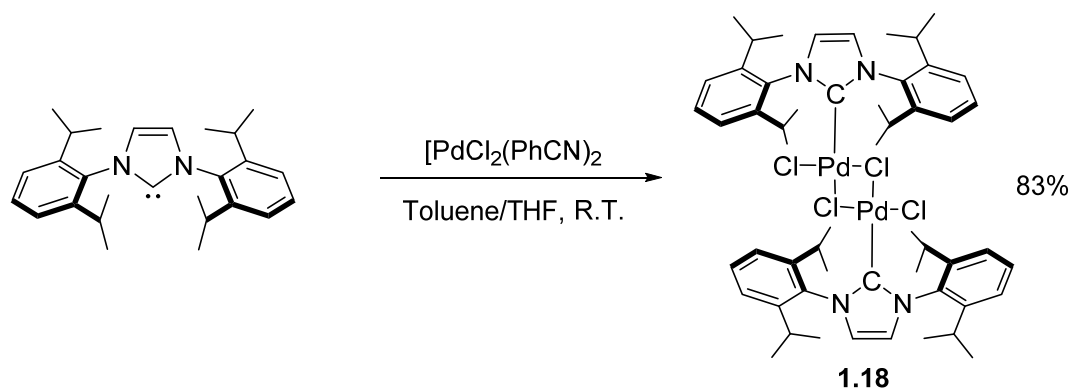
⁶⁴ (a) G. A. Grasa, M. S. Viciu, J. Huang, S. P. Nolan, *The Journal of Organic Chemistry* **2001**, 66, 7729. (b) I. Conesa Lerma, M. J. Cawley, F. G. N. Cloke, K. Arentsen, J. S. Scott, S. E. Pearson, J. Hayler, S. Caddick, *J. Organomet. Chem.* **2005**, 690, 5841.

⁶⁵ (a) S. Caddick, F. G. N. Cloke, G. K. B. Clentsmith, P. B. Hitchcock, D. McKerrecher, L. R. Titcomb, M. R. V. Williams, *J. Organomet. Chem.* **2001**, 617–618, 635.; (b) L. R. Titcomb, S. Caddick, F. G. N. Cloke, D. J. Wilson, D. McKerrecher, *Chem. Commun.* **2001**, 1388.



Scheme 1.4.4: Well-defined Pd(0)-NHC pre-catalysts **1.16** and **1.17** involved in aryl amination.

The first well-defined Pd(II) complex $[\text{Pd}(\text{IPr})(\mu\text{-Cl})\text{Cl}]_2$ (**1.18**) was successfully synthesized by Nolan and co-workers by treatment of $[\text{PdCl}_2(\text{PhCN})_2]$ with the **IPr** ligand (Scheme 1.4.5).

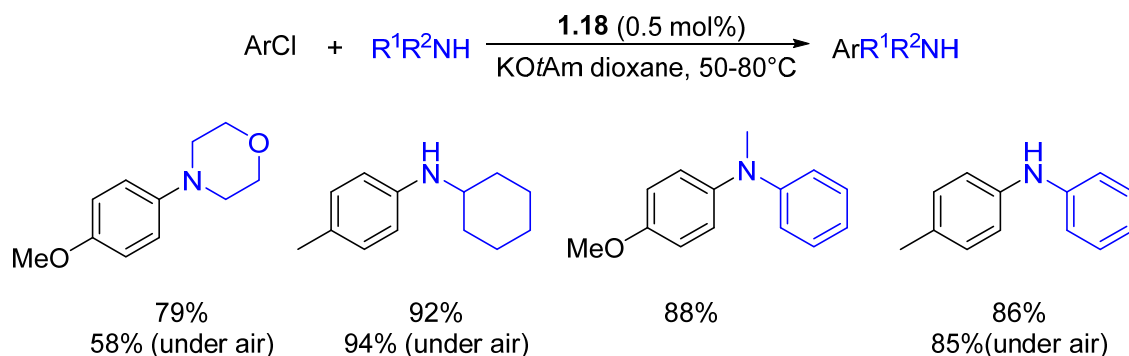


Scheme 1.4.5: Synthetic method of well-defined Pd(II)-NHC dimer complex **1.18**.

The reactivity of complex **1.18** was then investigated in Buchwald-Hartwig amination and a high efficiency with a variety of amine coupling partners under mild conditions was observed. Most notably, the reaction could proceed under air with technical grade solvents (Scheme 1.4.6).⁶⁶ The activation of the pre-catalyst was not clearly explained in this paper, but further theoretical and experimental studies highlighted the critical role of the amine or the aniline as reductive agent for this step.⁶⁷

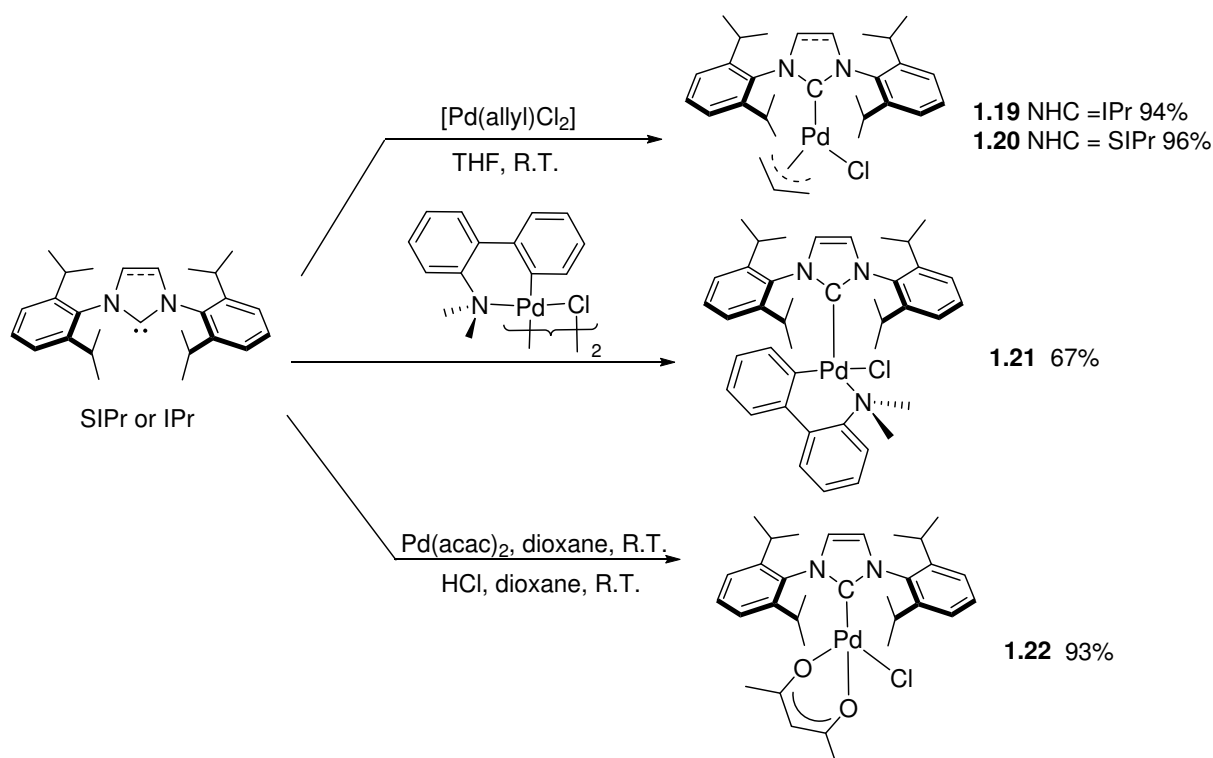
⁶⁶ M. S. Viciu, R. M. Kissling, E. D. Stevens, S. P. Nolan, *Org. Lett.* **2002**, 4, 2229.

⁶⁷ F. Wang, L. Zhu, Y. Zhou, X. Bao, H. F. Schaefer, *Chem. Eur. J.* **2015**, 21, 4153 and references cited therein.



Scheme 1.4.6: The catalytic activities of well-defined Pd-NHC pre-catalyst **1.18** in Buchwald-Hartwig amination.

Following the encouraging results presented above, further efforts were made in the development of well-defined Pd(II) complexes by Nolan and co-workers involving [Pd(NHC)(allyl)Cl] (**1.19** and **1.20**),⁶⁸ NHC-palladacycle (**1.21**),⁶⁹ and [Pd(NHC)(acac)Cl] (**1.22**)⁷⁰ whose synthetic methods are listed in Scheme 1.4.7. The times and temperatures used in coupling amination largely depended on simplicity of activation of the corresponding palladium pre-catalysts.



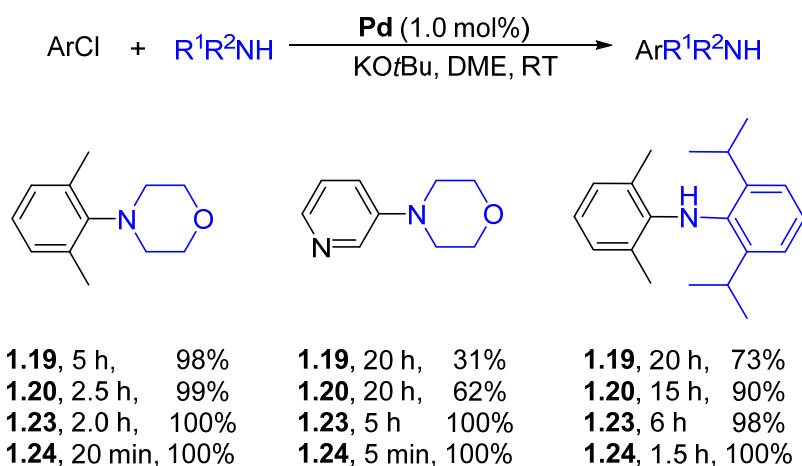
Scheme 1.4.7: Synthetic methods of different types of well-defined Pd(II) pre-catalysts.

⁶⁸ M. S. Viciu, R. F. Germaneau, O. Navarro-Fernandez, E. D. Stevens, S. P. Nolan, *Organometallics* **2002**, *21*, 5470.

⁶⁹ M. S. Viciu, R. A. Kelly, E. D. Stevens, F. Naud, M. Studer, S. P. Nolan, *Org. Lett.* **2003**, *5*, 1479.

⁷⁰ O. Navarro, N. Marion, N. M. Scott, J. González, D. Amoroso, A. Bell, S. P. Nolan, *Tetrahedron* **2005**, *61*, 9716.

A great breakthrough in the modification of palladium pre-catalyst has been achieved by replacement of the allyl moiety in **1.19** and **1.20** by a cinnamyl unit which led to drastic improvements in terms of reaction times and temperatures.⁷¹ The activities of [Pd(IPr)(cin)Cl] (**1.23**) and [Pd(SIPr)(cin)Cl] (**1.24**) in amination at room temperature were compared with the allyl analogues (**1.19** and **1.20**) (Scheme 1.4.8). More remarkably, the catalyst loading of **1.24** could be decreased to as low as 10 ppm in the case of aryl bromides as coupling partners.

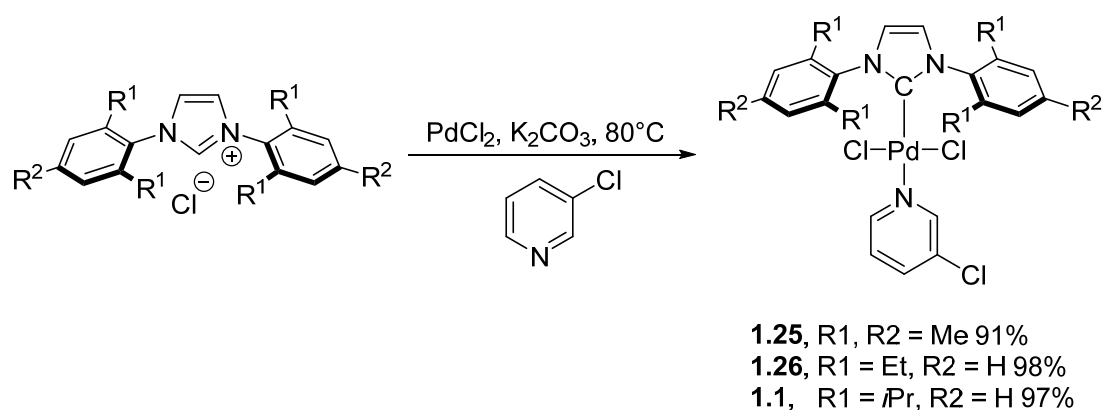


Scheme 1.4.8: Comparisons of efficiency between Pd pre-catalysts bearing allyl and cinnamyl ligands in aryl amination.

An obvious drawback inherent to the above described synthesis of palladium pre-catalyst for amination is the necessity to use free carbenes which makes the anhydrous and inert conditions unavoidable. A significant step was made with the development of a new type of Pd pre-catalyst named PEPPSI (Pyridine-Enhanced Precatalyst Preparation Stabilization and Initiation) by Organ and co-workers in 2006.⁷² A series of Pd-PEPPSI-NHC complexes could be prepared in excellent yields simply by heating a mixture of PdCl₂, imidazolium salts and K₂CO₃ in 3-chloropyridine without special precaution and even under air (Scheme 1.4.9). The reaction could be scaled up to kilogram scale and the excess of 3-chloropyridine could be recovered by distillation and reused.

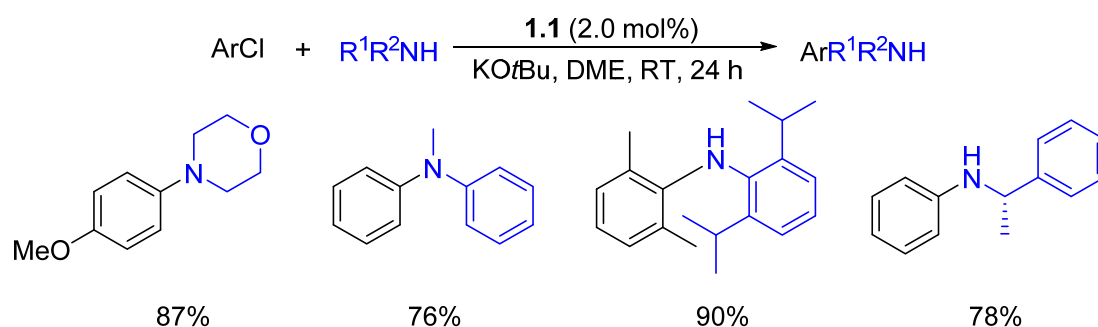
⁷¹ N. Marion, O. Navarro, J. Mei, E. D. Stevens, N. M. Scott, S. P. Nolan, *J. Am. Chem. Soc.* **2006**, 128, 4101.

⁷² C. J. O'Brien, E. A. B. Kantchev, C. Valente, N. Hadei, G. A. Chass, A. Lough, A. C. Hopkinson, M. G. Organ, *Chem. Eur. J.* **2006**, 12, 4743.



Scheme 1.4.9: The synthetic protocol of PEPPSI-Pd-NHC complexes reported by Organ group.

Later, investigation of Pd-PEPPSI complexes in amination reactions was carried out by the same group and the pre-catalyst **1.1** bearing **IPr** ligand was found to be the most active.⁷³ Various aryl chlorides and amines including certain sterically demanding amines were successfully employed in Buchwald-Hartwig amination in moderate to good yields (Scheme 1.4.10).



Scheme 1.4.10: The investigation of Pd-PEPPSI pre-catalyst **1.1** in Buchwald-Hartwig amination.

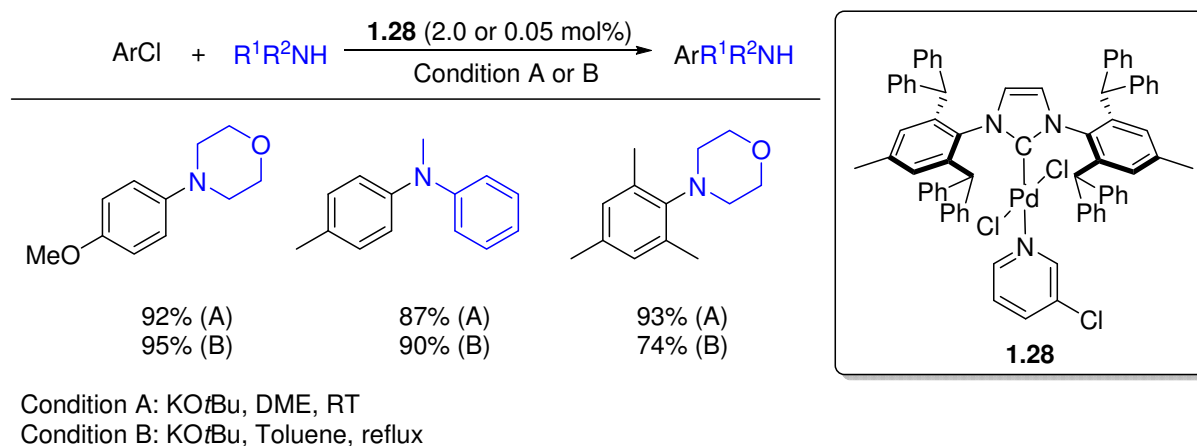
Since the increasing demand of the highly active pre-catalysts in Buchwald-Hartwig amination, the efforts have been made on the modification of the architecture of supporting NHC ligands. The most impressive example was the bulkier Pd-PEPPSI-IPent pre-catalyst (**1.2**) which was shown to greatly outperform Pd-PEPPSI-IPr (**1.1**) in the coupling of secondary amines and anilines over a wide range of aryl chlorides at 80 °C using Cs₂CO₃ as a mild base (detailed examples will be presented in Chapter 2).⁷⁴

The reactivity of palladium pre-catalyst [PdIPr*(cin)Cl] **1.27** bearing more sterically demanding **IPr*** developed by Markó and co-workers⁴⁰ was investigated by Nolan and co-

⁷³ M. G. Organ, M. Abdel-Hadi, S. Avola, I. Dubovyk, N. Hadei, E. A. B. Kantchev, C. J. O'Brien, M. Sayah, C. Valente, *Chem. Eur. J.* **2008**, *14*, 2443.

⁷⁴ (a) K. H. Hoi, S. Çalimsiz, R. D. J. Froese, A. C. Hopkinson, M. G. Organ, *Chem. Eur. J.* **2011**, *17*, 3086; (b) K. H. Hoi, S. Çalimsiz, R. D. J. Froese, A. C. Hopkinson, M. G. Organ, *Chem. Eur. J.* **2012**, *18*, 145.

workers in aryl amination. This pre-catalyst has been shown high stability due to the high electron donating and steric properties, which allows to use as low as 0.025 mol% of the catalyst loading under heating conditions for the coupling of various (hetero)aryl chlorides and amines.⁷⁵ The same benefit was observed later when using Pd-PEPSI type complex **1.28** in the same reaction (Scheme 1.4.11).⁷⁶



Scheme 1.4.11: Buchwald-Hartwig amine using Pd-PEPSI pre-catalyst **1.28** bearing IPr* as ancillary ligand.

Recently, Organ and co-workers disclosed an impressive work in amination using Cs₂CO₃ as base and showed that numerous aryl chlorides could be successfully coupled with a series of the most challenging anilines bearing electron-deficient substituents (detailed examples will be presented in Chapter 2 when using the Pd-PEPSI-IPent^{Cl₂} pre-catalyst.⁷⁷

4.4. Conclusion

Since the first time NHCs were introduced as ancillary ligands in palladium catalyzed Buchwald-Hartwig, collective efforts have been achieved in terms of a wider substrate scope and a more efficient and applicable reaction by means of modifying the architecture of supporting NHC ligands as well as the type of pre-catalysts. During the last decade, considerable contributions have been mainly made by Nolan and Organ groups toward the development of the highly active palladium-NHC catalysts. For the type of pre-catalyst, [Pd(NHC)(cinnamyl)Cl] and Pd-PEPSI have been demonstrated to be some of the most active pre-catalysts in terms of simplicity and efficiency for the activation of Pd(II) pre-catalyst into catalytic active NHC-Pd(0) species. On the other hand, optimization of NHC

⁷⁵ A. Chartoire, X. Frogneux, S. P. Nolan, *Adv. Synth. Catal.* **2012**, 354, 1897.

⁷⁶ A. Chartoire, X. Frogneux, A. Boreux, A. M. Z. Slawin, S. P. Nolan, *Organometallics* **2012**, 31, 6947.

⁷⁷ M. Pompeo, J. L. Farmer, R. D. J. Froese, M. G. Organ, *Angew. Chem. Int. Ed.* **2014**, 53, 3223.

ligands mostly focused on modification of the nitrogen substituents and backbone of the heterocycle on the basis of main frameworks of **IPr** or **SIPr** (**IPr***, **IPent**, **IPent^{Cl2}**).

More recently, Organ and co-workers proposed a catalyst performance rank order after a careful and precise evaluation based on the proven ability of Pd–NHCs in the previous literature which more or less indicates the catalytic strength of the existing active well-defined palladium–NHC catalysts (Figure 1.4.2).⁷⁸

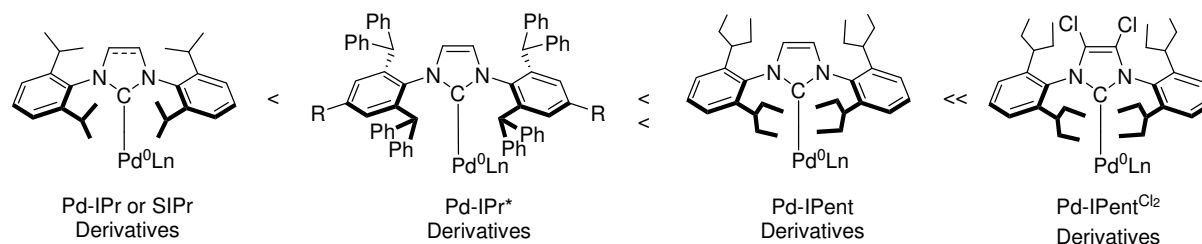


Figure 1.4.2: Proposed ranking of reactivity of selected Pd–NHC catalysts in C–N cross-coupling.

5. Thesis Overview

Since 2008, our group has developed a series of original NHCs based on six-membered ring and five-membered ring systems and containing a functionalized backbone (Figure 1.5.1).⁷⁹ The latter could be either an anionic unit, such as a malonate (**malonNHC**), an imidato (**imidNHC**), an enolate (**IMes^{O-}**), an imine anion (**IMes^{NR-}**) or an acetylacetonato unit (**IMes^{acac-}**). The development of these new NHC architectures involved a first study of their synthetic access, their structural and stereoelectronic characterization and their reactivity profile towards transition-metal complexes and small molecules. However, their application as ancillary ligands in organometallic catalysis has been relatively poorly explored. It is especially true concerning the five-membered, imidazol-2-ylidene-derived NHCs. The main reason is that the heterocyclic skeletons are still quite reactive in these NHCs (towards electrophiles, oxygen ...). In this context, the main target of this thesis was to develop new classes of skeleton-functionalized NHCs suitable to be employed in homogeneous catalysis.

⁷⁸ C. Valente, M. Pompeo, M. Sayah, M. G. Organ, *Organic Process Research & Development* **2013**, *18*, 18

⁷⁹ (a) V. César, S. Labat, K. Miqueu, J.-M. Sotiropoulos, R. Brousses, N. Lugan, G. Lavigne, *Chem. Eur. J.* **2013**, *19*, 17113; (b) L. Benhamou, N. Vujkovic, V. César, H. Gornitzka, N. I. Lugan, G. Lavigne, *Organometallics* **2010**, *29*, 2616; (c) V. Cesar, J.-C. Tourneux, N. Vujkovic, R. Brousses, N. Lugan, G. Lavigne, *Chem. Commun.* **2012**, *48*, 2349; (d) N. Vujkovic, V. César, N. Lugan, G. Lavigne, *Chem. Eur. J.* **2011**, *17*, 13151; (e) V. César, N. Lugan, G. Lavigne, *Chem. Eur. J.* **2010**, *16*, 11432; (f) V. César, N. Lugan, G. Lavigne, *J. Am. Chem. Soc.* **2008**, *130*, 11286; (g) L. Benhamou, V. Cesar, H. Gornitzka, N. Lugan, G. Lavigne, *Chem. Commun.* **2009**, 4720; (h) V. Cesar, V. Mallardo, A. Nano, G. Dahm, N. Lugan, G. Lavigne, S. Bellemin-Lapponnaz, *Chem. Commun.* **2015**, *51*, 5271.

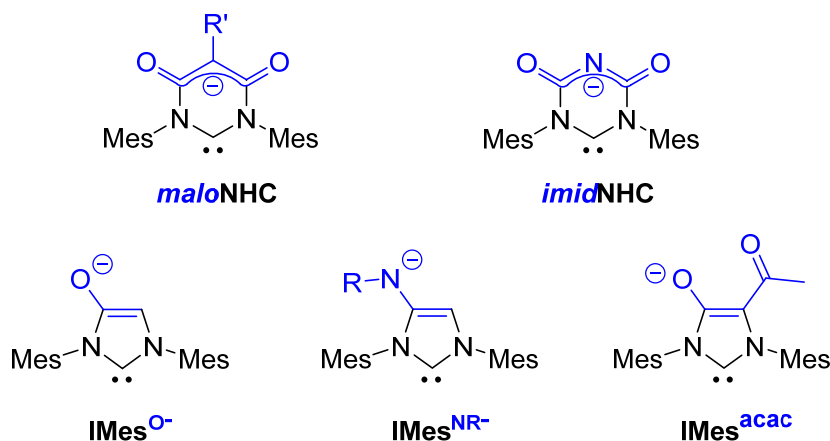


Figure 1.5.1: Previous systems of backbone functionalized anionic NHCs developed in our group.

At the beginning of this thesis, we intended to develop and study two new classes of imidazol-2-ylidenes, whose main characteristic is the presence of one or two neutral amino groups onto the imidazolyl ring (Figure 1.5.2). Our starting hypothesis was indeed based on the fact that the dimethylamino groups, as good π -mesomeric donors, are well-known to enrich the heteroaromatic cycles, the 4-(dimethylamino)pyridine (DMAP) being a textbook example.

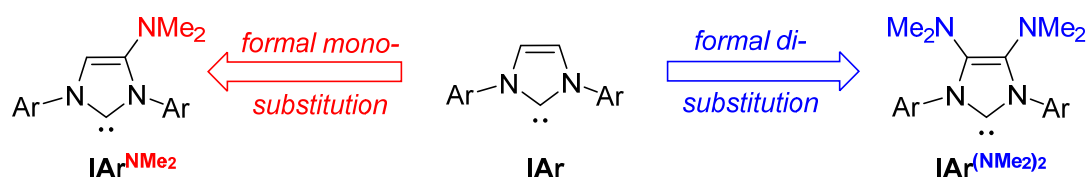


Figure 1.5.2: Target ligands (IAr^{XY}) studied in the thesis.

The influence of this decoration by amino groups will be then studied in Pd-catalyzed Buchwald-Hartwig Amination reaction (Figure 1.5.3). Due to their ease of preparation and activation, the $[\text{Pd}(\text{NHC})(\text{cin})\text{Cl}]$ and Pd-PEPPSI-NHC pre-catalysts were selected for this study.

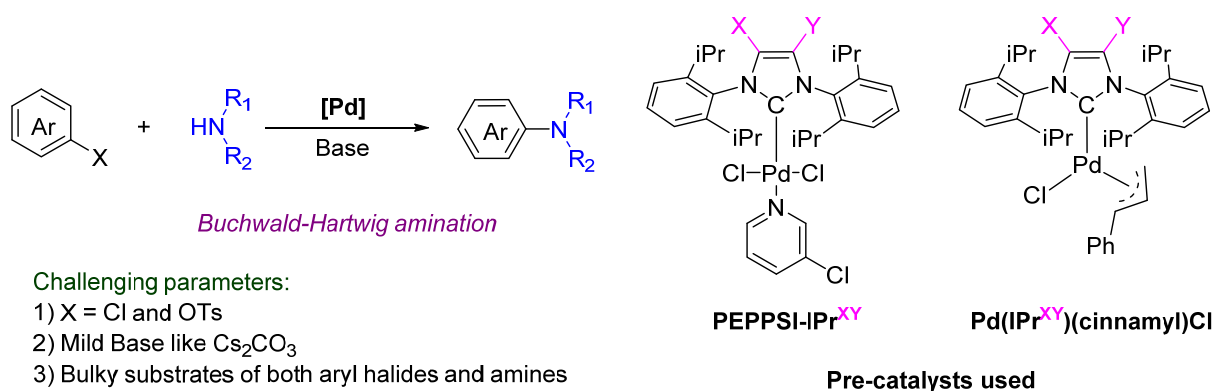


Figure 1.5.3: Target pre-catalyst and challenging aminations studied in the project.

In chapter 2, we will present the synthesis of imidazolium salts as precursors of the target carbenes, the generation and complexation of the latter onto Rh(I) and Pd(II) centers, and the catalytic studies in Buchwald-Hartwig amination. In chapter 3, we will present the development of the arylative amination of aryl tosylates as challenging electrophilic partners using a Pd-NHC catalytic system. In order to have a closer look at the critical stereoelectronic factors at play in these systems, the two first target NHC ligands will be further derivatized to produce other **IAr^{XY}** derivatives (where X = NMe₂, or NⁱPr₂, Y = H, Cl, Br) (Figure 1.5.4) and the respective efficiencies of the corresponding pre-catalysts will be evaluated in Buchwald-Hartwig amination. This will be the topic of chapter 4. Finally, the best ligand systems will be employed to optimize a more challenging coupling reaction involving aryl chlorides and bulky primary amines.

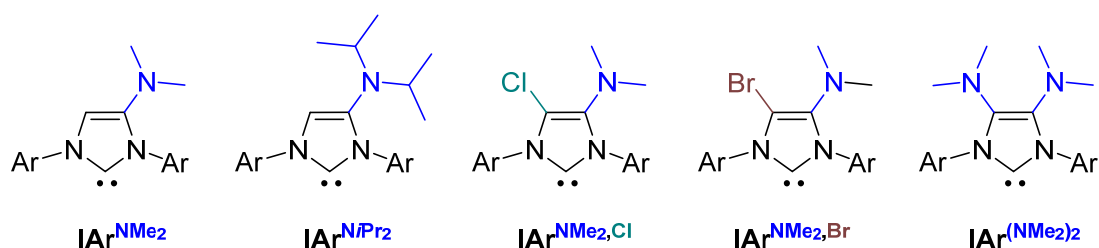


Figure 1.5.4: **IAr^{XY}** derivatives studied in the chapter 4.

-Chapitre 2-

1.	Introduction	35
2.	Synthesis of imidazolium salts	35
2.1.	Synthetic strategy	35
2.2.	Synthesis of the 4-(dimethylamino)imidazolium salts	36
2.3.	Synthesis of 4, 5-bis(dimethylamino)imidazolium triflates	40
3.	Quantification of the electronic properties of IMes^{NMe2} and IMes^{(NMe2)2}	46
3.1.	Synthesis of the [Rh(IMes ^{XY})Cl(CO) ₂] complexes	47
3.2.	Synthesis of the selenoureas [(IMes ^{XY})=Se]	49
4.	Study of the catalytic properties of new <i>NHC</i> ligands in palladium-catalyzed Buchwald-Hartwig amination	50
4.1.	Introduction	50
4.2.	Synthesis of PEPPSI-type palladium pre-catalysts	50
4.3.	Catalytic properties in Buchwald-Hartwig amination with KO ^t Bu	57
4.4.	Catalytic properties in Buchwald-Hartwig amination with Cs ₂ CO ₃	61
4.4.1.	State of the art	61
4.4.2.	Optimization of the reaction	65
4.4.3.	Scope of the substrates	66
4.	Conclusion	72

Chapter 2 : 4-(dimethylamino)-imidazol-2-ylidene and 4,5-bis(dimethylamino)-imidazol-2-ylidene: Synthesis, complexation and catalytic properties in Pd-catalyzed arylative amination

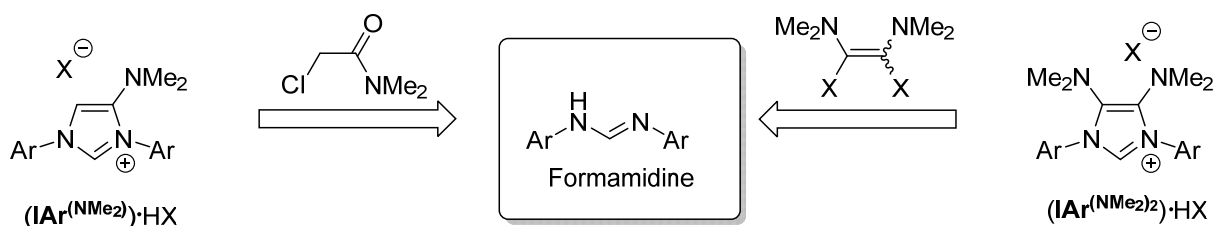
1. Introduction

This chapter deals with the chemistry of the 4-(dimethylamino)-imidazol-2-ylidene and 4,5-bis(dimethylamino)imidazol-2-ylidene ligands. In a first part, I will present the synthetic access towards their imidazolium salt precursors. Then, the generation and coordination abilities of these novel decorated NHCs will be described along with the quantification of their electronic properties. In a last part, the effect of the skeleton decoration will be studied in a model reaction, namely the Pd-catalyzed arylative amination which is better known as the Buchwald-Hartwig amination reaction.

2. Synthesis of imidazolium salts

2.1. Synthetic strategy

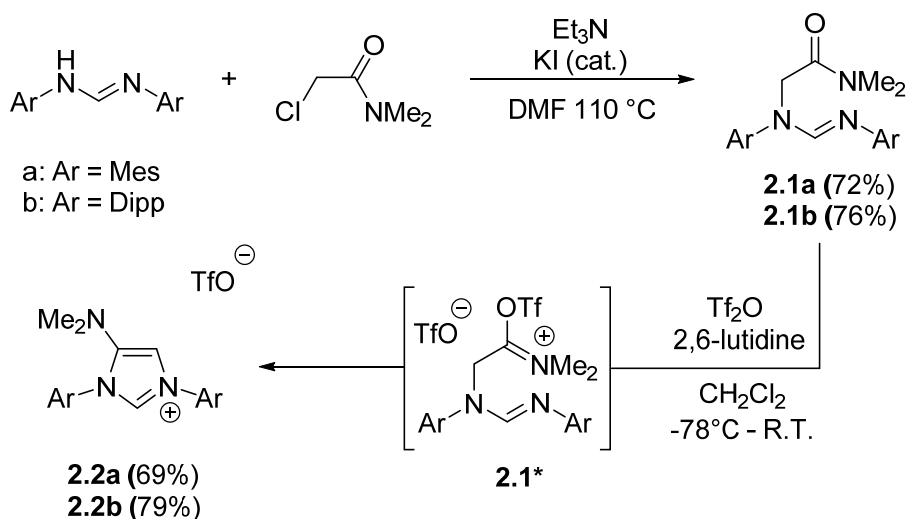
Based on the previous experience of the team in the synthesis of backbone-functionalized NHC precursors, the synthetic strategy of 4-(dimethylamino)imidazolium and 4,5-bis(dimethylamino)imidazolium salts was based on the grafting of the suitable C2-fragment reagent onto the corresponding disubstituted formamidine (Scheme 2.2.1). The synthesis of the mono-amino derivative would follow the same strategy as the one previously developed in the group for the synthesis of a 4-(isopropylamino)imidazolium salt, namely a two-step coupling between a formamidine with an α -chloroacetamide.^{79c} The heterocyclic skeleton of the bis-aminoimidazolium derivative would formally derive from a substituted diaminoethene possessing two leaving groups X.



Scheme 2.2.1: Retro-synthetic analysis for the synthesis of the target imidazolium salts

2.2. Synthesis of the 4-(dimethylamino)imidazolium salts

The imidazolium salts **2.2** were synthesized in two steps starting from the corresponding *N,N'*-diarylformamidines (Scheme 2.2.2).



Scheme 2.2.2: Synthetic procedure toward the 4-(dimethylamino)imidazolium triflates **2.2** (Mes = 2,4,6-trimethylphenyl; Dipp = 2,6-diisopropylphenyl).

The first step of the reaction consists in the acylation of the formamidine with *N,N*-dimethyl-2-chloroacetamide in the presence of Et_3N and a catalytic quantity of KI in DMF at 100°C . After purification by flash chromatography, compounds **2.1** were obtained in good yields (**2.1a**: 72%; **2.1b**: 76%). In the second step, the amide function was selectively activated using the triflic anhydride (Tf_2O)/2,6-lutidine system at low temperature (-78°C) to form the iminium triflate intermediate **2.1***.⁸⁰ Cyclization and aromatization readily occurred by the nucleophilic attack of the nitrogen on the formamidine moiety to the electrophilic carbon atom of the iminium and subsequent abstraction of a proton by 2,6-lutidine. Finally, by recrystallization through diffusion of diethyl ether to concentrated dichloromethane solutions of the crudes, mesityl substituted **2.2a** and 2,6-diisopropylphenyl derivative **2.2b** were readily obtained in good yields (69 % and 79% respectively) as white powders. The ^1H and ^{13}C NMR spectra of imidazolium triflates **2.2a** and **2.2b** were both recorded in CDCl_3 at 25°C . The ^1H NMR spectrum of **2.2a** is depicted in Figure 2.2.1.

⁸⁰ (a) S. Sforza, A. Dossena, R. Corradinni, E. Virgil, R. Marchelli, *Tetrahedron Lett.* **1998**, 39, 711; (b) A. B. Charette, M. Grenon, *Can. J. Chem.* **2001**, 79, 1694.

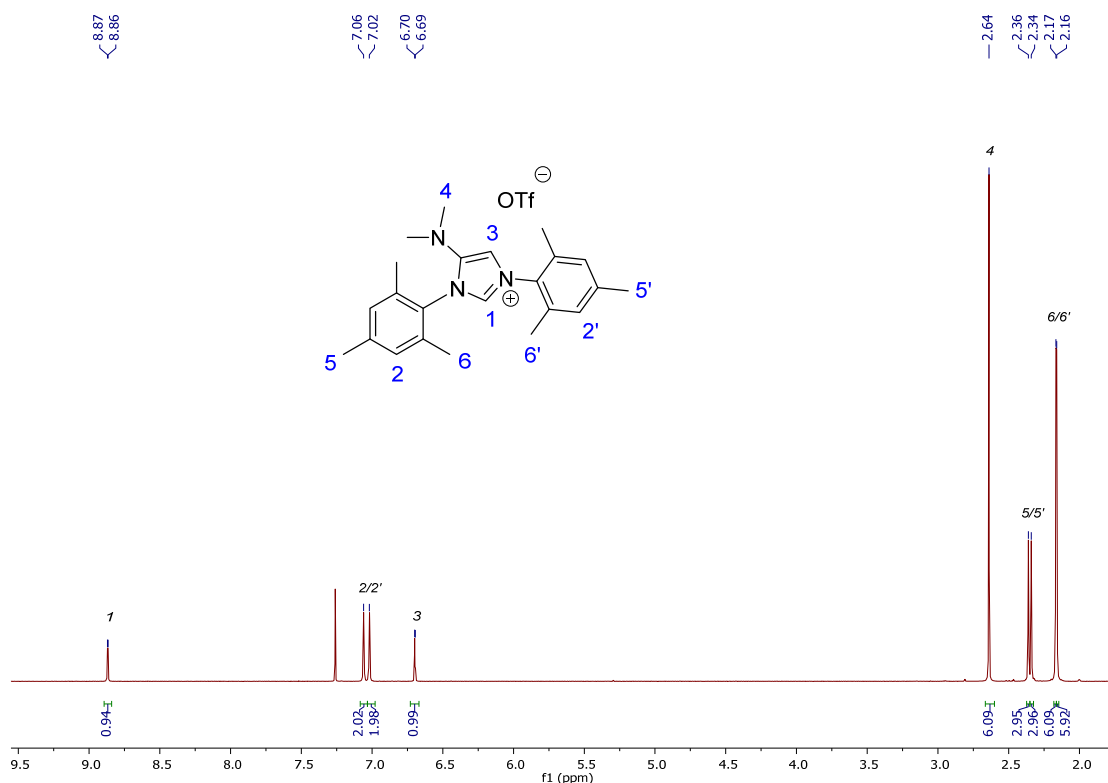


Figure 2.2.1: ^1H NMR spectrum of imidazolium triflate **2.2a** (CDCl_3 , 400 MHz).

The two protons on the cationic heterocycle appear as a characteristic set of two doublets at 8.87 ppm and 6.70 ppm with a coupling constant of 1.9 Hz. The slight different chemical shifts of the protons on mesityl group (signals 2, 5 and 6) indicate that the two mesityl substituents are no longer in the same magnetic environment due to the mono-substitution of the skeleton. The formulation of **2.2a** was confirmed by an X-ray diffraction analysis on a single-crystal of **2.2a** which was obtained by slow diffusion of pentane into a concentrated solution of **2.2a** in dichloromethane (Figure 2.2.2). The selected bond lengths and angles are shown in Table 2.2.1.

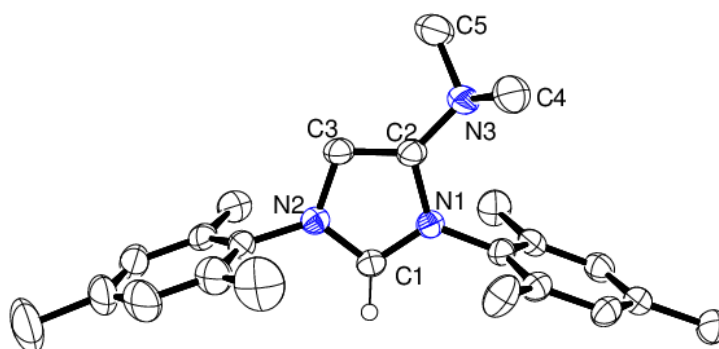


Figure 2.2.2: Molecular structure of imidazolium triflate **2.2a** (ellipsoids drawn at 30% probability level). Solvent molecules, triflate anion and all hydrogen atoms except the one on C1 were omitted for clarity.

Bond lengths (Å)		Bond angles (deg)	
C1-N2	1.326(2)	N2-C1-N1	108.80(17)
C1-N1	1.328(3)	C2-N3-C5	113.05(18)
C2-C3	1.358(3)	C2-N3-C4	115.78(19)
C2-N3	1.386(3)	C4-N3-C5	111.49(19)
N1-C2	1.397(2)	C3-C2-N3	133.10(18)
N2-C3	1.380(3)		

Table 2.2.1: Selected bond lengths (Å) and angles (deg) in **2.2a**.

In the X-Ray structure of **2.2a**, the NMe₂ group on the backbone of the imidazolyl ring is almost orientated orthogonally to the ring plane and the N3 nitrogen atom was found pyramidal ($\Sigma_{N3} = 342.3^\circ$). The N1-C2 bond length (1.397(2) Å) is markedly longer than that of the N2-C3 bond [1.380(3) Å]. These values are in agreement with those recorded in the reference 1,3-bis(mesityl)imidazolium chloride (**IMes·HCl**) [C-N: 1.383 Å],^{45a} and with the C-N lengths reported by Huber and Weiss in a related bis(dimethylamino)imidazolium triflate [C-N: 1.394–1.416 Å]. This may be explained in terms of an anomeric interaction between the lone pair of the amino group and the adjacent C-N σ^* orbital of the heterocycle, as already proposed by Huber and Weiss.⁸¹

The ¹H NMR spectrum of **2.2b** is shown in Figure 2.2.3. As similar to **2.2a**, the two heterocyclic protons in **2.2b** appear as two doublets at 8.67 ppm and 6.91 ppm. The chemical shifts of the protons on the Dipp substituents are slightly different. Single crystals of **2.2b** were obtained analogously as **2.2a**, and the X-Ray structure of **2.2b** is depicted in Figure 2.2.4. The molecular structure of **2.2b** has a similar fashion as **2.2a**.

⁸¹ S. M. Huber, F. W. Heinemann, P. Audebert, R. Weiss, *Chem. Eur. J.* **2011**, *17*, 13078.

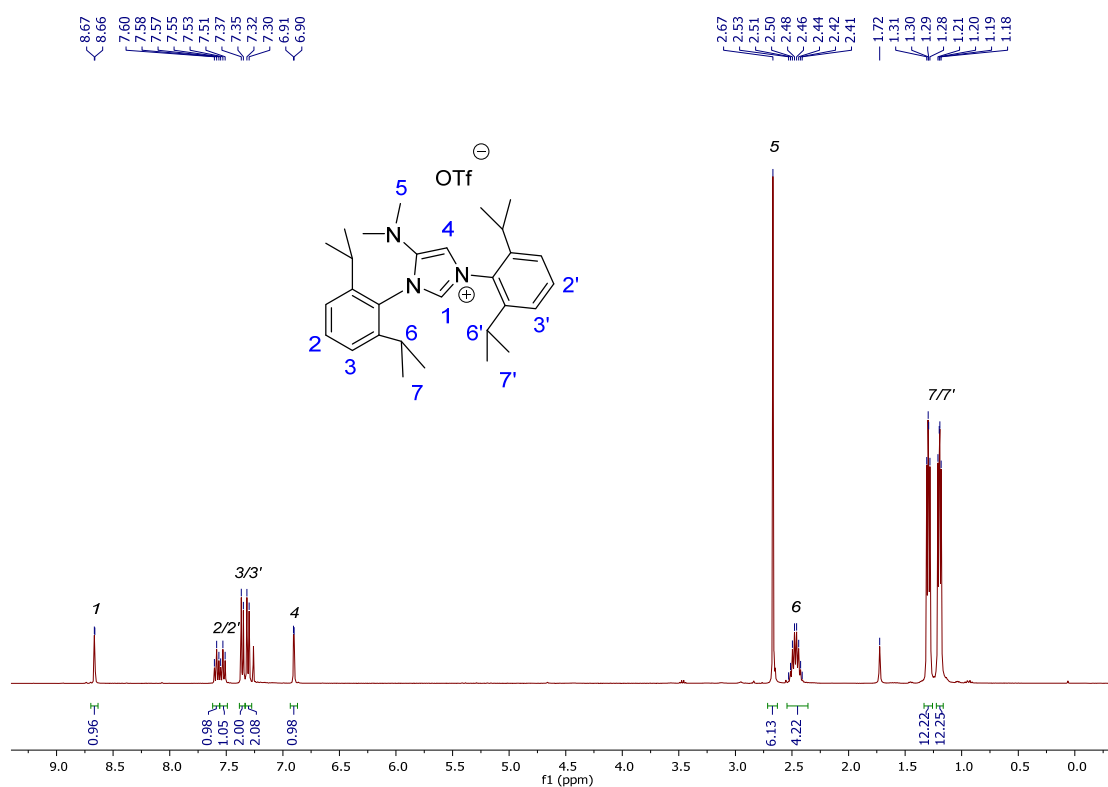


Figure 2.2.3: ^1H NMR spectrum of imidazolium triflate **2.2b** (CDCl_3 , 400 MHz).

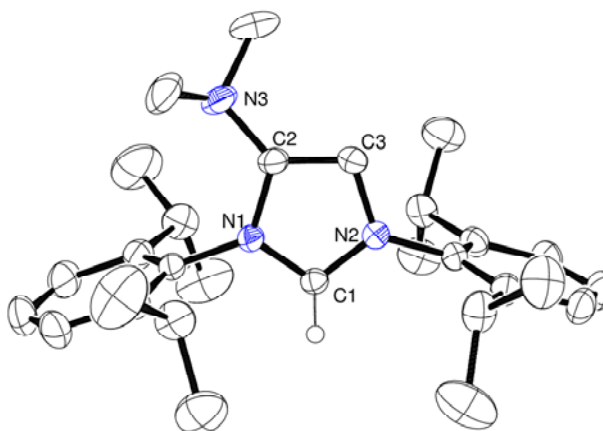


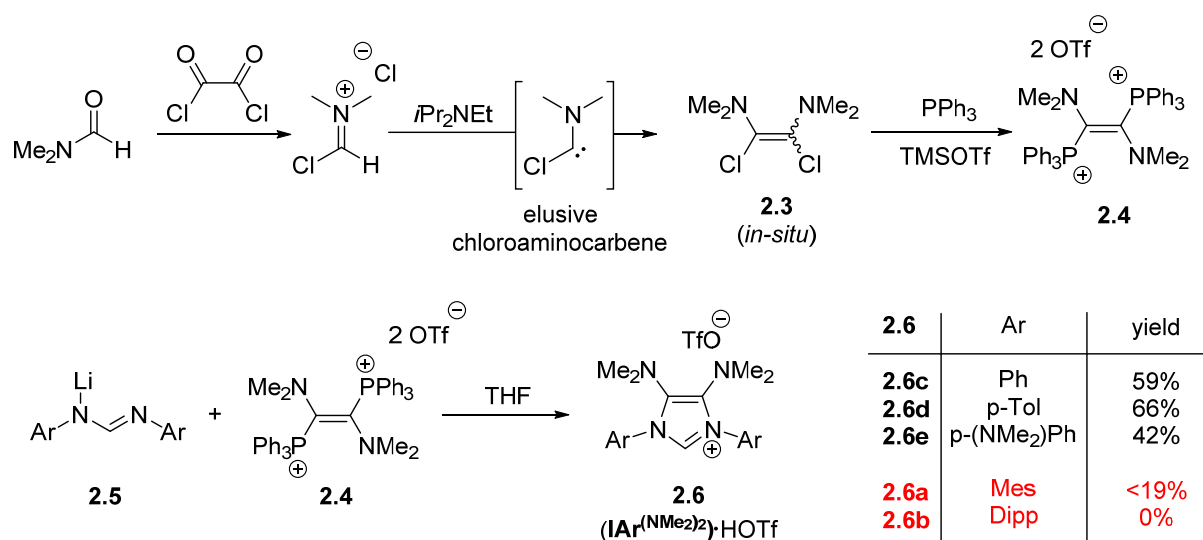
Figure 2.2.4: Molecular structure of imidazolium triflate **2.2a**. (ellipsoids drawn at 30% probability level). Solvent molecules, triflate anion and all hydrogen atoms except the one on C1 were omitted for clarity.

Bond lengths (Å)		Bond angles (deg)	
C1-N2	1.3209(17)	N2-C1-N1	108.70(11)
C1-N1	1.3332(17)	C3-C2-N3	131.20(14)
C2-C3	1.353(2)	N3-C2-N1	121.88(13)
C2-N3	1.3834(19)	C2-C3-N2	107.12(12)
N1-C2	1.3991(18)	C3-C2-N1	106.45(12)
N2-C3	1.3825(18)		

Table 2.2.2: Selected bond lengths (Å) and angles (deg) for **2.2a**.

2.3. Synthesis of 4, 5-bis(dimethylamino)imidazolium triflates

In a precedent work, Huber and Weiss reported that the synthesis of 4,5-bis(dimethylamino)imidazolium salts could be performed using the bis(phosphonio)diaminoethene salt **2.4** as C2 reagent. The formation of the latter includes the activation of DMF followed by the *in-situ* generation of a highly reactive chloroaminocarbene, which readily dimerizes to give the dichlorodiaminoethene intermediate **2.3**.⁸² This compound is highly unstable and reactive, and could not be isolated while it could be trapped with triphenylphosphine to yield compound **2.4**, which is a relatively stable and quite easy to handle solid. They successfully synthesized the 4,5-bis(dimethylamino)imidazolium triflates **2.6c-e** bearing phenyl, *para*-tolyl and *para*-dimethylaminophenyl in average yields by reacting **2.4** with the lithium formamidinates **2.5** (Scheme 2.2.3).



Scheme 2.2.3: Synthetic procedure reported by Weiss and Huber and its (unsuccessful) transposition to the synthesis of the target imidazolium salts **2.6a-b**.

Unfortunately, whereas this procedure worked well in our hands in the case of the *para*-tolyl derivative **2.6c**, it was shown that it is very sensitive to the steric hindrance of the formamidine derivative, since only a very poor yield of less than 19% was observed for the mesityl-substituted **2.6a**,⁸³ and even no product in the case of the Dipp-derivative **2.6b**. Obviously, the unsatisfied results could be attributed to the much higher steric congestion of the mesityl and 2,6-diisopropylphenyl groups which hinders the nucleophilic attack of the corresponding formamidinate onto **2.4** which already possesses two highly bulky triphenylphosphonium groups.

⁸² (a) R. Weiss, S. M. Huber, F. W. Heinemann, P. Audebert, F. G. Pühlhofer, *Angew. Chem. Int. Ed.* **2006**, *45*, 8059; (b) S. M. Huber, PhD thesis, Friedrich-Alexander-Universität Erlangen-Nürnberg, **2007**.

⁸³ G. Storch, master internship, Toulouse, **2011**.

We thus reasoned that the less sterically hindered and more reactive electrophile **2.3** could be the reagent of choice for this coupling. However, the highly reactive nature of **2.3** hampered its isolation and this reagent had to be used *in-situ* and “trapped” with a formamidine derivative.⁸⁴ After an intensive optimization of the reaction parameters, we found that the conditions described in Scheme 2.2.4 led to the synthesis of the target imidazolium triflates **2.6a-b** in moderate but still acceptable yields (38-47%). This synthesis is based on this developed with the bis(phosphonio)diaminoethene salt **2.4** and the following features are critical for a good completion of the procedure:

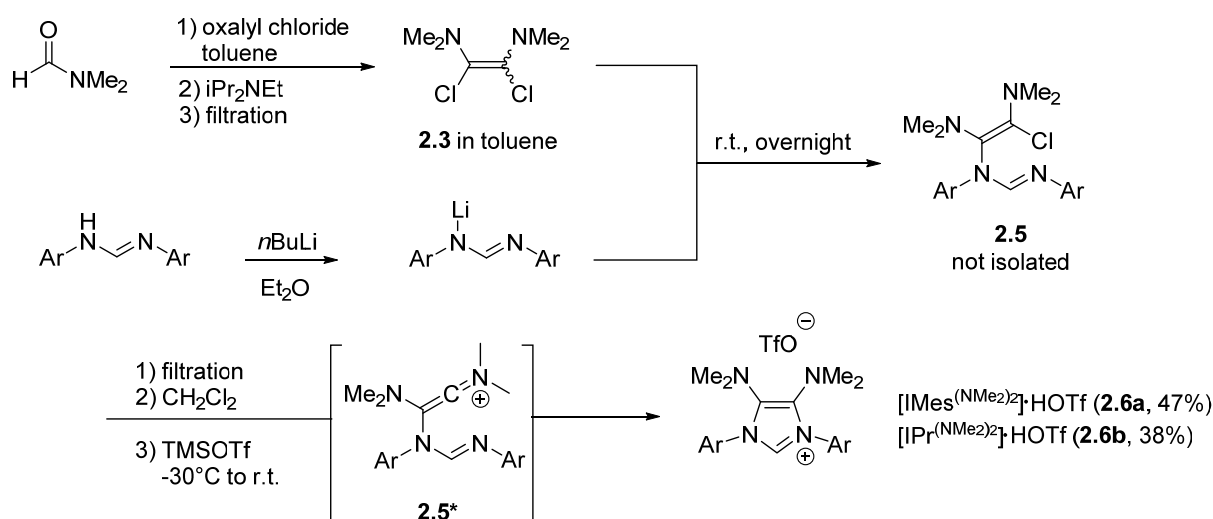
- the most critical point is the solvent system since it is a delicate balance among the solubility of the species, the required filtration of the salts and the compatibility of the solvents with the reactive species. In particular, whereas THF is usually employed for the deprotonation of the formamidines,⁸⁵ it could not be used in this synthesis since it polymerizes in presence of Me₃SiOTf, which is a strong Lewis acid. Deprotonation of the formamidines was thus carried out in Et₂O, in which the lithium formamidinates are either enough soluble for the mesityl derivative or even fully soluble in the case of the Dipp derivative. Moreover, we found that CH₂Cl₂ is necessary for the second step consisting in the addition of TMSOTf, but it could not be introduced at the beginning because of the strongly basic formamidinates.

- Two filtrations are carried out during the synthesis. The first one is performed to remove the ammonium salt (*i*Pr₂EtNH)Cl, which would react with the formamidinate in an acid-base reaction and the second one is to remove the LiCl salt, because it would consume one equivalent of the expensive TMSOTf reagent.

- Finally, the brown crude products of imidazolium triflates **2.6** are purified by flash chromatography to give light yellow, beige powders. The latter are usually repurified by recrystallization in CH₂Cl₂/Et₂O to give colorless or very pale beige powders. All these complex steps also explain the low yields of the synthetic procedure.

⁸⁴ The generation and trapping of this reagent was described in the following article: H. Böhme, P. Sutoyo, *Tetrahedron Lett.* **1981**, 22, 1671.

⁸⁵ (a) E. Despagnet-Ayoub, R. H. Grubbs, *J. Am. Chem. Soc.* **2004**, 126, 10198; (b) K. E. Krahulic, G. D. Enright, M. Parvez, R. Roesler, *J. Am. Chem. Soc.* **2005**, 127, 4142.



Scheme 2.2.4: Synthetic procedure to 4, 5-bis(dimethylamino)imidazolium **2.6**.

The proposed mechanism of the procedure is supported by the previous mechanistic proposal by Weiss and Huber. The first step consists in the formal substitution of a chloride atom by a nitrogen of the formamidine unit to yield the intermediate **2.5**, which is not isolated. TMSOTf is added to induce the cyclization, as it abstracts the chloride of **2.5** to form the highly reactive keteniminium **2.5***.

The imidazolium salts **2.6** are fully stable against air and water and their ^1H and ^{13}C NMR spectra were recorded in CDCl_3 , the ^1H NMR spectrum of **2.6a** being depicted in Figure 2.2.5. The carbenic proton appears as a singlet at 8.82 ppm shifting to high field compared to that of the mono-amino analogue **2.3a** at 8.87 ppm. The D_{2h} symmetry of the molecule is reflected by the simplicity of the NMR spectra, in which only signal for equivalent group of protons and carbons are observed. Additionally, the molecular structure of **2.6a** was confirmed by an X-Ray diffraction experiment on a single crystal (Figure 2.2.6).

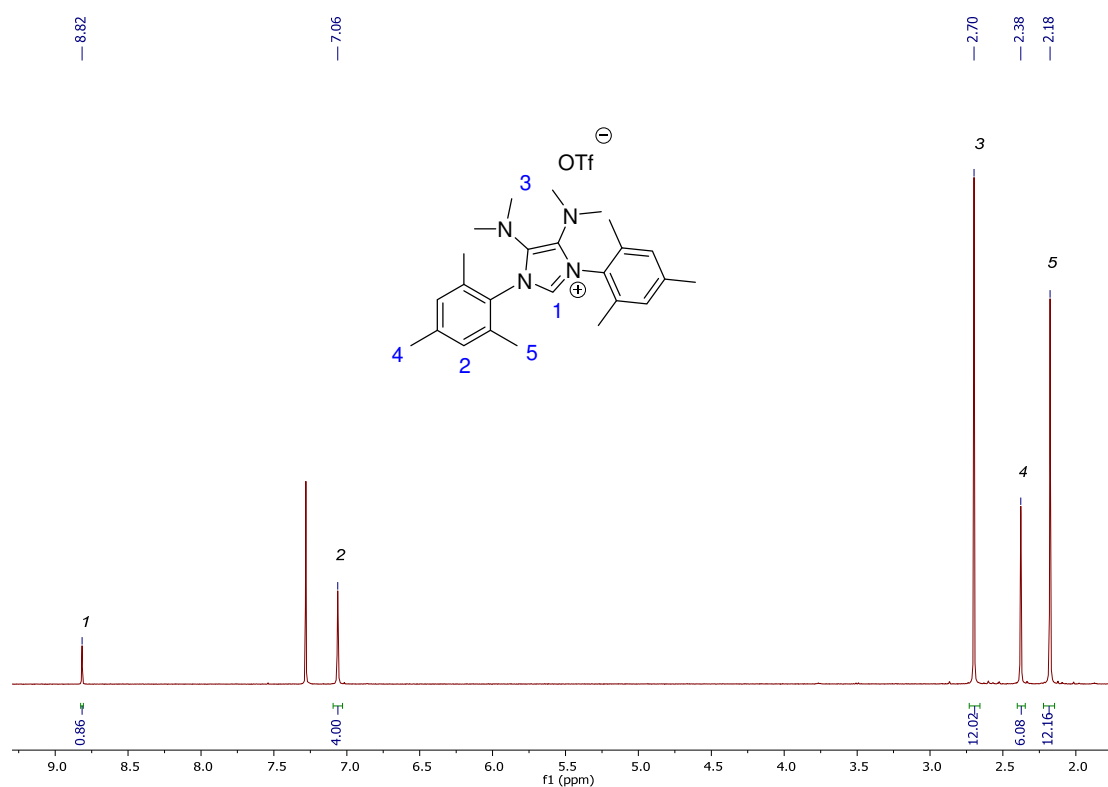


Figure 2.2.5: ^1H NMR spectrum of imidazolium triflate **2.6a** (CDCl_3 , 400 MHz).

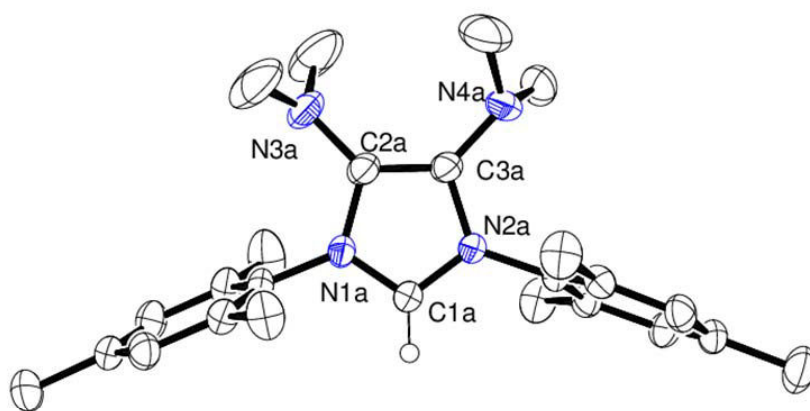


Figure 2.2.6: Molecular structure of imidazolium salt **2.6a** (Molecule A, Ellipsoids drawn at 30% probability level). Triflate anion and all hydrogen atoms except on C1a were omitted for clarity.

Bond lengths (Å)		Angles (deg)	
C1a-N2a	1.324(2)	N2a-C1a-N1a	108.76(15)
C1a-N1a	1.327(2)	C3a-C2a-N3a	133.18(18)
C2a-C3a	1.368(3)	N3a-C2a-N1a	120.56(17)
C2a-N3a	1.380(2)	C2a-C3a-N4a	134.19(17)
C3a-N4a	1.386(2)	C2a-C3a-N2a	106.45(15)
N1a-C2a	1.403(2)	C3a-C2a-N1a	106.15(15)
N2a-C3a	1.400(2)		

Table 2.2.3: Selected bond lengths (Å) and angles (deg) for **2.6a**.

Similar to **2.2a**, in the molecular structure of **2.6a**, both amino groups on the backbone of heterocyclic ring are orientated perpendicularly to the heterocyclic plane which results from an interaction between the lone pairs of NMe₂ and the adjacent C-N σ^* orbitals of the imidazolyl ring. Consequently, both N1a-C2a and N2a-C3a bond lengths are elongated to (1.403(2)Å) and (1.400(2)Å) respectively which are in the range of the reported results in **2.6c**, **2.6d** and **2.6e**.⁸¹

The same *D*_{2h} symmetry was observed in the ¹H and ¹³C{¹H} NMR spectra of **2.6b** (the ¹H NMR spectrum is depicted in Figure 2.2.7). Noteworthy, the methyl substituents on Dipp groups are divided into two sets of doublets. The single crystal structure of **2.6b** is similar to this of **2.6a** and is represented in Figure 2.2.8.

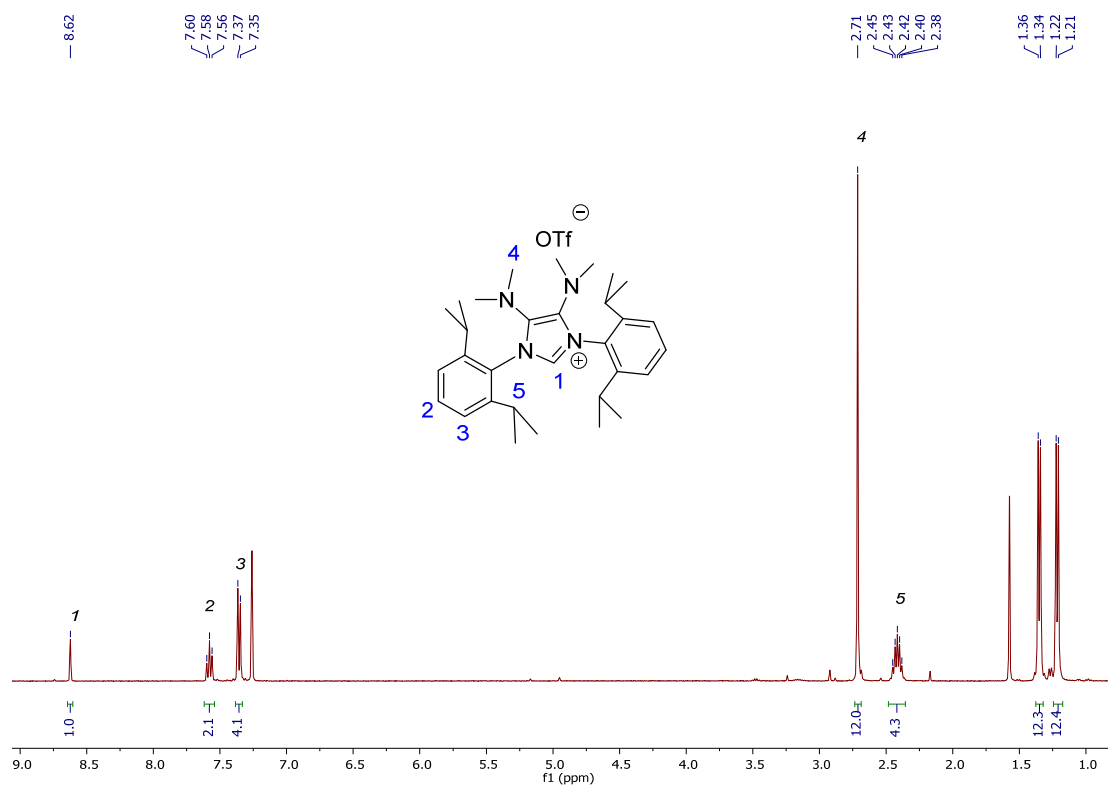


Figure 2.2.7: ¹H NMR spectrum of imidazolium salt **2.6b** (CDCl₃, 400 MHz).

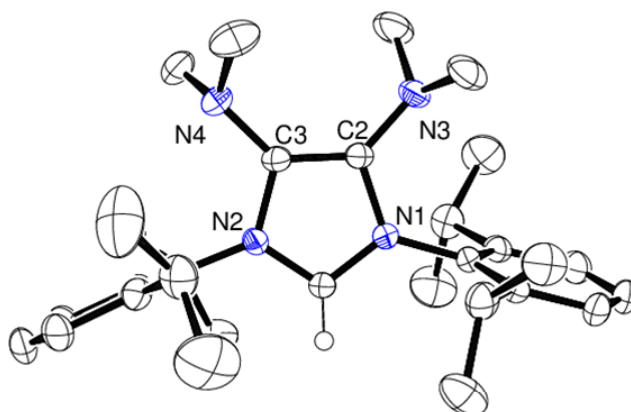
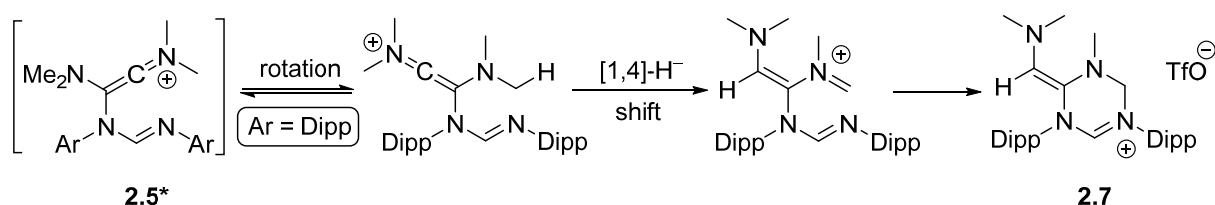


Figure 2.2.8: Molecular structure of imidazolium salt **2.6b** (Molecule A, Ellipsoids drawn at 30% probability level). Triflate anion and all hydrogen atoms except on C1a were omitted for clarity.

Bond lengths (Å)		Angles (deg)	
C1-N1	1.3279(17)	N2-C1-N1	108.76(12)
C1-N2	1.3298(18)	C3-C2-N3	134.12(13)
C2-C3	1.367(2)	N3-C2-N1	119.29(12)
C2-N3	1.3771(18)	C2-C3-N4	133.52(13)
C3-N4	1.3864(18)	C2-C3-N2	106.30(12)
N1-C2	1.4074(17)	C3-C2-N1	106.45(11)
N2-C3	1.4056(18)		

Table 2.2.3: Selected bond lengths (Å) and angles (deg) in **2.6b**.

During the optimization process, we isolated the by-product **2.7** in about 20% yield when starting from the N,N'-bis(2,6-diisopropylphenyl)formamidine. This compound consists of a six membered heterocyclic ring containing three nitrogen atoms which was finally confirmed by an X-Ray structure analysis of a single crystal of **2.7** (Figure 2.2.9). We hypothesized that the formation of **2.7** should be mostly attributed to the highly steric congestion of Dipp groups on the intermediate **2.5*** which delayed the nucleophilic attack of the second nitrogen atom to the keteniminium carbon, thus allowing the rotation of backbone group around the C-N bond followed by [1,4]-hydride shift to generate a new iminium species. Being less hindered, this compound undergoes a rapid cyclization to afford compound **2.7**.



Scheme 2.2.5: Proposed mechanism for the generation of the by-product **2.7**.

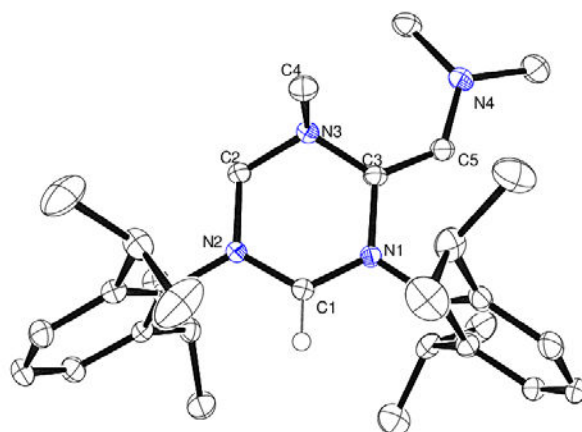


Figure 2.2.9: Molecular structure of imidazolium salt **2.7** (Molecule A, Ellipsoids drawn at 30% probability level). Triflate anion and all hydrogen atoms except on C1a were omitted for clarity.

Bond lengths (Å)		Angles (deg)	
C1-N1	1.3214(17)	N2-C1-N1	122.48(12)
C1-N2	1.3261(17)	C2-N3-C3	134.12(13)
C4-N3	1.4157(18)	C2-N3-C4	114.91(11)
C2-N3	1.4388(17)	C3-N3-C4	114.68(11)
C3-N3	1.4157(18)	C3-C5-N4	129.96(13)
C3-N4	1.3864(18)		
C5-N4	1.3864(18)		
C3-C5	1.350(2)		

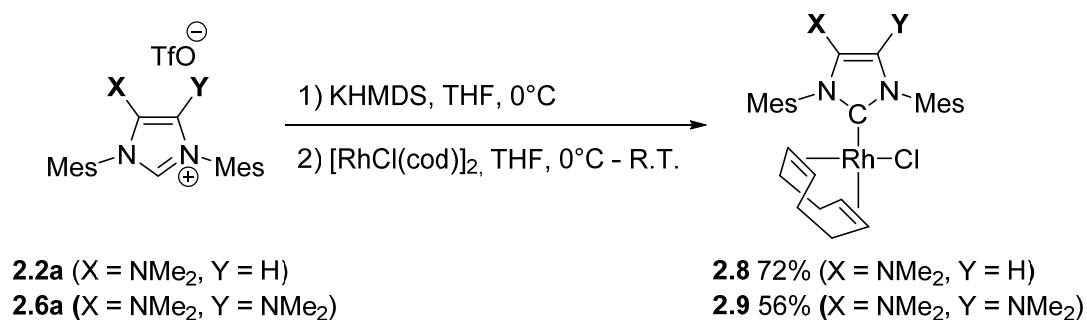
Table 2.2.4: Selected bond lengths (Å) and angles (deg) in **2.7**.

3. Quantification of the electronic properties of $\text{IMes}^{\text{NMe}_2}$ and $\text{IMes}^{(\text{NMe}_2)_2}$

As described in the chapter 1, the TEP values, calculated by linear correlation from the average $\nu_{\text{CO}}^{\text{av}}$ frequency of the two CO stretching bands in the IR spectrum of $[\text{Rh}(\text{NHC})\text{Cl}(\text{CO})_2]$ represents the total electron donicity of the NHC ligand, while the chemical shift of the signal of selenium atom in the ^{77}Se NMR spectra of the corresponding selenoureas adducts of type $\text{NHC}=\text{Se}$ allow the measurement of the π -accepting ability of NHCs. In this context, this part will describe the synthesis of the $[\text{RhCl}(\text{CO})_2(\text{IMes}^{\text{XY}})]$ complexes and selenoureas adducts $[(\text{IMes}^{\text{XY}})=\text{Se}]$. TEP values and δ_{Se} values will be measured in order to understand the electronic properties of the new NHC ligands. The mesityl derivatives were selected to allow an easier comparison with literature precedents.

3.1. Synthesis of the [Rh(IMes^{XY})Cl(CO)₂] complexes

The [RhCl(COD)(IMes^{XY})] **2.8** and **2.9** complexes were synthesized by reacting [RhCl(COD)]₂ with the corresponding free carbene IMes^{XY} which was generated *in situ* through deprotonation of the corresponding imidazolium salt by KHMDS in THF at 0°C. After purification by flash chromatography on silica gel, the Rh(I) complexes were obtained in good yields as yellow powder (Scheme 2.3.1). The ¹³C{¹H} NMR spectra of **2.8** and **2.9** display a doublet at 180.7 ppm (¹J_{RhC} = 52 Hz) and 175.8 ppm (¹J_{RhC} = 52 Hz) respectively which is the typical feature of a Rhodium-ligated imidazol-2-ylidene.⁸⁶ The chemical shifts δ(N₂C) of these signals are high-field shifted compared to the one of the analogous [RhCl(COD)(IMes)] which resonates at 183.5 ppm (¹J_{RhC} = 52 Hz), reflecting, in a first approach, a stronger electron donation of the carbenes IMes^{NMe₂} and IMes^{(NMe₂)₂}, due to the electronic donating dimethylamino groups on the imidazolyl skeleton.



Scheme 2.3.1: Synthetic procedure of [RhCl(COD)(IMes^{XY})] complexes **2.8** and **2.9**.

The solid-state molecular structure of **2.9** was confirmed by an X-Ray diffraction experiment and was displayed in Figure 2.3.1. As expected, the complex exhibits a square-planar arrangement of ligands around the rhodium centre, with the carbene ring being orthogonal to the mean coordination plane [torsion angle Cl1-Rh1-C1-N1 = 74.94 Å]. The Rh1-C1 distance [2.056(3) Å] falls into the normal range of rhodium imidazolylidene bond lengths. Here again, the nitrogen atoms N3 and N4 of the dimethylamino groups are pyramidalized (ΣN_{3α} = 344.45°; ΣN_{4α} = 354.90°) and the NMe₂ groups are twisted compared to the imidazolylidene ring, indicating that the lone pairs of the two nitrogens are not interacting with the π system of the NHC but rather with its σ, in-plane system.

⁸⁶ D. Tapu, D. A. Dixon, C. Roe, *Chem. Rev.* **2009**, 109, 3385.

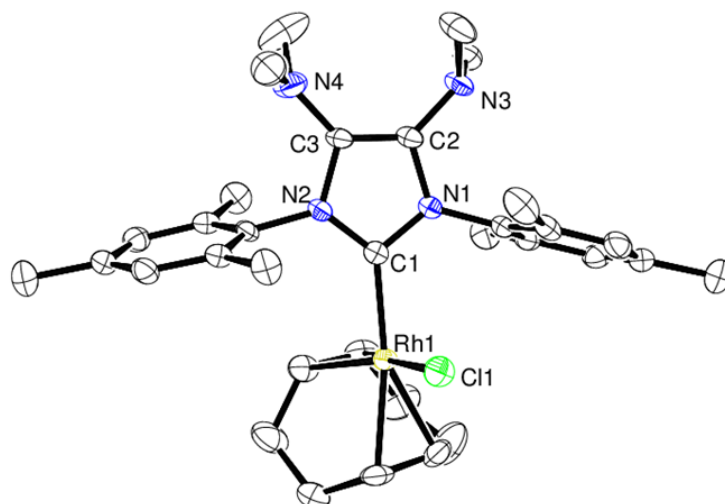


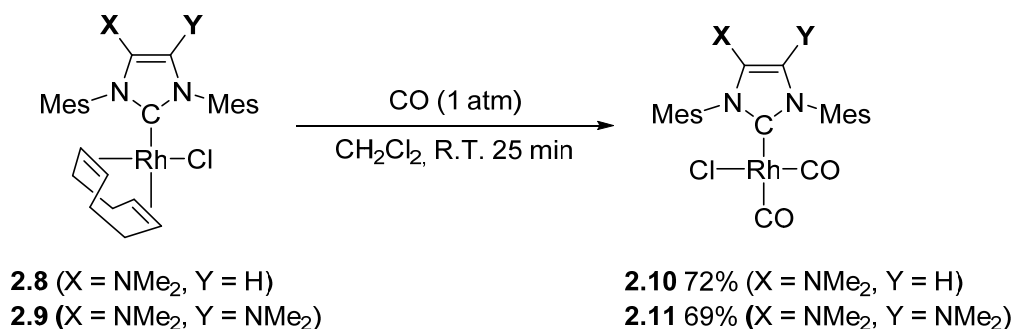
Figure 2.3.1: Molecular structure of rhodium complex **2.9** (Ellipsoids drawn at 30% probability level). Solvent molecule and hydrogen atoms were omitted for clarity.

Bond lengths (Å)		Angles (deg)	
Rh1-C1	2.056(3)	N2-C1-N1	103.4(2)
C1-N1	1.361(3)	C1-Rh1-Cl1	91.06(8)
C1-N2	1.356(4)	Cl1-Rh1-C1-N1	74.94
C2-C3	1.353(4)		
C2-N3	1.389(4)		
C3-N4	1.386(4)		
N1-C2	1.404(4)		
N2-C3	1.412(3)		

Table 2.3.1: Selected bond lengths (Å) and angles (deg) in **2.9**.

The corresponding rhodium dicarbonyl complexes $[\text{Rh}(\text{IMes}^{\text{XY}})\text{Cl}(\text{CO})_2]$ **2.10** and **2.11** were synthesized by bubbling CO gas into a CH_2Cl_2 solution of **2.8** and **2.9** respectively for about 15 min. A change of the solution color from bright yellow to light yellow was observed (Scheme 2.3.2). Three sets of doublets were observed in both $^{13}\text{C}\{^1\text{H}\}$ NMR spectra of **2.10** and **2.11**, which appear at 185.2 ppm ($J_{\text{RhC}} = 53$ Hz, Rh-CO), 183.0 ppm (d, $J_{\text{RhC}} = 75$ Hz, Rh-CO), and 174.2 ppm (d, $J_{\text{RhC}} = 45$ Hz, N_2C) for **2.10**, and 185.2 ppm (d, $J_{\text{RhC}} = 54$ Hz, Rh-CO), 183.0 ppm (d, $J_{\text{RhC}} = 75$ Hz, Rh-CO), and 169.3 ppm (d, $J_{\text{RhC}} = 45$ Hz, N_2C) for **2.11** respectively. The IR spectra of **2.10** and **2.11** were recorded in CH_2Cl_2 at 25°C and the TEP values were calculated from the average stretching frequency $\nu_{\text{CO}}^{\text{av}}$ of the CO ligands. Table 2.3.2 gathers the TEP values of several backbone-substituted IMes-derived NHCs. While the substitution of **IMes** by electron-withdrawing groups such as chlorine or bromine atoms leads to a decrease of the overall electronic donation of the corresponding NHCs (entries 4 and 5), the incorporation of electron-donating such as two methyl groups (entry 6), one methoxy group (entry 7) and one (entry 1) or two dimethylamino groups (entry 2) gives stronger donor NHCs compared to **IMes**. In particular, an increment of about -1.5 cm^{-1} is observed for each

addition of one dimethylamino group onto the heterocyclic ring. Moreover, whereas the anionic imidazol-2-ylidene-4-olate **IMes**⁰⁻ is the most electron donating of the series (and actually of all the five-membered imidazol-2-ylidene type carbenes),^{79g} the bis-aminated **IMes**^{(NMe₂)₂} was found to be the most nucleophilic among neutral imidazol-2-ylidenes.



Scheme 2.3.2: Synthetic procedure toward [Rh(IMes^{XY})Cl(CO)₂] complexes **2.10** and **2.11**.

Entry	IMes ^{XY}	ν_{CO} (CH ₂ Cl ₂ , cm ⁻¹)	ν_{COav}	TEP (cm ⁻¹) ^a
1	IMes ^{NMe₂}	2077.1, 1994.5	2035.8	2048.8
2	IMes ^{(NMe₂)₂}	2075.5, 1992.6	2034.0	2047.4
3	IMes	2079.1, 1996.0	2037.6	2050.3 ⁴⁶
4	IMes ^{Cl₂}	2084.7, 2000.2	2042.5	2054.2 ⁴⁶
5	IMes ^{Br₂}	2081.9, 1999.8	2041.3	2053.3 ⁴⁶
6	IMes ^{Me₂}	2077.0, 1992.5	2034.8	2048.0 ⁴⁶
7	IMes ^{OMe}	2079, 1995	2037	2048.5 ^{79b}
8	IMes ^{O⁻}	2071, 1988	2029.5	2043.0 ^{79g}

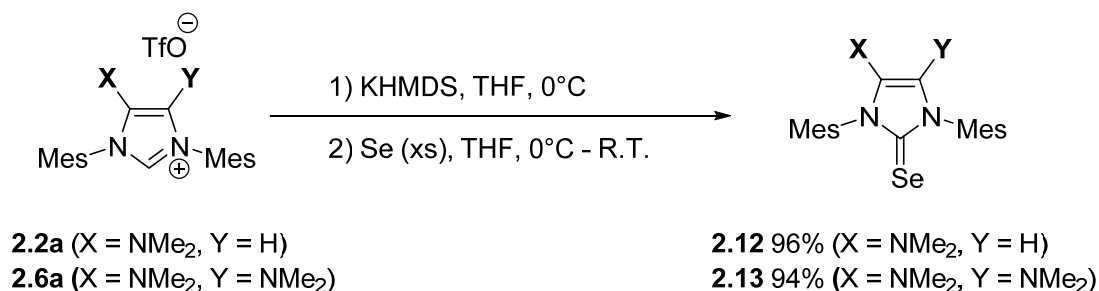
^aTEP calculated using equation $\text{TEP} = 0.8001 \nu_{\text{COav}} + 420.0 \text{ cm}^{-1}$

Table 2.3.2: TEP values of some backbone-functionalized imidazol-2-ylidenes extrapolated from their [Rh(IMes^{XY})Cl(CO)₂] complexes.

3.2. Synthesis of the selenoureas [(IMes^{XY})=Se]

In order to better understand the π -accepting abilities of the new NHCs, the corresponding selenoureas were synthesized by the classic way shown in

Scheme 2.3.3. Addition of an excess of selenium powder to a THF solution of *in situ* generated free carbene followed by a simple filtration through celite quantitatively afforded the compounds **2.12** and **2.13**.



Scheme 2.3.3: Synthesis of [(IMes^{XY})=Se] selenoureas **2.12** and **2.13**.

The ⁷⁷Se NMR spectra recorded in CDCl₃ at 25 °C show a single peak at 32.2 ppm for **2.12** and 26.5 ppm for **2.13**. These values are comparable with that reported by Nolan and co-workers for the **IMes** analogue ($\delta_{\text{Se}} = 27 \text{ ppm}$)²¹ within the experimental errors, and we can conclude that the dimethylamino substituents have a very weak, or even no influence on the π -system of the imidazol-2-ylidenes. This experimental result confirms Huber's and Weiss' assumption that the nitrogen lone pairs of the NMe₂ preferentially interact with the σ system of the heterocycle, leaving the π system unaffected.

4. Study of the catalytic properties of new *NHC* ligands in palladium-catalyzed Buchwald-Hartwig amination

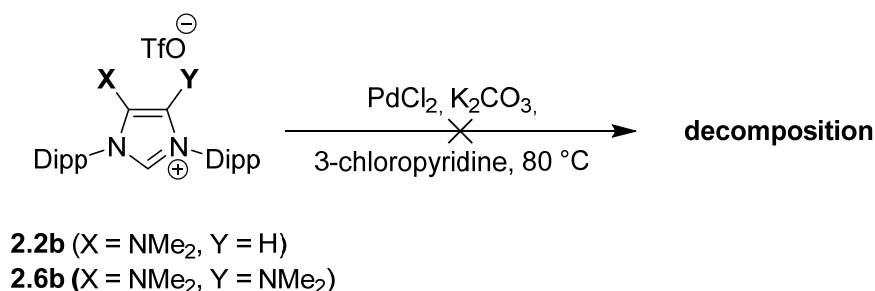
4.1. Introduction

The above studies allowed us well to understand the electronic effects of the backbone functionalization by one or two dimethylamino groups in terms of σ -donating and π -accepting abilities. This part will focus on the evaluation of the influence of this backbone-decoration in palladium-catalyzed arylation amination catalysis, and will start with the synthesis of the palladium pre-catalysts bearing the **IPr**^{NMe₂} and **IPr**^{(NMe₂)₂} ligands.

4.2. Synthesis of PEPPSI-type palladium pre-catalysts

As described in the chapter 1, Organ and co-workers have developed PEPPSI-type palladium pre-catalysts in 2006, whose general formula is [Pd(NHC)(3-ClPy)Cl₂] (3-ClPy = 3-chloropyridine) and which are abbreviated by Pd-PEPPSI-NHC. These complexes have been found to be air-stable, user-friendly and to display high efficiency in palladium-

catalyzed C-C bond formations,⁷² and in Buchwald-Hartwig amination.^{73,74,87} In this context, we decided to synthesize this type of pre-catalysts supported by the functionalized carbenes **IPr**^{NMe₂} and **IPr**^{(NMe₂)₂}, and to compare their catalytic activities with this of the **IPr** analogue in the Buchwald-Harwig amination. Unfortunately, the synthetic method reported by Organ and co-workers,⁷² namely heating a mixture of the imidazolium salt, PdCl₂ and K₂CO₃ in 3-chloropyridine at 80°C, only led to decomposition products as observed in the ¹H NMR spectra of the crude product (Scheme 2.4.1).

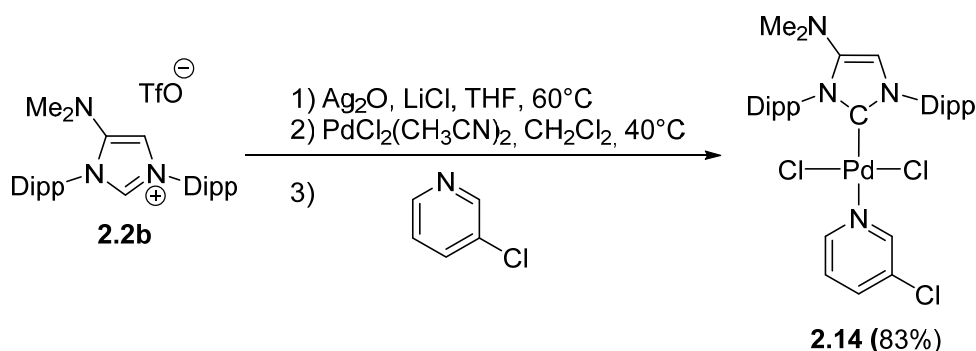


Scheme 2.4.1: Synthesis of palladium complexes using Organ's method.

Alternatively, we found that the imidazolium triflate **2.2b** smoothly and quantitatively reacted with Ag₂O in presence of LiCl and at 60°C to give the corresponding silver complex [Ag(IPr^{NMe₂})Cl]. The addition of LiCl was found to be decisive since it brings the choro ligand but, more importantly, it helps the deprotonation step by rendering the N₂CH proton more acidic by hydrogen interactions. The crude silver complex was recovered by simple filtration and evaporation and was directly engaged in the transmetalation step with the palladium precursor PdCl₂(CH₃CN)₂ to give the dimer [Pd(IPr^{NMe₂})(μ-Cl)Cl]₂.⁸⁸ The latter complex was broken by adding 3-chloropyridine to finally yield the palladium complex **2.14** as a light yellow solid. Although being quite long, this procedure is easy to perform and efficient since the overall yield is 83% (Scheme 2.4.2).

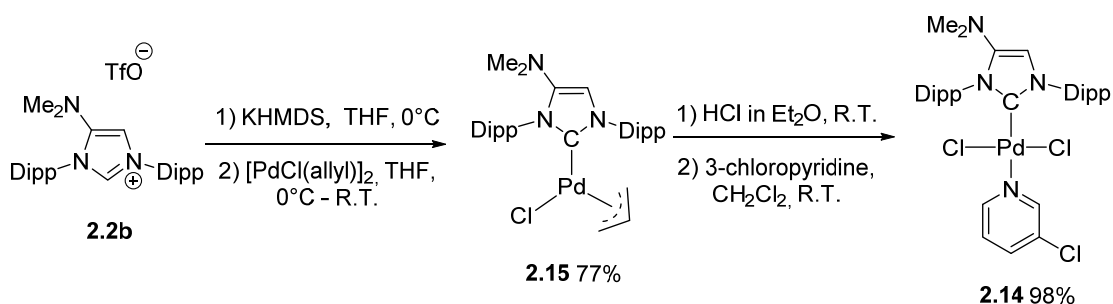
⁸⁷ K. H. Hoi, J. A. Coggan, M. G. Organ, *Chem. Eur. J.* **2013**, *19*, 843.

⁸⁸ For the related complex with IPr, see: (a) M. S. Viciu, R. M. Kissling, E. D. Stevens, S. P. Nolan, *Org. Lett.* **2002**, *4*, 2229; (b) O. Diebolt, P. Braunstein, S. P. Nolan, C. S. J. Cazin, *Chem. Commun.* **2008**, 3190; (c) C. E. Hartmann, S. P. Nolan, C. S. J. Cazin, *Organometallics* **2009**, *28*, 2915; (d) S. Akzinnay, F. Bisaro, C. S. J. Cazin, *Chem. Commun.* **2009**, 5752.



Scheme 2.4.2: Synthesis of palladium complex **2.14** by a transmetalation route.

Alternatively, by adding dimer palladium precursor $[\text{Pd}(\text{allyl})\text{Cl}]_2$ to a THF solution of the free carbene $\text{IPr}^{\text{NMe}_2}$ generated by deprotonation of **2.2b** with a slight excess of KHMDS at 0 °C, the $[\text{Pd}(\text{IPr}^{\text{NMe}_2})(\text{allyl})\text{Cl}]$ (**2.15**) complex could be obtained as a white powder after filtration through Al_2O_3 . **2.15** was then protonated by HCl solution in Et_2O at room temperature, which induced the precipitation of the same dimer $[\text{Pd}(\text{IPr}^{\text{NMe}_2})(\mu\text{-Cl})\text{Cl}]_2$ as before. Again, the latter was not isolated but in-situ reacted with an excess of 3-chloropyridine in CH_2Cl_2 to yield **2.14** in 98% yield (Scheme 2.4.3).



Scheme 2.4.3: Synthesis of palladium complex **2.14** by *in-situ* generation of the free NHC.

Complex **2.14** was fully characterized by spectroscopic and analytical methods. The ^1H NMR spectrum is depicted in the Figure 2.4.1. Noteworthy, the disappearance of the signal of the imidazolium proton in the ^1H NMR spectrum and the appearance of a signal at $\delta = 149.3$ ppm in the $^{13}\text{C}\{^1\text{H}\}$ NMR spectrum assigned to the carbenic carbon N_2C linked to the palladium center confirmed the formation of the complex. The number of signals for the protons of the Dipp groups in ^1H NMR spectrum of **2.14** is consistent with an apparent C_s -symmetry of the molecule in solution. As an example, the 24 protons of the methyl groups of the isopropyl groups resonate under 4 doublets, each integrating for 6 protons.

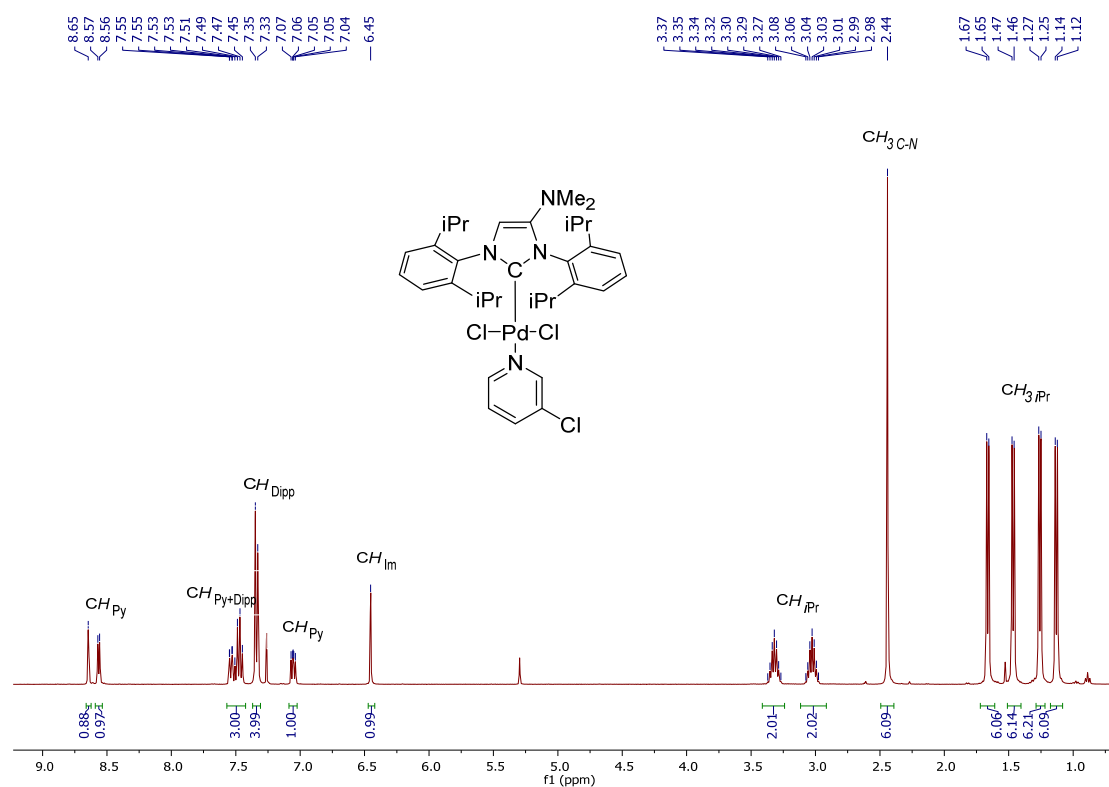


Figure 2.4.1: ^1H NMR spectrum of palladium complex **2.14** (CDCl_3 , 400 MHz).

Single crystals of **2.14** were grown by diffusion of pentane to a concentrated solution of **2.14** in CH_2Cl_2 , and its molecular structure is presented in the Figure 2.4.2. The coordination geometry around the Pd center is square-planar, as expected for a d^8 palladium(II) complex. The Pd1-C1 bond length of 1.9749(15) Å is similar to the one in the **IPr** analogue [$\text{Pd-C}_{\text{carb}}$ = 1.969(3) Å].⁷² The Pd1-N4 bond distance [2.1038(14) Å] is shorter than that of the PEPPSI-Pd-IPr analogue [2.137(2) Å]. As in the structure of the corresponding imidazolium precursor **2.2b**, the N2-C3 bond is longer than N1-C2 bond.

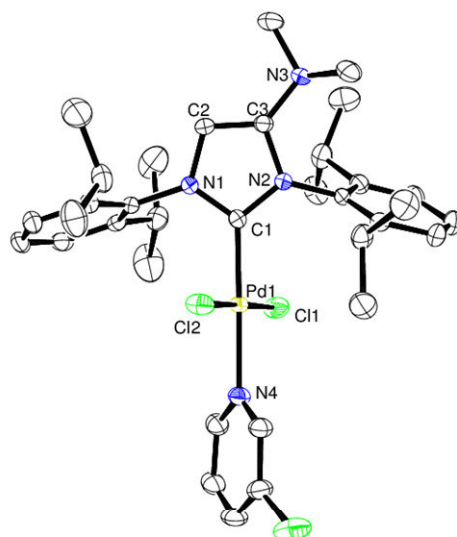
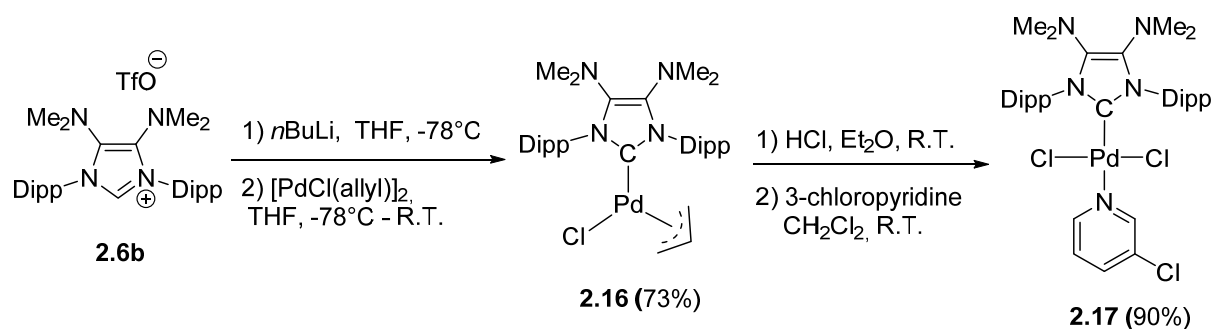


Figure 2.4.2: Molecular structure of palladium complex **2.14** (Ellipsoids drawn at 30% probability level). Hydrogen atoms and solvent molecules removed for clarity.

Bond length (Å)		Angles (deg)	
Pd1-C1	1.9749(15)	N1-C1-N2	105.43(13)
Pd1-N4	2.1038(14)	C1-Pd1-Cl1	93.53(5)
C1-N1	1.345(2)	C1-Pd1-Cl2	88.14(5)
C1-N2	1.3652(19)	C1-Pd1-N4	177.90(6)
C2-C3	1.348(2)	N2-C1-Pd1-Cl1	70.66
C3-N3	1.383(2)		
N1-C2	1.397(2)		
N2-C3	1.4052(19)		

Table 2.4.1: Selected bond lengths (Å) and angles (deg) in **2.14**.

Concerning the synthesis of the $[\text{Pd}(\text{IPr}^{(\text{NMe}_2)_2})(3\text{-ClPy})\text{Cl}_2]$ complex (**2.17**), the transmetalation route through the silver complex $\text{Ag}(\text{IPr}^{(\text{NMe}_2)_2})\text{Cl}$ failed at the stage of the transmetalation of $\text{IPr}^{(\text{NMe}_2)_2}$ from Ag(I) to the Pd(II) centers. This lack of reactivity of the silver complex could be explained by the stronger Ag-NHC bond in this complex due to the strong electron donation of the $\text{IPr}^{(\text{NMe}_2)_2}$ ligand. Fortunately, the free carbene $\text{IPr}^{(\text{NMe}_2)_2}$ could be generated by deprotonation of imidazolium salt **2.6b** in the presence of *n*BuLi in THF at -78 °C, and was further trapped by $[\text{Pd}(\text{allyl})\text{Cl}]_2$ affording the complex $[\text{Pd}(\text{IPr}^{(\text{NMe}_2)_2})(\text{allyl})\text{Cl}]$ (**2.16**) with a yield of 73% after purification by flash chromatography on neutral alumina. **2.16** was further protonated with HCl to give the dimer $[\text{Pd}(\text{IPr}^{(\text{NMe}_2)_2})(\mu\text{-Cl})\text{Cl}]_2$, which afforded the final palladium complex Pd-PEPPSI- $\text{IPr}^{(\text{NMe}_2)_2}$ (**2.17**) as a bright yellow powder in 90% yield.



Scheme 2.4.4: Synthesis of palladium complex Pd-PEPPSI-IPr^{(NMe₂)₂} (**2.17**).

The complex **2.17** was characterized by all spectroscopic and analytical methods and the ¹H NMR spectrum is displayed in the Figure 2.4.3. Obviously, as ligand IPr^{(NMe₂)₂} is more symmetric than IPr^{NMe₂}, the NMR spectra of complex **2.17** are simpler and are in accordance with an apparent *D*_{2h} symmetry of the molecule in solution. Molecular structure of **2.17** was confirmed by an X-Ray diffraction analysis (Figure 2.4.2). The Pd1-C1 bond length is 1.979(3) Å which is similar to that in the mono-amino analogue **2.14**. Noteworthy, the two Dipp substituents are significantly twisted compared to orthogonality to the imidazolyl ring, and it implies that one isopropyl group on each Dipp is brought closer to the palladium center. This specific arrangement could be the results of the accommodation of the steric constraint between the two NMe₂ groups on the backbone and the very bulky Dipp groups, as illustrated by the view along the C1-Pd1 bond from the top of the molecule in the “spacefill” mode.

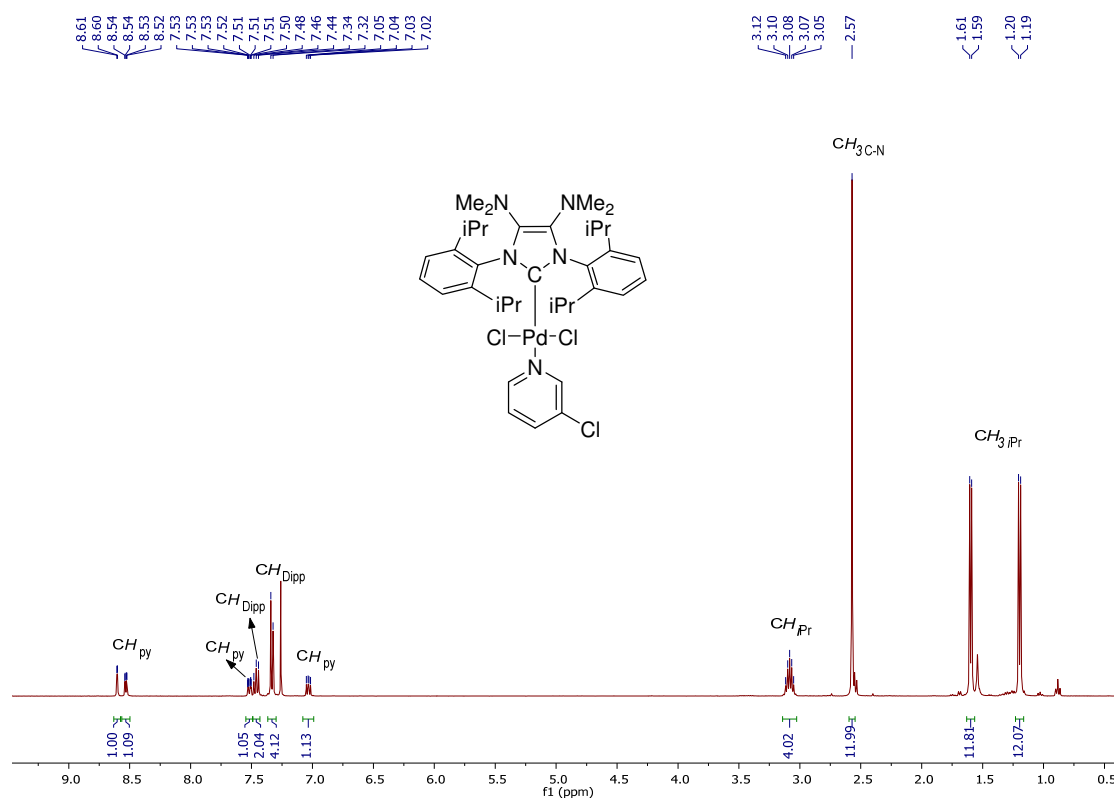


Figure 2.4.3: ^1H NMR spectrum of palladium complex **2.17** (CDCl_3 , 400 MHz).

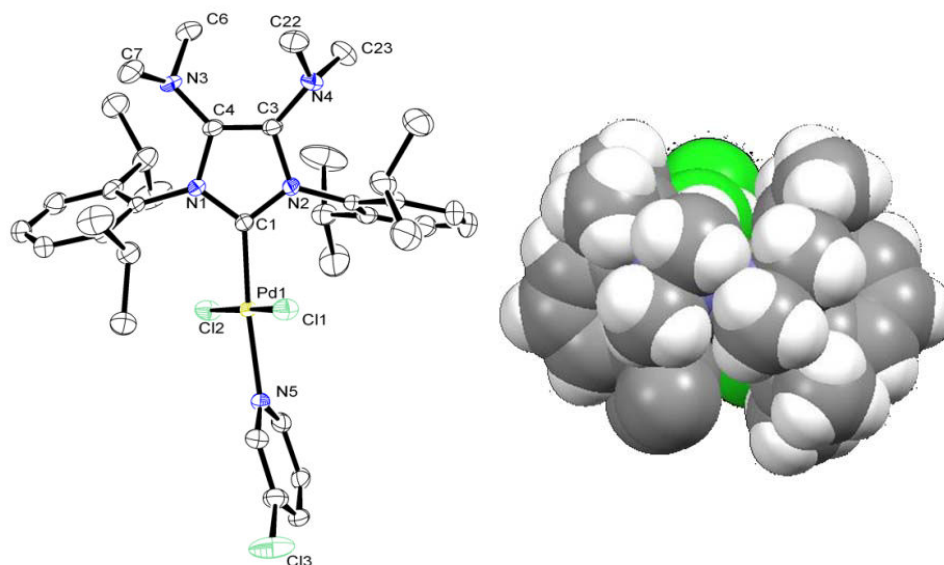


Figure 2.4.4: Left: Molecular structure of palladium complex **2.17** (molecule A, ellipsoids drawn at 30% probability level). Hydrogen atoms and solvent molecules removed for clarity. Right: view of **2.17** along the top of the molecule and along the C1-Pd1 bond.

Bond lengths (Å)		Angles (deg)	
Pd1-C1	1.979(3)	N2-C1-N1	106.1(3)
Pd1-N5	2.125(3)	C1-Pd1-Cl1	87.09(9)
C1-N1	1.349(4)	C1-Pd1-Cl2	93.35(9)
C1-N2	1.357(4)	C1-Pd1-N5	174.65(12)
C3-C4	1.350(5)	N2-C1-Pd1-Cl1	60.28
C3-N4	1.396(4)		
C4-N3	1.388(4)		
N1-C4	1.417(4)		
N2-C3	1.414(4)		

Table 2.4.2: Selected bond lengths (Å) and angles (deg) in **2.17**.

As another important parameter for NHC ligands, the steric properties of these two NHC ligands were calculated using the percent buried volume ($\%V_{\text{bur}}$) based on the crystal structures of **2.14** and **2.17**. The results are listed in Table 2.4.3. to the original PEPPSI-Pd-IPr complex (**1.1**) exhibiting a $\%V_{\text{bur}}$ value of 34.3%,⁸⁹ the stepwise incorporation of NMe_2 groups leads to a calculated $\%V_{\text{bur}}$ of 39.5% for $\text{IPr}^{\text{NMe}_2}$ ligand in **2.14**, and of 39.7% and 40.0% for $\text{IPr}^{(\text{NMe}_2)_2}$ in **2.17**.⁹⁰ These values reveal that the global effect of the skeleton decoration by dimethylamino groups is not only purely electronic as we expected at the beginning, but also involves a significant steric component. Apparently, from the data of $\%V_{\text{bur}}$ itself, it is shown

⁸⁹ Crystal data from the CCDC 761247 structure.

⁹⁰ The two values being associated with the two crystallographically independent molecular units of **2.17** in the lattice

that the steric issue has reached a maximum after introduction of the first NMe₂, and the %V_{bur} slightly increases 0.4 % after grafting the second NMe₂. But we should keep in mind that the crystal structure data collected by X-Ray diffraction represent only one frozen conformation of a molecule, and great care should be taken to avoid to extrapolate these values to the real behavior and steric constrain of the ligands in solution. In particular, the conformational flexibility is not taken into account by this measure.

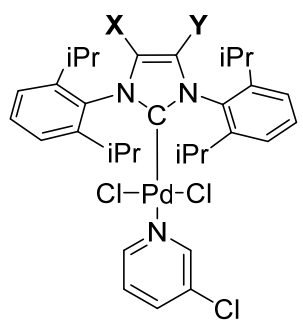
 <p>Pd(IPr^{XY})(3-ClPy)Cl₂</p>	Pd(IPr^{XY})(3-ClPy)Cl₂	
	NHC	buried volume(%V _{bur})
	IPr	34.3%
	IPr^{NMe₂}	39.5%
	IPr^{(NMe₂)₂}	39.7%, 40.0%

Table 2.4.3: Percent buried volume (%V_{bur}) of corresponding NHCs.

4.3. Catalytic properties in Buchwald-Hartwig amination with KO^tBu

The catalytic efficiencies of the PEPPSI-type pre-catalysts **2.14** and **2.17** were evaluated in Buchwald-Hartwig amination with respect to this of the reference PEPPSI-Pd-IPr complex **1.1**. As a first test, the room temperature (25°C) amination of 4-chloroanisole by morpholine was chosen as a model reaction, and the reaction conditions were fixed as follows: catalyst loading of 2.0 mol%, KO^tBu as base and DME as solvent. These conditions are actually the optimized ones that Organ and co-workers reported in their previous work.⁷³ Kinetic experiments were carried out with the three pre-catalysts **2.14**, **2.17**, **1.1**, and the kinetic curves are depicted in Figure 2.4.5. The conversions were determined by GC analysis against a calibrated internal standard (dodecane) by taking out a small aliquot of the solution under a flow of N₂ at regular intervals. The complex **2.17** was found to be by far the most active among the three pre-catalysts giving a full conversion within two hours, meanwhile the 4-chloroanisole was converted only in 43 % and 25 % in the cases of **2.14** and **1.1** respectively. When the reaction time was prolonged to 6 hours, the conversion reached 57% and 39% respectively for complexes **2.14** and **1.1** (Figure 2.4.5). Obviously, it appears that a clear incremental booster effect of the two amino groups on the backbone of NHC positively correlated with the catalytic performances of the corresponding complexes in the model

amination. With the result obtained here well matches the initially established assumption of the project.

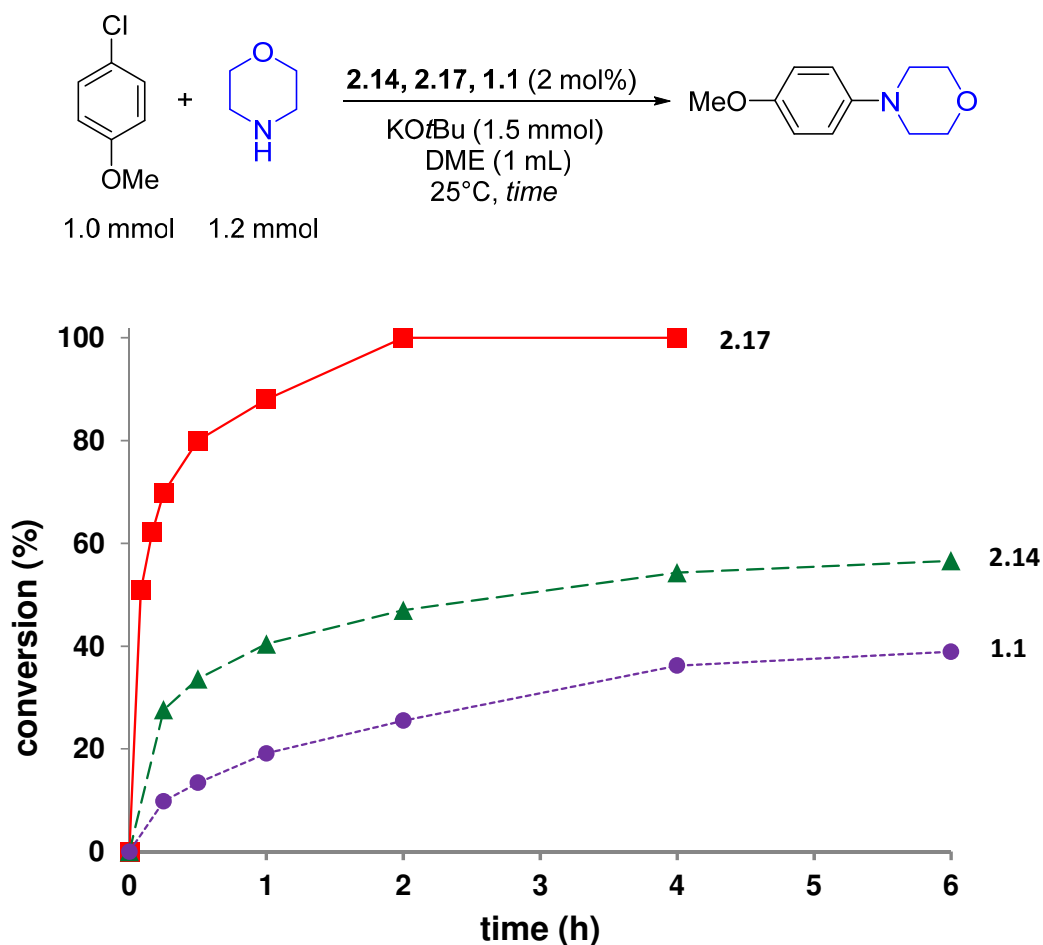


Figure 2.4.5: Parallel kinetic amination using **2.14**, **2.17** and **1.1** as pre-catalysts.

The above results prompted us to evaluate **2.17** in the room-temperature coupling of a variety of (hetero)aryl chlorides with aliphatic and aryl amines (Table 2.4.4). Under the standard conditions, the coupling product 4-(4-methoxyphenyl)morpholine **2.18a** was isolated in 92 % yield after 2 hours while the yields were 27% and 11% respectively when using **2.14** and **1.1** as pre-catalysts respectively. Moreover, the deactivated 4-(pyrrol-1-yl)- and 4-(dimethylamino)phenyl chlorides were efficiently coupled with morpholine using 2 mol% of **2.17** to give products **2.18b** and **2.18c** in excellent yields, whereas the use of catalysts **2.14** and **1.1** only led to modest conversions and yields under identical conditions. The reaction is unaffected by the nature of the amine partners as morpholine, pyrrolidine (**2.18d**), piperidine (**2.18i**), as well as *N*-methylaniline which are less nucleophilic than morpholine (**2.18h-j**), and the more crowded 2,6-dimethylaniline (**2.18g**) coupled efficiently. The catalytic efficiency

was found to be only slightly affected by the steric hindrance of one of the coupling partners, since a longer time or a slightly higher temperature were required to obtain **2.18f** and **2.18g**. Gratifyingly, catalyst **2.17** was also found to exhibit an excellent activity in the case of heteroaryl chlorides such as 2- and 3-chloropyridines (**2.18j-m**) and even for the quite difficult 3-chlorothiophene (**2.18n**, at 80 °C), for which catalysts **2.14** and **1.1** proved to be totally inefficient.

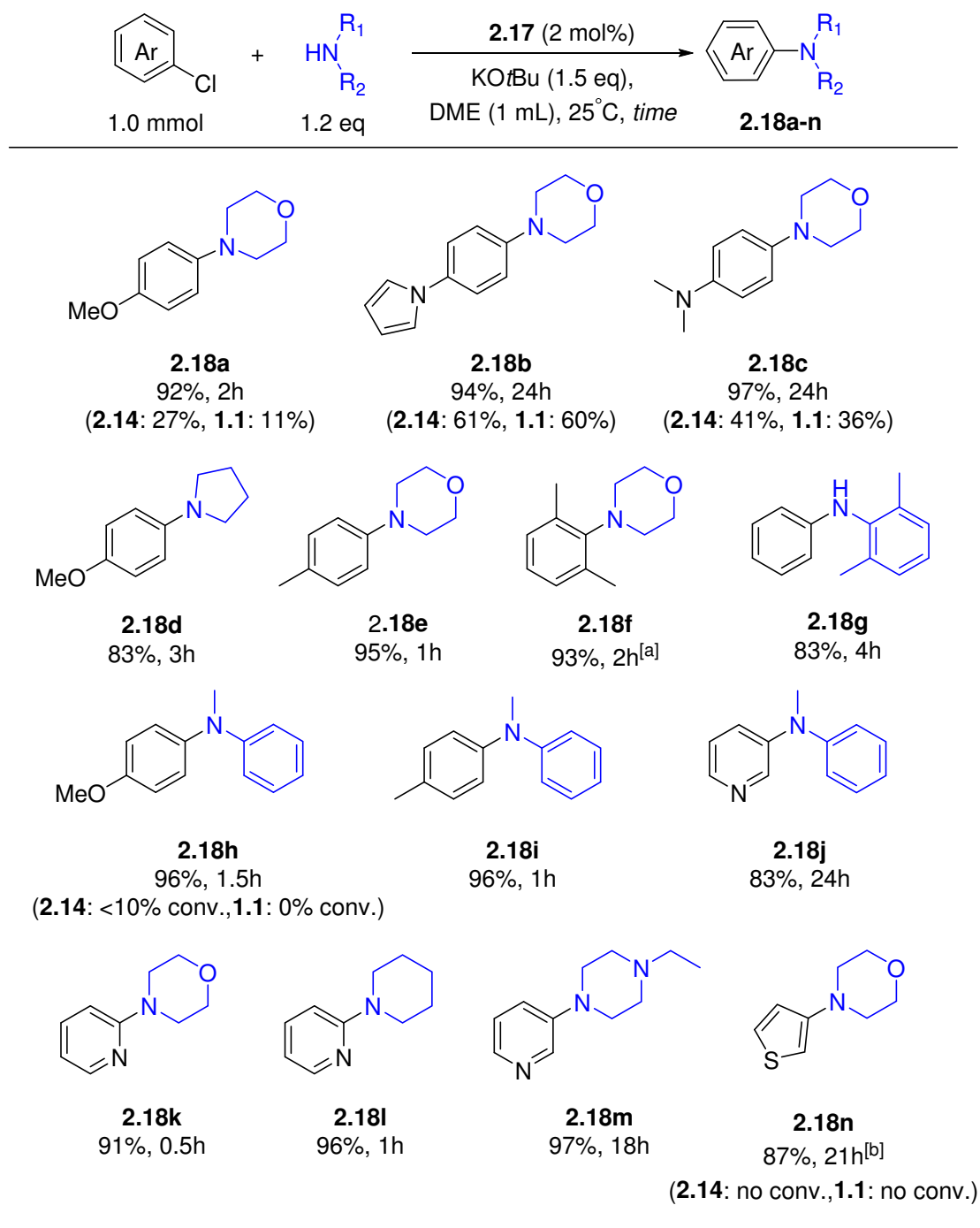


Table 2.4.4: Scope of the room-temperature Buchwald-Hartwig amination catalyzed by **2.17**. Yields refer to the average yields of isolated product from two runs after column chromatography. [a] at 50°C; [b] at 80°C.

The high efficiency of **2.17** shown in the above amination with certain challenging substrates inspired us to further evaluate it under even more difficult conditions, namely at low catalyst loading. These conditions require a high stability from the corresponding catalyst for a good completion. In this context, the scope of the Buchwald-Hartwig amination was then explored, and the catalyst loading of pre-catalyst **2.17** could be reduced to 0.005-0.1 mol% (it depends on the nature of the substrates) in dioxane at 80°C in the presence of KO^tBu (Table 2.4.5). Under identical conditions, a large scope of substrates with regard to (hetero)aryl chlorides and amines were suitable coupling partners resulting in excellent yields of the corresponding products (**2.19a-j**) indicating the high efficiency of **2.17**. Typically, non-activated aryl chlorides and pyridinyl chlorides were successfully coupled with morpholine or *N*-methylaniline (**2.19a-e**) at low catalyst loading (0.005-0.1 mol%) and remarkable turn-over numbers were observed (TON up to 19600 for **2.19e**) which is the highest TON value up to now for NHC-Pd catalysts.⁹¹ Anilines were also found to be suitable coupling partners, as illustrated by a 100% selectivity in the monoarylation of ArNH₂, and a total absence of bisarylation product (**2.19f-j**). Noteworthy, very good yields were obtained for electron-rich aryl chlorides and electron-deficient anilines (**2.19g**, **2.19j**), which are considered as very challenging coupling partners.⁹² These performances place the pre-catalyst **2.17** among the very best NHC-systems for the arylamination reaction,^{73,93} with performances matching those obtained with the Pd/phosphines systems for similar substrates.⁹⁴ The high efficiency of catalyst **2.17** can be reasonably attributed to the enhanced electron-donating ability which mostly enhances the stability of the active palladium species and in part to the increased steric shielding which well protects the Pd(0) center from decomposition – two complementary features known to be beneficial in Pd-catalyzed cross-coupling reactions – of bisamino-carbene compared to its **IPr** reference.

⁹¹ G. Le Duc, S. Meiries, S. P. Nolan, *Organometallics* **2013**, 32, 7547.

⁹² a) K. H. Hoi, S. Çalimsiz, R. D. J. Froese, A. C. Hopkinson, M. G. Organ, *Chem. Eur. J.* **2012**, 18, 145.

⁹³ a) S. Meiries, G. Le Duc, A. Chartoire, A. Collado, K. Speck, K. S. A. Arachchige, A. M. Z. Slawin, S. P. Nolan, *Chem. Eur. J.* **2013**, 19, 17358.

⁹⁴ a) R. J. Lundgren, M. Stradiotto, *Aldrichim. Acta* **2012**, 45, 59; b) R. J. Lundgren, A. Sappong-Kumankumah, M. Stradiotto, *Chem. Eur. J.* **2010**, 16, 1983; c) B. P. Fors, S. L. Buchwald, *J. Am. Chem. Soc.* **2010**, 132, 15914; d) Q. Shen, T. Ogata, J. F. Hartwig, *J. Am. Chem. Soc.* **2008**, 130, 6586.

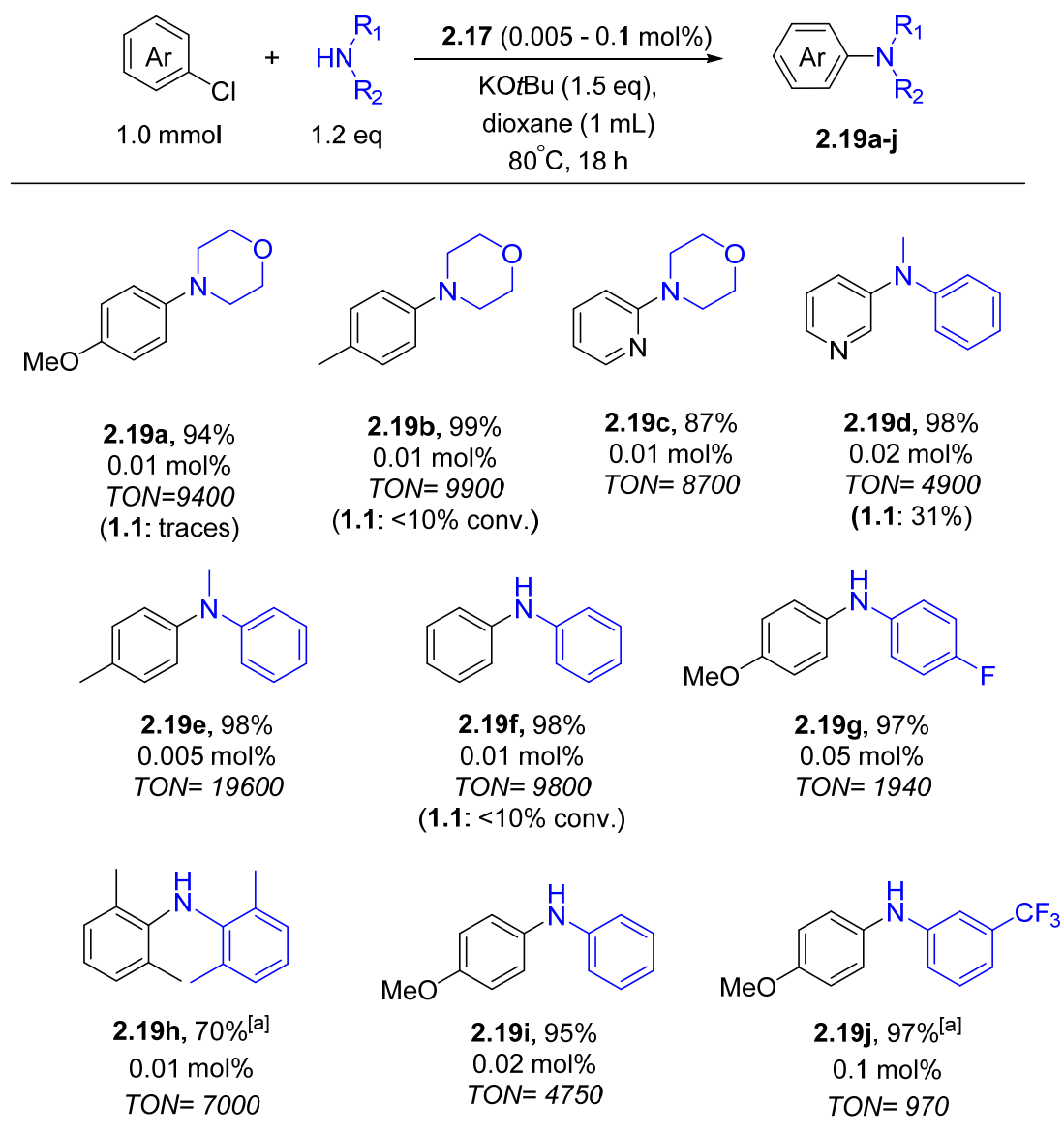


Table 2.4.5.: Scope of the Buchwald-Hartwig amination catalyzed with **2.17** at low catalyst loading, Yields refer to the average yields of isolated product from two runs after column chromatography [a] at 100°C.

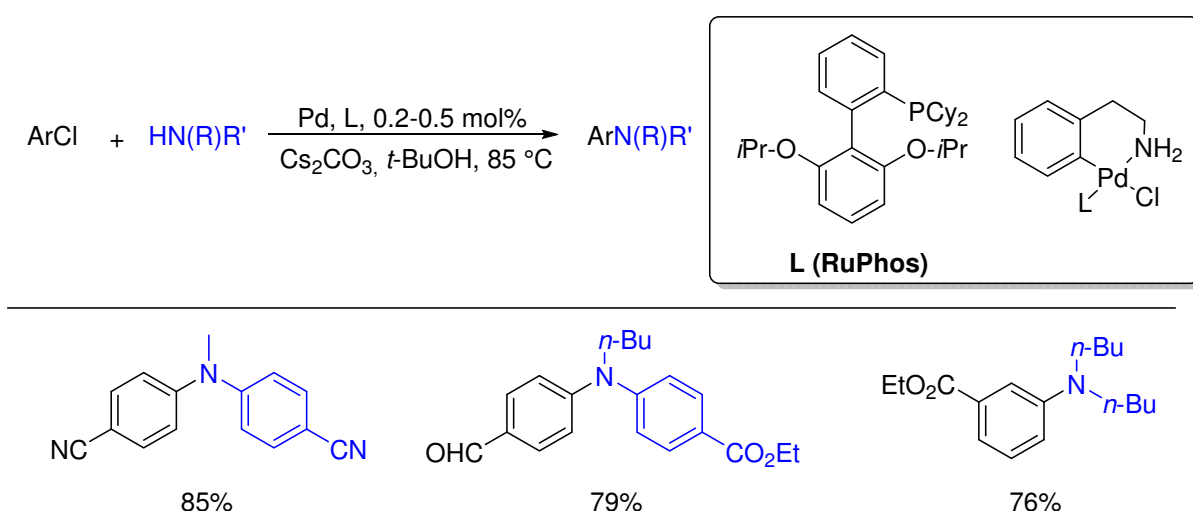
4.4. Catalytic properties in Buchwald-Hartwig amination with Cs_2CO_3

4.4.1. State of the art

In most cases, the bases involved in the Buchwald-Hartwig amination are usually aggressive alkoxide bases such as *tert*-butoxide for an efficient deprotonation of the Pd-coordinated ammonium species in the intermediate **B** (Figure 1.4.1). These strongly basic reaction conditions still severely restrict the applicability of the methodology, due to their incompatibility with base-sensitive functional groups, such as ketones, esters or nitro groups.

To circumvent this problem, the use of milder bases, and in particular of carbonate bases, has been proposed, but the reported examples are quite scarce and are mainly concerning phosphine-based catalysts.

Buchwald and co-workers demonstrated that by the use of catalyst system on the base of RuPhos and amino type palladium pre-catalyst, the amination could be effectively achieved using Cs_2CO_3 as base (Scheme 2.4.5).⁹⁵ Different substrates bearing sensitive functional groups were tolerated under these mildly basic conditions.

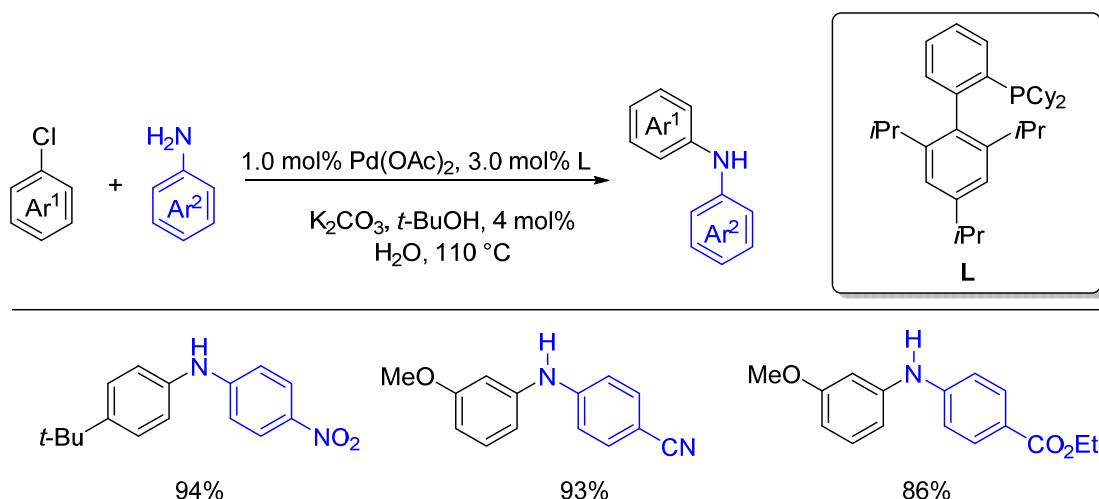


Scheme 2.4.5: Amination using Cs_2CO_3 as mild base employing RuPhos ligand reported by Buchwald.

The same research group also found that, by using a water-mediated catalyst pre-activation, the amination between aryl chlorides and deactivated aniline could be smoothly performed using K_2CO_3 as the base (Scheme 2.4.6).⁹⁶ High yields were obtained for the highly challenging anilines bearing electron deficiency substituent such as ester, cyano and nitro.

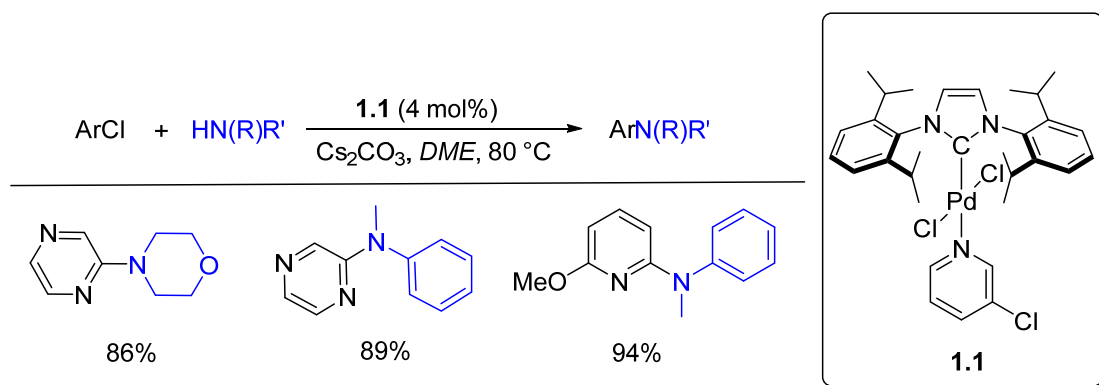
⁹⁵ D. Maiti, B. P. Fors, J. L. Henderson, Y. Nakamura, S. L. Buchwald, *Chem. Sci.* **2011**, 2, 57.

⁹⁶ B. P. Fors, P. Krattiger, E. Strieter, S. L. Buchwald, *Org. Lett.* **2008**, 10, 3505.



Scheme 2.4.6: Amination applying water-mediated pre-activation using K_2CO_3 as base with Xphos ligand reported by Buchwald.

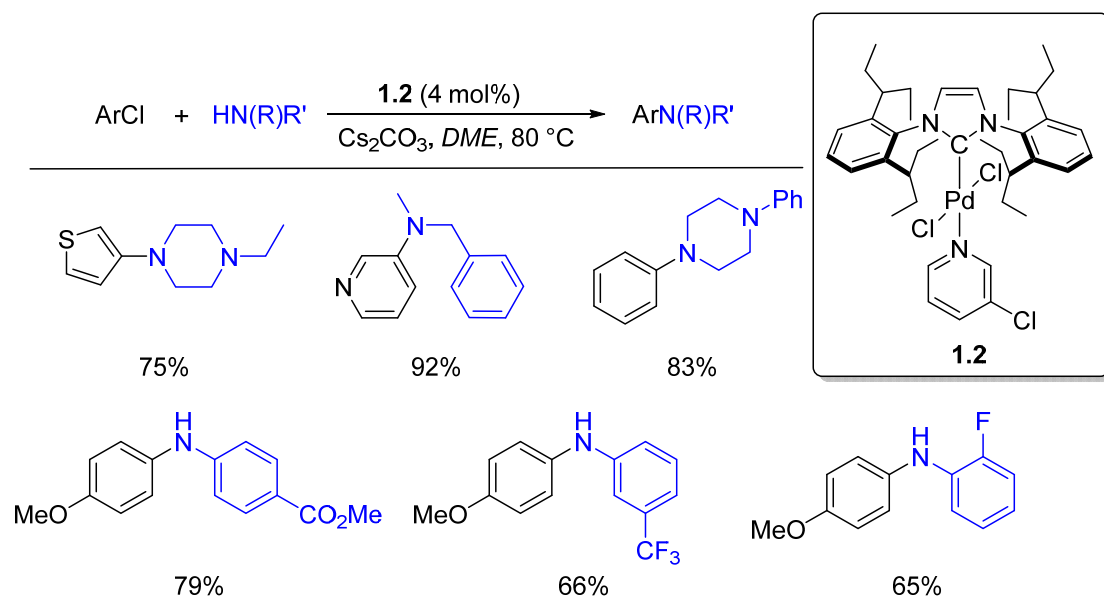
The most impressive breakthrough in this direction using NHC ligands was recently achieved by Organ and co-workers who developed first the PEPPSI-Pd-IPr complex **1.1** which was shown to catalyze the amination of certain heteroaryl chlorides with secondary amines in the presence of Cs_2CO_3 as the base (Scheme 2.4.7).⁹⁷ But the substrate scope of this protocol was only limited to the electron-deficient heteroaryl chlorides in order to facilitate the deprotonation step in the catalytic cycle.



Scheme 2.4.7: Amination containing heteroaryl chlorides as substrates using Cs_2CO_3 as base with PEPPSI-Pd-IPr pre-catalyst **1.1** reported by Organ.

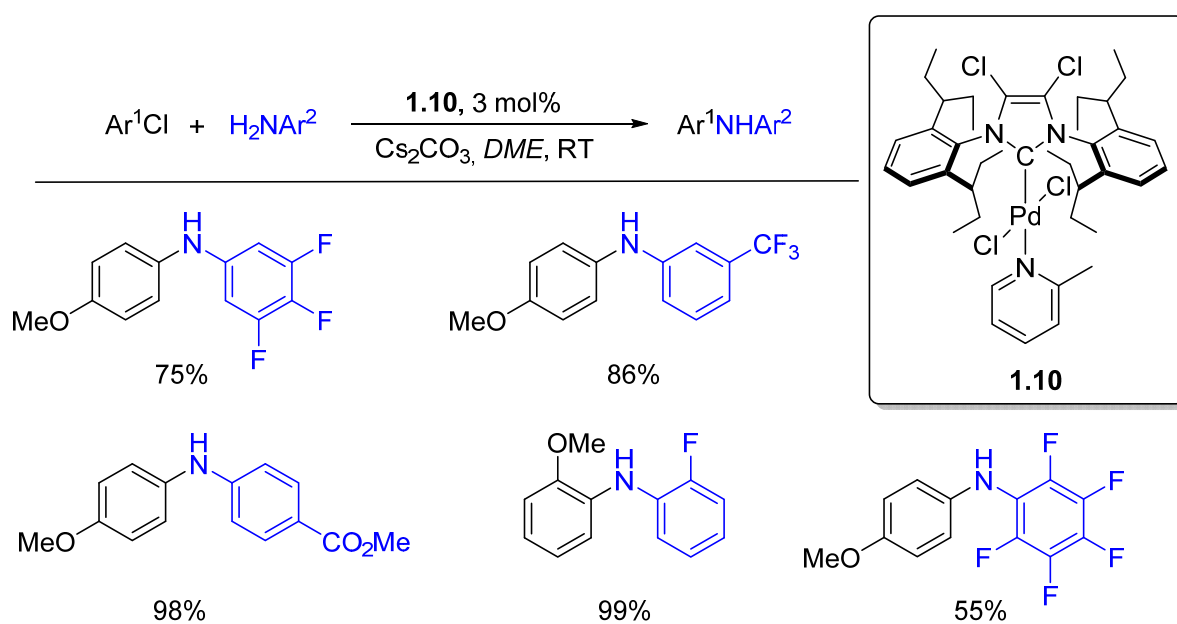
Later, the same group disclosed a second generation pre-catalyst, Pd-PEPPSI-IPent **1.2**, which was shown to greatly outperform pre-catalyst **1.1** in the amination of secondary amines and anilines with a great variety of aryl chlorides (Scheme 2.4.8).⁷⁴ Moderate to high yields were obtained for both electron rich aryl chlorides and also for the electron deficient anilines.

⁹⁷ M. G. Organ, M. Abdel-Hadi, S. Avola, I. Dubovyk, N. Hadei, E. A. B. Kantchev, C. J. O'Brien, M. Sayah, C. Valente, *Chem. Eur. J.* **2008**, *14*, 2443.



Scheme 2.4.8: Amination of aryl chlorides with variety of amines and anilines using Cs_2CO_3 as base using PEPPSI-Pd-IPent pre-catalyst **1.2** reported by Organ.

Finally, even the coupling of weakly nucleophilic anilines with electron-rich aryl chlorides, which represents the most challenging combination of coupling partners, was recently and efficiently achieved by chlorinated **IPent** as pre-catalyst **1.10** using Cs_2CO_3 as mild base even at room temperature.⁹⁸ In this work, they deduced that the observed enhancement of catalyst's performance is independent of the electronic nature of the backbone substituents, and is the result of steric rather than electronic effects.



⁹⁸ M. Pompeo, J. L. Farmer, R. D. J. Froese, M. G. Organ, *Angew. Chem. Int. Ed.* **2014**, 53, 3223.

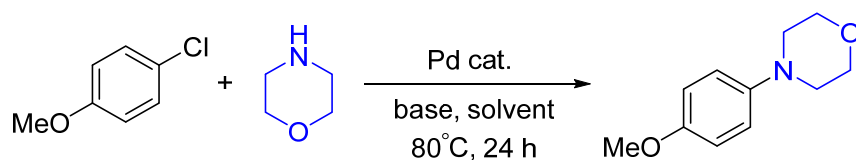
Scheme 2.4.9: The first example of Amination with aryl chlorides and anilines using Cs_2CO_3 catalyzed by PEPPSI-Pd-IPent pre-catalyst **1.10** at room temperature reported by Organ.

Nevertheless, there was no other example using a NHC-palladium pre-catalyst reported to catalyze the BH amination using a mild base. Based on the results obtained at room temperature and at low catalyst loadings, and keeping in mind Organ's conclusion, we were thus prompted to study the catalytic efficiency of our pre-catalysts **2.14** and **2.17** in this benchmark reaction using a mild base.

4.4.2. Optimization of the reaction

In a first comparative evaluation of the pre-catalysts, the experimental conditions required to perform the Buchwald-Hartwig amination in the presence of a mild base like cesium carbonate were taken from the earlier recent report by Organ, using the reaction between 4-chloroanisole and morpholine as a standard model (Table 2.4.6).

In a first catalytic test based on 4 mol% of Organ's pre-catalyst Pd-PEPPSI-IPr **1.1** (Entry 1), we were able to reproduce his previously reported result corresponding to 15% conversion after 24 h.^{21a} Under the same conditions, pre-catalyst **2.14** (Entry 2) led to an improved conversion rate of 75%, whereas 100% conversion was reached with the pre-catalyst **2.17** within the same duration (Entry 3). Gratifyingly, in the latter case, it was even possible to reduce the catalyst loading down to 1 mol% (Entry 5), in which 4 mol% of the **IPent** derivative pre-catalyst **1.2** was necessary to obtain a full conversion.^{74a} The lower limit of catalyst's efficiency was reached with 0.5 mol% of **2.17** (Entry 6), with a slight erosion of the conversion to 80%. In line with our previous results, these extended experimental observations provided convincing evidence that skeleton decoration of the heterocycle by two dimethylamino groups imparts high stability to the catalyst, whose lifetime then becomes much longer than that of the original unmodified complex Pd-PEPPSI-IPr (**1.1**) and might also than the **IPent** derivative **1.2** in this coupling amination. Further experiments focusing exclusively on the activity of **2.17**, indicated that DME is a better solvent than dioxane or toluene, and that Cs^+ is a much better counter-cation for the base than K^+ (Entries 7-9). Such a preference may be either due to the bigger size of Cs^+ , favoring a more efficient stabilization of the large anionic complex at intermediate stage, or to the higher solubility of its salts in the selected organic solvent. Reducing the quantity of base resulted in a lower conversion (Entries 10).



Entry	Pd cat. (mol%)	Solvent	Base	Conv. (%) ^[b]
1	1.1 (4)	DME	Cs ₂ CO ₃	15
2	2.14 (4)	DME	Cs ₂ CO ₃	75
3	2.17 (4)	DME	Cs ₂ CO ₃	100
4	2.17 (2)	DME	Cs ₂ CO ₃	100
5	2.17 (1)	DME	Cs ₂ CO ₃	100
6	2.17 (0.5)	DME	Cs ₂ CO ₃	80
7	2.17 (1)	Dioxane	Cs ₂ CO ₃	92
8	2.17 (1)	Toluene	Cs ₂ CO ₃	90
9	2.17 (1)	DME	K ₂ CO ₃	45
10	2.17 (1)	DME	Cs ₂ CO ₃	80

Table 2.4.6: Optimization of the Pd-catalyzed amination reaction in the presence of carbonate bases.^[a]

^[a] Reaction conditions: 4-chloroanisole (0.5 mmol), amine (0.75 mmol), base (1.5 mmol), solvent (0.5 mL), 80 °C. ^[b] Conversion rates were determined by GC based on 4-chloroanisole with dodecane as internal standard. ^[c] 1.5 equiv. of Cs₂CO₃ (0.75 mmol) was used.

4.4.3. Scope of the substrates

The optimized conditions described above were subsequently used as standard conditions in further attempts to extend the application of **2.17** to a variety of (hetero)aryl chlorides and secondary aliphatic amines as reaction partners (Table 2.4.7). We found that aryl chlorides bearing either electron-donating (OMe or Me) or electron-withdrawing substituents (CN, NO₂, or Ac) in the *para* position could be coupled with morpholine to give the desired products (i.e., **2.20a–2.20f**) in excellent yields. In the most favorable cases of aryl chlorides bearing electron-withdrawing substituents, even a drastic reduction of the catalyst loading down to 0.2 mol% did not affect the high yields of the resulting coupling products (i.e., **2.20d** and **2.20e**). This indicates that further optimization of the reaction time might be possible in such favorable cases. A good tolerance of steric hindrance in the aryl chloride component was noted in the coupling of 2-chlorotoluene with morpholine, which proceeded cleanly to give **2.20g**. The system was also found to be very efficient for the amination of heteroaryl chlorides such as 2-chloropyridine and 3-chloropyridine, which gave high yields of **2.20h** and **2.20i**, respectively. Impressively, even 3-chlorothiophene, which is considered to be quite a

challenging coupling partner, was also successfully coupled with morpholine to give **2.20j** in 84% yield.

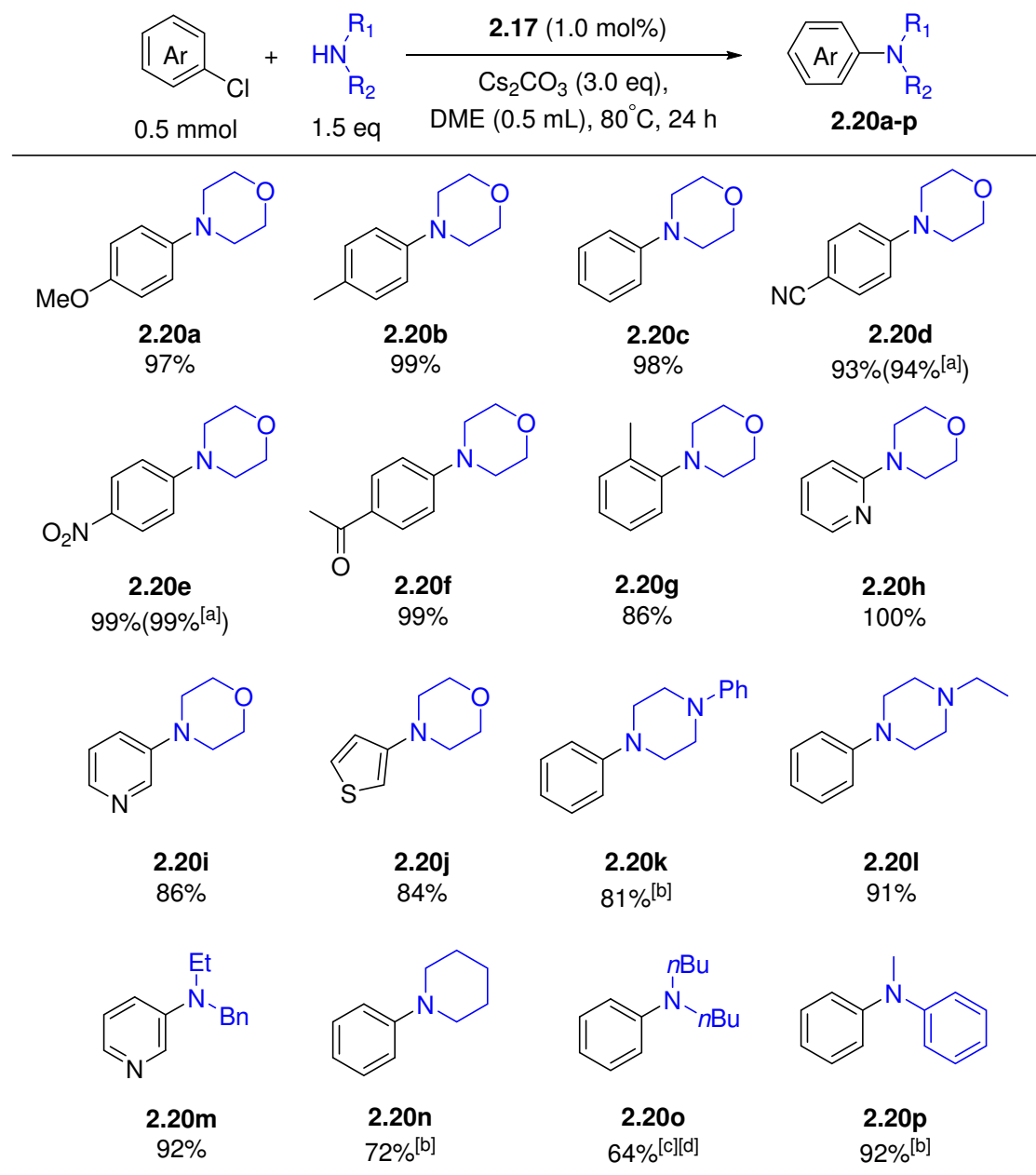
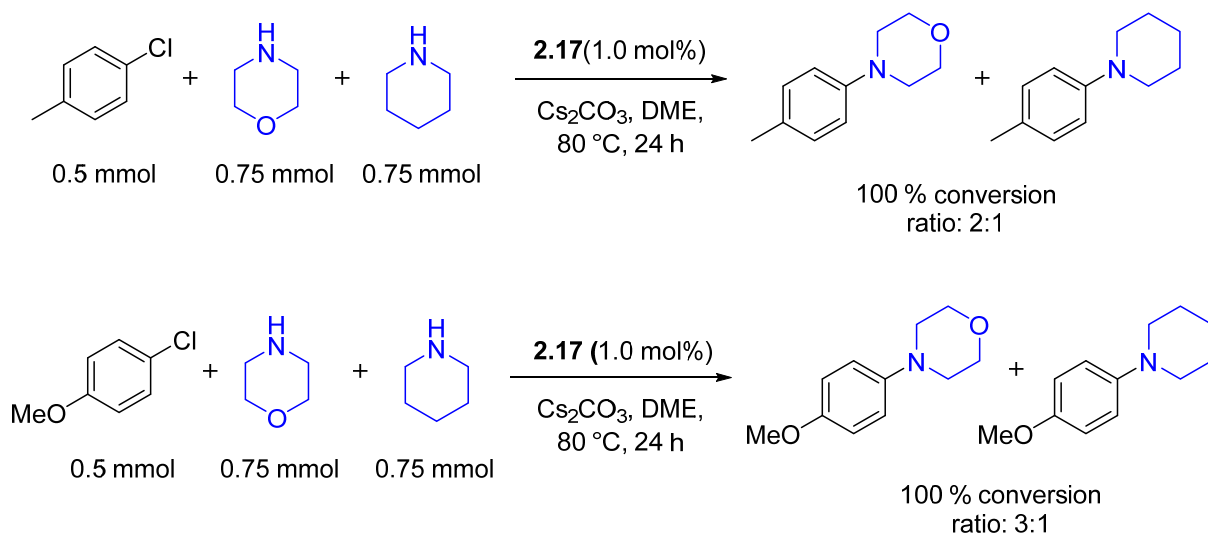


Table 2.4.7: Scope of the Buchwald-Hartwig amination with Cs₂CO₃ catalysed by **2.17**. Yields refer to the average yields of isolated product from two runs after column chromatography. [a] 0.2 mol% of **2.17**; [b] 2.0 mol% of **2.17**; [c] 4.0 mol% of **2.17**; [d] 100 °C in dioxane.

In further catalytic experiments, whose results are displayed in the lower part of Table 2.4.7, we investigated the coupling of aryl chlorides such as chlorobenzene with a series of amines more basic than morpholine ($pK_a = 8.36$), for which the deprotonation step is more difficult. Gratifyingly, *N*-phenylpiperazine ($pK_a = 8.8$) could be introduced as a coupling partner to give **2.20k** in a satisfactory 81% yield. It was also still possible to activate

piperidine, a strongly basic amine ($pK_a = 11.22$), but in that case, it was necessary to increase the amount of pre-catalyst to 2.0 mol% to obtain **2.20n** in 72% yield. The catalytic system also proved efficient for the introduction of acyclic dialkylamines as coupling partners (see the production of **2.20m** and **2.20o**). Dibutylamine, a highly challenging partner with both a high basicity and steric congestion, was successfully activated for the first time by a Pd-NHC catalyst under slightly modified standard conditions using a higher catalyst loading and higher temperature to produce **2.20o** in a reasonable 64% yield. Finally, to our delight, *N*-methylaniline, regarded as a much less nucleophilic amine, could be activated to produce **2.20p** in an impressive 92% yield. Taken together, these representative results establish the high efficiency of pre-catalyst **2.17**, whose performance can be seen to match and even sometimes surpass those of **IPent** derivative **1.2**. In a previous mechanistic investigation by Organ on the catalysts Pd-PEPPSI-IPr and Pd-PEPPSI-IPent,⁹⁸ it was proposed that the pK_a of the palladium(II)-amine species of type **B** (Figure 1.4.1) generated upon coordination of the amine might not only depend on the basicity of the amine, but that it might also be influenced by the donor properties of its coupling partner, namely, the aryl group in the adjacent position in the metal's coordination sphere. In order to corroborate such a hypothesis in the case of our modified pre-catalyst, two sets of parallel catalytic runs were conducted with two aryl chlorides showing different donor properties, namely, 4-chlorotoluene and 4-chloroanisole. In each experiment, 1.0 equiv. of the aryl chlorides together with a mixture of 1.5 equiv. of morpholine and 1.5 equiv. of piperidine was subjected to the reaction conditions. The first experiment, carried out with 4-chlorotoluene, gave a 2:1 ratio of *N*-(toluen-4-yl)morpholine and *N*-(toluen-4-yl)piperidine indicating that a coupling with a less basic amine was more favorable, whereas the second experiment (with 4-chloroanisole) gave a 3:1 ratio of *N*-(4-methoxyphenyl)morpholine and *N*-(4-methoxyphenyl)piperidine (Scheme 2.4.10). These results combined together are consistent with the hypothesis that variations in the electron-donating properties of the aryl group derived from the aryl chloride may influence the rate of deprotonation of the ammonium species, which is considered to be rate determining in this case.^{98a,99}

⁹⁹ C. Meyers, B. U. W. Maes, K. T. J. Loones, G. Bal, G. L. F. Lemi re, R. A. Dommissse, *J. Org. Chem.* **2004**, *69*, 6010.



Scheme 2.4.10: Competitive amination experiments of 4-chloroanisole and 4-chlorotoluene with morpholine and piperidine.

With the above optimized results in hand, we were encouraged to examine the scope of complex **2.17** in a series of even more challenging amination reactions using anilines as substrates exhibiting a much lower nucleophilicity than alkyl amines (Table 2.4.8). The coupling between aryl chlorides (indifferently incorporating electron rich or electron poor substituents) with various anilines proceeded smoothly to afford the mono-arylamination products in excellent yields. Nevertheless, in the most difficult cases of aryl chlorides bearing an electron-donating substituent like methoxy or methyl in *para*-position, it was necessary to increase the catalyst loading up to 3.0 mol% and 2.0 mol% in order to get almost quantitative production of the corresponding amines **2.21a** and **2.21b** respectively. The *ortho*-methyl substituted aryl chlorides still afforded an excellent yield of the coupling product **2.21h**. Significantly, aryl chlorides bearing sensitive *para*-substituents, such as cyanide or acetyl, were tolerated under these standard conditions, and, using a low catalyst loading of 1.0 mol%, it was even possible to achieve the coupling between the unprotected 4-chlorobenzaldehyde and aniline to produce **2.21g** in 89% yield.

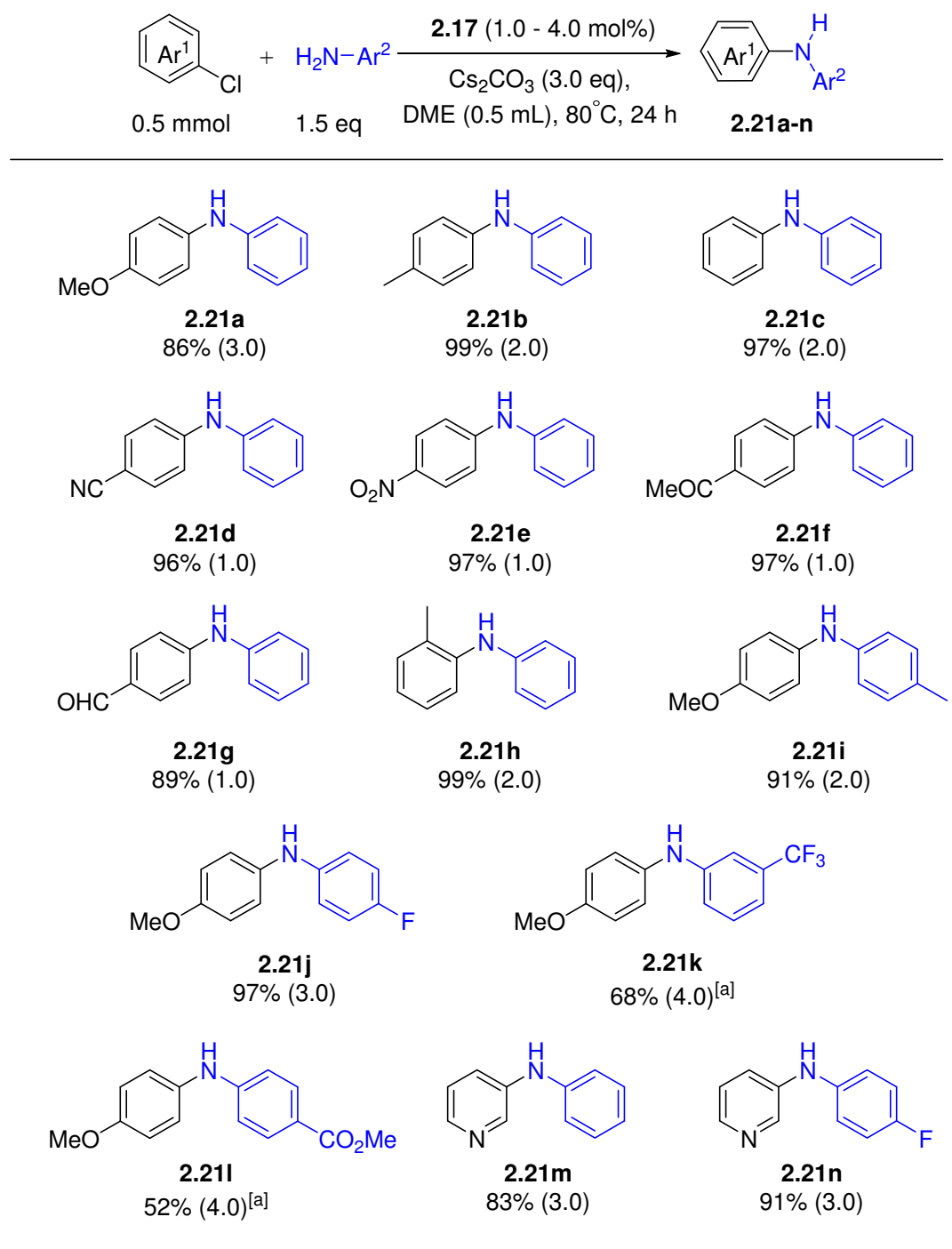


Table 2.4.8: Scope of the Buchwald-Hartwig amination with aniline derivatives catalyzed by **2.17**. Reaction conditions: ArCl (0.5 mmol), aniline (0.75 mmol), **2.17** (1.0-4.0 mol%, specified in parentheses), Cs₂CO₃ (1.5 mmol), DME (0.5 mL), 80 °C, 24 h. Yields refer to the average yields of isolated product from two runs after column chromatography. ^[a] 100 °C in dioxane.

Turning our attention to the coupling of electron-rich aryl chlorides with electron-poor anilines, previously identified as one of the most challenging combinations in BHA, we were pleased to observe that 4-chloroanisole can be efficiently coupled with 4-fluoroaniline and 3-trifluoromethylaniline in the presence of the pre-catalyst **2.17** (3.0 mol% and 4.0 mol% respectively) to produce **2.21j** in 97% yield, and **2.21k** in 68% yield (the latter requiring a

higher temperature). A test based on an aniline bearing an ester in *para* position was also conclusive, but required 4.0 mol% of the pre-catalyst **2.17** and a higher temperature of 100 °C to produce **2.21i** in an acceptable 52% yield. In parallel, using 3-chloropyridine as a hetero-aryl chloride in combination with aniline and *para*-fluoroaniline led to **2.21m** and **2.21n** respectively, in excellent yields. By comparing these results with those reported by Organ for the same couplings,^{98b,99} the following qualitative ranking of the supporting NHCs in the Pd-PEPPSI complexes could be drawn: **IPr** << **IPent** ~ **IPr**^{(NMe₂)₂} < **IPent**^{Cl₂} based on the above transformation and led to the conclusion that, starting from the classical **IPr** ligand, decorating the carbenic heterocycle is a viable and complementary strategy to the one consisting in varying the nitrogen-aryl substituents for optimizing catalyst efficiency in BHA.

Finally, we were led to consider the case of primary alkyl amines, which often tend to undergo competitive β-hydride elimination from the corresponding amido-Pd complexes,¹⁰⁰ an undesirable side reaction (ending with the reduction of aryl halides into arenes) which is avoided by using sterically demanding ligands. We were pleased to observe that the pre-catalyst **2.17** is highly active in their transformation (Table 2.4.9). For example, with 2 mol% of **2.17**, the reaction of 2-chlorotoluene or 2,6-dimethylchlorobenzene and octylamine gave 97% and 92% yield of the desired product **2.22a** and **2.22b** respectively. Under the same conditions, *N*-(cyclohexyl)aniline **2.22c**, was obtained with a slightly reduced, but still satisfactory yield of 74%. Reactions of 4-chloroanisole and 3-chloropyridine with octylamine also proceeded to completion, but appeared to be less selective, affording both mono and bis-arylation products. Finally benzylamine was also incorporated, and found to afford two products. The ratio of the mono and bisarylation products was found to depend both on the nature of aryl chlorides and amines.

¹⁰⁰ J. P. Wolfe, S. Wagaw, S. L. Buchwald, *J. Am. Chem. Soc.* **1996**, *118*, 7215.

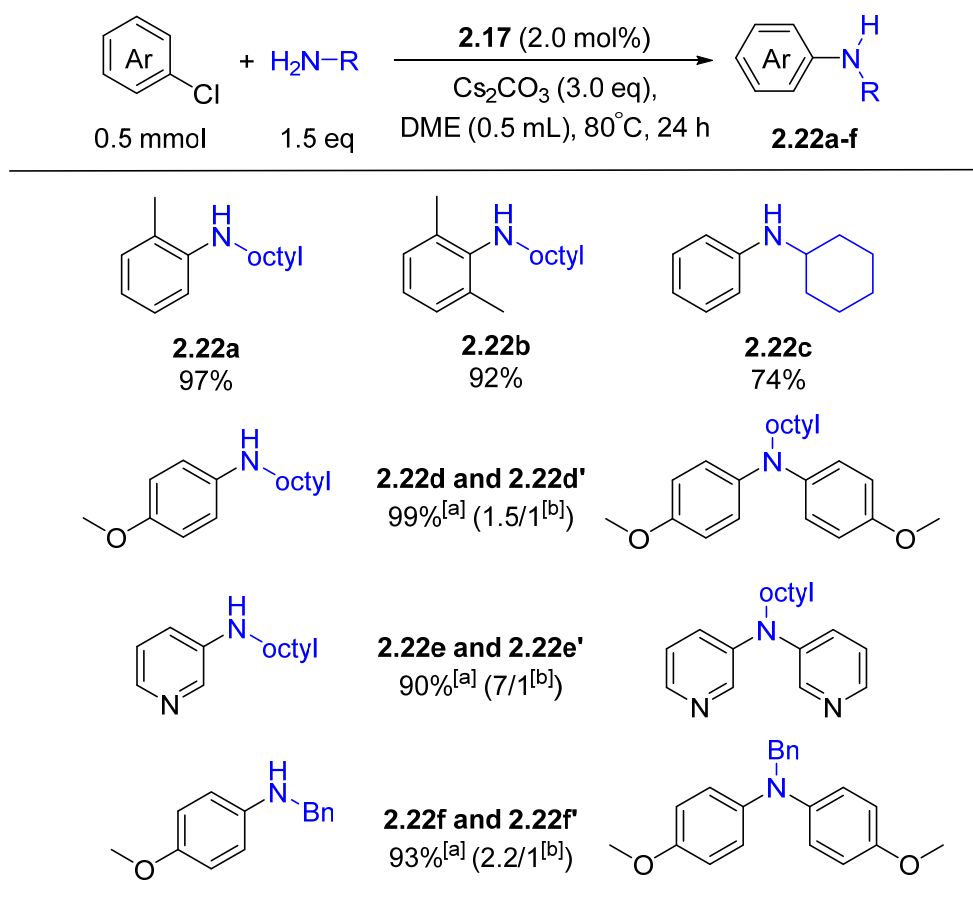


Table 2.4.9: Scope of the Buchwald-Hartwig amination with primary amine derivatives catalyzed by pre-catalyst **2.17**. Reaction conditions: ArCl (0.5 mmol), amine (0.75 mmol), **2.17** (2.0 mol%), Cs_2CO_3 (1.5 mmol), DME (0.5 mL), 80°C, 24 h. Yields refer to the average yields of isolated product from two runs after column chromatography. ^[a] The yield was based on the aryl chloride. ^[b] Ratio between mono and bis-arylation product.

4. Conclusion

In this chapter, we have presented the synthesis of the imidazolium salts (**IAr**^{NMe₂})-HOTf and (**IAr**^{(NMe₂)₂})-HOTf as the precursors of 4-(dimethylamino)-2*H*-imidazol-2-ylidene and 4,5-bis(dimethylamino)-2*H*-imidazol-2-ylidene ligands. For the purpose of studying electronic properties of these two new classes of NHC ligands, their TEP values were obtained from the IR spectra of the complexes $[\text{Rh}(\text{IMes}^{\text{XY}})\text{Cl}(\text{CO})_2]$ and δ_{Se} were measured by ⁷⁷Se NMR spectroscopy on the selenoureas $[(\text{IMes}^{\text{XY}})=\text{Se}]$, and it was found that the electronic donation of the carbenic carbon sequentially increased by decoration of mono- and bis-amino group respectively whereas the π -accepting properties of the NHC are only slightly or even not affected by the adjunction of the NMe₂ groups on the imidazolyl backbone. Later, the synthesis of the two new PEPPSI-type palladium pre-catalysts PEPPSI-Pd-IPr^{NMe₂} **2.14** and PEPPSI-Pd-IPr^{(NMe₂)₂} **2.17** was successfully achieved. From their crystal structures, we also calculated the percent buried volume %V_{bur} which is related to the steric properties of the

two supporting NHC ligands. It appears that grafting one backbone amino group leads to significant improvement of steric congestion while the second amino only results in a slight increase of the steric issue.

In the second part, the catalytic efficiencies of **2.14** and **2.17** were carefully evaluated in the benchmark Buchwald-Hartwig amination and were compared to the unsubstituted PEPPSI-Pd-IPr reference pre-catalyst. The palladium complex **2.17** bearing the bis-aminated **IPr**^{(NMe₂)₂} was shown to be the most active pre-catalyst, which most probably arises from a possible synergism between steric and electronic effects. Further studies consisted to explore the potentiality of the latter pre-catalyst, either at room temperature or at low catalyst loading (up to 50 ppm) at 80°C. Pre-catalyst **2.17** was shown to be one of the most active and efficient Pd-NHC catalysts reported up to date.

In the last part, the Buchwald-Hartwig amination was explored by using Cs₂CO₃ as a relative mild base. Again, the pre-catalyst **2.17** bearing the **IPr**^{(NMe₂)₂} ligand greatly outperforms the mono-substituted complex **2.14** and even more the unsubstituted representant **1.1**. Various aryl chlorides and an unprecedented broad range of amines including secondary amines and both primary alkyl and arylamines were involved as the suitable substrates in this transformation. It was assumed that this reaction is mainly controlled by the steric rather than the electronic feature of the NHC ligands.

-Chapitre 3-

1.	Introduction	77
2.	Results and Discussion	83
2.1.	Optimization of the reaction conditions	83
2.2.	Study of the substrate scope	86
3.	Conclusion.....	91

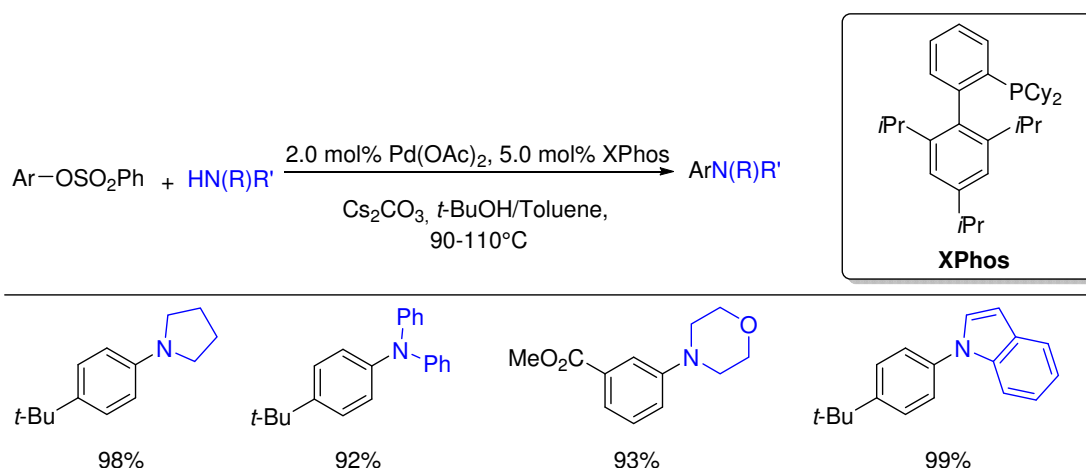
Chapter 3: Amination of (hetero)aryl tosylates catalysed by the Pd-PEPPSI-IPr^{(NMe₂)₂} pre-catalyst

1. Introduction

As outlined in Chapter 1, the palladium-catalyzed Buchwald-Hartwig amination has been successfully established as a highly valuable method for the formation of C(sp²)-N bonds, having important applications in both academia and industry.^{57,58} Usually in this transformation, aryl halides or triflates were abundantly employed as the electrophilic coupling partners and have been efficiently performed by numerous catalytic systems under very mild reaction conditions. Recent research's interest in this aspect has been focused on searching the electrophile alternatives, and aryl sulfonates which can be readily available from phenols, easy to purify and stable against hydrolysis are regarded as a series of significant electrophiles in this reaction. However, the activation/cleavage of the C_{aryl}-O bond remains a challenging problem which renders this amination elusive due to the difficulty in oxidative addition. Meanwhile, as the continuous requirements of developing more electron rich ancillary phosphine ligands, up to now, the most advanced ligand archetypes has enabled the access to these “non-activated” reaction partners.

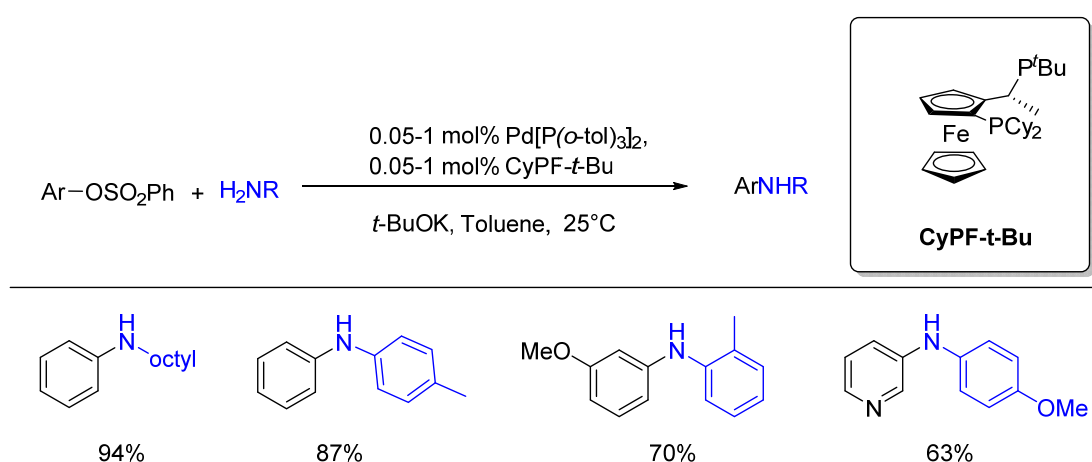
In 2003, Buchwald and co-workers firstly demonstrated that aryl tosylates and benzene sulfonates can be successfully aminated by various amines or amides when employing Pd(OAc)₂/XPhos catalysts (Scheme 3.1.1).¹⁰¹

¹⁰¹ X. Huang, K. W. Anderson, D. Zim, L. Jiang, A. Klapars, S. L. Buchwald, *J. Am. Chem. Soc.* **2003**, *125*, 6653.



Scheme 3.1.1: Amination of aryl tosylates and benzene sulfonates using Pd(OAc)₂/XPhos catalytic system reported by Buchwald.

Later, Hartwig and co-workers have shown that, by combining bidentate Josiphos ligand CyPF-*t*-Bu with the unconventional Pd(0) precursor Pd[P(*o*-tol)₃]₂, (hetero)aryl tosylates can be efficiently coupled with primary alkylamines, using as low as 0.05 mol% of catalyst loading at room temperature. Higher catalyst loading was necessary to obtain a satisfied yield when employing anilines as substrates (Scheme3.1.2).¹⁰²

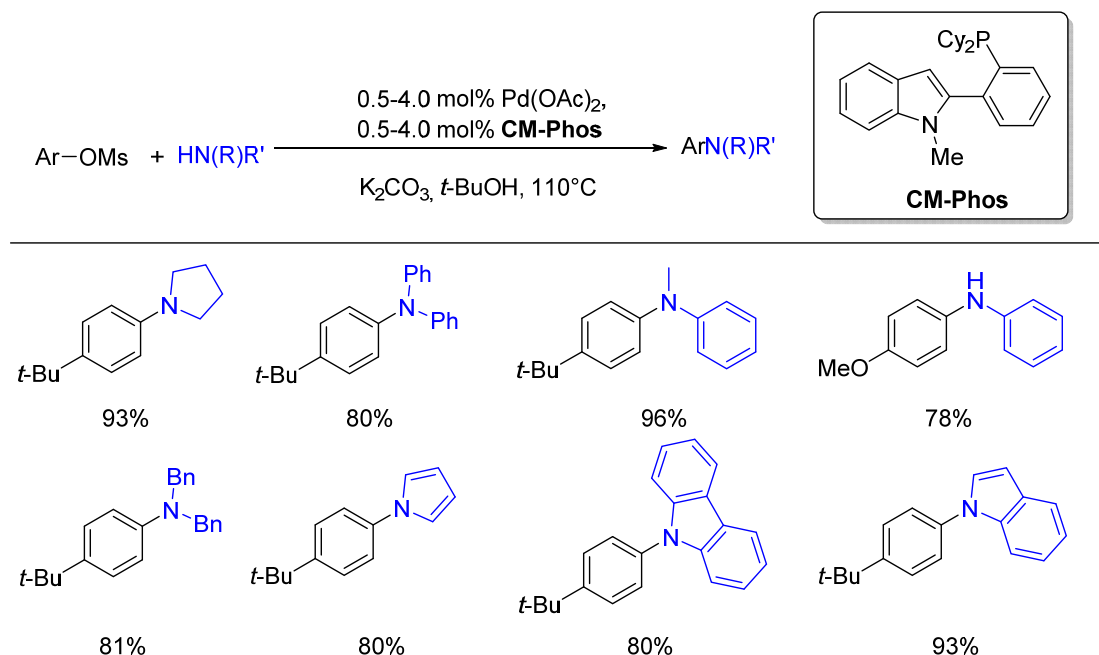


Scheme 3.1.2: Amination between (Hetero)aryl tosylates and primary amines at room temperature using a Pd[P(*o*-tol)₃]₂/CyPF-*t*-Bu catalytic system reported by Hartwig.

The first example involving aryl mesylates as coupling electrophiles in arylative amination was reported by Kwong and co-workers by using CM-Phos as an ancillary ligand, which formally derives from the Buchwald's *o*-biarylphosphines by the replacement of the distal aryl group by an indole unit. Using the catalytic system

¹⁰² T. Ogata, J. F. Hartwig, *J. Am. Chem. Soc.* **2008**, *130*, 13848.

$\text{Pd}(\text{OAc})_2/\text{CM-Phos}$, different kinds of amines as well as nitrogen heterocycles were applicable in this transformation (Scheme 3.1.3).¹⁰³

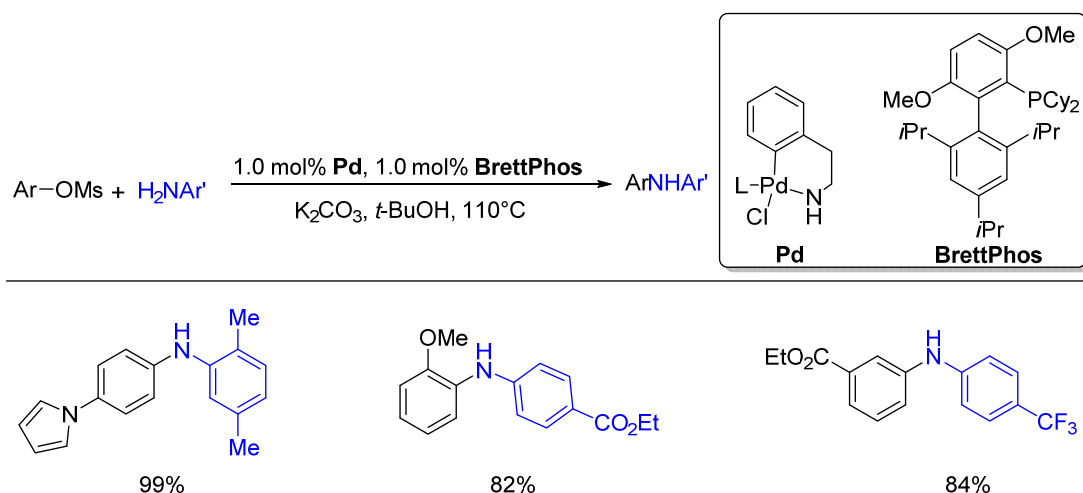


Scheme 3.1.3: First example of amination between aryl mesylates and amines and heterocycles using $\text{Pd}(\text{OAc})_2/\text{CM-Phos}$ catalytic system reported by Kwong.

At the same time, Buchwald and co-workers found that the BrettPhos ligand, in which the phosphine-containing arene was substituted with two methoxy groups, in combination with an efficient palladacyclic amino pre-catalyst, effective in the amination of mesylates.¹⁰⁴ Comparing these results with the above described for the coupling of aryl tosylates using the phosphine XPhos points out the importance of the electronic donation of the phosphine in this reaction. Various electron-deficient anilines were successfully employed in this protocol and usually led to excellent yields (Scheme 3.1.4). Noteworthy, no coupling with alkyl amines was reported with this system.

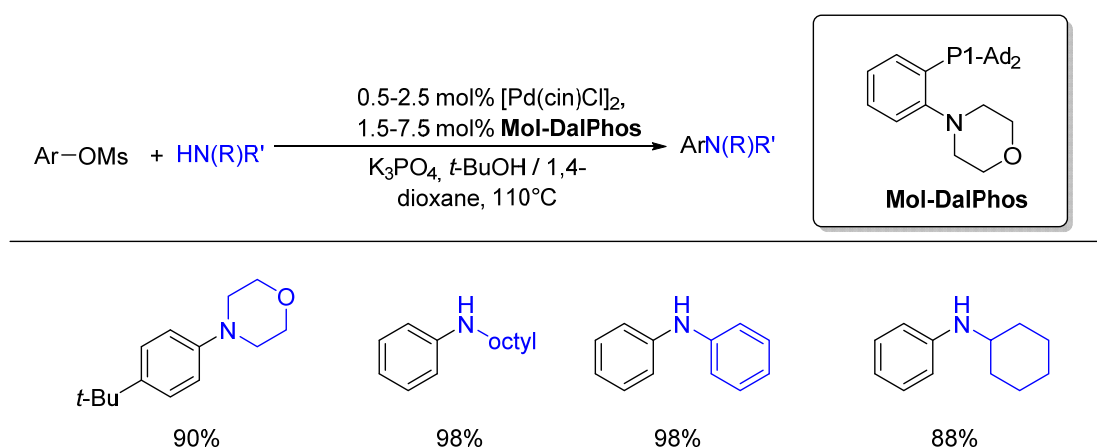
¹⁰³ C. M. So, Z. Zhou, C. P. Lau, F. Y. Kwong, *Angew. Chem. Int. Ed.* **2008**, 47, 6402.

¹⁰⁴ H. Munday, J. R. Martinelli, S. L. Buchwald, *J. Am. Chem. Soc.* **2008**, 130, 2754.



Scheme 3.1.4: Amination between aryl mesylates and anilines using palladacyclic amino pre-catalyst/BrettPhos catalytic system reported by Buchwald.

More recently, Stradiotto and co-workers reported that, using the $[\text{Pd}(\text{cin})\text{Cl}]_2/\text{Mor-DalPhos}$ catalytic system, different alkyl amines and anilines were efficiently coupled with aryl mesylates, and especially the primary alkyl amines could be selectively mono-arylated under this catalytic conditions (Scheme 3.1.5).¹⁰⁵ However, the scope of aryl mesylates was limited to neutral or electron deficient ones.



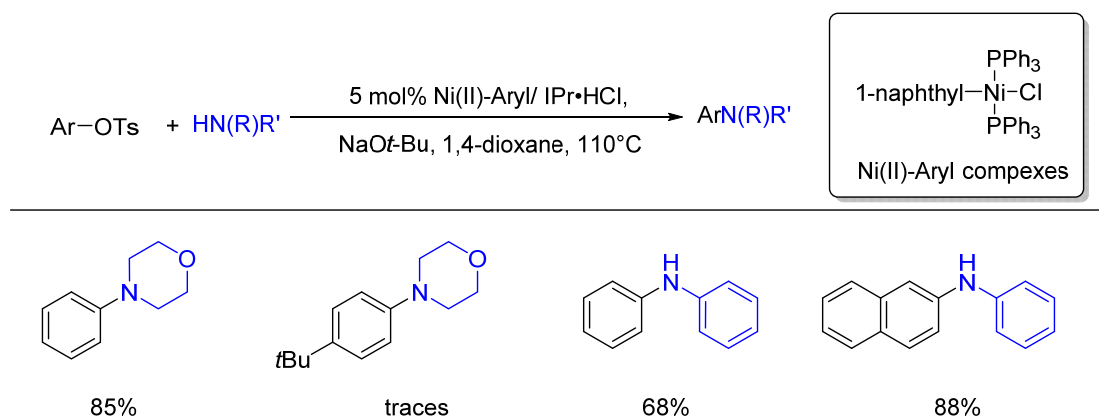
Scheme 3.1.5: Amination between aryl mesylates and amines using $[\text{Pd}(\text{cin})\text{Cl}]_2/\text{Mor-DalPhos}$ catalytic system reported by Stradiotto.

However, to our knowledge, whereas NHCs are stronger donors than phosphines, the amination of aryl sulfonates using a Pd-NHC catalyst has never been documented, and only a few Ni-NHC catalytic systems were reported to activate aryl tosylates in arylative amination. The higher nucleophilicity of Nickel complexes compared to the

¹⁰⁵ P. G. Alsabeh, M. Stradiotto, *Angew. Chem. Int. Ed.* **2013**, 52, 7242.

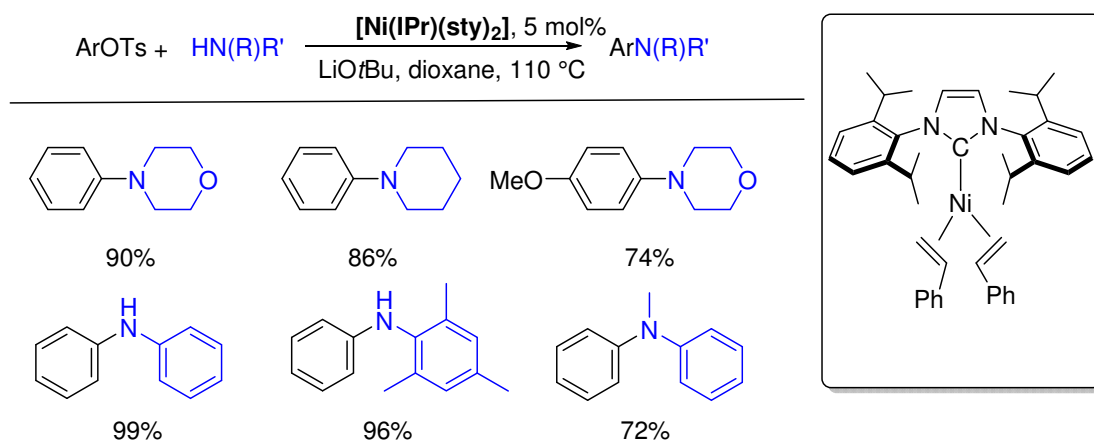
Palladium complexes would explain this reactivity discrepancy, since it facilitates the cleavage of the C-O bond.¹⁰⁶

In 2008, Yang and co-workers reported that, both amines and anilines were successfully coupled with aryl tosylates by use of the Ni(II)-(σ-aryl)/IPr catalytic system. But the latter failed to activate the aryl tosylates bearing electron-rich substituents such as *tert*-butyl or methoxy groups (Scheme 3.1.6).¹⁰⁷



Scheme 3.1.6: Amination between aryl tosylates and amines using Ni(II)/IPr catalytic system reported by Yang.

In 2012, Nicasio and co-workers reported that, by use of the well-defined Ni(0) complex $[\text{Ni(IPr)(styrene)}_2]$, several kinds of secondary alkyl amines and anilines could be efficiently coupled with aryl tosylates, having both electron-rich and deficient substituents (Scheme 3.1.7).¹⁰⁸



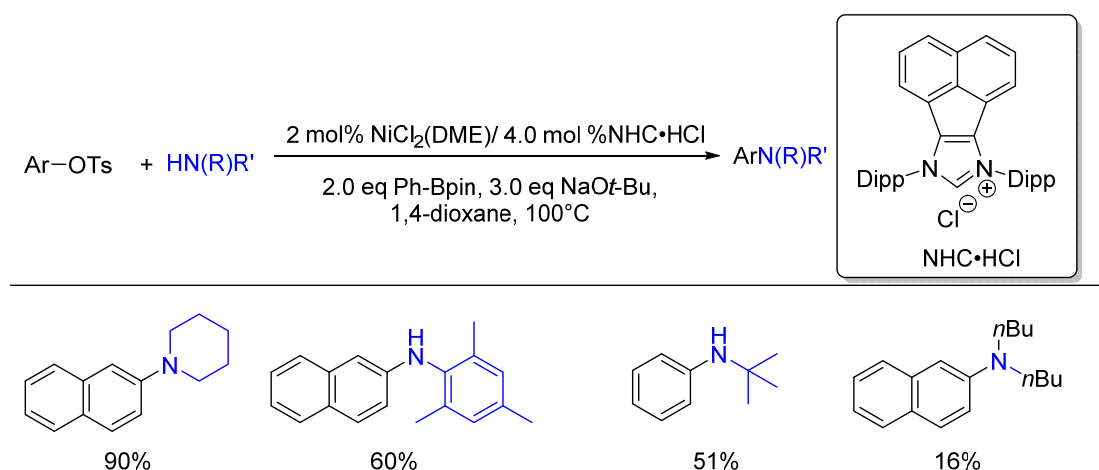
Scheme 3.1.7: Amination between aryl tosylates and amines using the $[\text{Ni(0)(IPr)(sty)}_2]$ pre-catalyst reported Nicasio.

¹⁰⁶ S. Z. Tasker, E. A. Standley, T. F. Jamison, *Nature* **2014**, 509, 299.

¹⁰⁷ C.-Y. Gao, L.-M. Yang, *J. Org. Chem.* **2008**, 73, 1624.

¹⁰⁸ M. J. Iglesias, J. F. Blandez, M. R. Frutos, A. Prieto, E. Álvarez, T. R. Belderrain, M. C. Nicasio, *Organometallics* **2012**, 31, 6312.

Very recently, Tu and co-workers reported a protocol for *in-situ* generating the Ni(0) active species, consisting of a mixture of the easily available and manipulable NiCl₂(dme)/NHC·HCl and the boronate ester PhBpin as reductant. This catalytic conditions were found to be efficient in coupling various heterocyclic aryl tosylates with primary and secondary amines and present the advantage to not use the air-sensitive Ni(0) precursors (Scheme 3.1.8).¹⁰⁹



Scheme 3.1.8: Amination between (hetero)aryl tosylates and amines using NiCl₂(dme)/NHC·HCl catalytic system reported by Tu.

However, whereas being active in catalyzing this arylation amination reaction, the Ni-NHC catalytic systems possess several disadvantages and drawbacks: (1) a high catalyst loading is usually necessary to achieve satisfied yields; (2) use of air sensitive Ni(0) complexes or adding external reducing agents is required; (3) and the use of strong bases (such as NaOtBu or LiOtBu) is inevitable, thus limiting the functional groups tolerance of the system; (4) the scope of either aryl tosylate or amine is still narrow.

In contrast, the features of efficiency and the simplicity of the generation of Pd(0) active species make palladium-catalysis a more suitable candidate for this transformation. The results presented in the chapter 2 have shown that the modification of the skeleton of 1,3-bis(2,6-disopropylphenyl)-2*H*-imidazol-2-ylidene (**IPr**) with two amino groups **IPr**^{(NMe₂)₂} and its palladium pre-catalyst [Pd(**IPr**^{(NMe₂)₂})(3-ClPy)Cl₂] **2.17** exhibits enhanced catalytic efficiency in the Buchwald-Hartwig amination relative to **IPr** derivative, and that catalyst **2.17** also allowed the utilization of Cs₂CO₃ as mild base which enlarge the scope of the aryl

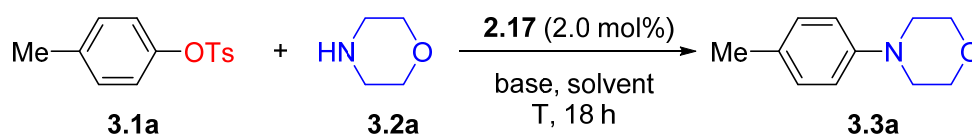
¹⁰⁹ J. Jiang, H. Zhu, Y. Shen, T. Tu, *Org. Chem. Front.* **2014**, *1*, 1172.

substrates bearing base-sensitive groups. We assumed that the enhancement of the electronic properties of the $\text{IPr}^{(\text{NMe}_2)_2}$ ligand should facilitate the oxidative addition of $\text{C}_{\text{aryl}}\text{-O}$ bond of the aryl sulfonates. In this chapter, we will describe the optimization of the reaction conditions for the amination of aryl tosylates as electrophilic partners, with a special emphasis on the ligand structure. The scope of the best catalytic system, bearing the $\text{IPr}^{(\text{NMe}_2)_2}$ ligand was studied in a second time.

2. Results and Discussion

2.1. Optimization of the reaction conditions

Initially, the coupling between 4-methylphenyl tosylate and morpholine using 2.0 mol% of the palladium pre-catalyst **2.17** was used as model reaction to find the optimized conditions (Table 3.2.1).



Entry	base	solvent	Temperature(°C)	GC Conversion (%)
1	K ₃ PO ₄	<i>t</i> BuOH	110	94
2	K ₃ PO ₄	<i>t</i> AmOH	110	96
3	K ₃ PO ₄	<i>t</i> AmOH	120	99
4	K ₃ PO ₄	<i>t</i> AmOH	100	44
5	K ₃ PO ₄	DMF	110	5
6	K ₃ PO ₄	Dioxane	110	26
7	K ₃ PO ₄ 2H ₂ O	<i>t</i> AmOH	110	95
8	K ₂ CO ₃	<i>t</i> AmOH	110	4
9	Cs ₂ CO ₃	<i>t</i> AmOH	110	73

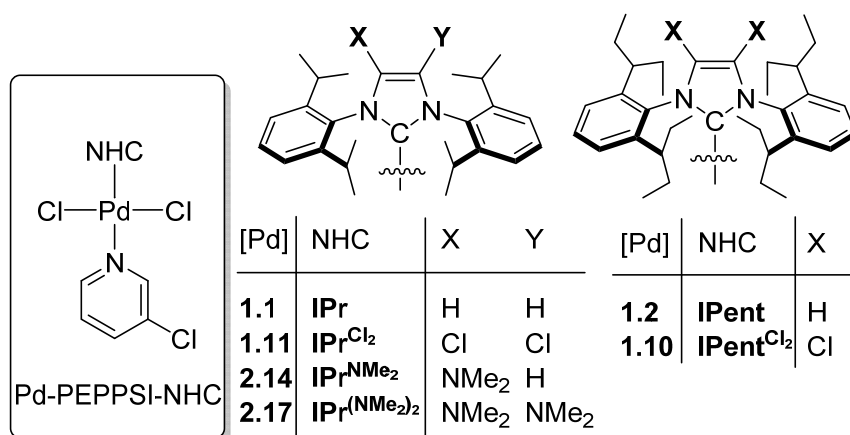
Table 3.2.1: Screening of the reaction conditions using pre-catalyst **2.17**.^[a]

[a] Reaction conditions: 4-tolyl tosylate (0.5 mmol), morpholine (0.75 mmol), catalyst (2.0 mol%), base (1.5 mmol), solvent (1.5 mL); Calibrated GC yields were reported using dodecane as the internal standard and were averaged over two runs.

Keeping in the mind the low solubility of aryl tosylates in nonpolar solvent, we chose *t*BuOH as the solvent which has already been shown to be the ideal solvent in most cases of amination involving aryl sulfonates as the substrates. Using palladium

pre-catalyst **2.17** and K_3PO_4 as the base, we were pleased to observe 94 % conversion of 4-tolyl tosylate, as measured by gas chromatography (Entry 1). Replacing *t*BuOH by *t*AmOH led to a slight improved conversion rate of 96 % mostly due to the higher boiling point of the latter (Entry 2). By increasing the reaction temperature to 120 °C, the reaction afforded a nearly full conversion while decreasing the reaction temperature to 100 °C dramatically affected the level of conversion (entry 3 and 4). Further investigations into the reaction parameters revealed that the choice of the base and solvent was critically crucial for the outcome of this transformation. The use of Cs_2CO_3 resulted in inferior conversion although it was a suitable base using aryl chlorides as the coupling partners presented in the previous chapter (Table 3.2.1, entry 6). The reaction was almost inhibited when K_2CO_3 was used as the base or using DMF or Dioxane as the solvent (Table 3.2.1, entries 6 and 7). Finally, anhydrous K_3PO_4 or hydrate $\text{K}_3\text{PO}_4 \cdot 2\text{H}_2\text{O}$ could be indifferently employed as base (entry 7 vs. entry 3).

As the fully optimized catalytic conditions have been established, we were next sought to investigate the effect of the ligand structure. In this context, the pre-catalyst **2.14** and **1.1** outlined in the chapter 2 were selected to compare the activity in this reaction with **2.17**. On the other hand, for comparative purposes, we also chose to test the pre-catalysts **1.2** and **1.10** bearing the sterically hindered, yet flexible NHCs IPent and IPent^{Cl₂}, since they are still the most efficient Pd-NHC catalytic systems in amination reaction up to date.^{98,99} For the sake of comparison, complex **1.11**, featuring the IPr^{Cl₂} ligand, was also included in the study.



Scheme 3.2.1: Palladium PEPPSI-type complexes considered in this study.

The coupling between aryl tosylates **3.1a-b** and morpholine **3.2a** was chosen as the model reaction to evaluate the respective catalytic efficiencies of the Pd-PEPPSI pre-catalysts (Table 3.2.2). Under the above optimized standard conditions, Pd-PEPPSI-IPr (**1.1**) showed almost no activity in the reaction to give products **3.3a** and **3.3b**. Whereas the more-electron deficient Pd-PEPPSI-IPr^{Cl₂} (**1.11**) gave even worse results, the incorporation of one dimethylamino group onto the backbone of **IPr** induced a clear, yet still limited improvement of the activity of Pd-PEPPSI-IPr^{NMe₂} (**2.14**). Compared with the results using Pd-PEPPSI-IPr^{(NMe₂)₂} (**2.17**) as pre-catalyst giving 99% and 43 % GC yield for the **3.3a** and **3.3b** respectively, the benefit should be again attributed to the synergetic effects of the two dimethylamino groups on the heterocycle backbone. Such performances were approached upon using the Pd-PEPPSI-IPent (**1.2**) but with a smaller 36% yield in **3.3b** starting from the more difficult 4-methoxyphenyl tosylate **3.1b** compared to the 43% yield obtained using **2.17**. As in the **IPr** series, diminishing the electron donation of **IPent** ligand by incorporating two chlorides in **1.10** led to a small decrease in product yields compared to **1.2**.⁹⁹ Taken together, these results suggest that the amination of aryl tosylates is facilitated by a synergy between an electronic enrichment of the metallic center and an increase in the steric crowding of the NHC ligand, with an optimal catalytic performance reached with the Pd-PEPPSI-IPr^{(NMe₂)₂} (**2.17**).

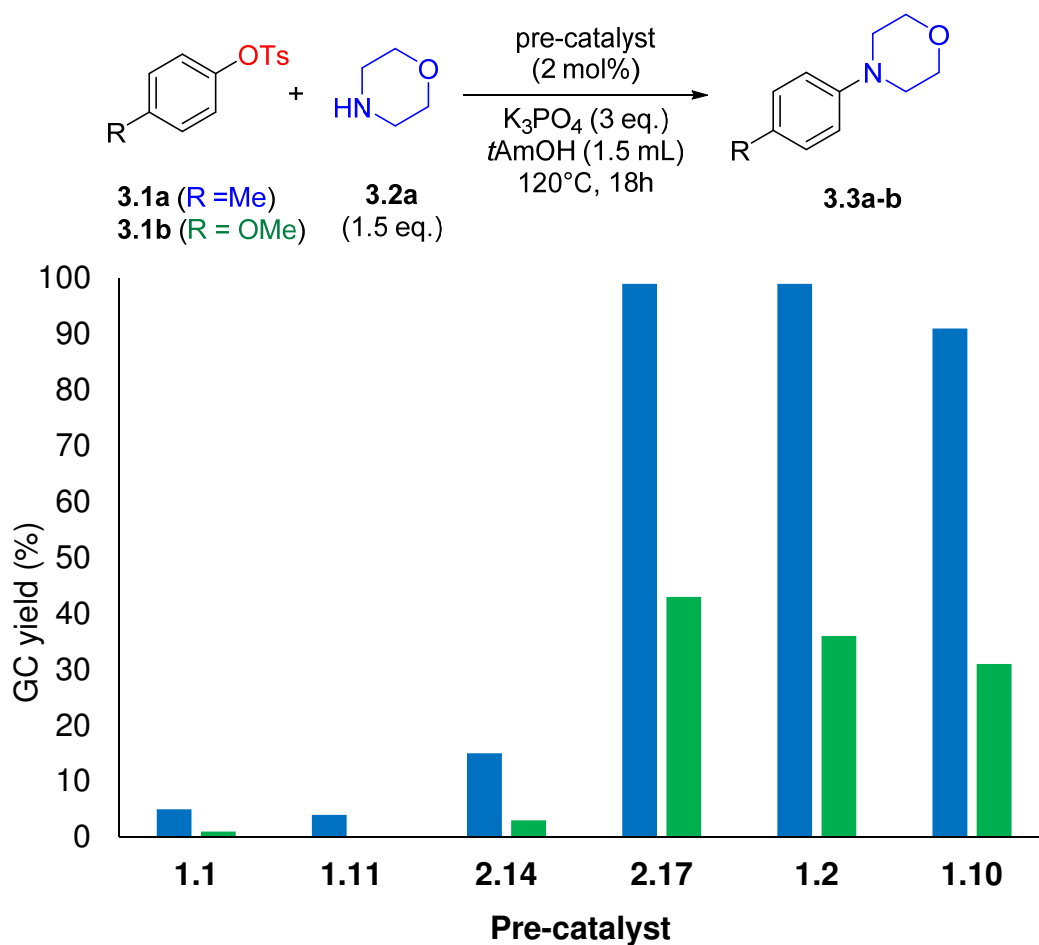
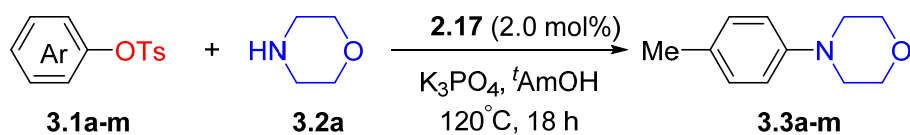


Table 3.2.2: Comparison of activities between different Pd-PEPPSI type pre-catalysts in amination using aryl tosylates **3.1a** and **3.1b**.

2.2. Study of the substrate scope

Having established the standard conditions for amination of aryl tosylates, the substrate scope was then investigated starting with the variation of the (hetero)aryl tosylate partner using morpholine **3.2a** as the common amine and 2 mol% of pre-catalyst **2.17** (Table 3.2.3).



Entry	ArOTs	Product	Yield (%) ^[b]
1	3.1a	3.3a	95
2	3.1b	3.3b	73 ^[c]

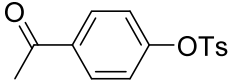
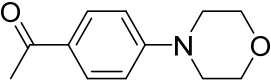
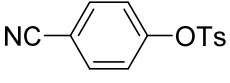
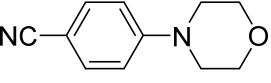
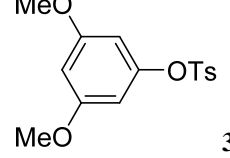
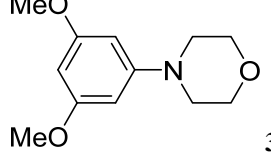
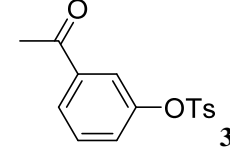
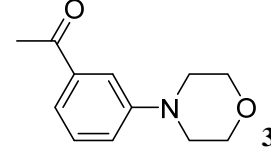
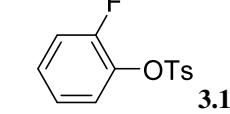
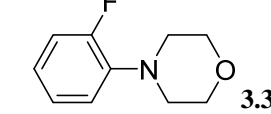
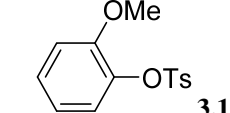
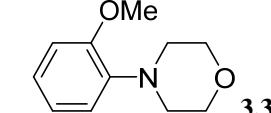
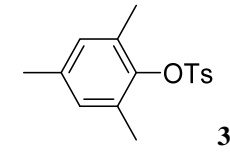
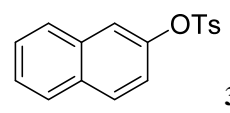
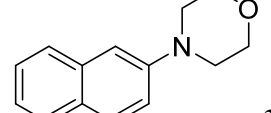
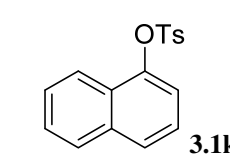
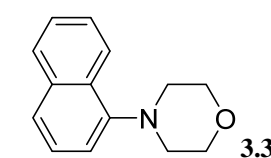
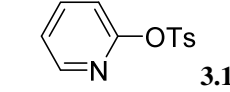
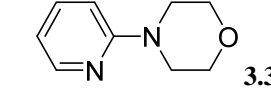
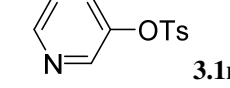
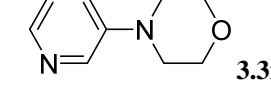
3	 3.1c	 3.3c	87
4	 3.1d	 3.3d	80 ^[d]
5	 3.1e	 3.3e	91
6	 3.1f	 3.3f	77
7	 3.1g	 3.3g	66
8	 3.1h	 3.3h	88 ^[c]
9	 3.1i	-	0
10	 3.1j	 3.3j	84
11	 3.1k	 3.3k	95
12	 3.1l	 3.3l	70
13	 3.1m	 3.3m	87

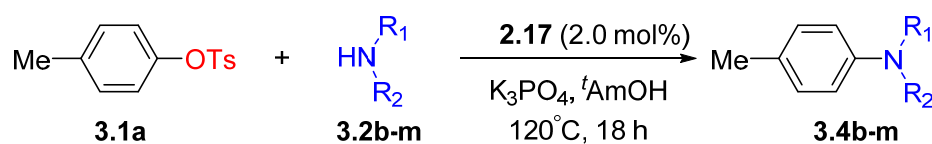
Table 3.2.3: Buchwald-Hartwig amination of (hetero)aryl tosylates **3.1a-l** with morpholine (**3.2a**) using pre-catalyst **2.17**.^[a]

[a] Reaction conditions: ArOTs (0.5 mmol), morpholine (0.75 mmol), **2.17** (2 mol%), K₃PO₄ (1.5 mmol), *t*AmOH (1.5 mL), 120°C. [b] Isolated yield, average of two runs. [c] 4 mol% of **2.17**. [d] 1 mol% of **2.17**.

Under the above reaction conditions, aryl tosylates **3.1a-d** bearing electronically-diverse *para*-substituents (methyl, methoxy, acetyl, cyano respectively) were efficiently coupled in good yields. Nevertheless, for the most difficult **3.1b**, it appeared necessary to increase the catalyst loading up to 4 mol% to reach an acceptable 73% isolated yield (Entries 1-4). The *meta* substitution of the aryl group was found not problematic (Entries 5-6), and the electron-rich 3,5-dimethoxyphenyl tosylate **3.1e** could be successfully employed to give **3.3e** in an excellent 91% yield (Entry 5). Gratifyingly, the mildly basic conditions of the reaction tolerate base-sensitive functional groups on the aryl groups. Whereas the sterically highly crowded mesityl tosylate **3.1i** remained untouched under these conditions (Entry 9), the coupling of *ortho*-substituted substrates **3.1g-h** bearing a fluoro or methoxy substituent smoothly proceeded to give **3.3g** and **3.3h** in 66% and 88% (with 4 mol% of **2.17** in the latter case) respectively, indicating that the catalytic species can adapt to some steric constraint in the aryl tosylate partner (Entries 7-8). Furthermore, whereas the naphthyl-based amines **3.1j-k** were obtained in very good yields (Entries 9-10), 2- and 3-pyridinyl tosylates **3.1l-m** were shown to be suitable substrates and yielded the corresponding amines in good yields (Entries 11-12).

We next turned our attention to the scope of the reaction with respect to the nature of the amine using 4-tolyl tosylate **3.1a** as the electrophile partner (Table 3.2.4). Irrespective to their electronic and steric nature, secondary cyclic (**3.2a-d**), acyclic (**3.2e**) amines, as well as *N*-methyl aniline **3.2f** and even the crowded and low nucleophilic diphenylamine **3.2g** underwent the transformation in good to excellent yields. Starting with unsubstituted aniline **3.2h** yielded the coupling product **3.3h** in 91% isolated yield and most notably no trace of the corresponding di-arylated aniline could be detected. Impressively, even more challenging anilines **3.2i-j** bearing electron-withdrawing groups such as 4-fluoro and 3-trifluoromethyl respectively and the crowded 2,6-dimethylaniline **3.2k** were smoothly engaged in this reaction in excellent yields, albeit requiring a small increase of the catalyst loading up to 4 mol% for the first two anilines. However, no conversion was detected when employing the low nucleophilic 2- and 3-aminopyridines **3.2l-m** (Entries 11-12), leaving the substrate **3.1a** untouched. The primary aliphatic amines were found to be suitable coupling partners, but exhibiting different outcomes according to their steric hindrance. The reaction between **3.1a** and octylamine **3.2n** proceeded well but appeared not very

selective, affording the mono- and bis-arylation products **3.4n** and **3.4n'** in a 27/73 ratio (Entry 13). Under the same conditions, the use of the slightly more crowded cyclohexylamine **3.3o** allowed the efficient isolation of the mono-arylated product **3.4o** in 93% yield (Entry 14), but the catalytic system appeared inefficient in coupling **3.1a** with the highly congested *tert*-butylamine **3.4p** (Entry 15). Finally, the procedure could be extended to the hydrazine derivative 4-aminomorpholine **3.4q** (Entry 16). The general applicability of the catalytic system throughout the above screening led us to conclude that the amine partner might not be involved in the rate determining step of the catalytic cycle, our observations being more consistent with the cleavage of the C_{Ar}-O bond of the aryl tosylate as being the rate limiting step of the catalytic cycle.



Entry	Amine	Product	Yield (%) ^[b]
1	3.2b	3.4b	91
2	3.2c	3.4c	82
3	3.2d	3.4d	96
4	3.2e	3.4e	91
5	3.2f	3.4f	91
6	3.2g	3.4g	94 ^[c]
7	3.2h	3.4h	91

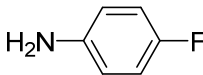
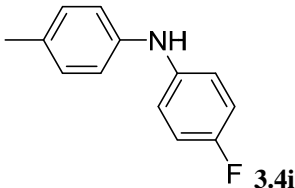
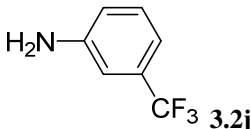
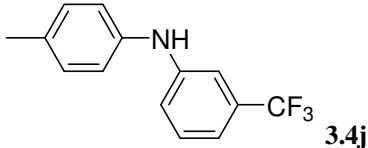
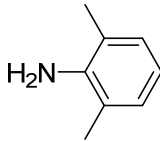
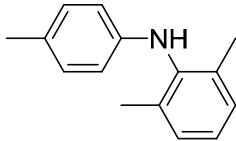
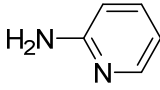
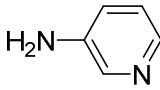
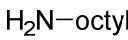
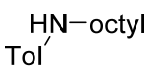
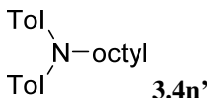
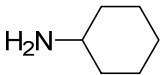
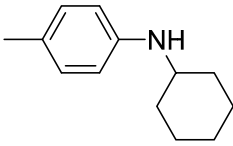
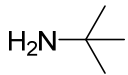
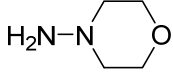
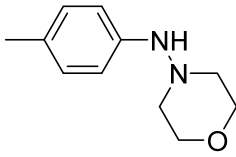
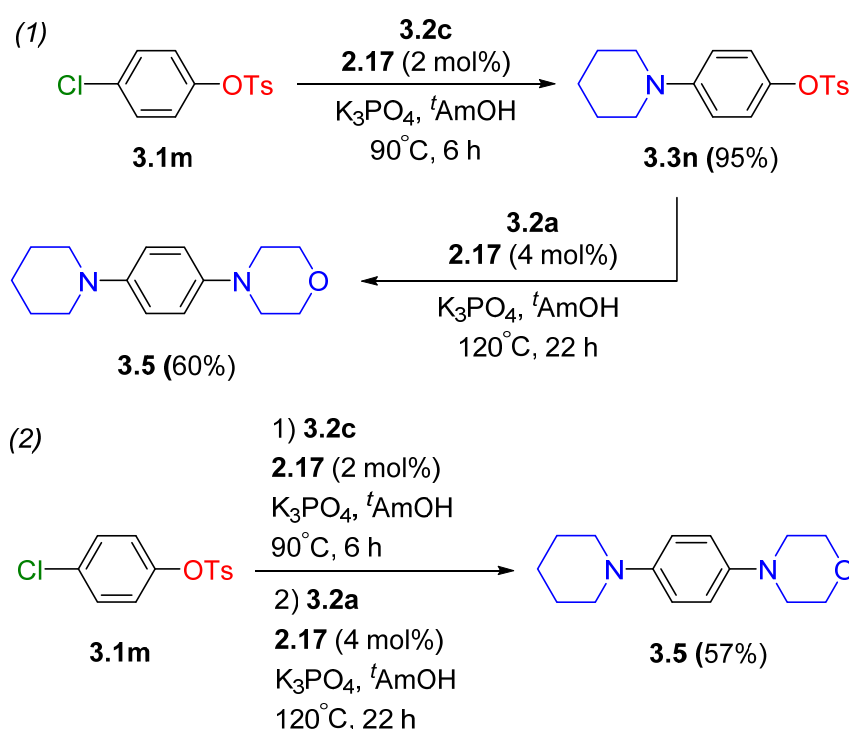
8	 3.2i	 3.4i	96 ^[c]
9	 3.2j	 3.4j	92 ^[c]
10	 3.2k	 3.4k	85
11	 3.2l	-	0
12	 3.2m	-	0
13 ^[d]	 3.2n	 3.4n  3.4n'	82 ^[e] (27/73 ^[f])
14	 3.2o	 3.4o	93
15	 3.2o		0
16	 3.2p	 3.4q	83

Table 3.2.4: [a] Reaction conditions: **3.1a** (0.5 mmol), amine (0.75 mmol), **1d** (2 mol%), K₃PO₄ (1.5 mmol), *t*AmOH (1.5 mL), 120°C. [b] Isolated yield, average of two runs. [c] 4 mol% of **1d**; [d] octyl = n-C₈H₁₇, Tol = p-tolyl; [e] Global yield based on **3a**; [f] Ratio between mono and bis arylation products **5an** and **5an'**.

To further extend the application potential of this methodology, we were thus prompted to take advantage of the different reactivity profiles between aryl chlorides and tosylates in Buchwald-Hartwig amination to selectively install different amines on the same bis-electrophilic substrate and under the same catalytic conditions. As representative example, *N*-(4-(piperidinyl)phenyl)morpholine **3.5** could be

synthesized from 4-chlorophenyl tosylate, readily available from 4-chlorophenol. Gratefully, when piperidine **3.2c** was employed as the amine partner under the standard conditions but at 90°C instead of 120°C, 4-(piperidinyl)phenyl tosylate **3.3n** was obtained as the sole product in 95% yield (Scheme 1, eq. 1). After purification and isolation, the latter was engaged in the second amination reaction with morpholine **3.2a** using the standard conditions. More remarkably, thanks to the high chemoselectivity of the transformation, it was possible to carry out the bis-amination in a one-pot protocol without the need to isolate the intermediate **3.3n**. The overall 57% yield in **3.5** was fully acceptable considering the strong electron-donating character of the piperidinyl-substituent in **3.3n**.



Scheme 3.2.1: Sequential (eq. 1) and one-pot (eq. 2) chemoselective bis-amination leading to bis-amine **3.5**

3. Conclusion

The results presented in this chapter establish the pre-catalyst the Pd-PEPPSI-IPr^{(NMe₂)₂} **2.17** as being a highly effective catalytic system for the Buchwald-Hartwig amination with (hetero)aryl tosylates as substrates. This study represents the first example of such kind of transformation involving a well-defined Pd/NHC catalytic system reported thus far in the literature. The benefit of this unique reactivity of pre-catalyst **2.17** should again rely on stereoelectronic modifications of the supporting imidazol-2-ylidene ligand. This optimized catalytic system was shown to achieve the

amination with a wide range of amines and anilines, and to be slightly more sensitive to the nature of the aryl tosylate, indicating that the limiting step of the catalytic cycle is the oxidative addition of the C_{Ar}-O bond onto the Pd(0) species. Moreover, the protocol which presents high chemoselectivity towards the chloride and tosyloxy group substituted on the same aryl ring provides an effective method for synthesizing aryl polyamines in “one pot” manipulation.

-Chapter 4-

1. Introduction	95
2. Established methods for the backbone functionalization of imidazol-2-ylidenes ...	95
2.1. Derivatization through the free carbenic species	96
2.2. <i>Via</i> stable NHC complexes	99
3. Synthesis of the imidazolium precursors	101
3.1. Synthesis of 4-(diisopropylamino)imidazolium salt	101
3.2. Synthesis of 4-dimethylamino-5-haloimidazolium salts	104
4. The electronic properties of new NHC ligands.....	108
4.1. Synthesis of Rh(IMes ^{XY})Cl(CO) ₂ complexes	108
4.2. Synthesis of the selenoureas [(IMes ^{XY})=Se].....	110
5. Studies of the catalytic properties in palladium-catalyzed Buchwald-Hartwig amination.....	111
5.1. Synthesis of PEPPSI-type Palladium pre-catalysts.....	111
5.2. Evaluation of catalytic properties in Buchwald-Hartwig amination.....	116
5.3. Conclusion	119
6. Buchwald-Hartwig Amination with challenging bulky primary alkyl amines ...	120
6.1. Introduction.....	120
6.2. Result and discussion.....	123
6.3. Conclusion	127
7. Conclusion and perspective	128

Chapter 4: Further skeleton derivatization of imidazol-2-ylidene ligands

1. Introduction

The results outlined in the previous two chapters have indicated considerable effects of backbone functionalization of **IPr** by bis-dimethylamino groups in palladium catalyzed Buchwald-Hartwig amination compared with the non-substituted **IPr** reference, whereas only a limited influent was observed with mono-dimethyl amino analogue. We assumed that the significant improvement in catalytic efficiency of palladium pre-catalyst bearing **IPr**^{(NMe₂)₂} in amination is mostly attributed to a possible synergism between steric and electronic effects. However, we do not understand well yet, which of these two factors is the most important for the outcome of the Pd-catalyzed arylation amination. Moreover, in their previous studies on **IPent** and **IPent**^{Cl₂} ligand in Buchwald-Hartwig amination, Organ and co-workers concluded that the steric factors are more important than electronic factors.¹¹⁰ In order to better understand the features at play in our systems, we thus envisaged to carry out further variations of the backbones of the amine-derived imidazol-2-ylidenes and to compare the corresponding pre-catalysts Pd-PEPPSI-IPr^{XY} in terms of catalytic efficiency. The principal concept for further modification of backbone of the imidazol-2-ylidenes will be focused on two aspects: (1) replacement of mono-dimethylamino substituent in **IAr**^{NMe₂} by a bulkier amino group like a diisopropylamino group (**IAr**^{NiPr₂}); (2) replacement of one of two dimethylamino groups in **IAr**^{(NMe₂)₂} by a less electron donating or even electronic withdrawing group like a halogen. In a second time, the catalytic results will allow us to obtain a reasonable conclusion and to rapidly optimize the catalytic system for a further amination reaction involving even more challenging substrates.

2. Established methods for the backbone functionalization of imidazol-2-ylidenes

Since it is well known that the electronic properties of the carbenic center are greatly sensitive to the nature of the carbenic heterocycle, great efforts have been made for developing efficient methods for the functionalization of the backbone of NHCs. Obviously,

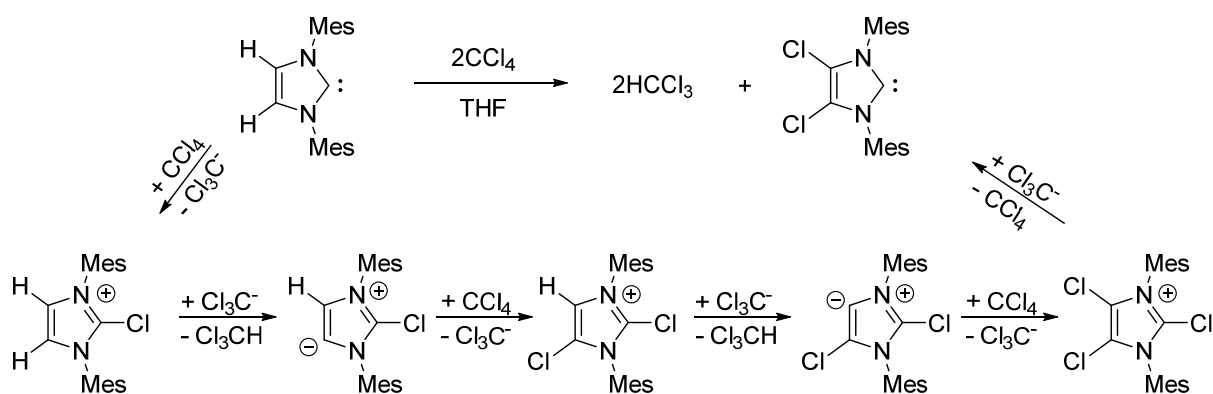
¹¹⁰ M. Pompeo, J. L. Farmer, R. D. J. Froese, M. G. Organ, *Angew. Chem. Int. Ed.* **2014**, 53, 3223.

direct modification of the backbone by means of an organic strategy is the most facile way and was mainly used in the previously reported works. In this section, we will describe some relevant literature precedents for the derivatization of imidazol-2-ylidenes.

2.1. Derivatization through the free carbenic species

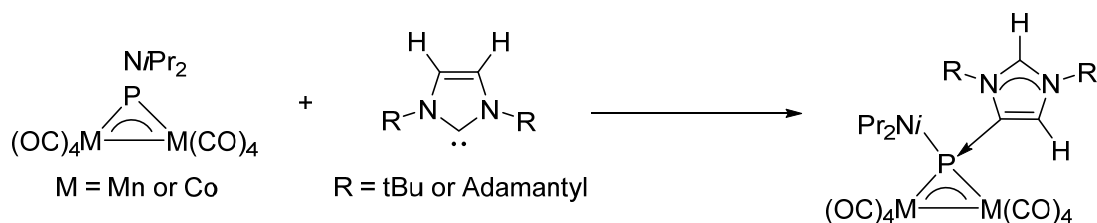
The free NHCs being more reactive than their imidazolium precursor salts, they served in the first examples as substrates for the substitution of the backbone.

In 1999, Arduengo and co-workers demonstrated a facile synthetic method to chlorinate the C4 and C5 positions of IMes by reacting the free carbene IMes with CCl_4 in THF at room temperature (Scheme 4.2.1).¹¹¹



Scheme 4.2.1: Chlorination of C4 and C5-positions of IMes and the reaction mechanism reported by Arduengo.

The first example of P-functionalization on the C4-position was described by Carty and co-workers.¹¹² Unexpectedly, reacting Mn_2 - and Co_2 -containing μ -P(NiPr₂) complexes $[\text{M}_2(\text{CO})_8\{\mu\text{-P}(\text{NiPr}_2)\}(4\text{-cyclo-C}_3\text{H}_2\text{-1,3-(NR)}_2)]$ with *It*Bu or IAd afforded C4-position substitution adducts instead of C2-position. The author assumed that the steric hindrance drives the reaction to the more thermodynamically-favored C4-isomer, exhibiting a mesoionic carbene (or “abnormal” carbene) (Scheme 4.2.2).

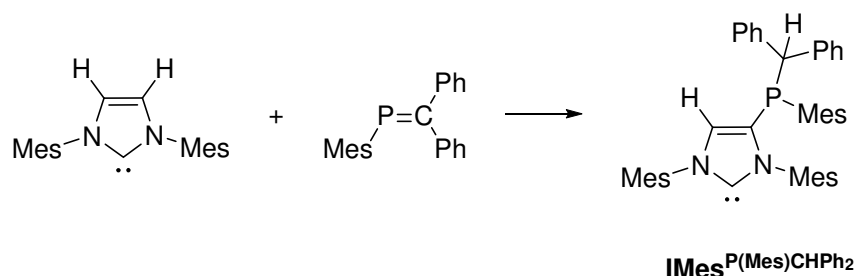


Scheme 4.2.2: The example of P-functionalization of the C4-position of NHC reported by Carty.

¹¹¹ A. J. Arduengo, F. Davidson, H. V. R. Dias, J. R. Goerlich, D. Khasnis, W. J. Marshall, T. K. Prakasha, *J. Am. Chem. Soc.* **1997**, 119, 12742.

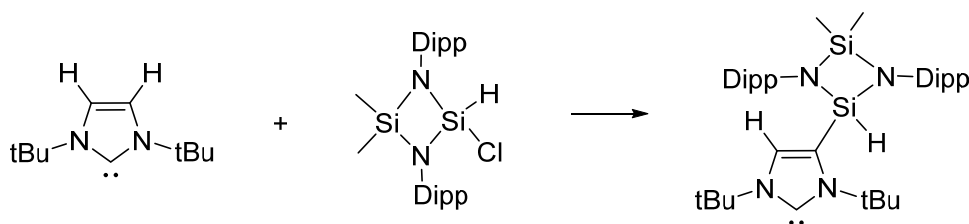
¹¹² T. W. Graham, K. A. Udachin, A. J. Carty, *Chem. Commun.* **2006**, 2699.

Another example of P-functionalization of the C4-position was reported by Gates and co-workers by use of a phosphalkene firstly affording the 4-phosphino-imidazol-2-ylidene **IMes**^{P(Mes)CHPh₂} which could further act as a bifunctional ligand for use of catalyst (Scheme 4.2.3).¹¹³ In this case, DFT calculations showed that the reaction proceeds through isomerization of the normal diaminocarbene to the mesoionic carbene, followed by reaction with the phosphalkene.



Scheme 4.2.3: P-functionalization on C4-position of NHC reported by Gates.

Furthermore, Cui and co-workers demonstrated that silyl-substituted NHCs could be formed by the reactions of *ItBu* with cyclic diaminochlorosilanes [Me₂Si-(NAr)₂]SiHCl (Ar=2,6-*i*Pr₂C₆H₃) (Scheme 4.2.4).¹¹⁴



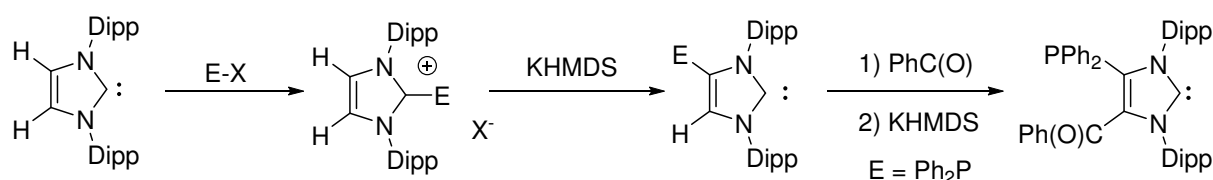
Scheme 4.2.4: Silyl-substituted NHC on C4-position reported by Cui.

Later, a systematic study of variation of backbone of **IPr** was carried out by Bertrand and co-workers, and detailed mechanism was also discussed.¹¹⁵ This method is quite flexible and allows the introduction of two functional groups in one pot (Scheme 4.2.5). The scope of electrophiles is the most general up to date.

¹¹³ (a) J. I. Bates, P. Kennepohl, D. P. Gates, *Angew. Chem. Int. Ed.* **2009**, 48, 9844; (b) J. I. Bates, D. P. Gates, *Organometallics* **2012**, 31, 4529.

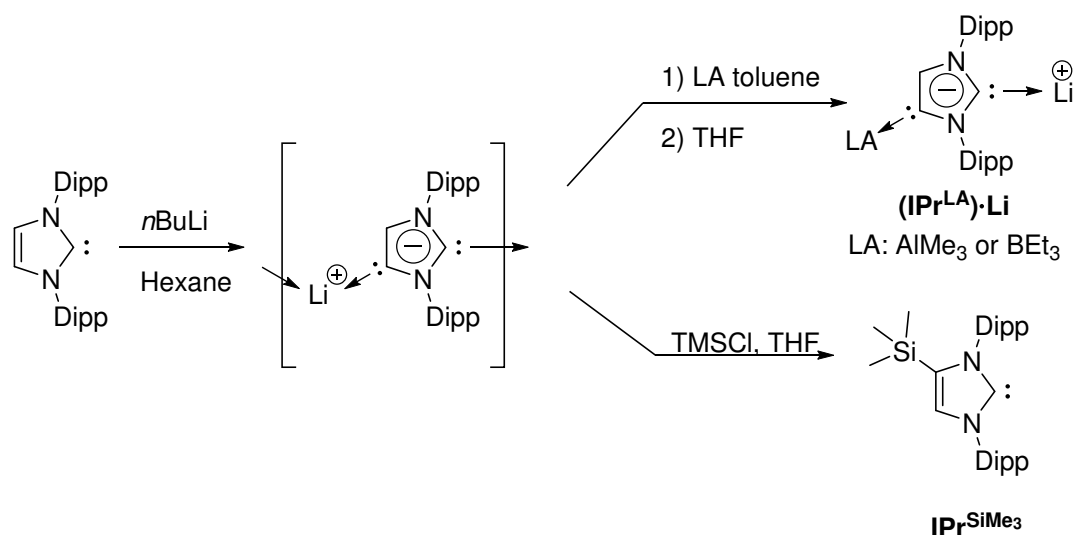
¹¹⁴ H. Cui, Y. Shao, X. Li, L. Kong, C. Cui, *Organometallics* **2009**, 28, 5191.

¹¹⁵ D. Mendoza-Espinosa, B. Donnadieu, G. Bertrand, *J. Am. Chem. Soc.* **2010**, 132, 7264.



Scheme 4.2.5: Versatile functionalization of C4 or/and C5-positions of IPr reported by Bertrand.

Robinson and co-workers found that an anionic *N*-heterocyclic dicarbene could be smoothly generated by adding *n*BuLi to **IPr** in hexane which could further react with group 13 Lewis acids AlMe₃ and BEt₃ to give the anionic NHCs of type (**IPr**^{LA})[−]Li⁺ revealing the anionic nature of the resulting dicarbene.¹¹⁶ The C4-substituted imidazol-2-ylidene **IPr**^{SiMe₃} was also obtained by reaction of the anionic dicarbene with TMSCl (Scheme 4.2.6).



Scheme 4.2.6: Reactivity of anionic dicarbene towards Lewis acid reported Robinson.

Inspired by this work, Ashfeld and co-workers developed a carboxylation of C4-position through exposing the above described anionic dicarbene to CO₂ (Figure 4.2.1).¹¹⁷ Based on the same protocol with the Lewis acid B(C₆F₅)₃, Tamm and co-workers further developed an anionic NHC bearing borate group.⁵²

¹¹⁶ Y. Wang, Y. Xie, M. Y. Abraham, P. Wei, H. F. Schaefer, P. v. R. Schleyer, G. H. Robinson, *J. Am. Chem. Soc.* **2010**, 132, 14370.

¹¹⁷ M. Vogt, C. Wu, A. G. Oliver, C. J. Meyer, W. F. Schneider, B. L. Ashfeld, *Chem. Commun.* **2013**, 49, 11527.

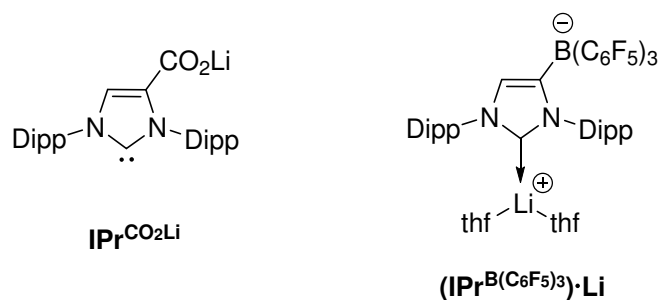


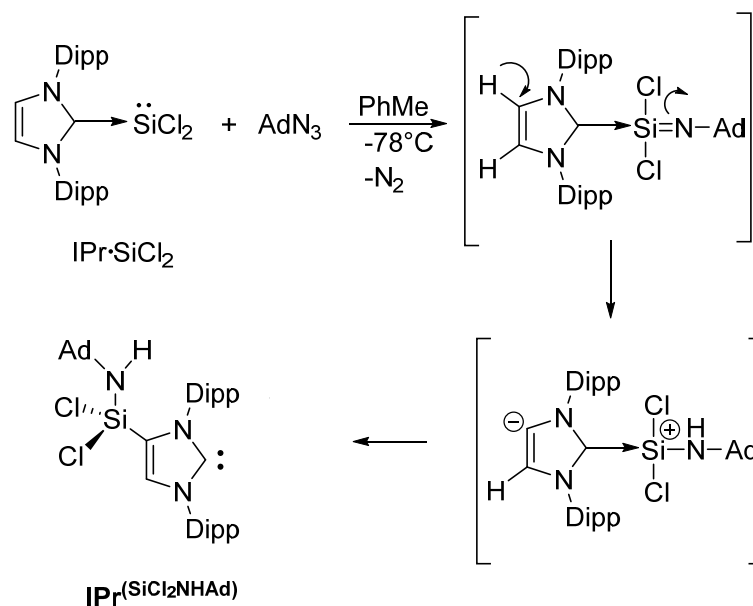
Figure 4.2.1: Functionalization of the C4 position of imidazol-2-ylidenes by anionic groups reported by Ashfeld and Tamm respectively.

2.2. Via stable NHC complexes

Usually, the direct backbone functionalization of the free NHC requires strict anhydrous and inert reaction conditions which limit the choice of the scope of both NHCs and electrophiles. In contrast, stable NHC complexes could be a better candidate in order to avoid using relative sensible free carbenes.

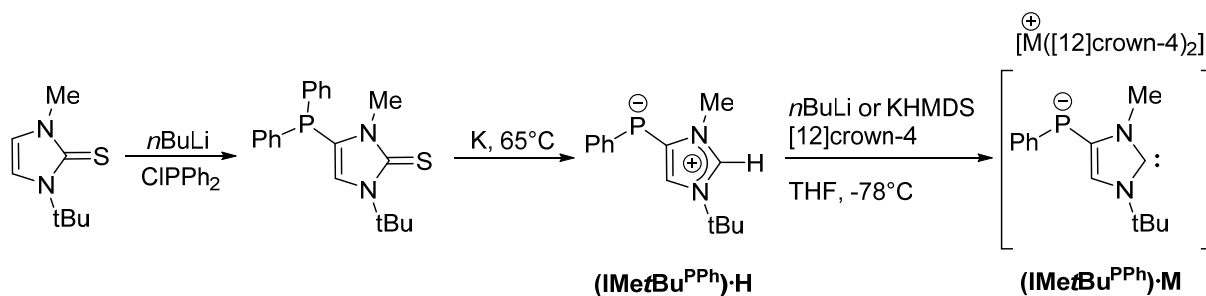
Roesky and co-workers demonstrated that the reaction between the IPr-stabilized dichlorosilylene $\text{IPr}\cdot\text{SiCl}_2$ and 1-adamantyl azide (AdN_3) led to the 4-(dichloroaminosilyl)imidazol-2-ylidene $\text{IPr}^{(\text{SiCl}_2\text{NHAd})}$ (Scheme 4.2.7).¹¹⁸ The mechanism was thought to proceed via a coupling between the azide and the silylene to give a silaimine, which is enough basic to deprotonate the C4 position of the imidazolyl ring. Subsequent migration of the silyl group from the normal carbene position to the “abnormal” carbene finally leads to the backbone-functionalized NHC.

¹¹⁸ R. S. Ghadwal, H. W. Roesky, M. Granitzka, D. Stalke, *J. Am. Chem. Soc.* **2010**, *132*, 10018.



Scheme 4.2.7: C4-silyl-substituted NHC using a IPr·SiCl₂ adduct reported by Roesky.

Streubel and co-workers has reported an efficient method to synthesize 4-phosphanylated 1,3-dialkyl-imidazol-2-thiones through substitution of C4-position by deprotonation of imidazol-2-thione.¹¹⁹ In a further study, when the same group tried to reduce the resulting product with an excess of potassium unexpectedly afforded the novel zwitterionic imidazolium (**IMetBu^{PPh}**)·H which could be deprotonated by *n*BuLi or KHMDS to form the anionic (**IMetBu^{PPh}**)[−]·M (Scheme 4.2.8).¹²⁰



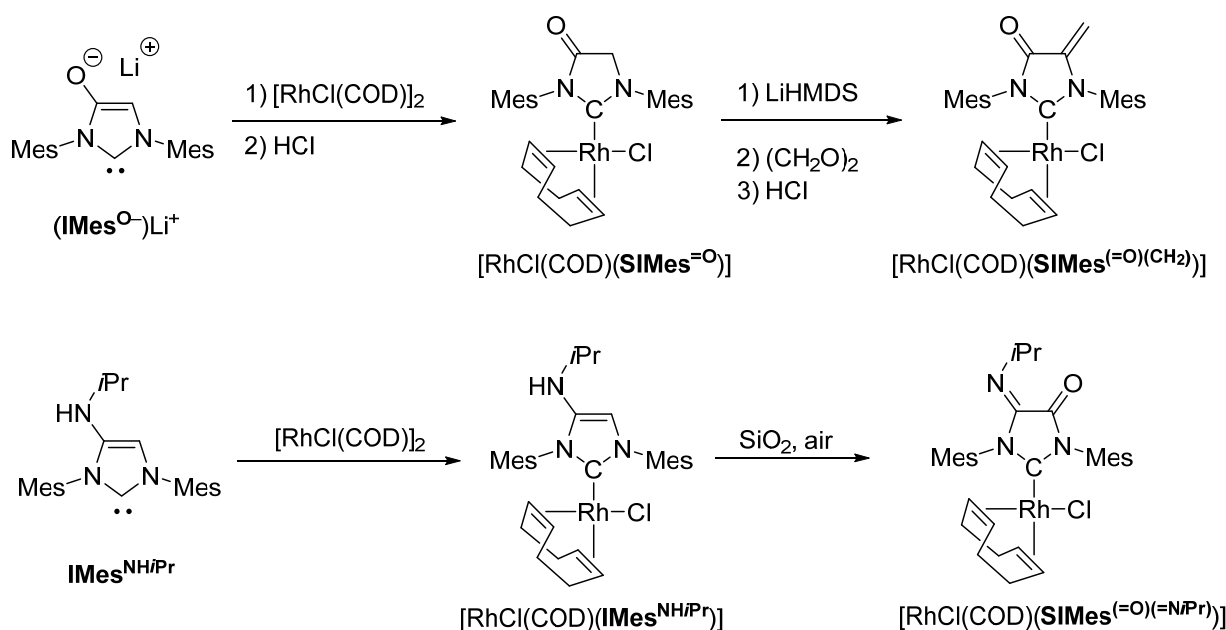
Scheme 4.2.8: Synthesis of phosphido-derived anionic NHC (**IMetBu^{PPh}**)[−] reported by Streubel.

In 2009 and more recently in 2012, our group developed a series of imidazol-2-ylidenes **IMes^{O−}** and **IMes^{NH[−]iPr}** substituted by an anionic oxygen atom and by an isopropylamino group respectively.⁷⁹ Thanks to these functions on the C4 position of the imidazolyl, the backbone was shown to react as an “enolate” or “enamine” analogue. Thus, when ligated to a rhodium(I) center, the NHCs could be further functionalized on their C5 position through a

¹¹⁹ S. Sauerbrey, P. K. Majhi, G. Schnakenburg, A. J. Arduengo, R. Streubel, *Dalton Trans.* **2012**, 41, 5368.

¹²⁰ P. K. Majhi, G. Schnakenburg, Z. Kelemen, L. Nyulaszi, D. P. Gates, R. Streubel, *Angew. Chem. Int. Ed.* **2013**, 52, 10080.

aldol condensation-elimination sequence by reacting paraformaldehyde or through a spontaneous 4e⁻ oxidation by air (Scheme 4.2.9). The first reactivity was actually the first report that the backbone of NHCs could be functionalized from a well-defined metal-NHC complex. This strategy presents the advantage to allow a rapid tuning of the electronic properties of the carbenic carbon and to afford a divergent optimization and construction of NHC-based catalysts in view to obtain better activities.^{79c,g}

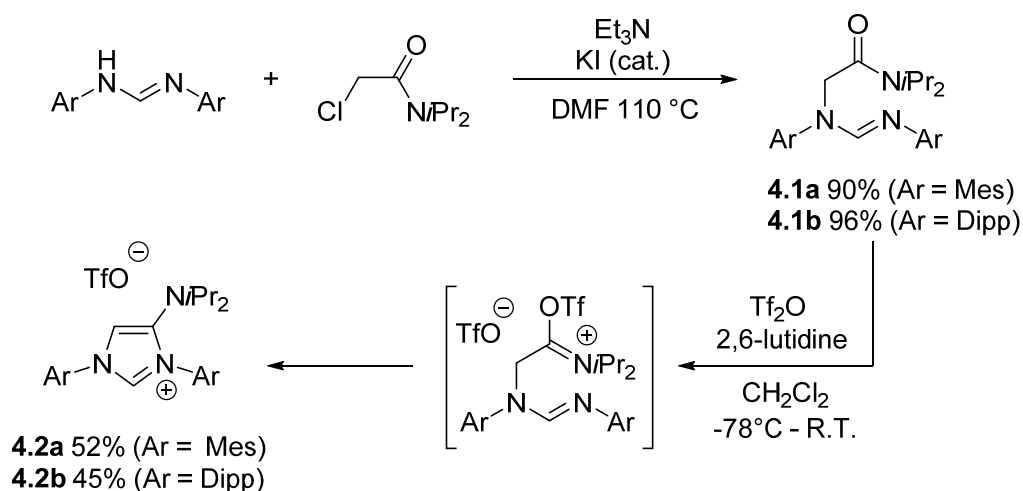


Scheme 4.2.9: Further derivatization with C4-N,O substituted [Rh(COD)CINHC] complexes developed in our group.

3. Synthesis of the imidazolium precursors

3.1. Synthesis of 4-(diisopropylamino)imidazolium salt

Following the synthetic method of 4-(dimethylamino)imidazolium **2.2** while using *N*, *N'*-diisopropyl-2-chloroacetamide, the imidazolium triflates (**IMes**^{NiPr₂})-HOTf **4.2a** and (**IPr**^{NiPr₂})-HOTf **4.2b** were obtained as white powders in average yields after recrystallization of the crude products (Scheme 4.3.1). The slightly decreased yields compared with that of dimethylamino derivatives could be mostly interpreted in terms of a higher steric hindrance of diisopropyl group compared to the dimethylamino group.



Scheme 4.3.1: Synthetic procedure towards 4-dimethylaminoimidazolium **4.2**.

The ^1H and $^{13}\text{C}\{^1\text{H}\}$ NMR spectra of imidazolium salts **4.2a** and **4.2b** were both recorded in CDCl_3 at 25°C . The ^1H NMR spectrum of **4.2a** is depicted in Figure 4.3.1. Similar to **2.2a**, the two protons on the imidazolium ring appear as a typical set of two doublets at 9.14 and 6.82 ppm with a coupling constant of 1.7 Hz. The presence of the amino group on the backbone of the imidazolyl ring renders the molecule unsymmetrical and the two mesityl substituents are inequivalents in NMR. This is reflected in the ^1H NMR spectrum by two singlet signals for the *ortho*-methyl groups. However, it appeared that the aromatic protons on the mesityl groups resonate at the same chemical shift as well as the two *para* methyl groups. This is only a coincidence. The two protons $\text{CH}(\text{CH}_3)_2$ of the two tertiary carbons of *isopropyl* group appear as one heptet at 3.4 ppm ($J = 6.8$ Hz), and each correlates with six protons $\text{CH}(\text{CH}_3)_2$ of the methyl groups, which resonate as a doublet at $\delta = 1.07$ ppm ($J = 6.8$ Hz).

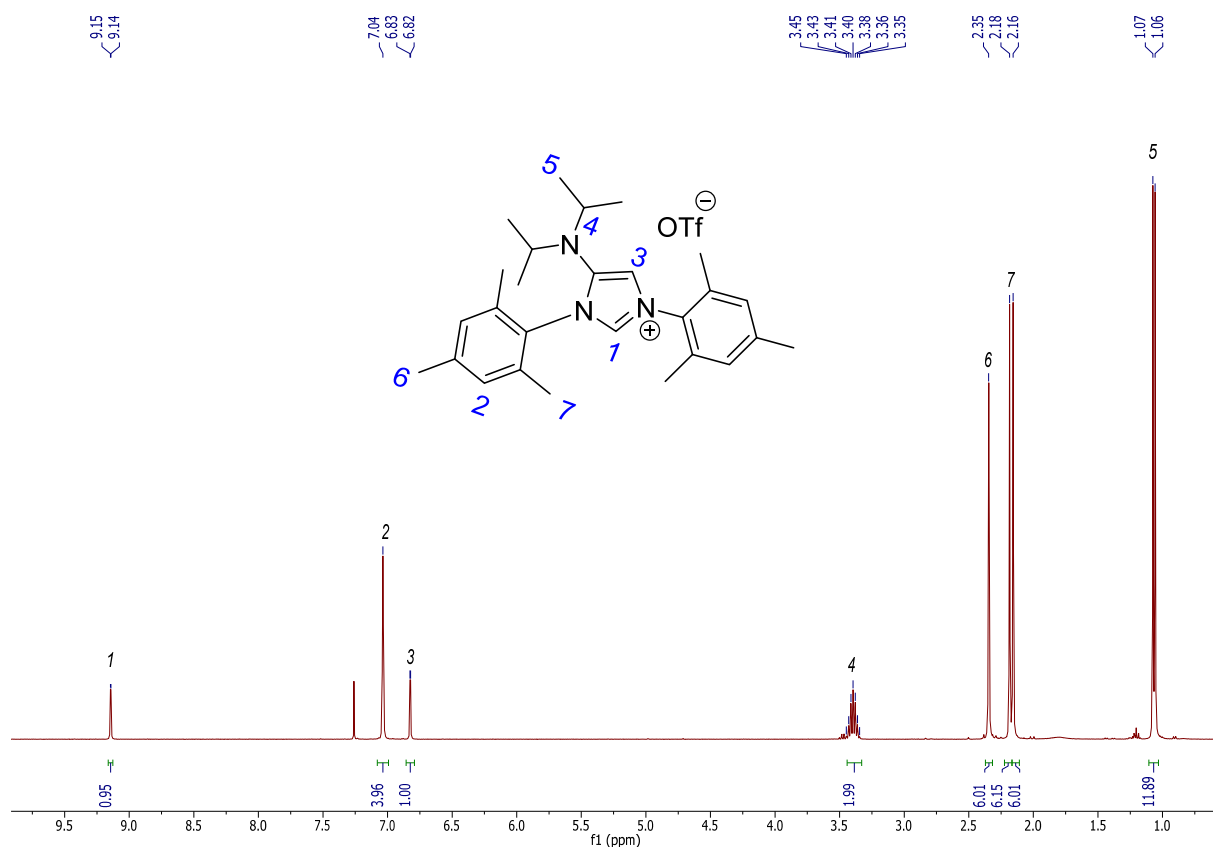


Figure 4.3.1: ^1H NMR spectrum of imidazolium salt **4.2a** (CDCl_3 , 400 MHz).

The ^1H NMR spectrum of **4.2b** is depicted in Figure 4.3.2. Similar to **2.2a**, two heterocyclic protons in **4.2b** appear as two doublets at 9.15 and 6.89 ppm. The introduction of the amino group also renders the *N*-substituents magnetically inequivalent, which could be confirmed by the different resonances of protons detected for Dipp group.

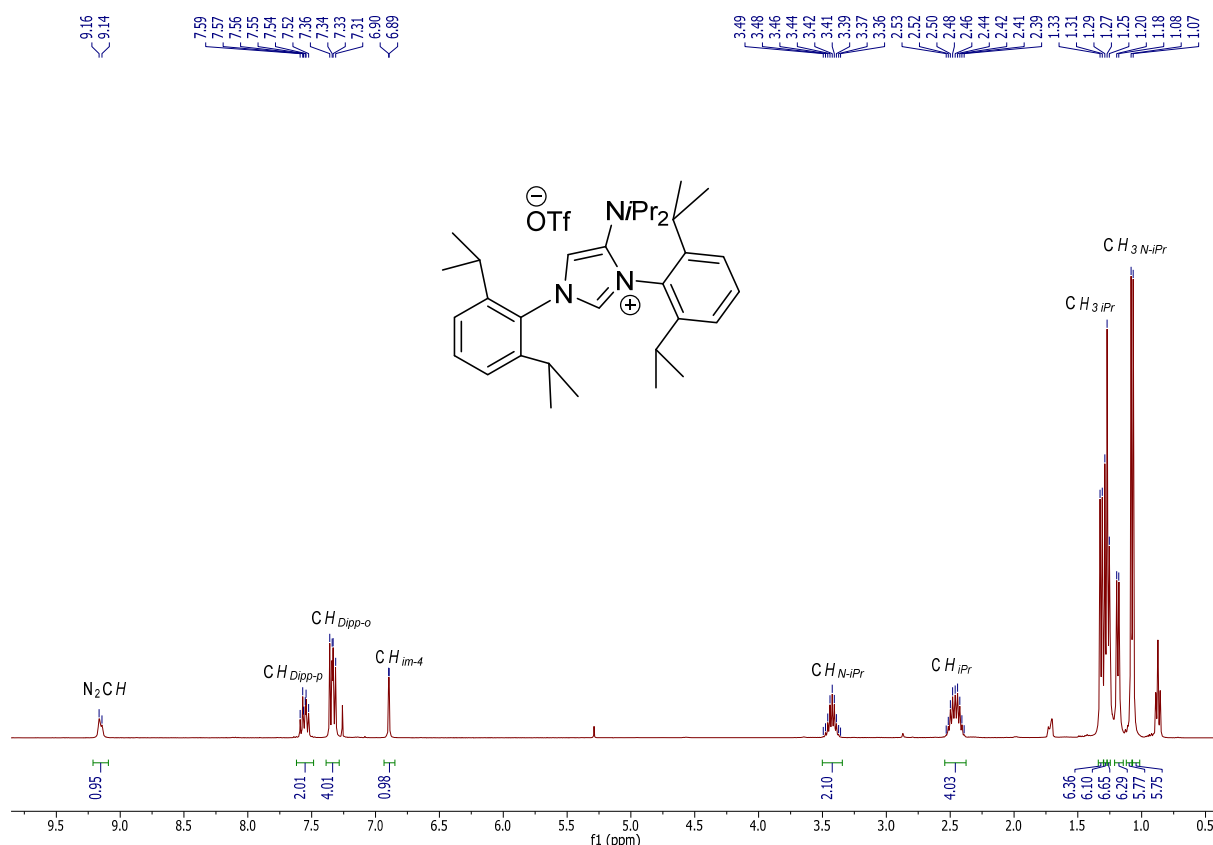
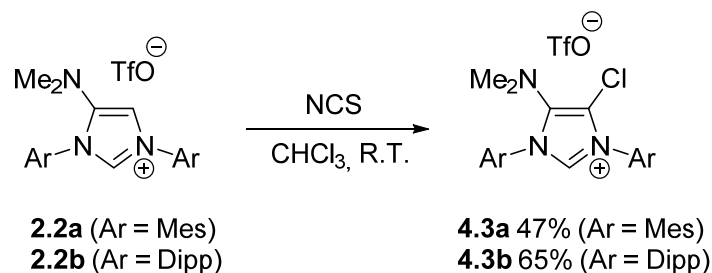


Figure 4.3.2: ^1H NMR spectrum of imidazolium salt **4.2b** (CDCl_3 , 400 MHz).

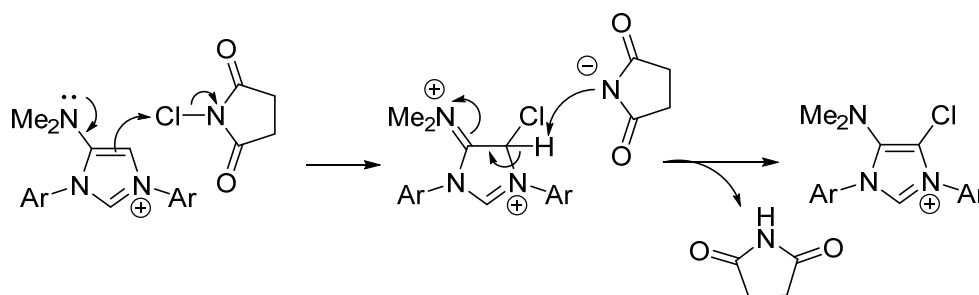
3.2. Synthesis of 4-dimethylamino-5-haloimidazolium salts

Based on the previous observation of characteristic reactivity on the further derivarization of imidazol-2-ylidene-4-olate IMes^{O^-} and 4-(isopropylamino)imidazol-2-ylidene $\text{IMes}^{\text{NH}i\text{Pr}}$ (Scheme 4.2.9), we assumed that the analogue 4-(dimethylamino)imidazol-2-ylidene $\text{IAr}^{\text{NMe}_2}$ should be able to possess the same reactivity towards electrophiles such as N-halosuccinimides as oxidative halogenating agents. Whereas no reaction occurred by mixing 4-(dimethylamino)imidazolium triflate **2.2a** with *N*-chlorosuccinimide (NCS) in CH_2Cl_2 , we were pleased to observe the disappearance of resonance of the proton on the C5 position of **2.2b** in the ^1H NMR spectrum of crude product after 30 minutes when carrying out the reaction in CHCl_3 (Scheme 4.3.2). The main reason of this discriminate reactivity in these two solvents could be the acidity of later which might assist this transformation. After quenching by water, the organic phase was separated, dried and filtered through silica to obtain the pure products (**4.3a** and **4.3b**) with average yields since a small amount of decomposition products was observed in the ^1H NMR spectrum of reaction residue.



Scheme 4.3.2: Chlorination of C5 position of monoamino imidazolium salts **4.3**.

We propose the possible mechanism shown in Scheme 4.3.3. We assumed that with the assistance of the lone electron pair of nitrogen on the C4 position, the olefinic-backbone nucleophilically attacks NCS to generate an intermediate species and succinimide which further plays the role of base to deprotonate the proton on the C5 position to regenerate the aromatic imidazolium ring.



Scheme 4.3.3: Proposed mechanism for the chlorination of the backbone of $(\text{IAr}^{\text{NMe}_2})\cdot\text{HOTf}$.

The ^1H NMR spectrum of **4.3a** is shown in Figure 4.3.3. The imidazolium proton was considerably upshifted to 9.41 ppm from that of **2.2a** at 8.86 ppm, and the resonance for carbenic carbon atom slightly upshifted to 135.7 ppm from the resonance of **2.2a** ($\delta = 134.4$ ppm), which indicates a decrease of electronic donation properties of carbenic carbon resulting from chlorinated C5-position. Meanwhile the resonance for the C5 carbon atom upshifted to 111.0 ppm from the resonance of **2.2a** ($\delta = 106.7$ ppm). The two *N*-substituted mesityl groups are magnetically inequivalent which is confirmed by the appearance of two sets of signals for *ortho* and *para* methyl groups.

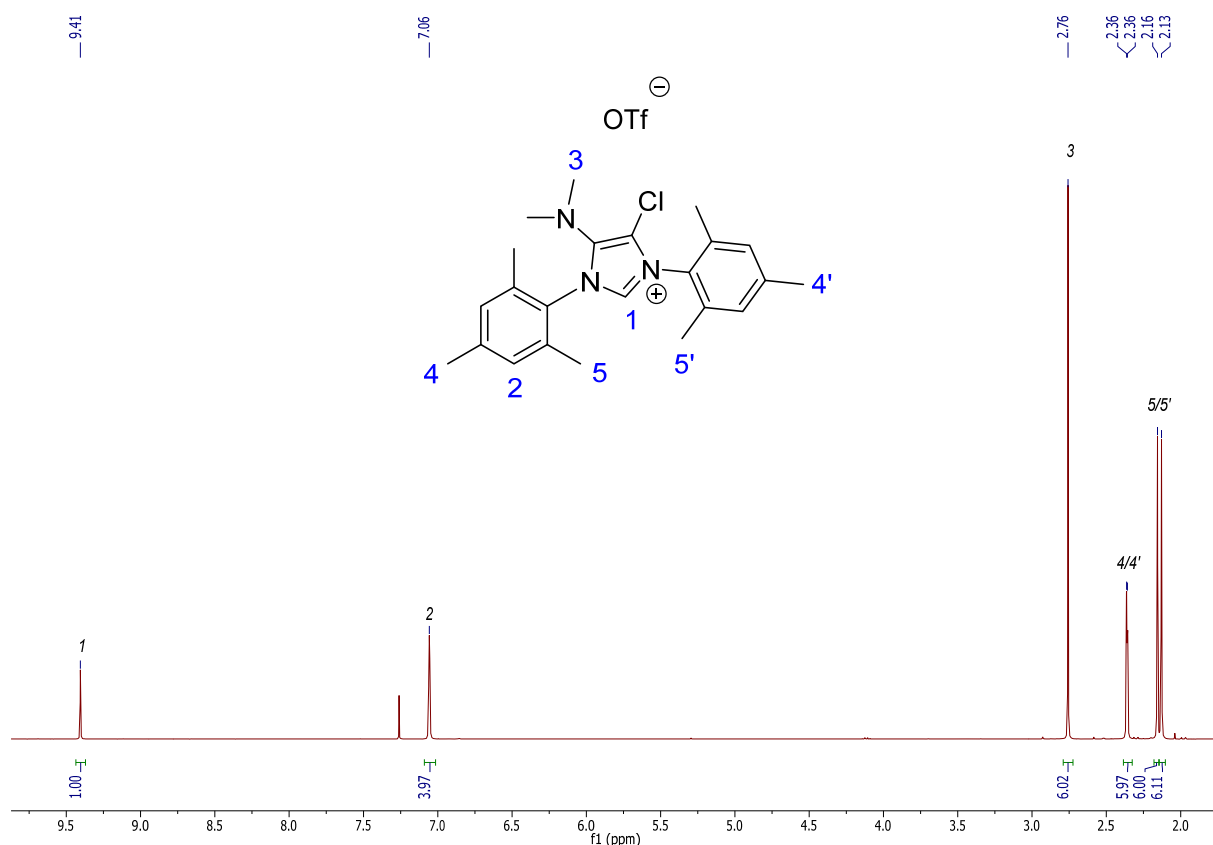


Figure 4.3.3: ^1H NMR spectrum of imidazolium salt **4.3a** (CDCl_3 , 400 MHz).

The shift of protons in **4.3b** is in the same manner as those of **4.3a** (Figure 4.3.4). The N_2CH proton (*1*) upshifted to 9.41 ppm from 8.66 ppm of **2.2b**, and the resonance for carbenic carbon atom slightly upshifted to 135.8 ppm from the resonance of **2.2a** ($\delta = 134.0$ ppm). Four sets of doublets corresponding to the four pairs of CH_3 on Dipp substituents were observed in the ^1H NMR spectrum in accordance to the C_s symmetry of the molecule. The structure of **4.3b** is confirmed by X-ray diffraction which is shown in Figure 4.3.5. The selected bond lengths and angles are shown in Table 4.3.1. The distance of new formed bond C3-Cl of 1.688(3) Å is the same as reported for IPr^{Cl_2} ,^{45a} and is typical of a C-Cl single bond.¹²¹ The C2-N1 distance [1.396(4) Å] is almost unchanged compared to those in **2.2b** as well as bond C3-N2 [1.385(4) Å]. Furthermore, bond C1-N2 slightly increases to 1.330(4) Å compared to 1.3209(17) Å in **2.2b**.

¹²¹ F. H. Allen, O. Kennard, D. G. Watson, L. Brammer, A. G. Orpen, R. Taylor, *J. Chem. Soc., Perkin Trans 2* **1987**, 0, S1.

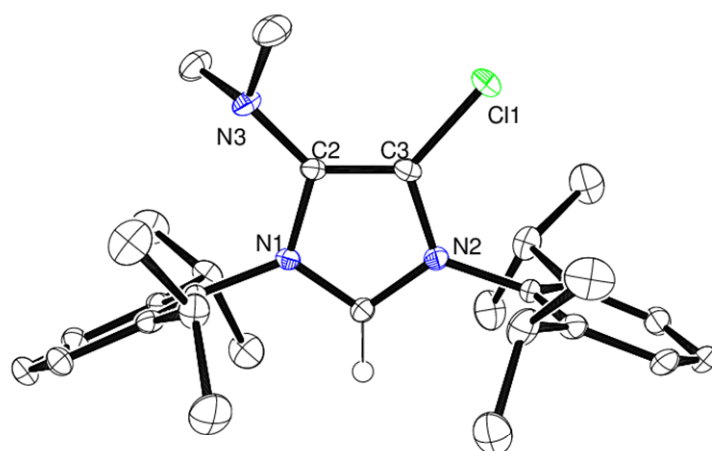
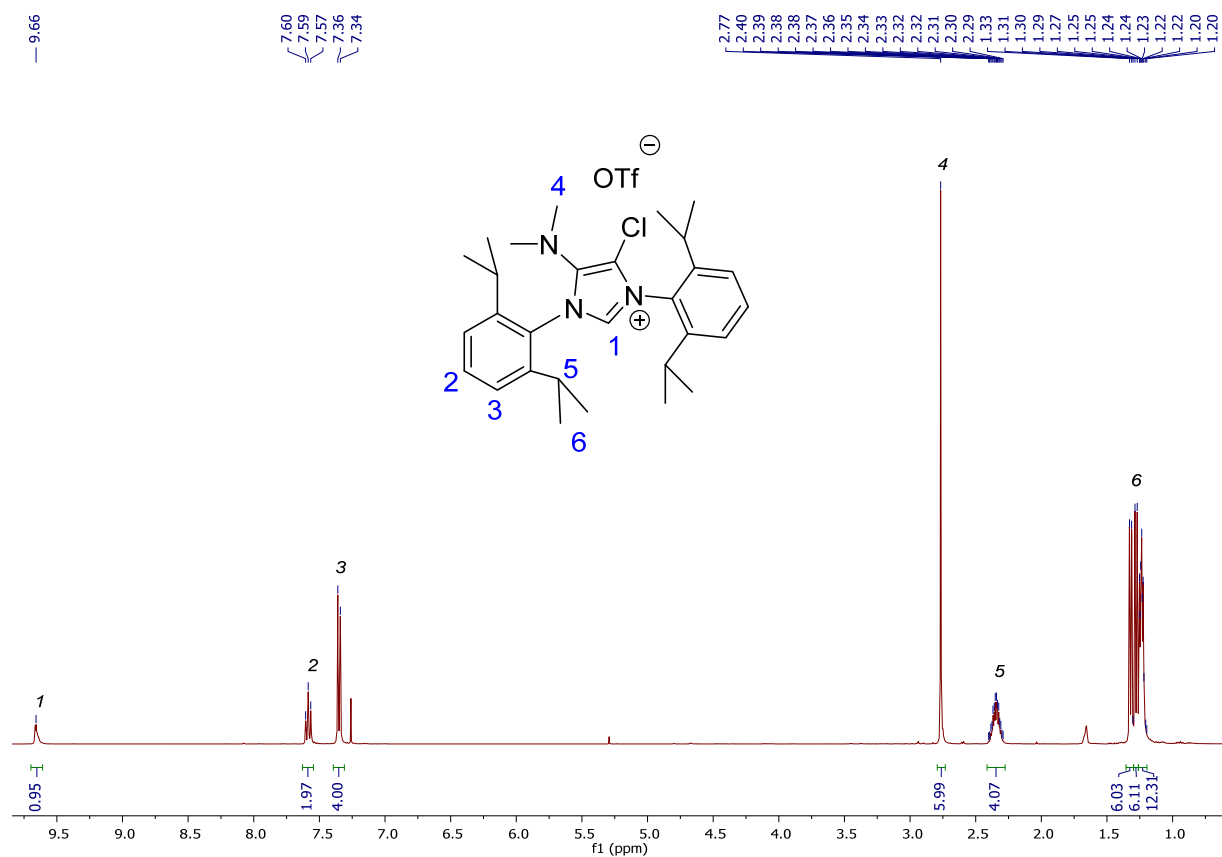


Figure 4.3.5: Molecular structure of rhodium complex **4.3b**. (Ellipsoids drawn at 30% probability level). Solvent molecule and hydrogen atoms were omitted for clarity.

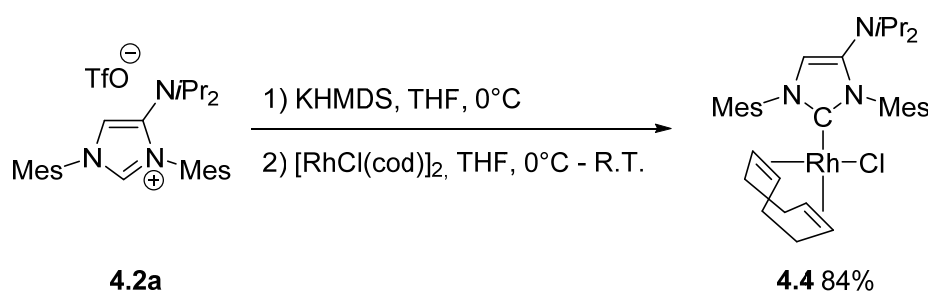
Bond length (Å)		Angles (deg)	
C1-N2	1.330(4)	N2-C1-N1	108.5(3)
C1-N1	1.330(4)	C3-C2-N3	134.0(3)
C2-C3	1.355(5)	N3-C2-N1	120.7(3)
C2-N3	1.377(4)	C2-C3-N2	108.6(3)
N1-C2	1.396(4)	C3-C2-N1	105.0(3)
N2-C3	1.385(4)	C2-C3-Cl1	130.9(3)
Cl1-C3	1.688(3)	N2-C3-Cl1	120.5(2)

Table 4.3.1: Selected bond lengths (Å) and angles (deg) in **4.3b**.

4. The electronic properties of new NHC ligands

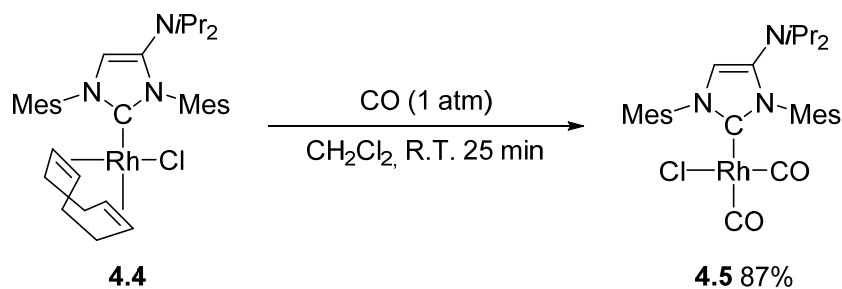
4.1. Synthesis of $[\text{Rh}(\text{IMes}^{\text{XY}})\text{Cl}(\text{CO})_2]$ complexes

In order to measure the TEP values of the new NHCs, the complexes $[\text{Rh}(\text{IMes}^{\text{XY}})\text{Cl}(\text{CO})_2]$ as model complexes are needed to be synthesized. Using the synthetic method described in Chapter 2, the complexes $[\text{RhCl}(\text{COD})(\text{IMes}^{\text{NiPr}_2})]$ (**4.4**) was obtained as a yellow powder in 84% yield after purification through flash chromatography using silica gel (Scheme 4.4.1). In the $^{13}\text{C}\{^1\text{H}\}$ NMR spectrum of **4.4**, the resonance of rhodium-ligated N_2C carbon atom appears as a doublet at 179.9 ppm ($^1J_{\text{RhC}} = 53$ Hz).



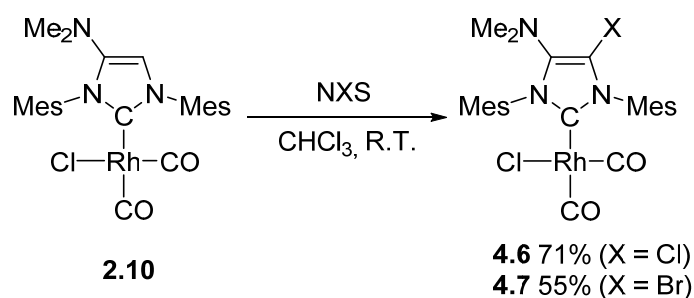
Scheme 4.4.1: Synthetic procedure of $[\text{RhCl}(\text{COD})(\text{IMes}^{\text{NiPr}_2})]$ complex **4.4**.

Bubbling CO gas into a CH_2Cl_2 solution of **4.4** until the colour of the solution turned to light yellow (for about 25 min) afforded the $[\text{Rh}(\text{IMes}^{\text{NiPr}_2})\text{Cl}(\text{CO})_2]$ complex in good yield as a pale powder after washing the residue with pentane (Scheme 4.4.2). The complex **4.5** was in particular confirmed by ^{13}C NMR spectroscopy where three sets of typical doublets appear at 185.3 (d, $J_{\text{RhC}} = 54$ Hz, Rh-CO), 183.1 (d, $J_{\text{RhC}} = 76$ Hz, Rh-CO), 173.9 (d, $J_{\text{RhC}} = 44$ Hz, $\text{N}_2\text{C}_{\text{carb}}$) respectively. The two carbonyl stretching frequencies ($\nu_{\text{CO}}^{\text{av}}$) were measured at 2076.4 and 1993.5 cm^{-1} in CH_2Cl_2 at 25°C. A TEP value of 2048.2 cm^{-1} for **4.5** is calculated by the equation ($\text{TEP} = 0.8001 \nu_{\text{COav}} + 420.0 \text{ cm}^{-1}$) which is 0.6 cm^{-1} less than $[\text{Rh}(\text{IMes}^{\text{NMe}_2})\text{Cl}(\text{CO})_2]$ **2.10**.



Scheme 4.4.2: Synthetic procedure for $\text{Rh}(\text{IMes}^{\text{NiPr}_2})\text{Cl}(\text{CO})_2$ complex **4.5**.

In analogy to the previous results obtained in the group on the functionalization of imidazol-2-ylidene ligands after complexation,^{79c,g} we decided to carry out the same chlorination procedure developed for the imidazolium precursors to derivative the backbone of Rh(IMes^{NMe₂})Cl(CO)₂ **2.10**. This would avoid the somewhat difficult complexation step starting from the imidazolium precursors. Fortunately, using the same reaction conditions, Rh(IMes^{NMe₂,Cl})Cl(CO)₂ **4.6** was formed in good yield after 2 hours at room temperature (Scheme 4.4.3). The disappearance of the signal of the proton on imidazolyl ring in the ¹H NMR spectrum proved the success of the chlorination on the backbone. Three new resonances in ¹³C NMR spectrum appeared at 185.0 ppm (d, *J*_{RhC} = 55 Hz, Rh-CO), 182.9 ppm (d, *J*_{RhC} = 75 Hz, Rh-CO), and 174.5 ppm (d, *J*_{RhC} = 46 Hz, N₂C_{carb}). The two carbonyl stretching frequencies (*ν*_{CO}^{av}) were recorded at 2079.6 and 1996.4 cm⁻¹ and the calculated TEP value is 2050.6 cm⁻¹ which is 1.8 cm⁻¹ higher than that of Rh(IMes^{NMe₂})Cl(CO)₂ **2.10** revealing the decrease of the electronic donation of the corresponding carbene center after chlorination. This result prompted us to study the halogenation with Br or I atoms. Under the same conditions using NBS instead of NCS, the target complex [Rh(IMes^{NMe₂,Br})Cl(CO)₂] **4.7** was obtained in average yields since a small amount of decomposition products was found at the end of the reaction (Scheme 4.4.3). The TEP value of **4.7** is 2050.3 cm⁻¹ which is close to that of **4.6**. Unfortunately, the less reactive NIS failed to react and only gave unidentified decomposition products. We assumed the size of iodine is much larger than that of chlorine and bromine and it would hamper the nucleophilic attack of the “enamine-type” backbone.



Scheme 4.4.3: Synthesis of [Rh(IMes^{NMe₂,X})Cl(CO)₂] complexes **4.6** and **4.7**.

Thereby, an overview of the electronic properties of the different backbone-substituted **IMes** ligands is presented in the Figure 4.4.1. For a complete comparison, we also added the relevant imidazole-2-ylidenes known in literature.

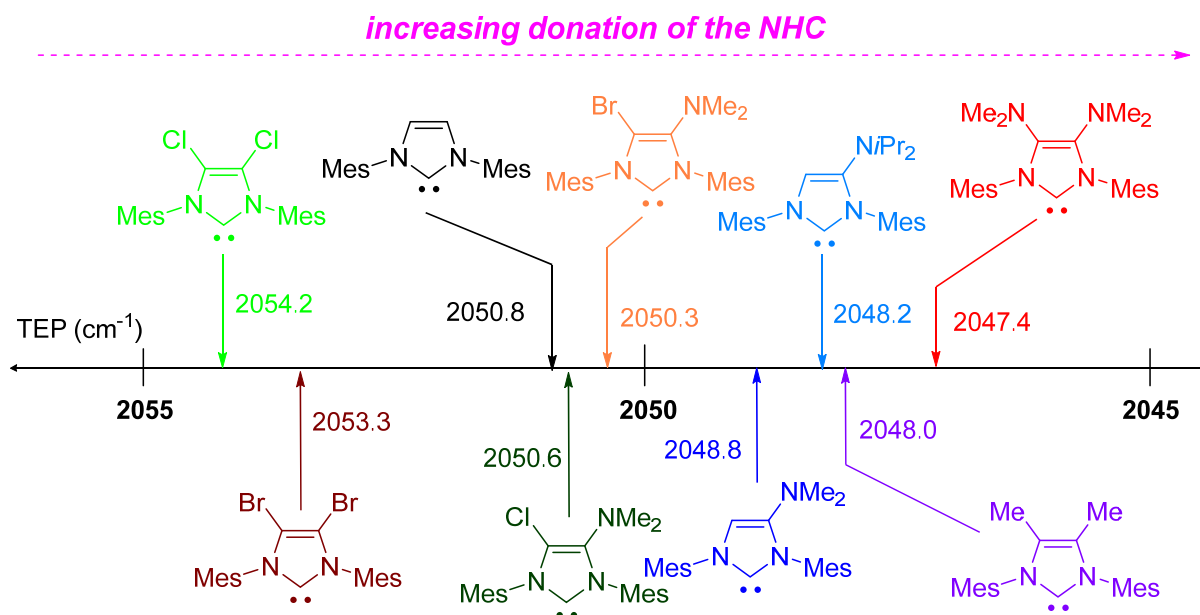
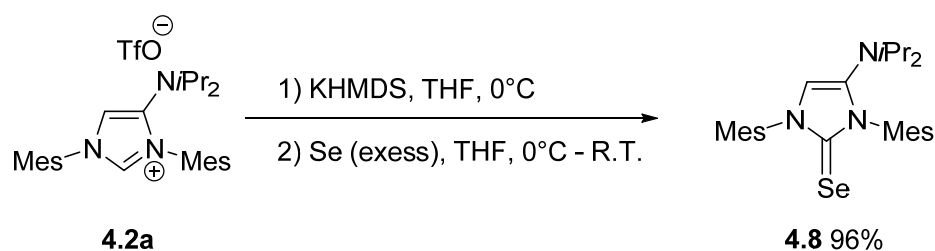


Figure 4.4.1: Electronic properties of backbone-substituted imidazol-2-ylidenes.

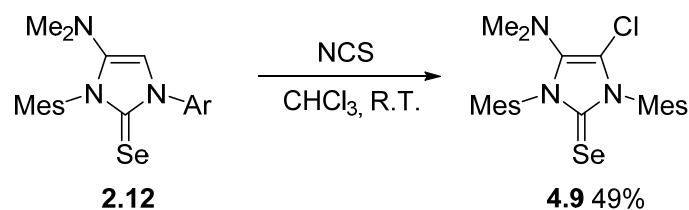
4.2. Synthesis of the selenoureas [(IMes^{XY})=Se]

In order to understand the π -accepting ability of the new ligands, the titled selenourea compounds are needed to be synthesized. Following the methods described in Chapter 2, compound [(IMes^{NiPr₂})=Se] **4.8** was obtained quantitatively. The ⁷⁷Se NMR spectrum recorded in CDCl₃ at 25 °C shows a resonance at 35.8 ppm which is 3.6 ppm upshifted compared to [(IMes^{NMe₂})=Se] **2.12** indicating a little increase of π -accepting ability with diisopropylamino on the backbone.



Scheme 4.4.4: Synthesis of [(IMes^{NiPr₂})=Se] compound **4.8**.

The same conditions as in Scheme 4.3.3 was applied for the synthesis of [(IMes^{NMe₂,Cl})=Se] **4.9** by adding NCS to a CHCl₃ solution of [(IMes^{NMe₂})=Se] **2.12**. Finally, **4.9** was obtained as a green-yellow powder in average yield after purification through a small plug of silica gel (Scheme 4.4.5). The ⁷⁷Se NMR spectrum was recorded in CDCl₃ at 25 °C showing a resonance of the ⁷⁷Se atom at 67.8 ppm which reveals a large increase of π -accepting ability of **4.9** attributed to the electron-withdrawing nature of the chlorine substituent.



Scheme 4.4.5: Synthesis of [(IMes^{NMe₂,Cl})=Se] compound **4.9**.

An overview of the ranking of the π -accepting abilities of the different backbone-functionalized imidazole-2-ylidenes is represented in Figure 4.4.2.

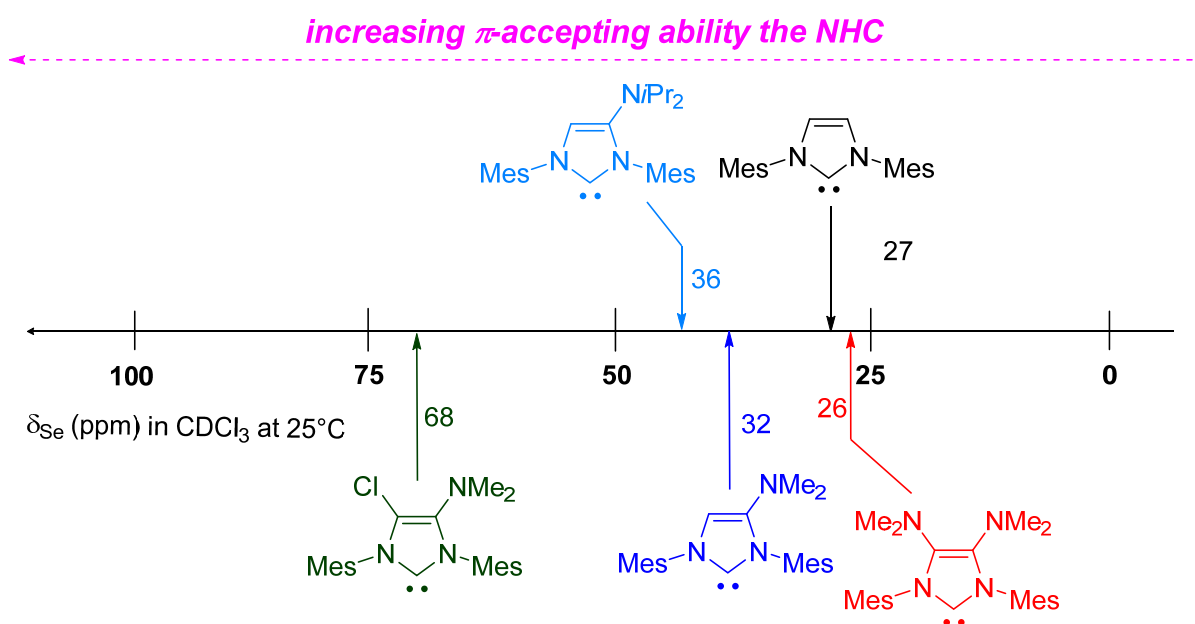


Figure 4.4.2: π -accepting ability ranking of the synthesized imidazol-2-ylidenes based on the chemical shift in ^{77}Se NMR spectra of selenoureas [(IMes^{XY})=Se].

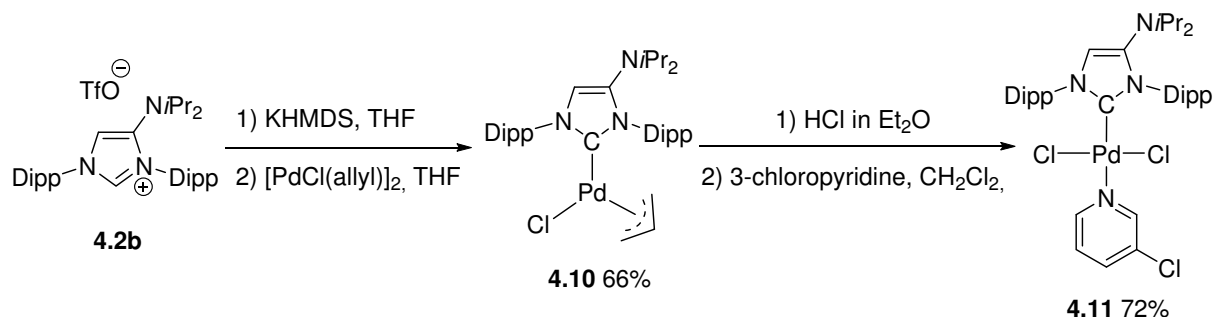
5. Studies of the catalytic properties in palladium-catalyzed Buchwald-Hartwig amination

5.1. Synthesis of PEPPSI-type Palladium pre-catalysts

In order to evaluate the catalytic influence of the further derivatization of imidazol-2-ylidenes in palladium-catalyzed arylative amination, the same type of PEPPSI-type palladium pre-catalyst was synthesized bearing newly functionalized **IPr**^{NiPr₂}, **IPr**^{NMe₂,Cl}, **IPr**^{NMe₂,Br} and tested in Buchwald-Hartwig amination comparing to the ones which have already been studied in the chapter 1 and the those reported in literature.

Following the synthetic method described in chapter 2 for complex **2.14**, the palladium complex Pd-PEPPSI-IPr^{NiPr₂} **4.11** was obtained in an overall yield of 47% in a two-step

sequence (Scheme 4.5.1). The lower yield compared to **2.14** could be attributed to the higher hindrance of corresponding generated NHC.



Scheme 4.5.1: Synthesis of PEPPSI-Pd-IPr^{NiPr₂} complex **4.11**.

The ¹H spectrum of complex **4.11** is depicted in Figure 4.5.1 and is similar to that of monodimethylamino analogue **2.14**. The four doublets ranging from 1.73 to 1.14 ppm correspond to the *iPr* group on aryl substituents while the ones on the amino group appear as one doublet at 1.07 ppm. The structure of **4.11** was established by an X-ray diffraction analysis (Figure 4.5.2). The Pd-C_{carb} bond length of 1.9718(16) Å is almost the same as that in **2.14**, while N1-C2 bond is slightly longer than that in **2.14** thanks to increase of electron donation which improved the n-σ* interaction.⁸¹ As the same observation of **2.17**, the two *Dipp* substituents are significantly twisted compared to orthogonality to the imidazolyl ring due to the much more sterically hindered *NiPr*₂ group compared to NMe₂ analogue.

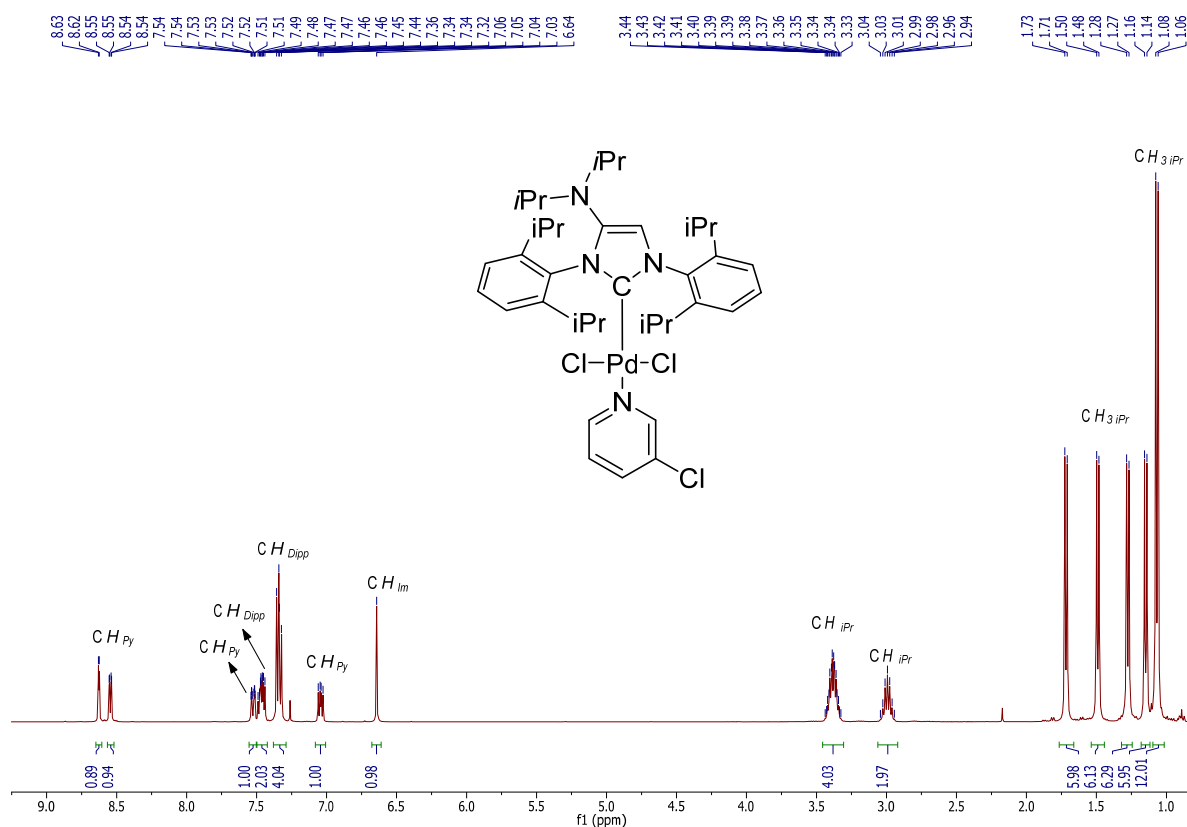


Figure 4.5.1: ^1H NMR spectrum of palladium complex **4.11** (CDCl₃, 400 MHz).

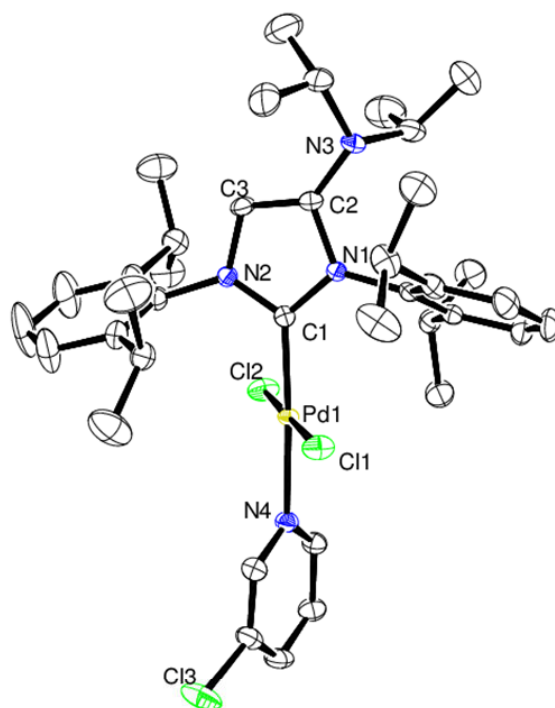
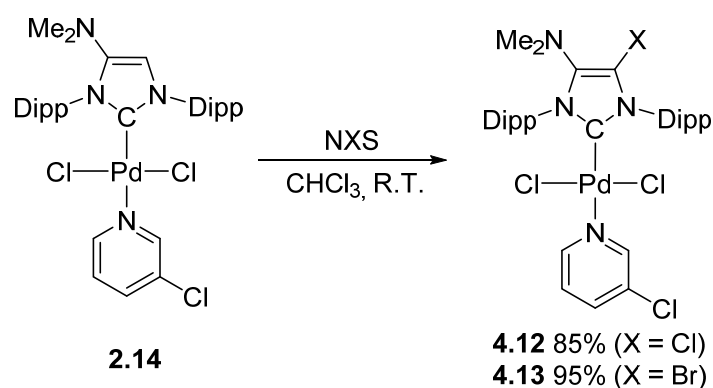


Figure 4.5.2: Molecular structure of palladium complex **4.11** (molecule A, ellipsoids drawn at 30% probability level). Hydrogen atoms and solvent molecules removed for clarity.

Bond length (Å)		Angles (deg)	
Pd1-C1	1.9718(16)	N1-C1-N2	105.54(13)
Pd1-N4	2.1047(14)	C1-Pd1-Cl1	91.88(5)
C1-N1	1.363(2)	C1-Pd1-Cl2	89.20(5)
C1-N2	1.348(2)	C1-Pd1-N4	177.06(6)
C2-C3	1.348(2)	N1-C1-Pd1-Cl1	64.68
C2-N3	1.391(2)		
N1-C2	1.421(2)		
N2-C3	1.388(2)		

Table 4.5.1: Selected bond lengths (Å) and angles (deg) in **4.11**.

Encouraged by the results of direct halogenation of $[\text{Rh}(\text{IMes}^{\text{NMe}_2})\text{Cl}(\text{CO})_2]$, we continued to study the same reactivity in palladium complexes. As expected, adding NCS to a CHCl_3 solution of $\text{Pd-PEPPSI-IPr}^{\text{NMe}_2}$ **2.14** at room temperature led to the synthesis of $\text{Pd-PEPPSI-IPr}^{\text{NMe}_2,\text{Cl}}$ **4.12** in 85% yield after purification through a small plug of silica gel. In the same manner, $\text{Pd-PEPPSI-IPr}^{\text{NMe}_2,\text{Br}}$ **4.13** was synthesized in 95% yield as a yellow powder (Scheme 4.5.2). The same decomposition was observed by ^1H NMR after adding NIS to a chloroform solution of **2.14**.



Scheme 4.5.2: Synthesis of $\text{PEPPSI-Pd-IPr}^{\text{NMe}_2,\text{X}}$ complexes **4.12** and **4.13** under very mild conditions.

In the ^1H spectrum of complex **4.12** depicted in Figure 4.5.3, there is only one multiplet signal for the protons of two tertiary carbons of *isopropyl* group after introduction of chlorine on backbone whereas they are both two individual resonances in the ^1H spectrum of **4.13**. The two *N*-substituted Dipp groups in both complexes are still in magnetically different environment since the nature of the two groups on the heterocyclic ring is different. Unfortunately, we did not succeed in obtaining single crystals of **4.12** suitable for an X-ray diffraction analysis. The carbenic carbons in **4.12** and **4.13** appear at 152.0 and 153.2 ppm respectively, these values are downfield-shifted compared to the resonance in **2.14** at 149.3 ppm.

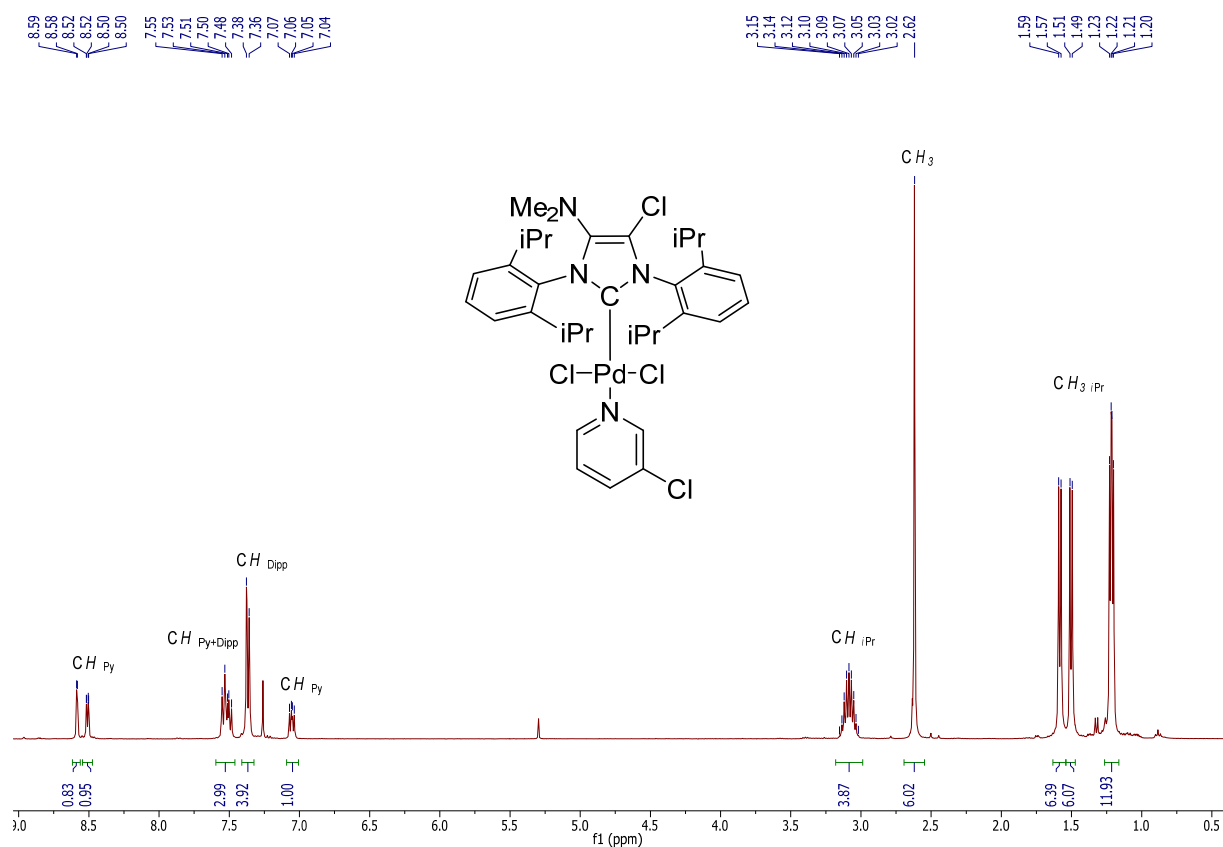


Figure 4.5.3: ¹H NMR spectrum of palladium complex **4.12** (CDCl₃, 400 MHz).

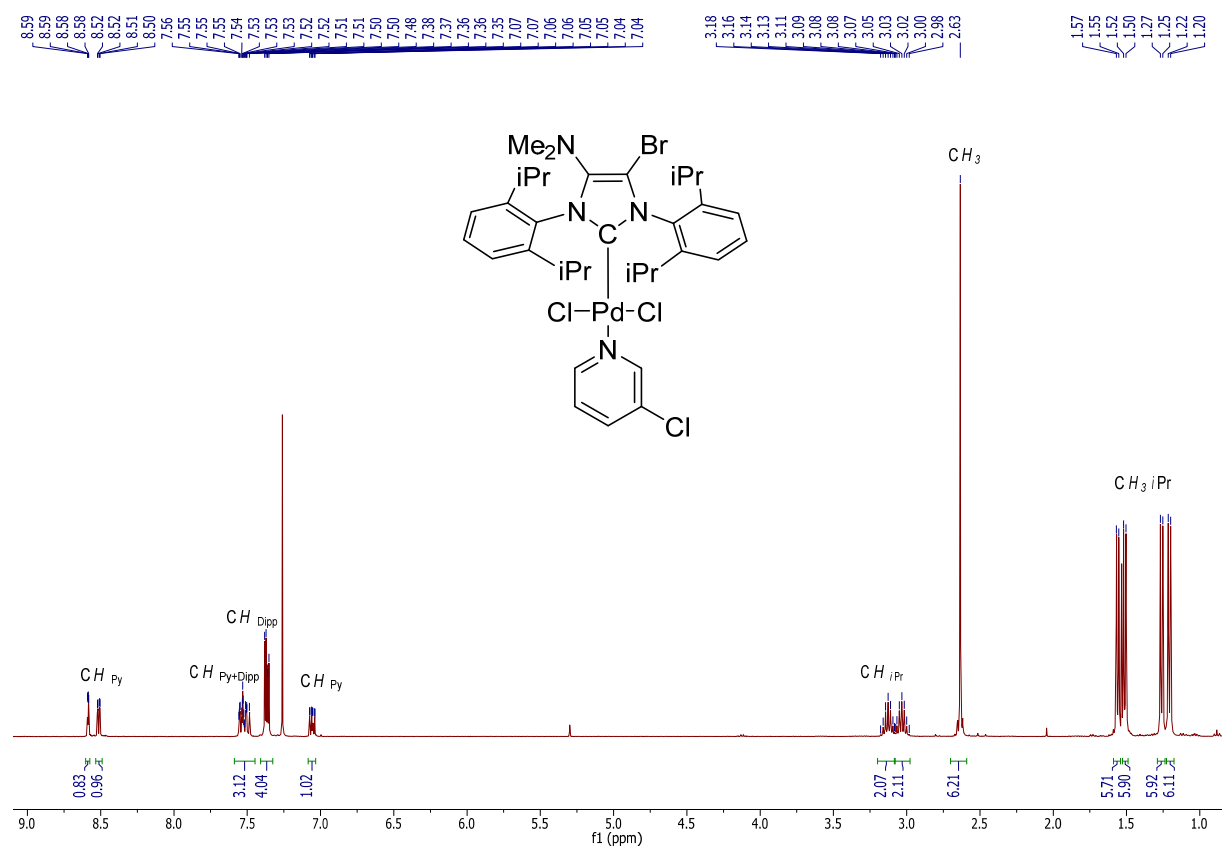


Figure 4.5.4: ¹H NMR spectrum of palladium complex **4.13** (CDCl₃, 400 MHz).

In contrast, the single crystals of **4.13** suitable for an X-ray diffraction experiment were obtained through the diffusion of pentane into a concentrated CH_2Cl_2 solution. However, the collected data were not good enough to describe the information of the bonds. The percent buried volume ($\%V_{\text{bur}}$) of the above described palladium complexes **4.11** and **4.13** were calculated by their crystal structure data. The results are summarized in Table 4.5.2 together with **2.14** and **2.17**. The results reveal that changing the size of mono-amino group or grafting another functional group can equally tune the steric properties of the corresponding NHCs while the later enables to modify the electronic pattern.

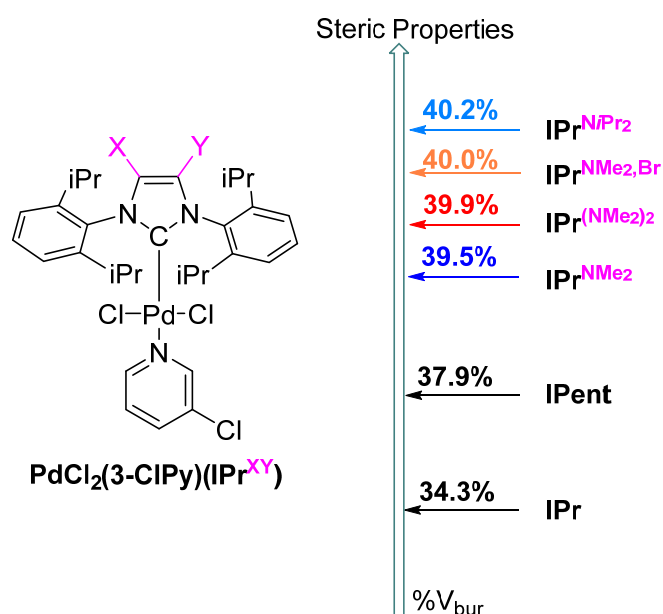


Table 4.5.2: Percent buried volume ($\%V_{\text{bur}}$) of corresponding backbone functionalized NHCs.

5.2. Evaluation of catalytic properties in Buchwald-Hartwig amination

The catalytic efficiencies of the newly formed Pd-PEPPSI pre-catalysts were then studied in the Buchwald-Hartwig amination at room temperature in order to evaluate the influence of the above NHC backbone functionalizations, and to understand which of the steric or electronic factors is prominent in this reaction. The amination of 4-chloroanisole by morpholine at 25 °C was chosen as the model reaction. In order to exclude the side effect coming from the impurity of base, we strictly purified the potassium *tert*-butoxide KO*t*Bu to remove any trace of KOH or *t*BuOH formed by the hydrolysis. This purified base was then stored and weighted in a glove box to avoid any further hydrolysis. Parallel kinetic experiments were carried out by using pre-catalysts **2.14**, **2.17**, **1.1**, **1.2**, **1.11**, **4.11**, **4.12**, and **4.13** respectively. The kinetic curves are displayed in Figure 4.5.5.

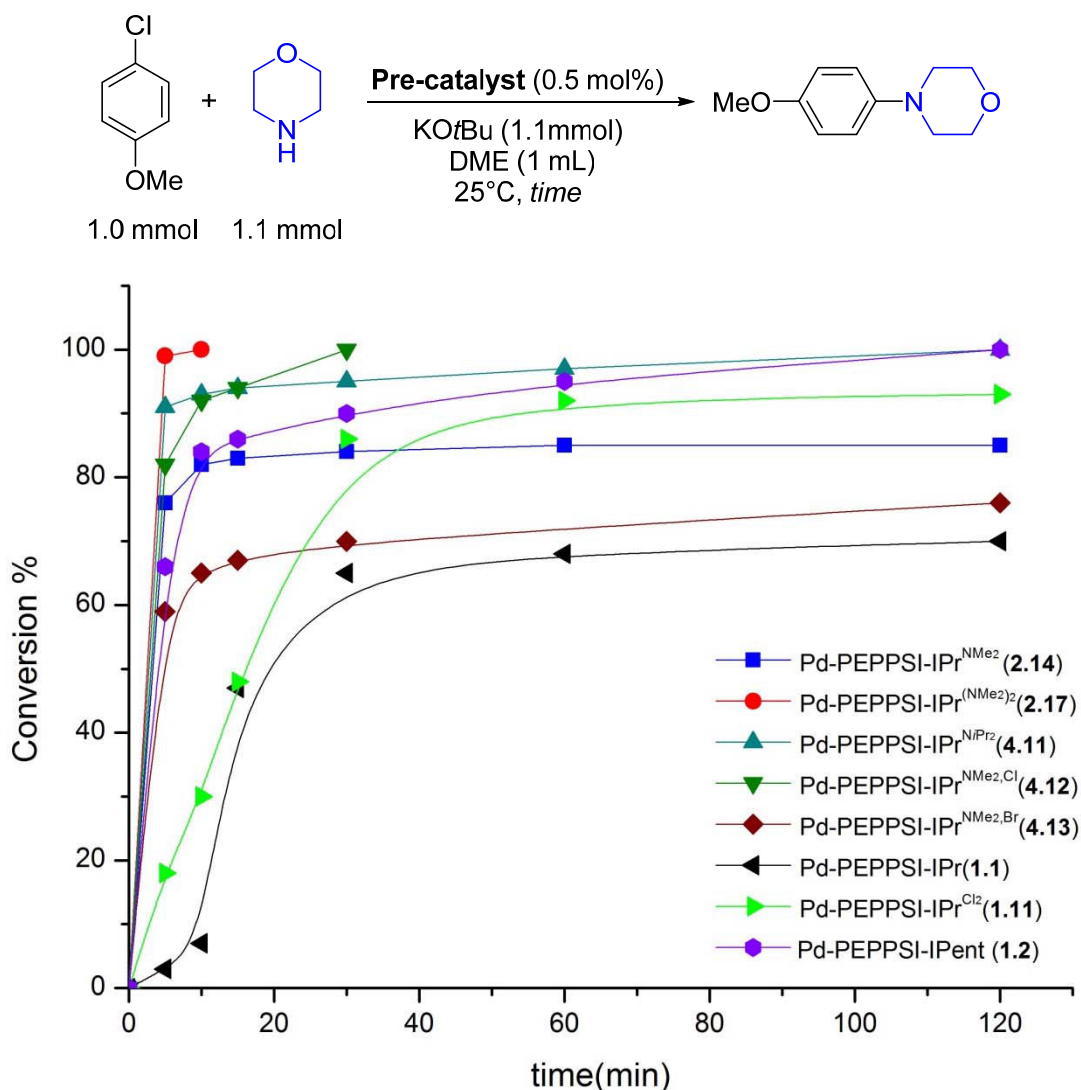


Figure 4.5.5: Parallel kinetic amination between 4-chloroanisole and morpholine at 25 °C.

First, it should be noticed that the catalytic efficiency of all the catalysts was significantly increased by using the purified KOtBu compared to the unpurified one (see chapter 2). The complex **2.17** was found to be still the most efficient catalyst in this transformation, with a total conversion in less 10 min (red curve). The complexes **2.14** and **1.1** showed less efficient giving 85% and 68% of conversion after 2 hours under the same conditions (blue and black curves). Replacing NMe₂ by more steric NiPr₂ has a positive effect on the outcome of this reaction, as the complex **4.11** was found to be more efficient than **2.14**. A 91% conversion was obtained after 5 min and the reaction totally finished in 2 hours (light blue curve). Moreover, the catalytic influence of the sequential halogenation of IPr^{NMe₂} led to an improved catalytic activity when chlorine was introduced (see deep green curve) while adding bromine on the backbone had a negative effect (see brown curve) might due to the lower catalyst stability. Finally, catalyst **1.2** bearing IPent was also tested to evaluate its catalyst activity towards the above amination and it was found to be less efficient than complexes **2.17**, **4.11**

and **4.12** (see violet curve). Furthermore, precatalyst **1.11** supported by **IPr**^{Cl₂} performed much better than **IPr** analogue (see bright green curve). The results of this preliminary catalytic evaluation well matches the assumption that the steric factors are more dominant than electronic factors in Pd-catalyzed arylation amination, which can be clearly rationalized by the observation of higher catalytic efficiency of catalysts **4.11** and **4.12** compared to **2.14**.

The outstanding results given by the above study encouraged us to explore the pre-catalysts in the more challenging amination of 2-chloroanisole which is more sterically hindered. Under the standard conditions, pre-catalyst **2.17** showed the best efficiency, with a 91% conversion after only 5 min and a full conversion in less than 1 hour (red curve). This result advantageously compares with the most active system known up to date reported by Nolan group and based on a [Pd(SIPr)(cin)Cl] pre-catalyst.⁷¹ Unlike the above amination with 4-chloroanisole as substrate, under the same conditions, pre-catalysts **2.14** and **1.1** with **IPr**^{NMe₂} and **IPr** respectively were much less efficient, and 34% and 15% of 2-chloroanisole were converted after 2 hours (blue and black curves). In contrast, pre-catalyst **4.11** bearing **IPr**^{NiPr₂} was much more efficient than **2.14** and 83% conversion was observed in the first 5 min and 90% conversion was obtained after 2 hours of the reaction (see light blue curve), indicating that the increase of the hindrance of amino groups had an important effect in this amination involving more sterically hindered substrates. Moreover, the same trend has been found when pre-catalyst **4.12** was employed as catalyst. In the first 5 min, 80% conversion was observed through GC chromatography and 96% conversion in 2 hours revealing that the chlorine atom on the second position of the backbone largely improves the catalytic activity (deep green curve). Once again, the **IPent** ligand has been found to be less efficient than **IPr**^{(NMe₂)₂}, **IPr**^{NiPr₂} and **IPr**^{NMe₂,Cl} in the amination with 2-chloroanisole as substrate (see violet curve). And finally we found that **IPr**^{Cl₂} performed even worse than **IPr** in this reaction mostly due to less stability of palladium catalyst in the medium of the reaction (see bright green curve).

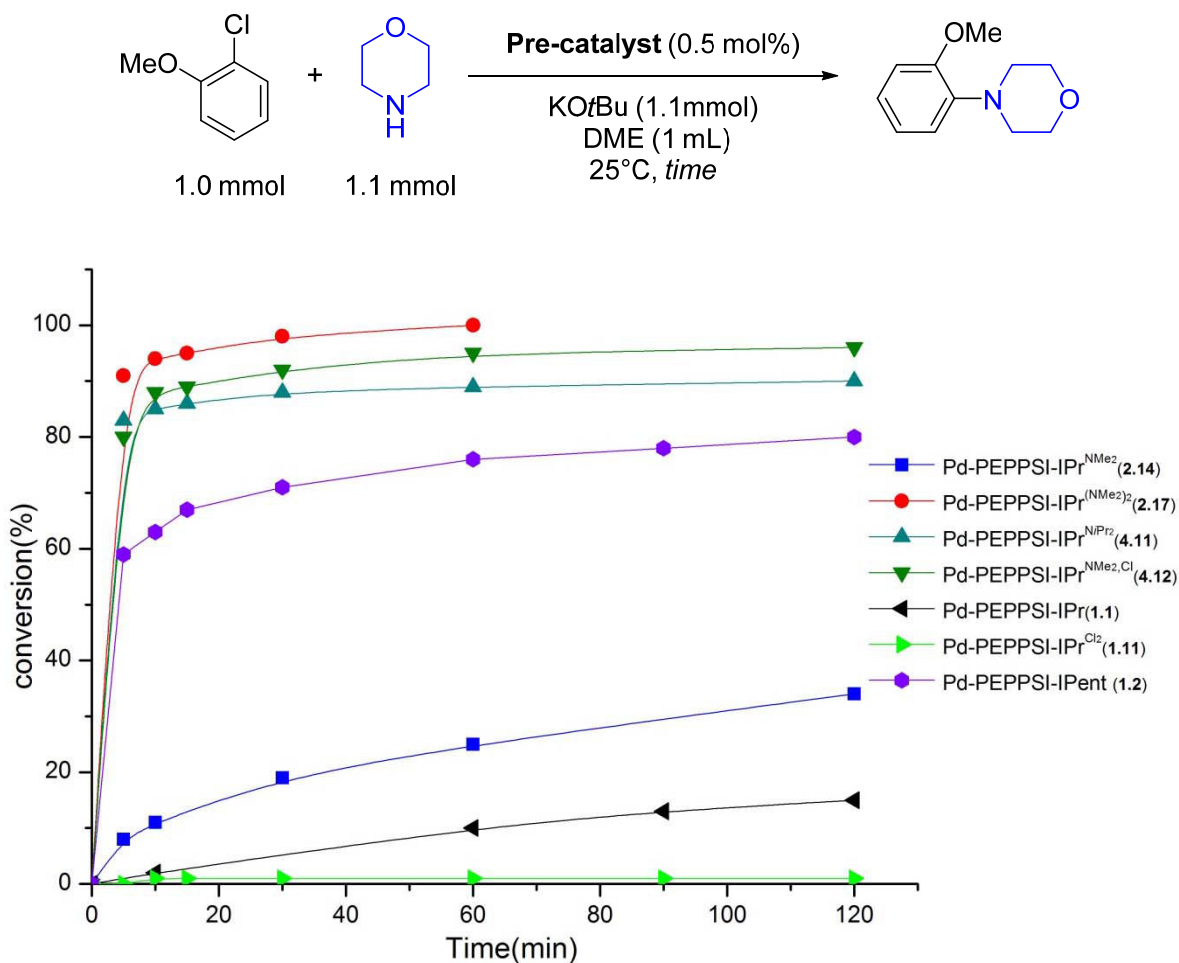


Figure 4.5.6: Parallel kinetic studies on the amination of 2-chloroanisole with morpholine at 25 °C.

5.3. Conclusion

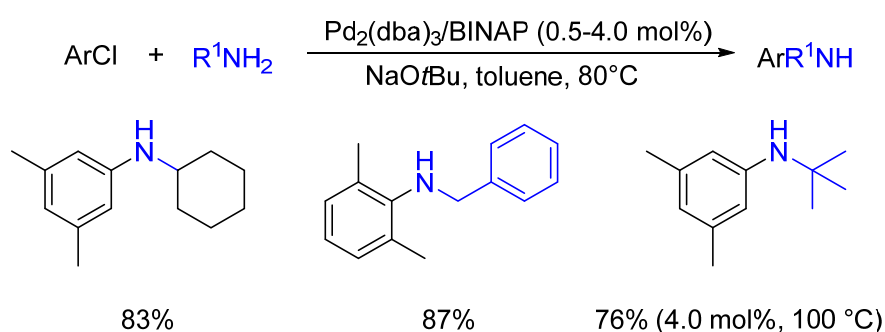
In this part, Pd-PEPPSI type pre-catalysts bearing further backbone derivatization $\text{IPr}^{\text{NiPr}_2}$ and $\text{IPr}^{\text{NMe}_2, \text{X}}$ have been prepared by use of classic complexation for Pd-PEPPSI- $\text{IPr}^{\text{NiPr}_2}$ and direct halogenation for Pd-PEPPSI- $\text{IPr}^{\text{NMe}_2, \text{X}}$, and its influence in Pd-catalyzed arylation amination has been evaluated by means of kinetic studies with 4-chloroanisole or 2-chloroanisole and morpholine as coupling partners. The comparison of catalytic efficiencies was carried out among different types of Pd-PEPPSI- $\text{IPr}^{\text{X}, \text{Y}}$ and one of the most efficient Pd-PEPPSI-IPent catalyst reported in literature. According to the catalytic results, it is obvious that the two different strategies which further modified $\text{IPr}^{\text{NMe}_2}$ to $\text{IPr}^{\text{NiPr}_2}$ and $\text{IPr}^{\text{NMe}_2, \text{Cl}}$ led to a significant improvement of the catalytic efficiencies of the corresponding palladium pre-catalysts, albeit to a lower extent compared to the bis-aminated carbene $\text{IPr}^{(\text{NMe}_2)_2}$, formally derived from $\text{IPr}^{\text{NMe}_2}$ by adjunction of a second dimethylamino group. The observed effect could be mostly assigned to steric factors while the supplementary electronic donation of $\text{IPr}^{(\text{NMe}_2)_2}$ would mostly enhance the stability of the catalytic species.

6. Buchwald-Hartwig Amination with challenging bulky primary alkyl amines

6.1. Introduction

In the last section we have demonstrated the different reactivity of each backbone functionalized PEPPSI type pre-catalyst $[\text{Pd}(\text{IPr}^{\text{X,Y}})(3\text{-ClPy})\text{Cl}_2]$ in Buchwald-Hartwig Amination revealing that $[\text{Pd}(\text{IPr}^{\text{NMe}_2})_2](3\text{-ClPy})\text{Cl}_2$ (**2.17**) and $[\text{Pd}(\text{IPr}^{\text{NiPr}_2})(3\text{-ClPy})\text{Cl}_2]$ (**4.11**) are the most active pre-catalysts in the model reactions while $[\text{Pd}(\text{IPr}^{\text{NMe}_2,\text{Cl}})(3\text{-ClPy})\text{Cl}_2]$ (**4.12**) shows slightly inferior catalytic properties. Furthermore, it has been found that in presence of sterically demanding substrates, the two former palladium pre-catalysts performed equally well. We were thus interested in employing them in more challenging arylative amination reaction utilizing highly hindered primary alkylamines which remains less explored in last decades mostly due to the lack of efficient ligands.

Indeed, looking at the literature, rare examples of the *N*-arylation of hindered primary amines have been reported. As early as 2000, Buchwald and co-workers reported a Pd/BINAP catalytic system which was shown to be more efficient in the Buchwald-Hartwig amination with a variety of amines including primary amines than the classic monodentate phosphine ligands. However, high catalyst loading (4.0 mol%) and temperature (100°C) were necessary to achieve a average yield of product while involving *tert*-butyl amine as a substrate (Scheme 4.6.1).¹²²

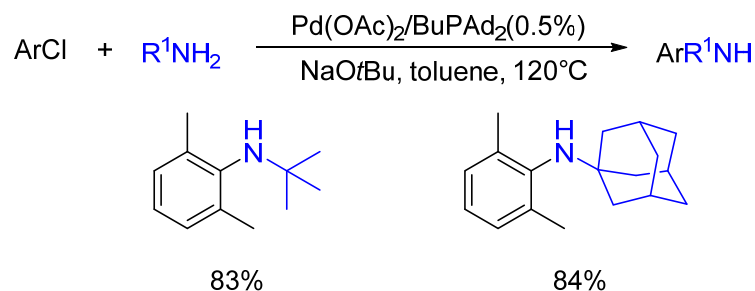


Scheme 4.6.1: Pd-catalyzed amination reaction with primary aliphatic amines using $\text{Pd}_2(\text{dba})_3/\text{BINAP}$ catalytic system reported by Buchwald.

Later, Beller and co-workers found that using more hindered phosphine ligand BuPAD₂, both aryl chlorides and primary amines bearing sterically demanding substituents could be

¹²² J. P. Wolfe, S. L. Buchwald, *J. Org. Chem.* **2000**, 65, 1144.

suitable coupling partners in *N*-arylation. However, elevated temperatures (120°C) were required which limited the scope of substrates (Scheme 4.6.2).¹²³

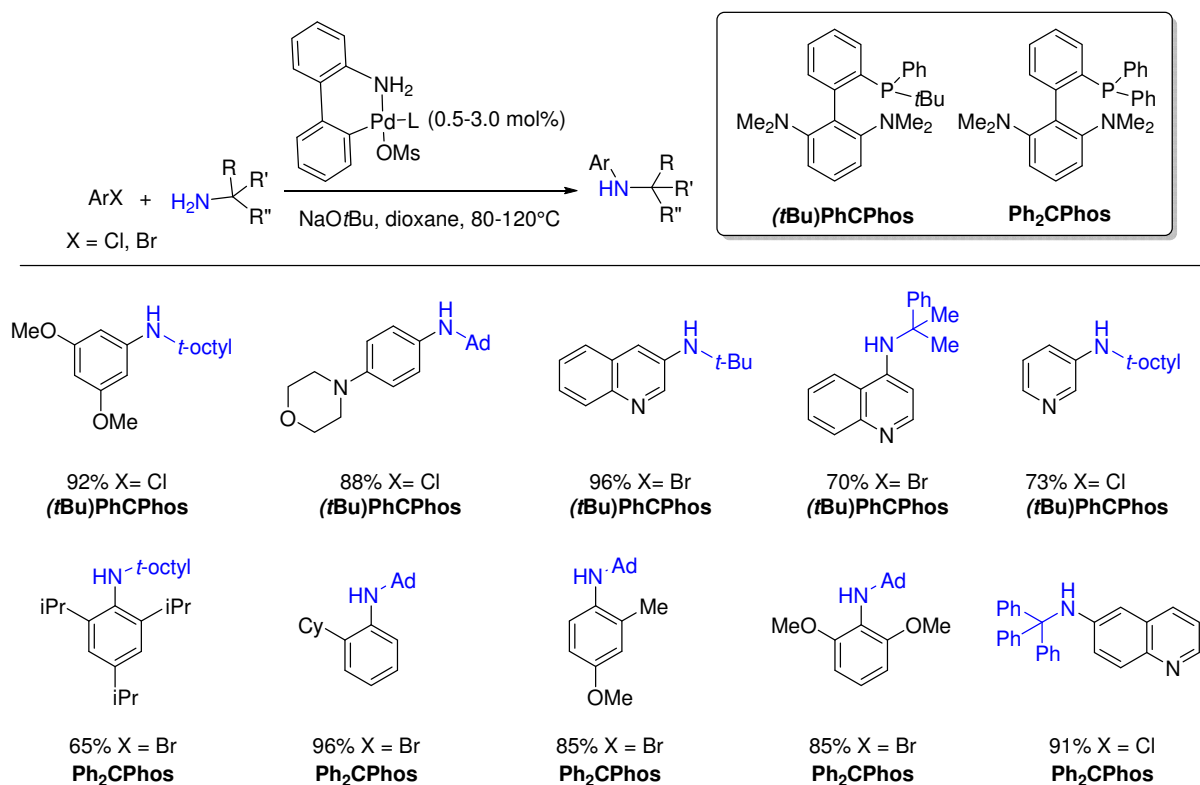


Scheme 4.6.2: Pd-catalyzed amination reaction with primary aliphatic amines using Pd(OAc)₂/BuPAd₂ catalytic system reported by Beller.

The use of NHCs as ancillary ligands in palladium-catalyzed amination was firstly investigated by Nolan and co-workers who later developed an efficient SIPr-Palladacycle pre-catalyst (**1.21**) which showed high activity in this transformation. However, with a few exceptions, the scope of amines was limited to secondary amines, while only the *N*-arylation of activated 3-fluorophenyl chloride with 1-adamantyl amine was demonstrated affording the coupling product in good yield.¹²⁴ On contrary, the use of a palladium complex bearing the annulated backbone (**1.12**) described in chapter 1 largely enlarges the substrate scope with regard to both sterically hindered aryl halides and primary amines. The *N*-arylation products 2,6-dimethyl-*N*-adamantyl aniline and 2,6-dimethyl-*N*-cyclohexyl aniline were obtained in good yields using a catalyst loading as low as 0.5 mol%, while only limited examples were described in this work.⁵⁰

¹²³ A. Ehrentraut, A. Zapf, M. Beller, *J. Mol. Catal. A: Chem.* **2002**, 182-183, 515.

¹²⁴ J. Broggi, H. Clavier, S. P. Nolan, *Organometallics* **2008**, 27, 5525.



Scheme 4.6.3: Efficient Pd-catalyzed amination reaction with sterically hindered aliphatic amines using palladacyclic amino pre-catalytic/(tBu)PhCPhos or Ph₂CPhos reported by Buchwald.

Very recently, Buchwald and co-workers have developed a new biaryl phosphine (tBu)PhCPhos for the mono-arylation of hindered primary amines after having carried out a careful investigation of the critical stereoelectronic factors of the phosphine ligands. By use of these ligands associated with a (2-aminobiphenyl)palladium methanesulfonate pre-catalyst, a large variety of hindered primary amines were successfully coupled with (hetero)aryl chlorides bearing *para* or *meta*-substituents. However, couplings using *ortho*-substituted substrates and/or tritylamine were sluggish with (tBu)PhCPhos, and the use of the smaller Ph₂CPhos ligand gave better results (Scheme 4.6.3). However, there still exists some drawbacks of this protocol, which refers to: (1) higher catalyst loading and temperature are still necessary to achieved a satisfied result; (2) In the cases of using aryl halides bearing *ortho* substituents, only aryl bromides were involved as suitable substrates to couple with amines.¹²⁵

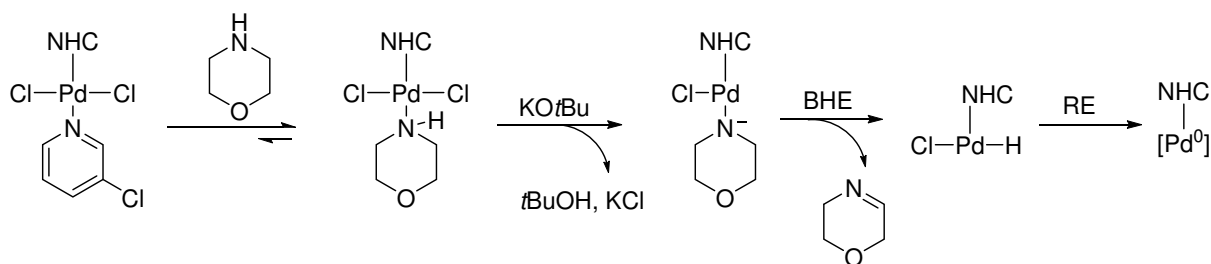
The previously outlined results indicate that the steric effect of the backbone functionalization has a dominant contribution to the outstanding catalytic efficiency of the corresponding palladium pre-catalyst. As it was explained in the literature, the amination involving sterically hindered primary amine usually requires the use of a bulky ligand. This

¹²⁵ P. Ruiz-Castillo, D. G. Blackmond, S. L. Buchwald, *J. Am. Chem. Soc.* **2015**, *137*, 3085.

prompted us to further investigate the above described two pre-catalysts $[\text{Pd}(\text{IPr}^{\text{NMe}_2})_2](3\text{-ClPy})\text{Cl}_2$ (**2.17**) and $[\text{Pd}(\text{IPr}^{\text{NiPr}_2})_2](3\text{-ClPy})\text{Cl}_2$ (**4.12**) in this transformation.

6.2. Results and discussion

In a first time, we chose 2-chloroanisole and *tert*-butyl amine as the model reaction since the two substrates are highly challenging and have never been reported before. As usual, KO*t*Bu and DME were selected as base and solvent for the reaction. In the initial optimization screening, palladium complexes **4.12** and **2.17** were employed as pre-catalysts to investigate their catalytic activity in this reaction. Surprisingly, the total conversion was 30% and 5% for **4.12** and **2.17** respectively after 4 hours at 60°C (Table 4.6.1, entries 1 and 2). We assumed that the low conversion should be mostly attributed to the sluggish activation of the pre-catalyst, since it was commonly accepted that the β -hydride elimination and reductive elimination of HCl from the resulting $[\text{LPdHCl}]$ intermediate is the major pathway to generate the Pd(0) active catalytic species. (Scheme 4.6.4)¹²⁶

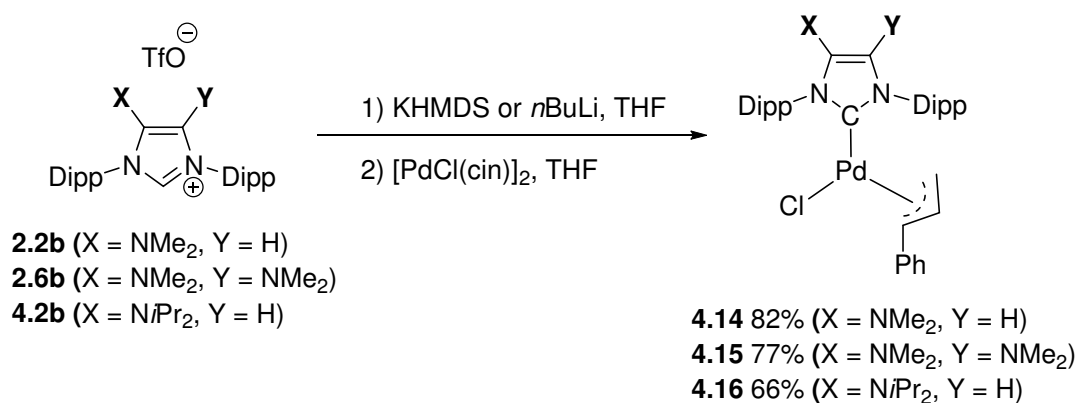


Scheme 4.6.4: Proposed mechanism of generation of Pd(0) active species from Pd-PEPPSI-NHC pre-catalysts.

Indeed, *tert*-butyl amine does not possess such hydrogen atoms on the β -position of the nitrogen and thus cannot activate the pre-catalyst by this pathway to generate the Pd(0) catalytic species. Consequently, we needed to consider pre-catalysts other than PEPPSI-type pre-catalysts to allow the entering in the catalytic cycle. Noteworthy, the pre-catalysts of type $[\text{Pd}(\text{NHC})(\text{cin})\text{Cl}]$ [cin = η^3 -cinnamyl] which were first developed by Nolan and whose mechanism to form Pd(0) species was carefully investigated by Hazari was shown to be readily activated in the presence of bases like KO*t*Bu.¹²⁷ In this context, the $[\text{Pd}(\text{IPr}^{\text{NMe}_2})(\text{cin})\text{Cl}]$ (**4.14**) $[\text{Pd}(\text{IPr}^{\text{NMe}_2})_2](\text{cin})\text{Cl}]$ (**4.15**) and $[\text{Pd}(\text{IPr}^{\text{NiPr}_2})(\text{cin})\text{Cl}]$ (**4.16**) were synthesized using the classical complexation of free carbene to palladium precursor $[\text{PdCl}(\text{cin})]_2$ (Scheme 4.6.5). These three palladium complexes present a yellow (for **4.14** and **4.16**) or deep yellow (for **4.15**) powder, and appear to be very stable against air and moisture.

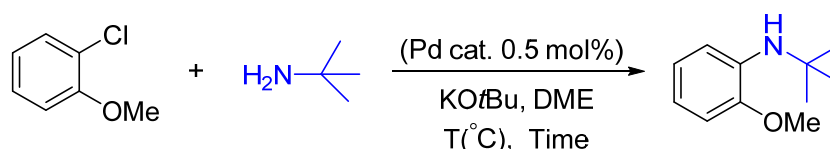
¹²⁶ J. L. Farmer, M. Pompeo, A. J. Lough, M. G. Organ, *Chem. Eur. J.* **2014**, 20, 15790.

¹²⁷ D. P. Hruszkewycz, D. Balcells, L. M. Guard, N. Hazari, M. Tilset, *J. Am. Chem. Soc.* **2014**, 136, 7300.



Scheme 4.6.5: Synthesis of [Pd(NHC)(cin)Cl] complex.

The newly synthesized pre-catalysts were then employed to evaluate their activity in the model reaction. To our delight, both complexes **4.15** and **4.16** were shown to be highly efficient, and full conversion was observed for **4.15** after 1 hour at 60°C while 95% of starting materials was converted in the presence of **4.16** after 2 hours (Table 4.6.1, entries 3 and 4). Pre-catalyst bearing less bulky ligand **IPr**^{NMe₂} **4.14** was less efficient while there was almost no conversion with [Pd(IPr)Cl(cin)] (**1.23**) as pre-catalyst (entries 5 and 6). Complex **4.15** remained efficient even when the reaction temperature was decreased to 40°C affording 97% conversion after 3 h while complex **4.16** showed to be less active under the same conditions (entries 7 and 8). Finally, the complex [Pd(IPent)(cin)Cl] (**4.17**), bearing the well-known bulky yet flexible **IPent** ligand, was found to exhibit about the same activity as the complex **4.16**.

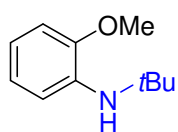
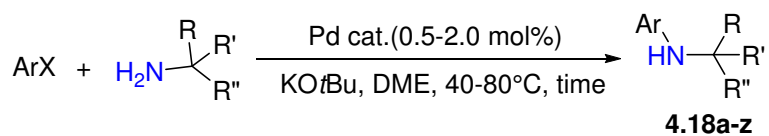


Entry	Pd cat.	Temp. (°C)	Time (h)	GC conversion (%) ^[b]
1	4.12	60	4	30
2	2.17	60	4	5
3	4.16	60	2	95
4	4.15	60	1	100
5	4.14	60	4	84
6	[Pd(IPr)(cin)Cl] (1.23)	60	3	0, 5 ^[c]
7	4.15	40	3	97
8	4.16	40	3	87
9	[Pd(IPent)(cin)Cl] (4.17)	40	3	88

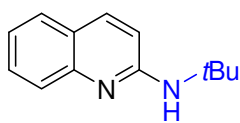
Table 4.6.1: Optimization of the Pd-catalyzed amination reaction with bulky primary amines.^[a]

^[a] Reaction conditions: 2-chloroanisole (1.0 mmol), amine (1.1 mmol), Pd cat. 0.5 mol%, KO^tBu (1.1 mmol), DME (1.0 mL); ^[b] Conversion rates were determined by GC based on 2-chloroanisole with dodecane as internal standard and were averaged over two runs; ^[c] After 24 h.

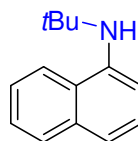
The above optimized conditions were then employed in the investigation of the coupling of various challenging (hetero)aryl chlorides with highly hindered tertiary alkyl amines (Table 4.6.2). We found that under these mild conditions, the catalyst **4.15** showed high efficiency when the unactivated aryl chlorides bearing *ortho*, *meta*, *para*-electronic rich substituents and heteroaryl or naphthyl chlorides are involved in coupling with *tert*-butyl amine and adamantly amine affording the desired coupling products in excellent yields in a very short time (**4.18a-4.18e** and **4.18h**), while a slightly higher temperature (60°C) was necessary in certain cases when using adamantly amine (**4.18f**, **4.18g** and **4.18i**). It is important to note that the conditions are much milder than the ones previously reported in literature. These encouraging results prompted us to further explore the possibility to introduce even more sterically hindered amines like *tert*-amyl amine, *tert*-octyl amine and trityl amine which appeared as suitable substrates of arylative amination only in the recently published work of Buchwald group. In these cases, we found that higher temperature (60°C) was also necessary to achieve a good conversion when more bulky *tert*-amyl amine and *tert*-octyl amine are involved as coupling partners. Surprisingly, complex **4.16** performed better than **4.15** in the presence of the bulky *tert*-amyl amine or *tert*-octyl amine. The full conversion was indeed observed for the reaction between 2-chloroanisole and *tert*-octyl amine while a 84% GC conversion was obtained using **4.15**. We proposed the higher flexibility of ligand **IPr**^{NiPr₂} compared with **IPr**^{(NMe₂)₂} bearing two amino groups might be a possible explanation. A variety of challenging (hetero)aryl chlorides were successfully engaged in this transformation affording the coupling products in good yields using 0.5 mol% of complex **4.16**, while an increase of catalyst loading and reaction time were needed to produce **4.18p** in an excellent yield. Impressively, using 1.0 mol% of **4.15**, the trityl amine could successfully couple with 2-chloroanisole to give **4.18r** in 83% yield. 4-chloroanisole and 3-chloropyridine could be equally aminated to afford the product **4.18s** and **4.18t** with reasonable yields of 82 % and 54% respectively.



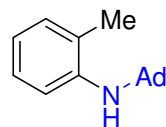
4.18a 82%^c
(40°C, 3H)



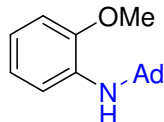
4.18b 75%^c
(40°C, 4H)



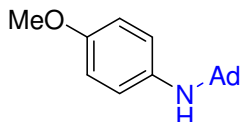
4.18c 83%^c
(40°C, 3H)



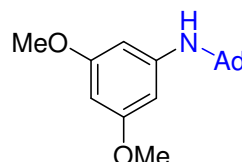
4.18d 97%^c
(40°C, 3H)



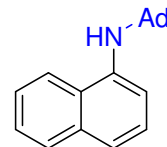
4.18e 81%^c
(40°C, 4H)



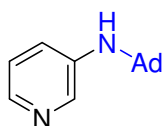
4.18f 93%^c
(60°C, 2H)



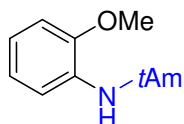
4.18g 88%^c
(60°C, 3H)



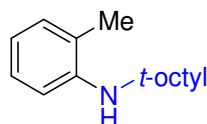
4.18h 65%^c
(40°C, 4H)



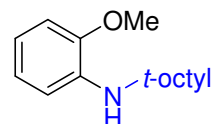
4.18i 81%^c
(60°C, 3H)



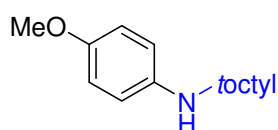
4.18j 96%^d
(60°C, 3H)



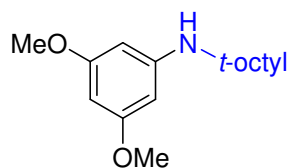
4.18k 82%^d
(60°C, 3H)



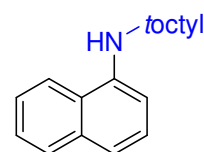
4.18l 95%^d
(60°C, 4H)



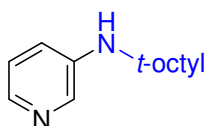
4.18m 80%^d
(60°C, 4H)



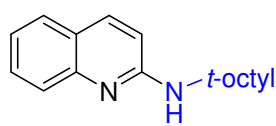
4.18n 91%^d
(60°C, 4H)



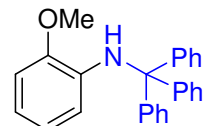
4.18o 83%^d
(60°C, 4H)



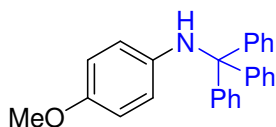
4.18p 99%^e
(60°C, 18H)



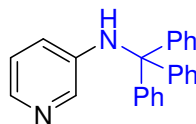
4.18q 61%^d
(60°C, 4H)



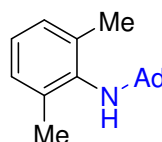
4.18r 83%^f
(60°C, 18H)



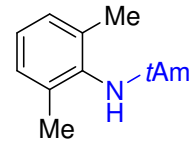
4.18s 82%^f
(60°C, 18H)



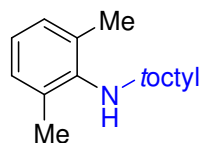
4.18t 54 %^f
(60°C, 18H)



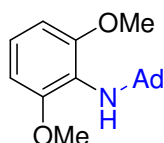
4.18u 87%^f
(60°C, 14H)



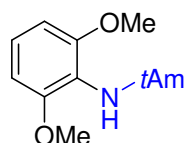
4.18v 68%^f
(60°C, 18H)



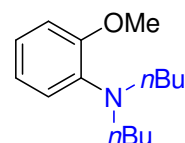
4.18w 69%^g
(60°C, 18H)



4.18x 77%^f
(60°C, 14H)



4.18y 93%^f
(60°C, 6H)



4.18z 85%^d
(60°C, 2H)

Table 4.6.2: Substrate scope of the Buchwald-Hartwig amination using pre-catalyst **4.15** and **4.16**.

^[a] Reaction conditions: aryl chloride (1.0 mmol), amine (1.1 mmol), KO^tBu (1.1 mmol), DME (1.0 mL); ^[b] Isolated yield; ^[c] 0.5 mol% of **4.15**; ^[d] 0.5 mol% of **4.16**; ^[e] 1.0 mol% of **4.16**; ^[f] 1.0 mol% of **4.15**; ^[g] 2.0 mol% of **4.15**.

Turning our attention to the di-*ortho*-substituted aryl chlorides, 2-chloroxylene was readily coupled with adamantyl amine, *tert*-amyl amine, *tert*-octyl amine to give the products **4.18u-w** using 1.0 mol% of **4.15** (2.0 mol% in the case of **4.18w**) at 60°C for a longer but still acceptable time of 14-18 h. Under the same conditions, complex **4.16** was much less efficient, and we assumed that it is mostly attributed to its lower catalyst stability compared to **4.15**. Unfortunately, the reaction only gave trace of the product when trityl amine was used as the amine source. Even more impressively, 2,6-dimethoxyphenyl chloride was also a suitable substrate to produce **4.18x-y** in good yields. It was well known that one of the most challenging substrates as amine is dibutyl amine, and finally it was employed in the coupling of 2-chloroanisole to produce **4.18z** in excellent yield under very mild conditions using pre-catalyst **4.16** as catalyst.

6.3. Conclusion

As continuation of the previous part of backbone variation where we found that both **IPr^{(NMe₂)₂}** and **IPr^{NiPr₂}** ligands dramatically improved the catalytic efficiency of the corresponding palladium PEPPSI-type pre-catalysts in amination at room temperature, we investigated these two ligands in more challenging Buchwald-Hartwig amination producing bulky anilines which was less explored in the last decade since rare efficient ligands enable to realize this transformation. Under mild conditions, both ligands are shown to be efficient in certain cases when [Pd(NHC)(cin)Cl] was utilized as pre-catalyst. A large variety of aryl chlorides bearing *ortho*, *meta* and *para*-electron rich substituents are found to be suitable coupling partners with steric primary alkyl amines. Even more sterically hindered di-*ortho* substituted aryl chlorides were found to efficiently produce the corresponding anilines. We believe that the improved steric influence on the metal centre as well as the increase in catalyst stability due to the stronger electron donation of ligands lead to this high catalytic efficiency of the palladium pre-catalysts.

7. Conclusion and perspective

In this chapter, we have further modified the $\text{IPr}^{\text{NMe}_2}$ ligand into its bulkier analogue $\text{IPr}^{\text{NiPr}_2}$ and have reduced the electron-donation of $\text{IPr}^{(\text{NMe}_2)_2}$ without greatly affecting its steric properties by formally replacing one dimethylamino group by a chlorine or bromine atom to give the $\text{IPr}^{\text{NMe}_2, \text{X}}$ ligands. Following the same synthetic method developed for $\text{IPr}^{\text{NMe}_2} \cdot \text{HOTf}$ **2.2b**, $\text{IPr}^{\text{NiPr}_2} \cdot \text{HOTf}$ **4.2b** was synthesized in good yields. Thanks to the amino group on the backbone of the imidazolyl ring in $\text{IAr}^{\text{NMe}_2}$, the latter was shown to react with *N*-chloro and *N*-bromosuccinimide in an oxidative halogenation reaction to produce the corresponding $\text{IAr}^{\text{NMe}_2, \text{X}}$ species, either under the imidazolium form or even directly into a metallic complex. The formal increase of the size of the amino group leads to a noticeable increase of the steric properties and a small increase of the electronic properties. As expected, the formal replacement of one dimethylamino group in $\text{IAr}^{(\text{NMe}_2)_2}$ by one halogen to give $\text{IAr}^{\text{NMe}_2, \text{X}}$ leads to a decrease of the electronic donation abilities while the steric hindrance remains about the same.

Finally, the catalytic influence of this modification was evaluated in the Buchwald-Hartwig amination reaction. The results of the kinetic studies at 25°C reveal that both derivatizations lead to a significant improvement of catalytic ability of the corresponding palladium pre-catalysts in two model aminations where Pd pre-catalysts supported by $\text{IPr}^{(\text{NMe}_2)_2}$, $\text{IPr}^{\text{NiPr}_2}$ and $\text{IPr}^{\text{NMe}_2, \text{Cl}}$ ligands showed higher efficiency than $\text{IPr}^{\text{NMe}_2}$ derivative. In light of this observation, and according to the previously results obtained from catalytic studies in the chapter 2, we draw the conclusion that the better catalytic activities of Pd-PEPPSI- $\text{IPr}^{(\text{NMe}_2)_2}$ compared with $\text{IPr}^{\text{NMe}_2}$ derivative should be more steric in nature while the higher electronic donation of the former leads to an increase of catalyst stability. Moreover, in a global point of view, the benefit for enhanced efficiency taken from backbone decoration of IPr in palladium-catalyzed arylative amination is mainly attributed to the incremental steric congestion of the resulting NHC ligands other than electronic issue.

In the second part of this chapter, the two most efficient ligands $\text{IPr}^{(\text{NMe}_2)_2}$ and $\text{IPr}^{\text{NiPr}_2}$ were then implemented in one of the most challenging aminations involving both sterically hindered aryl chlorides and bulky primary amines using the pre-catalysts $[\text{Pd}(\text{NHC})(\text{cin})\text{Cl}]$. The high activities were obtained under unprecedented mild conditions with a relative low catalyst loading.

-General Conclusion -

General Conclusion

The original concept of this thesis relied on the formal functionalization of imidazol-2-ylidenes by attachment of one or two neutral amino groups in attempt to enhance the inherent electronic donation of the carbenic center in view to improve the catalytic efficiency in the palladium-catalyzed arylation amination reaction.

Based on all the results obtained during the previous systematic studies in the precedent chapters, we are now able to draw the following conclusions:

(1) On contrary to our starting hypothesis, the substitution of imidazolyl skeleton of the IPr ligand by amino groups and halogen atoms not only affects the electronic donicity of the carbene center, but also the steric hindrance of the NHC ligand. By tuning the nature and the size of the substituents, these two parameters could be independently varied in a quite rational manner.

(2) The steric hindrance of the ancillary NHC ligand appears to be the main factor for the catalytic efficiency of the Pd-NHC catalysts in Buchwald-Hartwig amination. This study confirms the previous Organ's conclusions in the IPr, IPent and IPent^{Cl₂} series. Nevertheless, a stronger electronic donation of the NHC was also found beneficial in terms of catalyst stability and activity, since the bis-aminated IPr^{(NMe₂)₂} – being the strongest donor of the series and displaying one of the highest steric congestions – revealed to be the most efficient ancillary ligand in all cases of the above studied arylation aminations.

(3) This study confirms that the skeleton functionalization of IPr is an efficient alternative method to optimize the catalytic performances of the corresponding palladium catalysts in aryl amination and complements the previous strategies reported in literature, which focused on the modification of the aryl groups on the *N*-substituents of the imidazolyl ring.

(4) We have developed a relatively facile way to obtain a series of five new mono- and bis-substituted IPr-based NHCs: IPr^{NMe₂}, IPr^{NiPr₂}, IPr^{NMe₂,Cl}, IPr^{NMe₂,Br} and IPr^{(NMe₂)₂}. A ranking of the relative catalytic efficiencies of the Pd-PEPPSI-NHC pre-catalysts in Buchwald-Hartwig amination could be established: IPr^{Cl₂} < IPr < IPr^{NMe₂} << IPent ≈ IPr^{NMe₂,Cl} ≈ IPr^{NiPr₂} < IPr^{(NMe₂)₂}.

(5) The resulting series of newly functionalized IPr^{XY} ligands displaying a large palette of electronic and steric properties will serve as ligand library for the future optimization of other transition metal catalyzed organic transformations. A first proof of concept has been realized by developing an efficient coupling between aryl chlorides and bulky primary amines.

-Chapitre 5-

1	General procedure.....	137
1.1	Materials	137
1.2	Solvents.....	137
1.3	Nuclear Magnetic Resonance (NMR).....	138
1.4	Infrared spectroscopy	138
1.5	Mass spectroscopy	138
1.6	Elemental analysis	138
1.7	X-Ray Crystallography	138
1.8	Melting point.....	138
1.9	Gas chromatography	138
2	Chapter 2.....	139
2.1	Synthetic methods	139
	N-(N'',N''-dimethylcarbamoylmethyl)-N,N'-dimesitylformamidine (2.1a)	139
	N-(N'',N''-dimethylcarbamoylmethyl)-N',N'-di(2,6-diisopropylphenyl)formamidine (2.1b).....	139
	1,3-dimesityl-4-(dimethylamino)imidazolium triflate (2.2a).....	140
	1,3-bis(2,6-diisopropylphenyl)-4-(dimethylamino)imidazolium triflate (2.2b).....	141
	1,3-dimesityl-4,5-bis(dimethylamino)imidazolium triflate (2.6a)	141
	1,3-bis(2,6-diisopropylphenyl)-4,5-bis(dimethylamino)imidazolium triflate (2.6b). 143	
	Chloro-(η^4 -cycloocta-1,5-diene)-(1,3-dimesityl-4-(dimethylamino)imidazol-2-ylidene) rhodium(I) (2.8)	144
	Chloro-dicarbonyl-(1,3-dimesityl-4-(dimethylamino)imidazol-2-ylidene) rhodium(I) (2.10).....	145
	Chloro-dicarbonyl-(1,3-dimesityl-4,5-bis(dimethylamino)imidazol-2-ylidene) rhodium(I) (2.11)	146
	1,3-dimesityl-4-(dimethylamino)imidazolin-2-selenone (2.12).....	146
	1,3-dimesityl-4,5-bis(dimethylamino)imidazolin-2-selenone (2.13)	147
	Dichloro-(3-chloropyridine)(1,3-(diisopropylphenyl)-4-dimethylaminoimidazol-2-ylidene)palladium(II) (2.14)	147
	Chloro-(η^3 -allyl)-(1,3-(diisopropylphenyl)-4-dimethylaminoimidazol-2-ylidene)palladium(II) (2.15)	148
	Chloro-(η^3 -2-propen-1-yl)-(1,3-(diisopropylphenyl)-4,5-bis(dimethylamino)imidazol-2-ylidene)palladium(II) (2.16)	149
	Dichloro-(3-chloropyridine)(1,3-(diisopropylphenyl)-4,5-bis(dimethylamino)imidazol-2-ylidene)palladium(II) (2.17)	149

3	Palladium-Catalyzed Buchwald-Hartwig amination reaction	150
	Kinetic studies on the amination of 4-chloroanisole with morpholine	150
	Palladium-catalyzed amination at room temperature: general procedure A (Table 2.4.4)	150
	Palladium-catalyzed amination at low catalyst loadings: general procedure B (Table 2.4.5)	151
3.1	Catalytic products (Table 2.4.4 and 2.4.5)	151
3.2	Palladium-Catalyzed Buchwald-Hartwig amination reaction using a mild base. 155	
	General procedure for the optimization of Pd-catalyzed amination with carbonate base	155
	General procedure for Pd-catalyzed amination using cesium carbonate as the base (Table 2.4.7-2.4.9)	156
	Competitive amination experiments of 4-chlorotoluene with morpholine and piperidine (Scheme 2.4.10)	156
	Competitive amination experiments of 4-chloroanisole with morpholine and piperidine (Scheme 2.4.10)	157
3.3	Catalytic products (Table 2.4.7-2.4.9)	157
4	Chapter 3.....	165
4.1	Palladium-Catalyzed Buchwald-Hartwig amination reaction with aryl tosylates 165	
	General procedure for the optimization of the Pd-PEPPSI pre-catalyst (Table 3.2.1)	165
4.2	Catalytic products	166
5	Chapter 4.....	174
5.1	Synthetic methods	174
	N-(N'',N''-diisopropylcarbamoylmethyl)-N',N'-dimesitylformamidinium (4.1a)	174
	N-(N'',N''-diisopropylcarbamoylmethyl)-N',N'-di(2,6-diisopropylphenyl)formamidinium(4.1b)	174
	1,3-dimesityl-4-(diisopropylamino)imidazolium triflate (4.2a).....	174
	1,3-bis(2,6-diisopropylphenyl)-4-(dimethylamino)imidazolium triflate (4.2b).....	175
	1,3-dimesityl-4-(dimethylamino)-5-chloroimidazolium triflate(4.3a).....	176
	1,3-bis(2,6-diisopropylphenyl)-4-(dimethylamino)-5-chloroimidazolium triflate (4.3b)	176
	Chloro-(η^4 -cycloocta-1,5-diene)-(1,3-dimesityl-4-(diisopropylamino)imidazol-2-ylidene) rhodium(I) (4.4)	177
	Chloro-dicarbonyl-(1,3-dimesityl-4-(diisopropylamino)imidazol-2-ylidene) rhodium(I) (4.5)	178
	Chloro-dicarbonyl-(1,3-dimesityl-4-(dimethylamino)-5-chloroimidazol-2-ylidene) rhodium(I) (4.6)	178

Chloro-dicarbonyl-(1,3-dimesityl-4-(dimethylamino)-5-bromoimidazol-2-ylidene)rhodium(I) (4.7)	179
1,3-dimesityl-4-(diisopropylamino)imidazolin-2-selenone (4.8).....	179
1,3-dimesityl-4-(dimethylamino)-5-chloroimidazolin-2-selenone (4.9).....	180
Chloro-(η^3 -allyl)-(1,3-bis(2,6-diisopropylphenyl)-4-diisopropylaminoimidazol-2-ylidene)palladium(II) (4.10)	180
Dichloro-(3-chloropyridine)(1,3-bis(2,6-diisopropylphenyl)-4-(dimethylamino)-5-chloroimidazol-2-ylidene)palladium(II) (4.12).....	181
Dichloro-(3-chloropyridine)(1,3-bis(2,6-diisopropylphenyl)-4-(dimethylamino)-5-bromo(imidazol-2-ylidene)palladium(II) (4.13)	182
Chloro-(η^3 -2-cinnam-1-yl)-(1,3-bis(2,6-diisopropylphenyl)-4-(dimethylamino)imidazol-2-ylidene)palladium(II) (4.14)	182
Chloro-(η^3 -2-cinnam-1-yl)-(1,3-bis(2,6-diisopropylphenyl)-4,5-bis(dimethylamino)imidazol-2-ylidene)palladium(II) (4.15)	183
Chloro-(η^3 -2-cinnam-1-yl)-(1,3-bis(2,6-diisopropylphenyl)-4-(diisopropylamino)imidazol-2-ylidene)palladium(II) (4.16).....	184
5.2 Palladium-Catalyzed Buchwald-Hartwig amination reaction	184
Kinetic studies on the amination of 4-chloroanisole with morpholine	184
Kinetic studies on the amination of 2-chloroanisole with morpholine	185
General procedure for the optimization of the Pd-catalyzed amination reaction (Table 4.6.1)	185
Palladium-catalyzed amination with bulky primary amines (Table 4.6.2)	185
5.3 Catalytic products (Table 4.6.2).....	186
6 X-Ray experimental data.....	193

Experimental section

1 General procedure

1.1 Materials

All manipulations were performed under an inert atmosphere of dry nitrogen by using standard vacuum line and Schlenk tube techniques. Glassware was dried at 120°C in an oven for at least three hours.

N,N'-dimesitylformamidine,¹²⁸ N,N'-bis(2,6-diisopropylphenyl)formamidine,¹ [RhCl(cod)]₂,¹²⁹ [PdCl(allyl)]₂, [PdCl(cinnamyl)]₂,⁷¹ PdCl₂(CH₃CN)₂,¹³⁰ Pd-PEPPSI-IPr,¹³¹ Pd-PEPPSI-IPr^{Cl},¹³² Pd-PEPPSI-IPent,¹³³ Pd-PEPPSI-IPent^{Cl},⁶ (IPr)Pd(cinnamyl)Cl,⁷¹ and (IPent)Pd(cinnamyl)Cl,¹³⁴ were synthesized according to literature procedures. 2-chloro-N,N-dimethylacetamide was synthesized by reacting dimethylamine with chloroacetyl chloride. Aryl tosylate substrates were synthesized upon reaction of the corresponding phenol derivative with *para*-toluenesulfonyl chloride according to literature procedure.¹³⁵ All other reagents were commercially available and used as received except the liquid amines which were distilled by a trap to trap distillation. Anhydrous K₃PO₄ was purchased from Acros and Cs₂CO₃ was purchased from Alfa Aesar. KO^tBu was purchased from Aldrich and was pre-purified and weighted in the glove box as base for the catalytic procedure of chapter 4.

1.2 Solvents

THF, diethyl ether, DME and 1,4-dioxane were freshly distilled from sodium/benzophenone, toluene, *t*BuOH and *t*AmOH from molten sodium. Pentane, ethyl acetate and dichloromethane were dried over CaH₂ and subsequently distilled. DMF was dried over CaH₂ and distilled under reduced pressure. Ethanol was dried with sodium before distillation.

¹²⁸ K. E. Krahulic, G. D. Enright, M. Parvez, R. Roesler, *J. Am. Chem. Soc.* **2005**, *127*, 4142.

¹²⁹ G. Giordiano, R. H. Crabtree, *Inorg. Synth.* **1990**, *28*, 88.

¹³⁰ M. Rimoldi, F. Ragaini, E. Gallo, F. Ferretti, P. Macchi, N. Casati, *Dalton Trans.* **2012**, *41*, 3648.

¹³¹ C. J. O'Brien, E. A. Kantchev, C. Valente, N. Hadei, G. A. Chass, A. Lough, A. C. Hopkinson, M. G. Organ, *Chem. Eur. J.* **2006**, *12*, 4743-4748

¹³² M. Pompeo, N. Hadei, R. D. J. Froese, M. G. Organ, *Angew. Chem. Int. Ed.* **2012**, *51*, 11354-11357.

¹³³ M. G. Organ, S. Çalimsiz, M. Sayah, K. H. Hoi, A. J. Lough, *Angew. Chem. Int. Ed.* **2009**, *48*, 2383-2387.

¹³⁴ J. L. Farmer, M. Pompeo, A. J. Lough, M. G. Organ, *Chem. Eur. J.* **2014**, *20*, 15790-15798.

¹³⁵ D. A. Wilson, C. J. Wilson, C. Moldoveanu, A.-M. Resmerita, P. Corcoran, L. M. Hoang, B. M. Rosen, V. Percec, *J. Am. Chem. Soc.* **2010**, *132*, 1800-1801.

1.3 Nuclear Magnetic Resonance (NMR)

NMR spectra were recorded on Bruker AV300 or AV400 spectrometers. Chemical shifts are reported in ppm (δ) compared to TMS (^1H and ^{13}C) using the residual peak of deuterated solvent as internal standard.¹³⁶

1.4 Infrared spectroscopy

Infrared spectra were recovered on a Perkin-Elmer Spectrum 100 FT-IR spectrometer.

1.5 Mass spectroscopy

MS spectra were recorded by the mass spectrometry service of the "Institut de chimie de Toulouse".

1.6 Elemental analysis

Microanalyses were performed by the Microanalytical Services of the LCC or of the ICSN (Gif-sur-Yvette, France).

1.7 X-Ray Crystallography

X-Ray diffraction studies were carried out by Dr. N. Lugan. Crystal data were collected using a MoK α graphite monochromated (λ 0.71373 Å) on a Stoe IPDS diffractometer and an Oxford-Diffraction XCALIBUR diffractometer.

1.8 Melting point

Melting points were recovered with a Stuart Scientific Melting Point apparatus SMP1 and were not corrected.

1.9 Gas chromatography

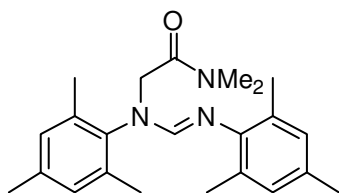
GC analyses were performed on a Shimadzu GC-2014 chromatograph equipped with a 30-m capillary column (Supelco, SLB 5-ms, fused silica capillary column, 30 m \times 0.32 mm \times 0.25 μm film thickness), using Helium as the vector gas. The following GC conditions were used: Initial temperature 40 °C, for 1 minutes, then rate 30 °C/min. until 250° C and 250° C for 2 minutes. Linear velocity of carrier gas: 30 cm.s⁻¹.

¹³⁶ G. R. Fulmer, A. J. M. Miller, N. H. Sherden, H. E. Gottlieb, A. Nudelman, B. M. Stoltz, J. E. Bercaw, K. I. Goldberg, *Organometallics* **2010**, 29, 2176.

2 Chapter 2

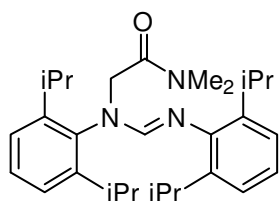
2.1 Synthetic methods

N-(N'',N''-dimethylcarbamoylmethyl)-N,N'-dimesitylformamidinium (2.1a)



To a solution of N,N'-dimesitylformamidinium (1.5 g, 5.35 mmol) and KI (0.088 g, 0.53 mmol, 0.1 eq) in DMF (15 mL), 2-chloro-N,N-dimethylacetamide (0.78 g, 6.4 mmol, 1.2 eq.) and triethylamine (1.1 mL, 8 mmol, 1.5 eq.) were added respectively at room temperature. The resulting mixture was stirred at 100°C overnight. After cooling down to room temperature, the reaction mixture was diluted with Et₂O (150 mL) and the organic phase was washed with water (50 mL). The aqueous phase was then extracted with ether (3×30 mL) and the organic layers were combined and washed again with water (30 mL) and brine (30 mL). After drying over Na₂SO₄, the solution was filtered and evaporated under reduced pressure. The crude residue was purified by flash chromatography (SiO₂, Hexane/EtOAc : 2/1 then 1/1) to afford a colorless, sticky foam (1.4 g, 72%). **¹H NMR (400 MHz, CDCl₃)** δ = 7.22 (s, 1H, N₂CH), 6.89 (s, 2H, CH_{Mes}), 6.81 (s, 2H, CH_{Mes}), 4.43 (s, 2H, CH₂), 3.16 (s, 3H, N-CH₃), 2.95 (s, 3H, N-CH₃), 2.37 (s, 6H, CH₃ ortho), 2.26 (s, 3H, CH₃ para), 2.22 (s, 3H, CH₃ para), 2.15 (s, 6H, CH₃ ortho); **¹³C{¹H} NMR (101 MHz, CDCl₃)** δ = 168.3 (C=O), 152.2 (N₂CH), 139.8, 137.4, 137.0, 131.4 (C_{Mes}), 129.6 (CH_{Mes}), 129.4 (C_{Mes}), 128.6 (CH_{Mes}), 49.5 (CH₂), 37.4, 36.2 (N-CH₃), 21.0, 20.8 (CH₃ para), 18.8, 18.6 (CH₃ ortho); **MS (ESI):** m/z (%): 366 (100) [M + H]⁺; **HRMS (ESI):** m/z calcd. for C₂₃H₃₂N₃O: 366.2545; found: 366.2548, ε_r = 0.8 ppm.

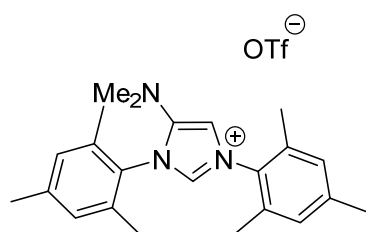
N-(N'',N''-dimethylcarbamoylmethyl)-N',N'-di(2,6-diisopropylphenyl)formamidinium (2.1b)



To a solution of N,N'-di(2,6-diisopropylphenyl)formamidinium (3.646 g, 10.0 mmol) and KI (0.16 g, 1.0 mmol, 0.1 eq) in DMF (30 mL), 2-chloro-N,N-dimethylacetamide (1.46 g, 12.0 mmol, 1.2 eq.) and triethylamine (2.1 mL, 15.0 mmol) were added respectively at room temperature. The resulting mixture was stirred at 100°C overnight. After cooling down to room temperature, water (100 mL) was added to the solution and the mixture was extracted with ether (3×60 mL) and the organic layers were combined and washed again with water (60 mL) and brine (60 mL). After drying over Na₂SO₄, the solution was filtered and evaporated under reduced pressure. The crude residue was purified by flash

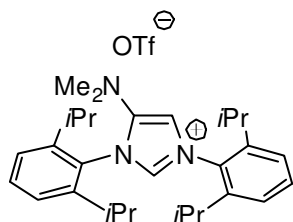
chromatography (SiO₂, Hexane/EtOAc : 6/1) to afford a white solid (3.42 g, 76%). mp = 163°C; ¹H NMR (400 MHz, CDCl₃) δ = 7.31 (t, *J* = 7.7 Hz, 1H, CH_{Ar}), 7.23 (s, 1H, N₂CH), 7.18 (d, *J* = 7.6 Hz, 2H, CH_{Ar}), 7.07 (d, *J* = 7.6 Hz, 2H, CH_{Ar}), 6.99 (t, *J* = 7.7 Hz, 1H, CH_{Ar}), 4.43 (s, 2H, CH₂), 3.65-3.55 (m, 2H, CH_{iPr}), 3.28-3.21 (m, 2H, CH_{iPr}), 3.15 (s, 3H, N-CH₃), 2.95 (s, 3H, N-CH₃), 1.30 (d, *J* = 6.8 Hz, 6H, CH_{3 iPr}), 1.17 (d, *J* = 6.7 Hz, 12H, CH_{3 iPr}), 1.14 (d, *J* = 6.9 Hz, 6H, CH_{3 iPr}); ¹³C{¹H} NMR (101 MHz, CDCl₃) δ = 167.9 (C=O), 151.1 (N₂CH), 148.5, 147.0, 140.1, 139.3 (C_{Ar}), 128.9, 124.5, 122.9, 122.8 (CH_{Ar}), 51.1 (CH₂), 37.5, 36.3 (N-CH₃), 28.1, 27.7 (CH_{iPr}) 25.3, 24.6 (CH_{3 iPr}), 23.8; IR (ATR): ν = 2962, 2928, 2867, 1651, 1633, 1584, 1463, 1445, 1331, 1314, 1237, 1181, 1157, 1098, 1056, 802, 769, 755 cm⁻¹; MS (ESI): *m/z* (%): 450 (100) [M + H]⁺; HRMS (ESI): *m/z* calcd. for C₂₉H₄₄N₃O: 450.3484; found: 450.3485, ε_r = 0.2 ppm.

1,3-dimesityl-4-(dimethylamino)imidazolium triflate (2.2a)



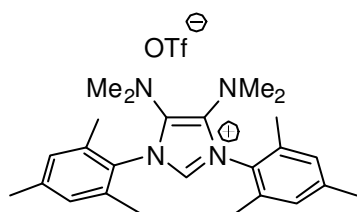
2,6-lutidine (1.65 mL, 14.25 mmol, 1.5 eq) was added to a solution of compound **2.1a** (3.5 g, 9.5 mmol) in CH₂Cl₂ (40 mL) at -78°C. Triflic anhydride (1.76 mL, 10.45 mmol, 1.1 eq) was then added dropwise. The solution became brown and the mixture was stirred for another 2.5 h in the cooling bath and then allowed to warm to room temperature. A saturated solution of NaHCO₃ (60 mL) was added to the resulting solution and the biphasic mixture was stirred for another 30 minutes. The organic phase was separated and washed again with NaHCO₃ (2 × 60 mL), dried over Na₂SO₄ and evaporated under reduced pressure. The crude product was washed with Et₂O and dried to get a white powder (3.24 g, 69%). Single crystals suitable for an X-Ray diffraction experiment were grown by layering a solution of **2.2a** in CH₂Cl₂ with pentane. mp = 149°C; ¹H NMR (400 MHz, CDCl₃) δ = 8.86 (d, *J* = 1.9 Hz, 1H, N₂CH), 7.06 (s, 2H, CH_{Mes}), 7.02 (s, 2H, CH_{Mes}), 6.70 (d, *J* = 1.9 Hz, 1H, CH_{Im}), 2.64 (s, 6H, N-CH₃), 2.36 (s, 6H, CH_{3 para}), 2.34 (s, 3H, CH_{3 para}), 2.17 (s, 6H, CH_{3 ortho}), 2.16 (s, 6H, CH_{3 ortho}); ¹³C{¹H} NMR (101 MHz, CDCl₃) δ = 145.8, 141.7, 141.3, 134.8 (C_{Ar}), 134.4 (N₂CH), 134.2, 131.0 (C_{Ar}), 130.3 (CH_{Mes}), 129.9 (CH_{Mes}), 129.0 (C_{Ar}), 120.6 (q, *J*_{CF} = 320 Hz, CF₃SO₃), 106.7 (CH_{Im}), 42.2 (N-CH₃), 21.4, 21.3 (CH_{3 para}), 17.8, 17.3 (CH_{3 ortho}); IR (ATR): ν = 3114, 3053, 2923, 1666, 1643, 1604, 1549, 1483, 1456, 1281, 1250, 1224, 1151, 1028, 924, 853, 755, 674 cm⁻¹; MS (ESI): *m/z* (%): 348 (100) [M – OTf]⁺; HRMS (ESI): *m/z* calcd. for C₂₃H₃₀N₃: 348.2440; found: 348.244, ε_r = 1.1 ppm.

1,3-bis(2,6-diisopropylphenyl)-4-(dimethylamino)imidazolium triflate (**2.2b**)



2,6-lutidine (0.87 mL, 7.5 mmol, 1.5 eq) was added at room temperature to a solution of compound **2.1b** (2.25 g, 5.0 mmol) in CH₂Cl₂ (35 mL) and the solution was cooled down to -78°C. At this temperature, triflic anhydride (0.93 mL, 5.5 mmol, 1.1 eq) was added dropwise. The mixture was then allowed to warm up to room temperature overnight. A saturated solution of NaHCO₃ (60 mL) was added to the resulting solution and the biphasic mixture was stirred for another 30 minutes. The organic phase was separated and washed again with NaHCO₃ (2×60 mL), dried over Na₂SO₄ and evaporated under reduced pressure to give a crude product which was solubilized in CH₂Cl₂ and recrystallized by slow addition of ether, giving a colorless crystalline solid which was collected by filtration and dried under vacuum (2.3 g, 79%). Single crystals suitable for an X-Ray diffraction experiment were grown by layering a solution of **2.2b** in CH₂Cl₂ with pentane. mp = 202°C; ¹H NMR (400 MHz, CDCl₃) δ = 8.71 (s, 1H, N₂CH), 7.57 (t, *J* = 7.8 Hz, 1H, CH_{Ar}), 7.52 (t, *J* = 7.8 Hz, 1H, CH_{Ar}), 7.35 (d, *J* = 7.8 Hz, 2H, CH_{Ar}), 7.30 (d, *J* = 7.8 Hz, 2H, CH_{Ar}), 6.89 (s, 1H, CH_{Im}), 2.66 (s, 6H, N-CH₃), 2.56-2.36 (m, 4H, CH_{iPr}), 1.33-1.28 (m, 12H, CH_{3 iPr}), 1.22-1.18 (m, 12H, CH_{3 iPr}); ¹³C{¹H} NMR (101 MHz, CDCl₃) δ = 146.2, 145.5, 145.0 (C_{Ar}), 134.0 (N₂CH), 132.4, 132.0 (CH_{Ar}), 130.2, 128.3 (C_{Ar} + C_{Im}), 125.3, 124.7 (CH_{Ar}), 120.6 (q, *J*_{CF} = 321 Hz, CF₃SO₃⁻), 107.9 (CH_{Im}), 42.1 (N-CH₃), 29.5, 29.2 (CH_{iPr}), 25.1, 24.7, 24.1, 23.0 (CH_{3 iPr}); IR (ATR): ν = 2966, 2929, 2870, 2061, 1980, 1635, 1612, 1544, 1464, 1408, 1331, 1280, 1257, 1223, 1148, 1030, 933, 810, 757 (cm⁻¹); MS (ESI, positive mode): *m/z* (%): 432 (100) [M – TfO]⁺; Elemental analysis calcd (%) for C₃₀H₄₂F₃N₃O₃S (MW = 581.73): C 61.94, H 7.28, N 7.22, found: C 61.71, H 7.01, N 7.08.

1,3-dimesityl-4,5-bis(dimethylamino)imidazolium triflate (**2.6a**)



*n*BuLi (1.6 M in hexane, 1.4 mL, 2.2 mmol, 1.1 eq.) was added dropwise to a solution of N,N'-dimesitylformamidine (560 mg, 2.0 mmol) in Et₂O (15 mL) at 0 °C, and the mixture was stirred at this temperature for 1 h to afford a white suspension of the corresponding lithium formamidinate. In a separated experiment, oxalyl chloride (0.6 mL, 7.0 mmol, 3.5 eq.) was added to a solution of DMF (0.55 mL, 7.0 mmol, 3.5 eq.) in toluene (15 mL) at 0°C, leading to an intense gas evolution (CO₂ + CO) and precipitation of a white solid. After stirring at room temperature for 2 h, the

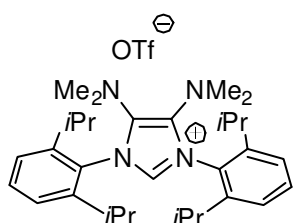
solution was again cooled down to 0°C, and diisopropylethylamine (1.05 mL, 6.0 mmol, 3.0 eq.) was added dropwise. The reaction mixture slowly became orange. After stirring for 1 h at 0°C and 2 h at room temperature, the precipitate was filtered off through a Celite plug (about 2 cm). The resulting orange mother solution was then added to the previously prepared solution of lithium dimesitylformamidinate at room temperature through cannula. The resulting mixture was stirred at room temperature overnight, filtered through celite to remove LiCl, diluted with CH₂Cl₂ (25 mL) and then cooled down to -30°C. TMSOTf (0.36 mL, 2.0 mmol) was added dropwise, resulting in a color change from orange to dark brown. The solution was allowed to warm up to room temperature in the cooling bath and after 6 h at room temperature, all volatiles were evaporated, leading to a crude residue which was purified by flash chromatography (SiO₂, pure CH₂Cl₂ then CH₂Cl₂/MeOH : 99/1) to afford an off-white powder (492 mg, 47%). Single crystals suitable for an X-Ray diffraction experiment were grown by slow diffusion of Et₂O into a solution of **2.6a** in CH₂Cl₂. **¹H NMR (400 MHz, CDCl₃)** δ = 8.57 (s, 1H, N₂CH), 7.02 (s, 4H, CH_{Mes}), 2.65 (s, 12H, N-CH₃), 2.34 (s, 6H, CH_{3 para}), 2.12 (s, 12H, CH_{3 ortho}); **¹³C{¹H} NMR (101 MHz, CDCl₃)** δ = 141.0, 134.6, 134.2 (C_{Ar}), 130.2 (N₂CH), 129.9 (CH_{Mes}), 128.9 (C_{Ar}), 120.7 (q, J_{CF} = 321 Hz, CF₃SO₃⁻), 42.7 (N-CH₃), 21.1 (CH_{3 para}), 17.6 (CH_{3 ortho}); **IR(ATR):** ν = 3109, 2989, 2924, 1612, 1548, 1493, 1390, 1278, 1256, 1223, 1148, 1048, 1030, 855, 635, 573 cm⁻¹; **MS (ESI, positive mode):** m/z (%): 391 (100) [M – TfO]⁺; **Elemental analysis** *calcd* (%) for C₂₆H₃₅F₃N₄O₃S (MW = 540.64) + 0.3 CH₂Cl₂: C 55.80, H 6.34, N 9.90; *found*: C 55.92, H 6.39, N 9.54.

Alternative synthesis: starting from N-(trimethylsilyl)formamidine

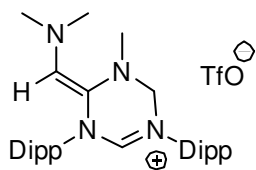
Addition of oxalyl chloride (0.61 mL, 7.2 mmol, 4.5 eq.) to a solution of DMF (0.56 mL, 7.2 mmol, 4.5 eq.) in toluene (6 mL) at 0°C, resulting in an intense gas evolution (CO and CO₂) and formation of a white precipitate. After stirring the mixture for 40 min at room temperature, diisopropylethylamine (0.84 mL, 4.82 mmol, 3.0 eq.) was added dropwise at 0°C and stirring was continued for 1 h at 0°C and then 2 h at room temperature. The resulting orange suspension was diluted with toluene (10 mL) and filtered using a fritted glass to separate the salts (4 mL of toluene were used to rinse). A solution of N,N'-dimesityl-N-(trimethylsilyl)formamidine (565 mg, 1.60 mmol) in CH₂Cl₂ (10 mL) was added into the reaction mixture and the resulting orange solution was stirred at room temperature overnight. TMSOTf (290 μL, 1.60 mmol, 1.0 eq.) was added dropwise at room temperature immediately forming a black solution. After 6 h of stirring, all volatiles were removed in vacuo and the dark gum-like residue was purified by flash column chromatography (SiO₂, hexane/EtOAc:

1/1 then pure EtOAc then CH₂Cl₂/MeOH: 95/5) yielding a red solid. This crude product was further purified by washing with small amounts of Et₂O and dissolution/evaporation cycles with CH₂Cl₂ to yield a white solid (450 mg, 55%).

1,3-bis(2,6-diisopropylphenyl)-4,5-bis(dimethylamino)imidazolium triflate (**2.6b**)

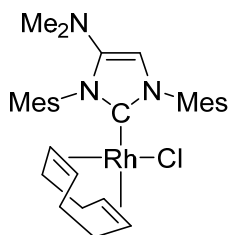


*n*BuLi (1.6 M in hexane, 1.31 mL, 2.1 mmol, 1.05 eq.) was added dropwise to a solution of di(2,6-diisopropylphenyl)formamidine (0.73 g, 2.0 mmol) in Et₂O (10 mL) at 0 °C, and the mixture was stirred at this temperature for 1 h to afford a light yellow solution of the corresponding lithium formamidinate. In a separate experiment, oxalyl chloride (0.6 mL, 7.0 mmol, 3.5 eq.) was added to a solution of DMF (0.55 mL, 7.0 mmol, 3.5 eq.) in toluene (20 mL) at 0°C, leading to an intense gas evolution (CO₂ + CO) and precipitation of a white solid. After stirring at room temperature for 1 h, the solution was again cooled to 0°C, and diisopropylethylamine (1.05 mL, 6.0 mmol, 3.0 eq.) was added dropwise. The reaction mixture slowly became orange. After stirring for 1 h at 0°C and then 2 h at room temperature, the precipitate was filtered off through a Celite plug (about 2 cm). The previously prepared orange mother solution was then added to the solution of lithium di(2,6-diisopropylphenyl)formamidinate at room temperature through cannula. The resulting mixture was stirred at room temperature for 6 h, filtered through celite to remove LiCl, diluted with CH₂Cl₂ (25 mL) and then cooled at -30°C. TMSOTf (0.36 mL, 2.0 mmol) was added dropwise resulting in a color change from orange to dark brown. The solution was then allowed to warm up to room temperature in the cooling bath, and after 6 h at room temperature, all volatiles were evaporated to give a crude residue which was purified by flash chromatography (SiO₂, pure CH₂Cl₂ then CH₂Cl₂/MeOH: 98/2) to afford a light yellow powder which was further purified by recrystallization in CH₂Cl₂/Et₂O to give an off-white powder (480 mg, 38%). Single crystals suitable for an X-Ray diffraction experiment were grown by layering a solution of **2.6b** in CH₂Cl₂ with pentane. **¹H NMR (400 MHz, CDCl₃)** δ = 8.62 (s, 1H, N₂CH), 7.58 (t, *J* = 7.8 Hz, 2H, CH_{Ar}), 7.36 (d, *J* = 7.8 Hz, 4H, CH_{Ar}), 2.71 (s, 12H, N-CH₃), 2.45-2.38 (m, 4H, CH_{iPr}), 1.35 (d, *J* = 6.7 Hz, 12H, CH_{3 iPr}), 1.22 (d, *J* = 6.8 Hz, 12H, CH_{3 iPr}); **¹³C{¹H} NMR (101 MHz, CDCl₃)** δ = 145.7, 135.0 (C_{Ar}), 132.0 (CH_{Ar}), 129.5 (N₂CH), 128.1 (C_{Ar}), 124.8 (CH_{Ar}), 120.7 (q, *J*_{CF} = 321 Hz, CF₃SO₃⁻), 43.0 (N-CH₃), 29.4 (CH_{iPr}), 25.8, 22.7 (CH_{3 iPr}); MS (ESI, positive mode): *m/z* (%): 475 (100) [M – TfO]⁺; **Elemental analysis calcd (%)** for C₃₂H₄₇F₃N₄O₃S (MW = 624.81): C 61.51, H 7.58, N 8.97; **found:** C 61.30, H 7.45, N 8.69.



During the optimization of synthesis of **2.6b**, we observed another by-product **2.7** which was purified by flash chromatography (SiO₂, pure CH₂Cl₂ then CH₂Cl₂/MeOH: 98/2) to afford a yellow powder (249.7 mg, 20 %). Single crystals suitable for an X-Ray diffraction experiment were grown by layering a solution of **2.7** in CH₂Cl₂ with pentane. **¹H NMR (400 MHz, CDCl₃)** δ = 7.53 (t, J = 7.8 Hz, 1H, CH_{Ar}), 7.45 (t, J = 7.9 Hz, 1H, CH_{Ar}), 7.40 (s, 1H, N₂CH), 7.32 (d, J = 7.8 Hz, 2H, CH_{Ar}), 7.26 (d, J = 7.3 Hz, 2H, CH_{Ar}), 5.17 (s, 1H, CH), 4.95 (s, 2H, CH₂), 3.24 (s, 3H, N-CH₃), 3.23-3.07 (m, 4H, CH_{iPr}), 2.92 (s, 6H, N-(CH₃)₂), 1.38 (d, J = 6.7 Hz, 6H, CH_{3 iPr}), 1.32 (d, J = 6.7 Hz, 6H, CH_{3 iPr}), 1.27 (d, J = 6.8 Hz, 12H, CH_{3 iPr}). **¹³C{¹H} NMR (101 MHz, CDCl₃)** δ = 146.6 (CH_{Ar}), 146.2, 145.9 (C_{Ar}), 133.2, 132.1 (C_{Ar}), 132.0, 131.4, 128.1, 125.6, 125.4 (CH_{Ar}), 115.5 (C_{Ar}), 71.1 (CH₂), 44.2 (N-CH₃), 42.1 (N-(CH₃)₂), 29.0, 28.8 (CH_{iPr}), 25.3, 25.1, 24.7, 24.6 (CH_{3 iPr}). MS (ESI, positive mode): m/z (%): 475 (100) [M – TfO]⁺.

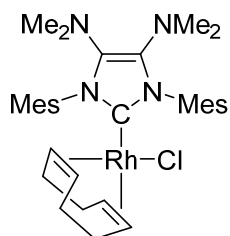
Chloro-(η^4 -cycloocta-1,5-diene)-(1,3-dimesityl-4-(dimethylamino)imidazol-2-ylidene)rhodium(I) (**2.8**)



A solution of KHMDS (0.5 M in toluene, 514 μ L, 0.257 mmol, 1.05 eq.) was added dropwise to a solution of **2.2a** (121.9 mg, 0.245 mmol) in THF (10 mL) at 0°C. After 30 min, solid [RhCl(1,5-cod)]₂ (60 mg, 0.122 mmol, 0.5 eq.) was added as a solid and the ice-water bath was removed. After 1 h, all volatiles were removed *in vacuo* and the crude residue was purified by flash chromatography (SiO₂, CH₂Cl₂) to give a yellow powder (105 mg, 72%). **¹H NMR (400 MHz, CDCl₃)** δ = 7.08 (s, 1H, CH_{Mes}), 7.04 (s, 1H, CH_{Mes}), 6.98 (s, 2H, CH_{Mes}), 6.31 (s, 1H, CH_{Im}), 4.55-4.50 (m, 1H, CH_{COD}), 4.47-4.42 (m, 1H, CH_{COD}), 3.36-3.33 (m, 1H, CH_{COD}), 3.07-3.03 (m, 1H, CH_{COD}), 2.50 (s, 3H, CH_{3 Mes}), 2.44 (s, 6H, N-CH₃), 2.43 (s, 3H, CH_{3 Mes}), 2.38 (s, 6H, CH_{3 Mes}), 2.37 (s, 6H, CH_{3 Mes}), 2.12 (s, 3H, CH_{3 Mes}), 2.05 (s, 3H, CH_{3 Mes}), 1.87-1.79 (m, 3H, CH_{2 COD}), 1.79-1.71 (m, 1H, CH_{2 COD}), 1.54-1.49 (m, 3H, CH_{2 COD}), 1.33-1.24 (m, 1H, CH_{2 COD}); **¹³C{¹H} NMR (101 MHz, CDCl₃)** δ = 180.7 (d, J_{RhC} = 53 HZ, N₂C_{carb}), 152.1, 147.2, 138.5, 138.4, 138.0, 137.8, 136.8, 135.6, 134.5 (C_{Ar}), 129.9, 129.7, 128.3, 128.1 (CH_{Mes}), 108.4 (CH_{Im}), 95.9 (d, J_{CRh} = 8 Hz, CH_{COD}), 95.6 (d, J_{CRh} = 8 Hz, CH_{COD}), 67.7 (d, J_{CRh} = 15 Hz, CH_{COD}), 43.3 (N-CH₃), 33.0, 32.6, 28.6, 28.2 (CH_{2 COD}), 21.3, 21.2 (CH_{3 para}), 20.6, 20.0, 18.7, 18.3 (CH_{3 ortho}); **IR (ATR):** ν = 3156, 2908, 2871, 2825, 1625, 1474, 1447, 1427, 1384, 1364, 1313, 1244, 1214, 1187, 1153, 1092, 1048, 1035, 1013, 956, 922, 866, 850,

816, 768, 736, 728, 668 cm^{-1} ; **MS (ESI):** m/z (%): 558 (100) $[\text{M} - \text{Cl}]^+$; **HRMS (ESI):** m/z calcd. for $\text{C}_{31}\text{H}_{41}\text{N}_3^{103}\text{Rh}$: 558.2356; found: 558.2358, $\epsilon_r = 0.4$ ppm.

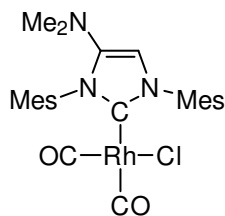
Chloro-(η^4 -cycloocta-1,5-diene)-(1,3-dimesityl-4,5-bis(dimethylamino)imidazol-2-ylidene) rhodium(I) (2.9)



A solution of KHMDS (0.5 M in toluene, 357 μL , 0.178 mmol, 2.2 eq.) was added dropwise to a solution of $[\text{Rh}(\text{cod})\text{Cl}]_2$ (40.0 mg, 81 μmol , 1.0 eq.) in toluene (5 mL) at room temperature. After 20 min of stirring, **2.6a** (87.7 mg, 162.2 μmol , 2.0 eq.) was added to the dark solution at 0°C .

Stirring was continued at room temperature for 2 h. All volatiles were evaporated and the crude product was purified by flash column chromatography (SiO_2 , hexane/EtOAc: 8/1 then 4/1) to yield a yellow powder (58 mg, 56 %). Single crystals suitable for an X-Ray diffraction experiment were grown by layering a solution of **2.9** in CH_2Cl_2 with pentane. **^1H NMR (400 MHz, CDCl_3)** δ = 7.03 (s, 2H, CH_{Mes}), 6.96 (s, 2H, CH_{Mes}), 4.40 (br, 2H, CH_{COD}), 3.23 (br, 2H, CH_{COD}), 2.54 (s, 12H, N- CH_3), 2.41 (s, 6H, CH_3_{Mes}), 2.36 (s, 6H, CH_3_{Mes}), 2.08 (s, 6H, CH_3_{Mes}), 1.82-1.72 (m, 4H, CH_2_{COD}), 1.48-1.45 (m, 4H, CH_2_{COD}); **$^{13}\text{C}\{^1\text{H}\}$ NMR (101 MHz, CDCl_3)** δ = 175.8 (d, $J_{\text{RhC}} = 52$ Hz, $\text{N}_2\text{C}_{\text{carb}}$), 140.0, 138.1, 137.9, 135.4, 135.2, 134.7 (C_{Ar}), 129.5 (CH_{Mes}), 127.7 (CH_{Mes}), 95.1 (d, $J_{\text{RhC}} = 8$ Hz, CH_{COD}), 67.2 (d, $J_{\text{RhC}} = 15$ Hz, CH_{COD}), 43.4 (N- CH_3), 32.7 (CH_2_{COD}), 28.3 (CH_2_{COD}), 21.1 (CH_3_{Mes}), 20.6 (CH_3_{Mes}), 18.7 (CH_3_{Mes}); **IR(ATR):** ν = 2982, 2929, 2913, 2872, 2827, 1739, 1649, 1485, 1448, 1360, 1297, 1239, 1123, 1052, 1031, 990, 957, 949, 850, 783, 733 cm^{-1} ; **MS (ESI, positive mode):** m/z (%): 601 (100) $[\text{M} - \text{Cl}]^+$; **Elemental analysis** calcd (%) for $\text{C}_{33}\text{H}_{46}\text{ClN}_4\text{Rh}$ (MW = 637.10): C 62.21, H 7.28, N 8.79; found: C 61.85, H 7.22, N 8.65.

Chloro-dicarbonyl-(1,3-dimesityl-4-(dimethylamino)imidazol-2-ylidene) rhodium(I) (2.10)

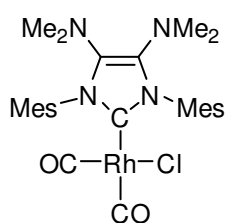


CO gas was bubbled into a solution of **2.8** (34.9 mg, 58.7 μmol) in CH_2Cl_2 (5 mL) for 10 min during which the color changed from bright yellow to very pale yellow. After 30 minutes, all volatiles were removed under

vacuum and the residue was washed with pentane (2 x 5 mL) to yield after drying a pale yellow powder (22.8 mg, 72%). **^1H NMR (400 MHz, CDCl_3)** δ = 7.00 (s, 2H, CH_{Mes}), 6.98 (s, 2H, CH_{Mes}), 6.43 (s, 1H, CH_{Im}), 2.49 (s, 6H, N- CH_3), 2.36 (s, 3H, $\text{CH}_3_{\text{para}}$), 2.35 (s, 3H, $\text{CH}_3_{\text{para}}$), 2.25 (s, 6H, $\text{CH}_3_{\text{ortho}}$), 2.23 (s, 6H, $\text{CH}_3_{\text{ortho}}$); **$^{13}\text{C}\{^1\text{H}\}$ NMR (101 MHz, CDCl_3)** δ = 185.2 (d, $J_{\text{RhC}} = 53.2$ Hz, Rh-CO), 183.0 (d, $J_{\text{RhC}} = 74.9$ Hz, Rh-CO), 174.2 (d, $J_{\text{RhC}} = 44.6$

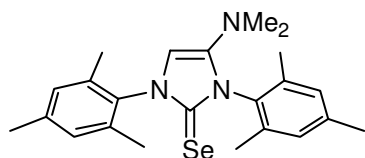
Hz, N_2C_{carb}), 147.0, 139.2, 139.1, 136.0, 135.8, 135.5, 133.5 (C_{Ar}), 129.5, 129.2 (CH_{Mes}), 108.2 (CH_{Im}), 43.1 (N-CH₃), 21.4, 21.3 (CH_3_{para}), 19.1, 18.6 (CH_3_{ortho}); **IR (CH₂Cl₂):** ν_{CO} = 2077.1, 1994.5 cm⁻¹; **IR (ATR):** ν = 3124, 2960, 2924, 2840, 2063, 1984, 1610, 1484, 1459, 1406, 1381, 1330, 1226, 1187, 1157, 1050, 923, 853 cm⁻¹; **MS (ESI):** m/z (%): 843 (17) [Rh(NHC)₂(CO)(H₂O)]⁺, 519 (100) [Rh(NHC)CO](CH₃CN)]⁺, 478 (31) [Rh(NHC)(CO)]⁺.

Chloro-dicarbonyl-(1,3-dimesityl-4,5-bis(dimethylamino)imidazol-2-ylidene) rhodium(I) (2.11)



CO gas was bubbled into a solution of **2.9** (71.2 mg, 0.112 mmol) in CH₂Cl₂ (5 mL) for 10 min during which the color changed from bright yellow to very pale yellow. After 30 minutes, all volatiles were removed under vacuum and the residue was washed with pentane (3 x 5 mL) to yield after drying a pale yellow powder (45.5 mg, 69%). **¹H NMR (400 MHz, CDCl₃)** δ = 6.97 (s, 4H, CH_{Mes}), 2.58 (s, 12H, N-CH₃), 2.35 (s, 6H, CH_3_{para}), 2.22 (s, 12H, CH_3_{ortho}); **¹³C{¹H} NMR (101 MHz, CDCl₃)** δ = 185.2 (d, J_{RhC} = 54 Hz, Rh-CO), 183.0 (d, J_{RhC} = 75 Hz, Rh-CO), 169.3 (d, J_{RhC} = 45 Hz, N_2C_{carb}), 138.6, 135.9, 135.4, 133.8 (C_{Ar}), 129.1 (CH_{Mes}), 43.2 (N-CH₃), 21.2 (CH_3_{para}), 19.0 (CH_3_{ortho}); **IR (CH₂Cl₂):** ν_{CO} = 2075.5, 1992.6 cm⁻¹; **IR (ATR):** ν = 2980, 2920, 2868, 2061, 1980, 1631, 1486, 1452, 1378, 1314, 1298, 1200, 1124, 1050, 1031, 991, 957, 924, 850, 716 cm⁻¹; **MS (ESI):** m/z (%): 576 (17) [Rh(NHC)(CH₃CN)₂]⁺, 562 (22) [Rh(NHC)(CO)(CH₃CN)]⁺, 549 (100) [Rh(NHC)(CO)₂]⁺, 521 (27) [Rh(NHC)(CO)₂]⁺, 391 (15) [NHC + H]⁺; **Elemental analysis calcd (%)** for C₂₇H₃₆ClN₄O₂Rh (MW = 586.96): C 55.25, H 6.18, N 9.55; *found*: C 55.56, H 6.17, N 9.22.

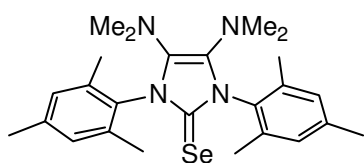
1,3-dimesityl-4-(dimethylamino)imidazolin-2-selenone (2.12)



A solution of KHMDS (0.5 M in toluene, 980 μ L, 0.49 mmol, 1.1 eq.) was added dropwise to a solution of **2.2a** (223 mg, 0.45 mmol, 1.0 eq) in THF (10 mL) at 0°C. After 30 min, selenium element (excess, *ca.* 75 mg) was added as a solid and the ice-water bath was removed. After 2 h, the solution was filtered by celite and silica and rinsed by CH₂Cl₂ until the solution was colorless. Evaporated the solvent under reduced pressure and the residue was washed by pentane to get a grey powder (185 mg, 96 %). **¹H NMR (400 MHz, CDCl₃)** δ = 7.01 (s, 2H, CH_{Mes}), 6.99 (s, 2H, CH_{Mes}), 6.28 (s, 1H, CH_{Im}), 2.51 (s, 6H, N-CH₃), 2.34 (s, 3H, CH_3_{para}), 2.33 (s, 3H, CH_3_{para}), 2.16 (s, 6H, CH_3_{ortho}), 2.15 (s, 6H, CH_3_{ortho}). **¹³C{¹H} NMR (101 MHz,**

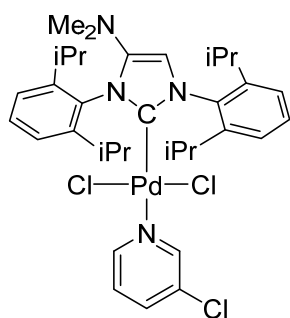
CDCl_3) δ = 154.4 (NCN), 144.4, 139.3, 139.1, 136.1, 135.5, 134.7, 132.9 ($C_{q\text{ Ar}}$), 129.6, 129.3 (CH_{Ar}), 103.9 ($\text{CH}_{\text{Im-5}}$), 42.9 (N- CH_3), 21.4, 21.3, 18.4, 18.2 (CH_3_{Mes}). $^{77}\text{Se}\{\text{1H}\}$ NMR (95 MHz, CDCl_3) δ = 32.2. **Elemental analysis calcd (%)** for $\text{C}_{23}\text{H}_{29}\text{N}_3\text{Se}$ (MW = 426.47): C 64.78, H 6.85, N 9.85; *found*: C 64.70, H 6.50, N 9.74.

1,3-dimesityl-4,5-bis(dimethylamino)imidazolin-2-selenone (2.13)



A solution of KHMDS (0.5 M in toluene, 440 μL , 0.22 mmol, 1.1 eq.) was added dropwise to a solution of **2.6a** (108.2 mg, 0.2 mmol, 1.0 eq) in THF (8 mL) at 0°C. After 30 min, selenium element (excess, *ca.* 37 mg) was added as a solid and the ice-water bath was removed. After 2 h, the solution was filtered by celite and silica and rinsed by CH_2Cl_2 until the solution was colorless. Evaporated the solvent under reduced pressure and the residue was washed by pentane to get the grey powder (80 mg, 94 %). ^1H NMR (400 MHz, CDCl_3) δ = 6.98 (s, 4H, CH_{Mes}), 2.59 (s, 12H, N- CH_3), 2.33 (s, 6H, $\text{CH}_3_{\text{para}}$), 2.16 (s, 12H, $\text{CH}_3_{\text{ortho}}$). $^{13}\text{C}\{\text{1H}\}$ NMR (101 MHz, CDCl_3) δ = 151.3 (NCN), 138.9, 136.0, 133.1, 132.9 ($C_{q\text{ Ar}}$), 129.3 (CH_{Ar}), 43.6 (N- CH_3), 21.4, 18.5 (CH_3_{Mes}). $^{77}\text{Se}\{\text{1H}\}$ NMR (95 MHz, CDCl_3) δ = 26.5. **Elemental analysis calcd (%)** for $\text{C}_{25}\text{H}_{34}\text{N}_4\text{Se}$ (MW = 469.54): C 63.95, H 7.30, N 11.93; *found*: C 63.87, H 7.19, N 11.83.

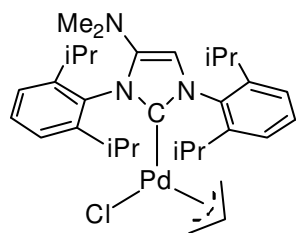
Dichloro-(3-chloropyridine)(1,3-(diisopropylphenyl)-4-dimethylaminoimidazol-2-ylidene)palladium(II) (2.14)



2.2b (291 mg, 0.50 mmol), Ag_2O (69.5 mg, 0.30 mmol, 0.6 eq) and LiCl (106 mg, 2.50 mmol, 5.0 eq) were placed in a Schlenk tube. Dry THF (10 mL) was added and the mixture was stirred at 70 °C for 2 h with exclusion of light. The solvent was removed under vacuum and the residue was suspended in CH_2Cl_2 (*ca.* 20 mL), then filtered through a plug of Al_2O_3 (Brockmann's type 3) and washed with CH_2Cl_2 until all the complex was eluted (checked by TLC). The solvent was concentrated to *ca.* 10 mL and $\text{PdCl}_2(\text{CH}_3\text{CN})_2$ (155.7 mg, 0.60 mmol, 1.2 eq) was added as a solid and the mixture was stirred overnight at 35°C. The resulting mixture was filtered through a plug of Al_2O_3 to give an orange solution which was concentrated to *ca.* 10 mL. To this solution, 3-chloropyridine (47 μL , 0.50 mmol, 1.0 eq) was added and the solution immediately changed from orange to bright yellow. After 1 hour at room temperature, the solution was filtered again through a plug of Al_2O_3 , washed with CH_2Cl_2 and the volatiles were removed under vacuum to leave a light

yellow solid (300 mg, 83%). Single crystals suitable for an X-Ray diffraction experiment were grown by layering a solution of **2.14** in CH₂Cl₂ with pentane. **¹H NMR (400 MHz, CDCl₃):** δ = 8.65 (s, 1H, CH_{py-2}), 8.56 (d, J = 5.5 Hz, 1H, CH_{py-6}), 7.54 (d, J = 8.2 Hz, 1H, CH_{py-4}), 7.48 (t, J = 7.7 Hz, 2H, CH_{Dipp-p}), 7.34 (d, J = 7.7 Hz, 4H, CH_{Dipp-m}), 7.05 (dd, J = 7.7, 6.0 Hz, 1H, CH_{py-5}), 6.45 (s, 1H, CH_{Im-5}), 3.37-3.27 (m, 2H, CH_{iPr}), 3.08-2.98 (m, 2H, CH_{iPr}), 2.44 (s, 6H, N-CH₃), 1.66 (d, J = 6.6 Hz, 6H, CH_{3 iPr}), 1.47 (d, J = 6.6 Hz, 6H, CH_{3 iPr}), 1.26 (d, J = 6.7 Hz, 6H, CH_{3 iPr}), 1.13 (d, J = 6.8 Hz, 6H, CH_{3 iPr}); **¹³C{¹H} NMR (101 MHz, CDCl₃):** δ = 150.6 (CH_{py}), 149.6 (CH_{py}), 149.3 (N₂C_{carbene}), 147.4, 147.0, 146.7 (C_{Ar}), 137.5 (CH_{py}), 136.2 (C_{q DIPP}), 133.0, 132.0 (C_{Ar}), 130.1 (CH_{Dipp}), 130.0 (CH_{Dipp}), 124.9 (CH_{Dipp}), 124.4 (CH_{py}), 124.2 (CH_{Dipp}), 110.2 (CH_{Im-5}), 42.7 (N-CH₃), 28.9 (CH_{iPr}), 26.6, 26.2, 25.0, 23.3 (CH_{3 iPr}); **IR (ATR):** ν = 2967, 2929, 2868, 1618, 1593, 1466, 1410, 1381, 1334, 1183, 1119, 1100, 1051, 932, 802, 758, 689 (cm⁻¹); **elemental analysis calcd (%)** for C₃₄H₄₅Cl₃N₄Pd (MW = 722.53): C 56.52, H 6.28, N 7.75; *found*: C 56.25, H 6.21, N 7.48.

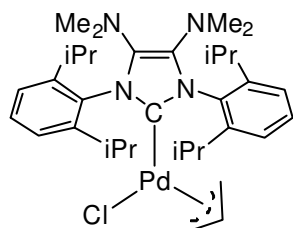
Chloro-(η^3 -allyl)-(1,3-(diisopropylphenyl)-4-dimethylaminoimidazol-2-ylidene)palladium(II) (2.15**)**



2.2b (116.4 mg, 0.20 mmol, 1.0 eq) was dissolved in dry THF (10 mL) and the solution was cooled to 0 °C. KHMDS (solution at 0.5 M in toluene, 0.44 mL, 0.22 mmol, 1.1 eq) was added dropwise and the solution became light yellow. After 30 min reacting at 0°C, [Pd(allyl)Cl]₂ (36.7 mg, 0.10 mmol, 0.5 eq) was added as a solid and the mixture was warmed to room temperature and allowed to stir for another 3 h. Volatiles were evaporated under vacuum and the crude residue was purified through flash chromatography (Al₂O₃ Brockmann's type III, CH₂Cl₂) to give a white powder (80 mg, 65 %). **¹H NMR (400 MHz, CDCl₃):** δ = 7.43 (t, J = 7.7 Hz, 1H, CH_{Ar}), 7.37 (t, J = 7.7 Hz, 1H, CH_{Ar}), 7.32-7.17 (m, 4H, CH_{Ar}), 6.45 (s, 1H, CH_{Im}), 4.82-4.67 (m, 1H, CH_{allyl}), 3.88 (d, J = 7.5 Hz, 1H, CH_{2 allyl}), 3.25-3.19 (m, 1H, CH_{iPr}), 3.15-3.09 (m, 1H, CH_{iPr}), 3.06-3.00 (m, 1H, CH_{iPr}), 2.86-2.77 (m, 2H, CH_{2 allyl}), 2.72-2.63 (m, 1H, CH_{iPr}), 2.47 (s, 6H, N-CH₃), 1.45 (d, J = 6.6 Hz, 6H, CH_{3 iPr}), 1.41 (d, J = 6.2 Hz, 6H, CH_{3 iPr}), 1.35 (d, J = 6.5 Hz, 6H, CH_{3 iPr}), 1.29 (d, J = 6.5 Hz, 6H, CH_{3 iPr}), 1.25-1.21 (m, 12H, CH_{3 iPr}), 1.19 (d, J = 6.4 Hz, 6H, CH_{3 iPr}), 1.08 (d, J = 6.6 Hz, 6H, CH_{3 iPr}); **¹³C{¹H} NMR (100.6 MHz, CDCl₃):** δ = 183.1 (N₂C_{carbene}), 146.8, 146.7, 146.2, 145.9, 136.7, 134.5 (C_{Ar}), 129.7 (CH_{p-Dipp}), 129.7 (CH_{p-Dipp}), 124.8, 124.6, 124.1, 123.7 (CH_{m-Dipp}), 114.1 (CH_{allyl}), 109.3 (CH_{Im}), 72.7 (CH_{2 allyl}), 49.4 (CH_{2 allyl}), 43.0 (N-CH₃), 28.8, 28.7, 28.6, 28.5 (CH_{iPr}), 26.8, 26.1, 26.0,

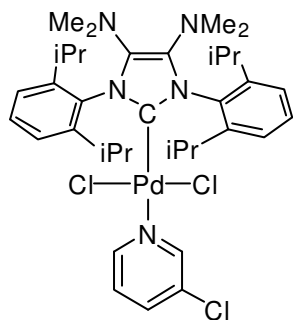
25.1, 25.0, 24.7, 23.2, 22.8 (CH_3 *i*Pr); IR (ATR): ν = 2963, 2927, 2867, 1619, 1468, 1450, 1397, 1380, 1360, 1320, 1178, 1053, 930, 805, 757, 680 (cm^{-1}); **MS (ESI, positive mode):** m/z (%): 578 (100) $[\text{M} - \text{Cl}]^+$; **elemental analysis calcd (%)** for $\text{C}_{32}\text{H}_{46}\text{ClN}_3\text{Pd}$: C 62.54, H 7.54, N 6.84; *found*: C 62.69, H 7.80, N 6.68.

Chloro-(η^3 -2-propen-1-yl)-(1,3-(diisopropylphenyl)-4,5-bis(dimethylamino)imidazol-2-ylidene)palladium(II) (2.16)



*n*BuLi (1.51 M in hexane, 364 mL, 0.55 mmol, 1.1 eq.) was added dropwise to a solution of **2.6b** (313 mg, 0.5 mmol) in THF (20 mL) at -70°C . After 40 min, solid $[\text{PdCl}(\text{allyl})]_2$ (92 mg, 0.25 mmol, 0.5 eq.) was added all at once and the solution was stirred for 1 h at -70°C and 1 h at room temperature. The volatiles were evaporated under vacuum and the crude residue was purified by flash chromatography (Al_2O_3 , CH_2Cl_2), giving a light yellow powder (240 mg, 73%), which was directly engaged in the next reaction. **^1H NMR (300 MHz, CDCl_3):** δ = 7.42-7.37 (m, 2H, CH_{Dipp}), 7.25-7.22 (m, 4H, CH_{Dipp}), 4.86-4.52 (m, 1H, CH_{allyl}), 3.84 (d, J = 7.4 Hz, 1H, $\text{CH}_2_{\text{allyl}}$), 2.98-2.72 (m, 5H, 1H, $\text{CH}_2_{\text{allyl}}$ and 4H, $\text{CH}_{i\text{Pr}}$), 2.60 (s, 12H, N- CH_3), 1.43 (d, J = 6.7 Hz, 12H, CH_3 *i*Pr), 1.21 (d, J = 6.8 Hz, 12H, CH_3 *i*Pr). **$^{13}\text{C}\{^1\text{H}\}$ NMR (101 MHz, CDCl_3)** δ = 175.8 ($\text{N}_2\text{C}_{\text{carbene}}$), 146.8, 135.1, 135.0 (C_{Dipp} + $\text{C}_{\text{Im-4,5}}$), 129.3, 124.3 (CH_{Dipp}), 113.5 (CH_{allyl}), 73.2 ($\text{CH}_2_{\text{allyl}}$), 51.3 ($\text{CH}_2_{\text{allyl}}$), 43.8 (N- CH_3), 28.8 ($\text{CH}_{i\text{Pr}}$), 25.3 (CH_3 *i*Pr); **MS (ESI, positive mode):** m/z (%): 621 (100) $[\text{M} - \text{Cl}]^+$; **HRMS (ESI):** m/z calcd. for $\text{C}_{34}\text{H}_{51}\text{N}_4^{104}\text{Pd}$: 619.3154; *found*: 619.3154, ϵ_r = 0.0 ppm; **Elemental analysis calcd (%)** for $\text{C}_{34}\text{H}_{51}\text{ClN}_4\text{Pd}$ (MW = 657.67): C 62.09, H 7.82, N 8.52; *found*: C 61.72, H 7.95, N 8.34.

Dichloro-(3-chloropyridine)(1,3-(diisopropylphenyl)-4,5-bis(dimethylamino)imidazol-2-ylidene)palladium(II) (2.17)



A solution of HCl (2M in Et_2O , 2.3 mL, 4.6 mmol, 12 eq.) was added to solid $[(\mathbf{2b})\text{Pd}(\text{allyl})\text{Cl}]$ (240 mg, 0.364 mmol) at room temperature. The color of the solution changed from light yellow to orange and soon after an orange solid began to precipitate. After 2 h, the volatiles were evaporated under vacuum and the solid was dissolved in CH_2Cl_2 (10 mL). Further addition of morpholine (238 μL , 2.5 mmol, 7 eq.) led to a color change from orange to bright yellow. The reaction mixture was stirred for another 1 h and filtered through a plug of silica gel. The solvent was removed under vacuum to leave a yellow solid (250 mg, 90%, 66% from the imidazolium). Single crystals suitable for an X-Ray

diffraction experiment were grown by layering a solution of **2.17** in CH₂Cl₂ with pentane. **¹H NMR (400 MHz, CDCl₃):** δ = 8.60 (d, J = 2.3 Hz, 1H, CH_{py-2}), 8.53 (dd, J = 5.5, 1.4 Hz, 1H, CH_{py-6}), 7.52 (ddd, J = 8.2, 2.4, 1.3 Hz, 1H, CH_{py-4}), 7.46 (t, J = 8.0 Hz, 2H, CH_{Dipp-p}), 7.33 (d, J = 7.7 Hz, 4H, CH_{Dipp-m}), 7.03 (dd, J = 8.2, 5.6 Hz, 1H, CH_{py-5}), 3.08 (p, J = 6.6 Hz, 4H, CH_{iPr}), 2.57 (s, 12H, N-CH₃), 1.60 (d, J = 6.5 Hz, 12H, CH_{3 iPr}), 1.20 (d, J = 6.7 Hz, 12H, CH_{3 iPr}); **¹³C{¹H} NMR (101 MHz, CDCl₃):** δ = 150.7 (CH_{py-2}), 149.7 (CH_{py-6}), 147.5 (C_{Dipp-o}), 145.3 (N₂C_{carb}), 137.3 (CH_{py-4}), 136.3 (C_{Im-4,5}), 133.6 (C_{Dipp-ipso}), 131.9 (C_{py-3}), 129.7 (CH_{Dipp-p}), 124.7 (CH_{Dipp-m}), 124.3 (CH_{py-5}), 43.8 (N-CH₃), 29.0 (CH_{iPr}), 26.1, 25.9 (CH_{3 iPr}); **IR (ATR):** ν = 2968, 2927, 2868, 1637, 1464, 1451, 1380, 1369, 1297, 1118, 1100, 1049, 989, 961, 929, 805, 767, 747, 711, 691 (cm⁻¹); **MS (ESI, positive mode):** m/z (%): 475 (100) [imidazolium]⁺; **Elemental analysis calcd (%)** for C₃₆H₅₀Cl₃N₅Pd (MW = 765.59): C 56.48, H 6.58, N 9.15; *found*: C 56.37, H 6.41, N 9.21.

3 Palladium-Catalyzed Buchwald-Hartwig amination reaction

Kinetic studies on the amination of 4-chloroanisole with morpholine

Pre-catalysts **1.1**, **2.14**, **2.17** (0.02 mmol, 2 mol%) and KO^tBu (168 mg, 1.5 mmol) were placed in three separate Schlenk tubes, which were closed with a septum, put under nitrogen by three vacuum/N₂ cycles and placed in a thermostatic bath at 25°C. Dodecane (224 μ L, 1.0 mmol, internal standard) and morpholine (109 μ L, 1.2 mmol) were syringed into and the reaction mixture was stirred for 2 minutes. DME (1.0 mL) was then injected via syringe followed by 4-chloroanisole (122 μ L, 1.0 mmol) and the time was started at this point. Conversions were measured by passing an aliquot of the solution through a plug of silica gel using EtOAc as eluant and monitoring the relative areas of the peaks compared to that of dodecane in the GC chromatogram.

Palladium-catalyzed amination at room temperature: general procedure A (Table 2.4.4)

KO^tBu (168 mg, 1.5 mmol, 1.5 eq) and pre-catalyst **2.17** (15.4 mg, 20 μ mol, 2 mol%) were charged into a Schlenk tube that was sealed with a septum, then evacuated and purged with nitrogen by three times. The amine (1.2 mmol, 1.2 eq) was added via syringe, and the reaction was allowed to stir for about 2 minutes. DME (1.0 mL) was then injected via syringe followed by the aryl halide (1.0 mmol, 1.0 eq). If the aryl halide was a solid, it was introduced into the tube prior to purging with nitrogen. The reaction mixture was stirred at 25 °C for the indicated

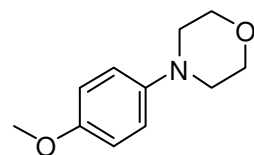
time. The reaction mixture was diluted with EtOAc (10 mL), filtered through a small plug of silica gel and washed with ethyl acetate. The filtrate was concentrated under reduced pressure and purified via silica gel flash chromatography. The reported yields are the average of at least two runs.

Palladium-catalyzed amination at low catalyst loadings: general procedure B (Table 2.4.5)

Under air, KO^tBu (168 mg, 1.5 mmol, 1.5 eq) was charged into a Schlenk tube that was sealed with a septum, then evacuated and purged with nitrogen by three times. The desired volume of a stock solution of pre-catalyst **2.17** (x mL, 0.003 M, prepared by dissolving 1.7 mg of **18** in 0.75 mL of dioxane) was added via syringe, followed by the addition of the amine (1.2, mmol, 1.2 eq). The mixture was stirred at room temperature for 2-3 min. Dioxane ((1-x) mL) was added and finally the aryl halide (1.0 mmol, 1.0 eq). Then the mixture was put into a preheated oil bath (80 °C), and was allowed to stir for 18 h. The reaction mixture was diluted with EtOAc (10 mL), filtered through a small plug of Silica gel and washed with ethyl acetate. The filtrate was concentrated under reduced pressure and purified via silica gel flash chromatography. The reported yields are the average of at least two runs

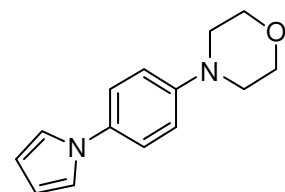
3.1 Catalytic products (Table 2.4.4 and 2.4.5)

4-(4-methoxyphenyl)morpholine (2.18a): After flash chromatography on silica gel (Pentane/Et₂O: 4/1), the general procedure A yielded 176.6 mg (91 %, **2.18a**), and the procedure B yielded 182.0 mg (94%, **2.19a**) of the title compound as a white solid.



¹H NMR (400 MHz, CDCl₃): δ = 6.99-6.76 (m, 4H), 3.86 (t, *J* = 4.7 Hz, 4H), 3.77 (s, 3H), 3.06 (t, *J* = 4.8 Hz, 4H). ¹³C{¹H} NMR (101 MHz, CDCl₃): δ = 154.1, 145.8, 117.9, 114.6, 67.2, 55.7, 51.0.

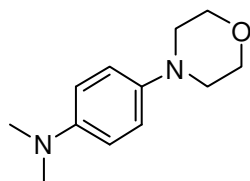
4-(4-(pyrrol-1-yl)phenyl)morpholine (2.18b): After flash chromatography on silica gel (DCM/MeOH: 99/1), the general procedure A yielded 209.7 mg (92%) of the title compound as a white solid.



¹H NMR (400 MHz, CDCl₃): δ = 7.35-7.28 (m, 2H), 7.02 (t, *J* = 2.2 Hz, 2H), 6.99-6.93 (m, 2H), 6.33 (t, *J* = 2.2 Hz, 2H), 3.95-3.82 (m,

4H), 3.23-3.12 (m, 4H). $^{13}\text{C}\{^1\text{H}\}$ NMR (101 MHz, CDCl_3): δ = 149.5, 134.0, 121.9, 119.6, 116.6, 109.9, 67.0, 49.7.

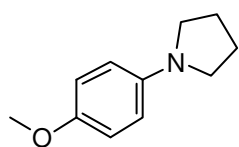
4-[4-(N,N-dimethylamino)phenyl]morpholine (2.18c): After flash chromatography on silica gel (Pentane/Ethyl Acetate: 2/3), the general procedure A yielded 202.4 mg (98%) of the title compound as a white solid.



^1H NMR (400 MHz, CDCl_3): δ = 6.94-6.86 (m, 2H), 6.80-6.72 (m, 2H), 3.86 (t, J = 4.7 Hz, 4H), 3.05 (t, J = 4.8 Hz, 4H), 2.88 (s, 6H).

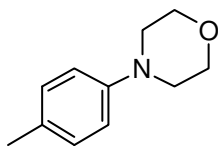
$^{13}\text{C}\{^1\text{H}\}$ NMR (101 MHz, CDCl_3): δ = 146.0, 143.3, 118.1, 114.6, 67.2, 51.2, 41.6.

1-(4-methoxyphenyl)pyrrolidine (2.18d): After flash chromatography on silica gel (Pentane/ Et_2O : 9/1), the general procedure A yielded 146.5 mg (83%) of the title compound as a white solid.



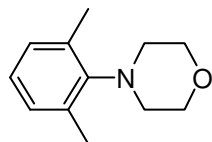
^1H NMR (400 MHz, CDCl_3): δ = 6.95-6.75 (m, 2H), 6.66-6.46 (m, 2H), 3.77 (s, 3H), 3.29-3.17 (m, 4H), 2.05-1.93 (m, 4H). $^{13}\text{C}\{^1\text{H}\}$ NMR (101 MHz, CDCl_3): δ = 151.0, 143.3, 115.2, 112.8, 56.1, 48.5, 25.5.

4-(4-methylphenyl)morpholine (2.18e): After flash chromatography on silica gel (Pentane/ Et_2O : 5/1), the general procedure A yielded 167.3 mg (94 %, **2.18e**), and the procedure B yielded 176.5 mg (99%, **2.19b**) of the title compound as a white solid.



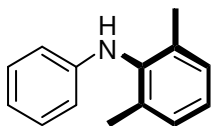
^1H NMR (400 MHz, CDCl_3): δ = 7.10 (d, J = 8.3 Hz, 2H), 6.84 (d, J = 8.5 Hz, 2H), 3.86 (t, J = 4.8 Hz, 3H), 3.11 (t, J = 4.9 Hz, 3H), 2.29 (s, 3H). $^{13}\text{C}\{^1\text{H}\}$ NMR (101 MHz, CDCl_3): δ = 149.3, 129.8, 129.7, 116.2, 67.1, 50.1, 20.5.

4-(2,6-dimethylphenyl)morpholine (2.18f): After flash chromatography on silica gel (Pentane/Ethyl Acetate: 95/5), the general procedure A at 50°C yielded 179.2 mg (94%) as colorless crystals.



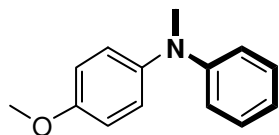
^1H NMR (400 MHz, CDCl_3): δ = 7.08-6.89 (m, 3H), 3.82 (t, J = 4.3 Hz, 4H), 3.12 (t, J = 4.3 Hz, 4H), 2.37 (s, 6H). $^{13}\text{C}\{^1\text{H}\}$ NMR (101 MHz, CDCl_3): δ = 148.0, 137.1, 129.2, 125.5, 68.3, 50.1, 19.7.

2,6-dimethyl-N-phenylaniline (2.18g): After flash chromatography on silica gel (Pentane/ Et_2O : 9/1), the general procedure A yielded 163.2 mg (83%) of the title compound as an orange solid.



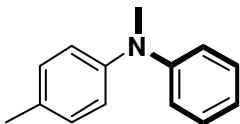
¹H NMR (400 MHz, CDCl₃): δ = 7.25-7.04 (m, 5H), 6.86-6.70 (m, 1H), 6.60-6.46 (m, 2H), 5.21 (br, s, 1H), 2.32-2.20 (m, 6H). **¹³C{¹H} NMR (101 MHz, CDCl₃):** δ = 146.4, 138.3, 136.0, 129.3, 128.66, 125.9, 118.3, 113.6, 18.5.

4-methoxy-*N*-methyl-*N*-phenylaniline (2.18h): After flash chromatography on silica gel (Pentane/Et₂O: 9/1), the general procedure **A** yielded 206.0 mg (97%, **2.18h**), and the procedure **B** yielded 211.8 mg (99%, **2.19i**) of the title compound as a yellow oil.



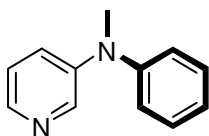
¹H NMR (400 MHz, CDCl₃): δ = 7.25-7.17 (m, 2H), 7.15-7.06 (m, 2H), 6.95-6.87 (m, 2H), 6.84-6.77 (m, 3H), 3.83 (s, 3H), 3.27 (s, 3H). **¹³C{¹H} NMR (101 MHz, CDCl₃):** δ = 156.4, 149.9, 142.4, 129.1, 126.3, 118.5, 115.9, 114.9, 55.6, 40.6.

4-Methyl-*N*-methyl-*N*-phenylaniline (2.18i): After flash chromatography on silica gel (Pentane/Ethyl Acetate: 99/1), the general procedure **A** yielded 188.2 mg (95%, **2.18i**), and the procedure **B** yielded 192.6 mg (98%, **2.19e**) of the title compound as a light yellow oil.



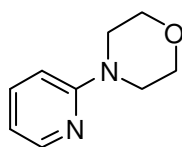
¹H NMR (400 MHz, CDCl₃): δ = 7.39-7.30 (m, 2H), 7.23 (d, J = 7.9 Hz, 2H), 7.11 (dd, J = 8.5, 1.7 Hz, 2H), 7.04 (d, J = 8.7 Hz, 2H), 6.98 (td, J = 7.4, 1.1 Hz, 1H), 3.39 (d, J = 1.4 Hz, 3H), 2.44 (s, 3H). **¹³C{¹H} NMR (101 MHz, CDCl₃):** δ = 149.5, 146.7, 132.1, 130.0, 129.1, 122.6, 119.9, 118.3, 40.4, 20.9.

***N*-methyl-*N*-(pyridin-3-yl)aniline (2.18j):** After flash chromatography on silica gel (Pentane/Ethyl Acetate: 9/1), the general procedure **A** yielded 147.1 mg (80%, **2.18j**) and the procedure **B** yielded 180.8 mg (98%, **2.19d**) of the title compound as a yellowish oil.



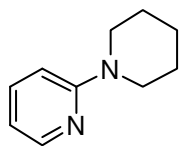
¹H NMR (400 MHz, CDCl₃): δ = 8.31 (s, 1H), 8.13 (d, J = 4.0 Hz, 1H), 7.35-7.27 (m, 2H), 7.23-7.17 (m, 1H), 7.15-6.99 (m, 4H), 3.31 (s, 3H). **¹³C{¹H} NMR (101 MHz, CDCl₃):** δ = 147.9, 145.1, 141.2, 140.6, 129.6, 124.7, 123.4, 123.3, 122.4, 40.0.

4-(pyridin-2-yl)morpholine (2.18k): After flash chromatography on silica gel (Pentane/Et₂O: 5/1), the general procedure **A** yielded 149.7 mg (91%, **2.18k**), and the procedure **B** yielded 142.0 mg (87%, **2.19c**) of the title compound as a colorless oil.



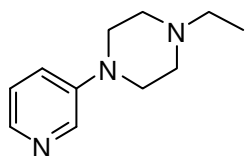
¹H NMR (400 MHz, CDCl₃): δ = 8.30-7.92 (m, 1H), 7.62-7.34 (m, 1H), 6.73-6.46 (m, 2H), 3.88-3.68 (m, 4H), 3.55-3.37 (m, 4H). **¹³C{¹H} NMR (101 MHz, CDCl₃):** δ = 159.6, 148.0, 137.5, 113.8, 106.9, 66.8, 45.6.

2-piperidinylpyridine (2.18l): After flash chromatography on silica gel (Pentane/Et₂O: 5/1), the general procedure A yielded 151.3 mg (93%) of the title compound as a yellowish oil.



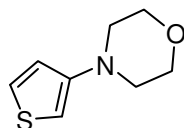
¹H NMR (400 MHz, CDCl₃): δ = 8.17 (ddd, J = 4.9, 2.0, 0.9 Hz, 1H), 7.44 (ddd, J = 8.9, 7.1, 2.0 Hz, 1H), 6.64 (d, J = 8.7 Hz, 1H), 6.55 (ddd, J = 7.1, 4.9, 0.9 Hz, 1H), 3.52 (s, 4H), 1.64 (s, 6H). **¹³C{¹H} NMR (101 MHz, CDCl₃):** δ = 159.8, 148.0, 137.5, 112.5, 107.3, 46.5, 25.7, 24.9.

1-ethyl-4-(pyridin-3-yl)piperazine (2.18m): After flash chromatography on silica gel



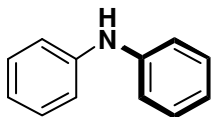
(MeOH/Ethyl Acetate: 1/1), the general procedure A yielded 184.6 mg (97%) of the title compound as an orange oil. **¹H NMR (400 MHz, CDCl₃):** δ = 8.28 (dd, J = 2.7, 1.1 Hz, 1H), 8.06 (dd, J = 4.2, 1.8 Hz, 1H), 7.20-7.06 (m, 2H), 3.22 (d, J = 5.1 Hz, 3H), 2.61 (d, J = 5.2 Hz, 4H), 2.46 (q, J = 7.2 Hz, 2H), 1.10 (t, J = 7.2 Hz, 3H). **¹³C{¹H} NMR (101 MHz, CDCl₃):** δ = 147.0, 140.6, 138.5, 123.6, 122.4, 52.5, 52.4, 48.4, 12.0.

4-(thiophen-3-yl)morpholine (2.18n): After flash chromatography on silica gel (Pentane/Ethyl Acetate: 3/1), the general procedure A at 80 °C yielded 146.3 mg (87%) of the title compound as a yellow solid.



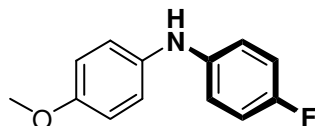
¹H NMR (400 MHz, CDCl₃): δ = 7.25 (dd, J = 5.3, 3.1 Hz, 1H), 6.86 (dd, J = 5.3, 1.6 Hz, 1H), 6.20 (dd, J = 3.1, 1.6 Hz, 1H), 3.90-3.79 (m, 4H), 3.13-3.03 (m, 4H). **¹³C{¹H} NMR (101 MHz, CDCl₃):** δ = 152.5, 125.7, 119.7, 100.5, 66.8, 50.9.

Diphenylamine (2.19f): After flash chromatography on silica gel (Pentane/Ethyl Acetate: 95/5), the general procedure B yielded 166.6 mg (98%) of the title compound as a white solid.



¹H NMR (400 MHz, CDCl₃): δ = 7.34-7.26 (m, 4H), 7.14-7.07 (m, 4H), 7.01-6.92 (m, 2H), 5.73 (br, s, 1H). **¹³C{¹H} NMR (101 MHz, CDCl₃):** δ = 143.2, 129.5, 121.1, 117.9.

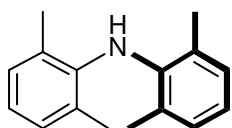
4-Fluoro-N-(4-methoxyphenyl)aniline (2.19g): After flash chromatography on silica gel



(Pentane/Et₂O: 90/10), the general procedure **B** yielded 212.3 mg (98%) of the title compound as a yellow-green solid.

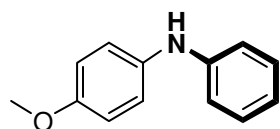
¹H NMR (400 MHz, CDCl₃): δ = 7.06-6.97 (m, 2H), 6.97-6.82 (m, 6H), 5.37 (br, s, 1H), 3.80 (s, 3H). **¹³C{¹H} NMR (101 MHz, CDCl₃):** δ = 158.5, 156.1, 155.1, 141.2 (d, J = 2 Hz), 136.6, 121.3, 117.9, 117.8, 116.0, 115.8, 114.9, 55.7.

Bis(2,6-dimethylphenyl)amine (2.19h): After flash chromatography on silica gel (Pentane), the general procedure **B** yielded 158.0 mg (70%) of the title compound as a white solid.



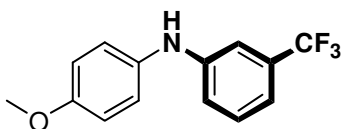
¹H NMR (400 MHz, CDCl₃): δ = 7.00 (d, J = 7.5 Hz, 4H), 6.86 (t, J = 7.4 Hz, 2H), 4.81 (br, s, 1H), 2.03 (s, 12H). **¹³C{¹H} NMR (75 MHz, CDCl₃):** δ = 141.9, 129.7, 128.8, 121.9, 19.3.

4-Methoxy-N-phenylaniline (2.19i): After flash chromatography on silica gel (Pentane/Et₂O: 95/5), the general procedure **B** yielded 190.4 mg (96%) of the title compound as a beige solid.



¹H NMR (400 MHz, CDCl₃): δ = 7.26-7.20 (m, 2H), 7.12-7.06 (m, 2H), 6.96-6.90 (m, 2H), 6.90-6.82 (m, 3H), 5.54 (br, s, 1H), 3.81 (s, 3H). **¹³C{¹H} NMR (101 MHz, CDCl₃):** δ = 155.4, 145.3, 135.8, 129.4, 122.3, 119.7, 115.8, 114.8, 55.7.

N-(4-methoxyphenyl)-3-(trifluoromethyl)aniline (2.19j): After flash chromatography on silica gel (Pentane/Et₂O: 85/15), the general procedure **B** yielded 258.5 mg (97%) of the title compound as a white powder.



¹H NMR (400 MHz, CDCl₃): δ = 7.28 (t, J = 7.9 Hz, 2H), 7.13-7.07 (m, 3H), 7.07-6.98 (m, 2H), 6.95-6.88 (m, 2H), 5.64 (br, s, 1H), 3.83 (s, 3H). **¹³C{¹H} NMR (75 MHz, CDCl₃):** δ = 156.2, 146.1, 134.4, 131.7 (q, J_{CF} = 32 Hz), 129.9, 123.5, 117.9 (q, J_{CF} = 1 Hz), 115.6 (q, J_{CF} = 4 Hz), 114.9, 11.3 (q, J_{CF} = 4 Hz), 55.6.

3.2 Palladium-Catalyzed Buchwald-Hartwig amination reaction using a mild base

General procedure for the optimization of Pd-catalyzed amination with carbonate base

Base (1.5 mmol, 3.0 eq) and palladium catalyst were charged under air into a Schlenk tube that was sealed with a septum and purged three times with nitrogen. 4-chloroanisole (55 μ L,

0.5 mmol, 1.0 eq), morpholine (69 μ L, 0.75 mmol, 1.5 eq) and solvent (0.5 mL) were subsequently added via syringe at room temperature. The mixture was stirred for about one minute at room temperature and was then transferred to a pre-heated oil bath (80 $^{\circ}$ C). The reaction was then allowed to proceed for 24 h, unless otherwise specified. The reaction mixture was diluted with ethyl acetate (10 mL), and dodecane (112 μ L, 0.5 mmol) was added as internal standard. Conversions were measured by passing an aliquot of the solution through a plug of silica gel using EtOAc as eluent and monitoring the relative areas of the peaks compared to that of dodecane in the GC chromatogram.

General procedure for Pd-catalyzed amination using cesium carbonate as the base (Table 2.4.7-2.4.9)

Cesium carbonate (488 mg, 1.5 mmol, 3.0 eq) and **2.17** (1.0-4.0 mol%) were charged under air into a Schlenk tube that was then sealed with a septum and purged three times with nitrogen. The aryl halide (0.5 mmol), the amine (0.75 mmol, 1.5 eq) and DME (0.5 mL) were subsequently added via syringe at room temperature. In cases where the aryl halide or amine was a solid at room temperature, it was introduced into the tube prior to purging with nitrogen. The mixture was stirred for about one minute at room temperature and was then transferred to a pre-heated oil bath (80 $^{\circ}$ C). Then the reaction was allowed to proceed for 24 h. The reaction mixture was diluted with ethyl acetate (10 mL), filtered through a small plug of Silica gel and washed with ethyl acetate. The filtrate was concentrated under reduced pressure and purified via silica gel flash chromatography.

Competitive amination experiments of 4-chlorotoluene with morpholine and piperidine (Scheme 2.4.10)

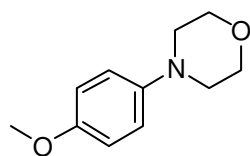
Cesium carbonate (488 mg, 1.5 mmol, 3.0 eq) and complex **2.17** (3.9 mg, 0.005 mmol, 1.0 mol%) were charged under air into a Schlenk tube that was sealed with a septum and purged three times with nitrogen. 4-chlorotoluene (59 μ L, 0.5 mmol, 1.0 eq), morpholine (69 μ L, 0.75 mmol, 1.5 eq), piperidine (59 μ L, 0.75 mmol, 1.5 eq) and DME (0.5 mL) were subsequently added via syringe at room temperature. The mixture was stirred for about one minute at room temperature and was then transferred to a preheated oil bath (80 $^{\circ}$ C). Then the reaction was allowed to proceed for 24 h. The ratio between the two products was determined by NMR spectrum of the crude mixture.

Competitive amination experiments of 4-chloroanisole with morpholine and piperidine (Scheme 2.4.10)

Cesium carbonate (488 mg, 1.5 mmol, 3.0 eq) and pre-catalyst **2.17** (3.9 mg, 0.005 mmol, 1.0 mol%) were charged under air into a Schlenk tube that was then sealed with a septum and purged with nitrogen by three times. 4-chlorotoluene (61 μ L, 0.5 mmol, 1.0 eq), morpholine (69 μ L, 0.75 mmol, 1.5 eq), piperidine (68 μ L, 0.75 mmol, 1.5 eq) and DME (0.5 mL) were subsequently added via syringe at room temperature. The mixture was stirred for about one minute at room temperature and was then transferred to a preheated oil bath (80 $^{\circ}$ C). The reaction was then allowed to proceed for 24 h. The ratio between the two products was determined by NMR spectrum of the crude mixture.

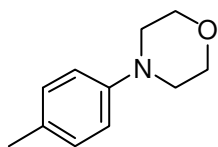
3.3 Catalytic products (Table 2.4.7-2.4.9)

4-(4-methoxyphenyl)morpholine (2.20a): After flash chromatography on silica gel (Pentane/Et₂O: 4/1), the title compound was recovered as a white solid: 94.0 mg (97 % yield).



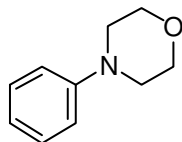
¹H NMR (400 MHz, CDCl₃): δ = 6.94-6.82 (m, 4H), 3.90-3.82 (m, 4H), 3.77 (s, 3H), 3.09-3.02 (m, 4H). ¹³C{¹H} NMR (101 MHz, CDCl₃): δ = 154.1, 145.7, 117.9, 114.6, 67.2, 55.7, 50.9.

4-(4-methylphenyl)morpholine (2.20b): After flash chromatography on silica gel (Pentane/Et₂O: 4/1), the title compound was recovered as a white solid: 88.0 mg (99 % yield).



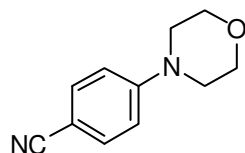
¹H NMR (400 MHz, CDCl₃): δ = 7.10 (d, *J* = 8.7 Hz, 2H), 6.85 (d, *J* = 8.4 Hz, 2H), 3.96-3.77 (m, 4H), 3.20-3.03 (m, 4H), 2.29 (s, 3H). ¹³C{¹H} NMR (101 MHz, CDCl₃): δ = 149.3, 129.8, 129.7, 116.2, 67.1, 50.1, 20.5.

4-phenylmorpholine (2.20c): After flash chromatography on silica gel (Pentane/Et₂O: 10/1), the title compound was recovered as a white solid: 79.9 mg (98 %).



¹H NMR (400 MHz, CDCl₃): δ = 7.32-7.27 (m, 2H), 7.00-6.82 (m, 3H), 3.91-3.83 (m, 4H), 3.20-3.13 (m, 4H). ¹³C{¹H} NMR (101 MHz, CDCl₃): δ = 151.4, 129.3, 120.2, 115.9, 67.1, 49.6.

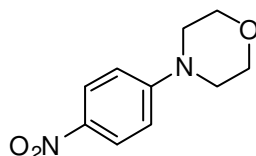
4-morpholinobenzonitrile (2.20d): After flash chromatography on silica gel (Pentane/Et₂O:



3/2), the title compound was recovered as a yellow solid: 87.4 mg (93 % yield).

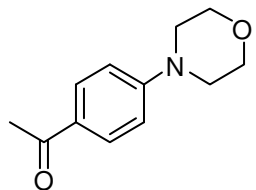
¹H NMR (400 MHz, CDCl₃): δ = 7.52-7.48 (m, 2H), 6.87-6.83 (m, 2H), 3.86-3.82 (m, 4H), 3.28-3.25 (m, 4H). **¹³C{¹H} NMR (101 MHz, CDCl₃):** δ = 153.6, 133.6, 120.0, 114.1, 101.0, 66.5, 47.4.

4-(4-nitrophenyl)morpholine (2.20e): After flash chromatography on silica gel (Pentane/Et₂O: 4/1), the title compound was recovered as an orange solid: 103.0 mg (99 % yield).



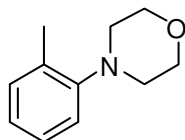
¹H NMR (400 MHz, CDCl₃): δ = 8.12 (dd, *J* = 9.2, 3.7 Hz, 2H), 6.82 (d, *J* = 9.3 Hz, 2H), 3.94-3.76 (m, 4H), 3.42-3.26 (m, 4H). **¹³C{¹H} NMR (101 MHz, CDCl₃):** δ = 155.1, 139.1, 126.0, 112.7, 66.5, 47.2.

4-(4-acetylphenyl)morpholine (2.20f): After flash chromatography on silica gel (Hexane/EtOAc: 1/1), the title compound was recovered as an orange solid: 102.0 mg (99 % yield).



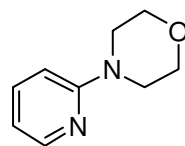
¹H NMR (400 MHz, CDCl₃): δ = 7.93-7.83 (m, 2H), 6.90-6.80 (m, 2H), 3.92-3.77 (m, 4H), 3.38-3.16 (m, 4H), 2.52 (s, 3H). **¹³C{¹H} NMR (101 MHz, CDCl₃):** δ = 196.7, 154.3, 130.5, 128.3, 113.4, 66.7, 47.7, 26.3.

4-(2-methylphenyl)morpholine (2.20g): After flash chromatography on silica gel (Hexane/EtOAc: 10/1), the title compound was recovered as a colorless oil: 76 mg (86 % yield).



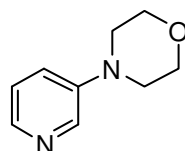
¹H NMR (400 MHz, CDCl₃): δ = 7.21 (t, *J* = 7.2 Hz, 2H), 7.09-6.98 (m, 2H), 3.88 (t, *J* = 4.5 Hz, 4H), 2.94 (t, *J* = 4.6 Hz, 4H), 2.35 (s, 3H). **¹³C{¹H} NMR (101 MHz, CDCl₃):** δ = 151.4, 132.7, 131.3, 126.7, 123.5, 119.0, 67.6, 52.4, 18.0.

4-(pyridin-2-yl)morpholine (2.20h): After flash chromatography on silica gel (Pentane/Et₂O: 2/1), the title compound was recovered as a colorless oil: 81.9 mg (100% yield).



¹H NMR (400 MHz, CDCl₃): δ = 8.16 (ddd, *J* = 5.0, 2.0, 0.9 Hz, 1H), 7.45 (ddd, *J* = 8.5, 7.2, 2.0 Hz, 1H), 6.64-6.54 (m, 2H), 3.82-3.71 (m, 4H), 3.49-3.40 (m, 4H). **¹³C{¹H} NMR (101 MHz, CDCl₃):** δ = 159.6, 148.0, 137.5, 113.8, 106.9, 66.8, 45.6.

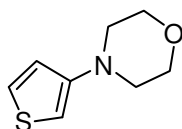
4-(pyridin-3-yl)morpholine (2.20i): After flash chromatography on silica gel (100 % Ethyl



acetate), the title compound was recovered as a yellow oil: 70.2 mg (86% yield).

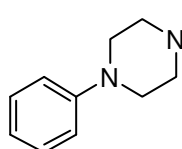
¹H NMR (400 MHz, CDCl₃): δ = 8.34-8.19 (m, 1H), 8.19-7.98 (m, 1H), 7.0-7.07 (m, 2H), 3.94-3.67 (m, 4H), 3.24-3.04 (m, 4H). **¹³C{¹H} NMR (101 MHz, CDCl₃):** δ = 147.0, 141.2, 141.2, 138.4, 123.6, 122.2, 66.8, 48.7.

4-(thiophen-3-yl)morpholine (2.20j): After flash chromatography on silica gel (Pentane/Ethyl Acetate: 3/1), the title compound was recovered as a yellow solid: 71.2 mg (84% yield).



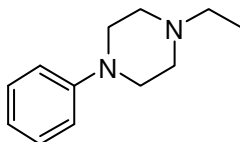
¹H NMR (400 MHz, CDCl₃): δ = 7.25 (dd, *J* = 5.2, 3.1 Hz, 1H), 6.86 (dd, *J* = 5.2, 1.5 Hz, 1H), 6.21 (dd, *J* = 2.9, 1.5 Hz, 1H), 3.91-3.72 (m, 4H), 3.18-2.96 (m, 4H). **¹³C{¹H} NMR (101 MHz, CDCl₃):** δ = 152.5, 125.7, 119.7, 100.6, 66.8, 50.9.

1,4-diphenylpiperazine (2.20k): After flash chromatography on silica gel (Pentane/Et₂O: 95/5), the title compound was recovered as white shiny crystals: 95.9 mg (81% yield).



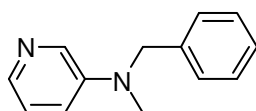
¹H NMR (400 MHz, CDCl₃): δ = 7.37-7.28 (m, 4H), 7.05-6.98 (m, 4H), 6.96-6.87 (m, 2H), 3.37 (d, *J* = 1.4 Hz, 8H). **¹³C{¹H} NMR (101 MHz, CDCl₃):** δ = 151.4, 129.3, 120.2, 116.5, 49.6.

1-ethyl-4-phenylpiperazine (2.20l): After flash chromatography on silica gel (DCM/MeOH: 90/10), the title compound was recovered as an orange oil: 86.4 mg (91% yield).



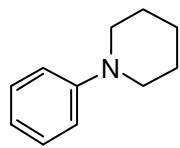
¹H NMR (400 MHz, CDCl₃): δ = 7.31-7.20 (m, 2H), 6.98-6.91 (m, 2H), 6.90-6.81 (m, 1H), 3.23 (t, *J* = 5.0 Hz, 4H), 2.63 (t, *J* = 5.2 Hz, 4H), 2.49 (q, *J* = 7.2 Hz, 2H), 1.14 (t, *J* = 7.2 Hz, 3H). **¹³C{¹H} NMR (101 MHz, CDCl₃):** δ = 151.4, 129.2, 119.8, 116.2, 53.0, 52.5, 49.2, 12.1.

***N*-benzyl-*N*-ethylpyridin-3-amine (2.20m):** After flash chromatography on silica gel (EtOAc/Pentane: 3/7), the title compound was recovered as a yellow oil: 97.5 mg (92% yield).



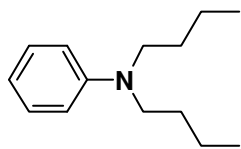
¹H NMR (400 MHz, CDCl₃): δ = 8.14 (d, *J* = 3.1 Hz, 1H), 7.92 (dd, *J* = 4.7, 1.3 Hz, 1H), 7.37-7.15 (m, 5H), 7.05 (dd, *J* = 8.5, 4.5 Hz, 1H), 6.97-6.84 (m, 1H), 4.51 (s, 2H), 3.50 (q, *J* = 7.1 Hz, 2H), 1.22 (t, *J* = 7.1 Hz, 3H). **¹³C{¹H} NMR (101 MHz, CDCl₃):** δ = 144.4, 138.1, 137.2, 134.5, 128.9, 127.2, 126.5, 123.8, 118.9, 53.8, 45.3, 12.1.

1-phenylpiperidine (2.20n): After flash chromatography on silica gel (Pentane/Et₂O: 95/5), the title compound was recovered as a colorless oil: 57.4 mg (71 % yield).



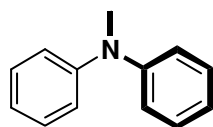
¹H NMR (400 MHz, CDCl₃): δ = 7.33-7.21 (m, 2H), 6.97 (d, *J* = 7.9 Hz, 2H), 6.85 (t, *J* = 7.3 Hz, 1H), 3.18 (t, *J* = 5.4 Hz, 4H), 1.80-1.70 (m, 4H), 1.65-1.56 (m, 2H). ¹³C{¹H} NMR (101 MHz, CDCl₃): δ = 152.4, 129.1, 119.3, 116.6, 50.8, 26.0, 24.5.

***N,N*-dibutylaniline (2.20o):** After flash chromatography on silica gel (Hexane/Ethyl Acetate: 20/1), the title compound was recovered as a colorless oil: 65.8 mg (64% yield).



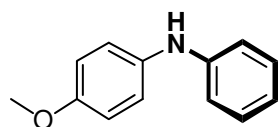
¹H NMR (400 MHz, CDCl₃): δ = 7.25-7.18 (m, 2H), 6.73-6.57 (m, 3H), 3.32-3.23 (m, 4H), 1.66-1.52 (m, 4H), 1.44-1.31 (m, 4H), 1.02-0.94 (m, 6H). ¹³C{¹H} NMR (101 MHz, CDCl₃): δ = 148.3, 129.3, 115.2, 111.8, 50.9, 29.6, 20.5, 14.2.

***N*-methyl-*N*-phenylamine (2.20p):** After flash chromatography on silica gel (Hexane/Ethyl Acetate: 99/1), the title compound was recovered as a colorless oil: 84.5 mg (92% yield).



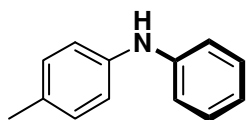
¹H NMR (400 MHz, CDCl₃): δ = 7.34 (t, *J* = 7.5 Hz, 4H), 7.09 (d, *J* = 7.7 Hz, 4H), 7.02 (t, *J* = 7.3 Hz, 2H), 3.38 (s, 3H). ¹³C{¹H} NMR (101 MHz, CDCl₃): δ = 149.1, 129.3, 121.4, 120.6, 40.3.

***N*-phenyl-4-methoxyaniline (2.21a):** After flash chromatography on silica gel (Pentane/Et₂O: 95/5), the title compound was recovered as a beige solid: 86.1 mg (86% yield).



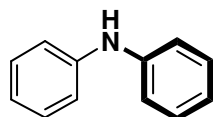
¹H NMR (300 MHz, CDCl₃): δ = 7.32-7.20 (m, 2H), 7.17-7.06 (m, 2H), 7.00-6.83 (m, 5H), 5.52 (br, s, 1H), 3.84 (s, 3H). ¹³C{¹H} NMR (75 MHz, CDCl₃): δ = 155.4, 145.3, 135.8, 129.4, 122.3, 119.7, 115.8, 114.8, 55.7

***N*-phenyl-4-methylaniline (2.21b):** After flash chromatography on silica gel (Hexane/Ethyl Acetate: 97/3), the title compound was recovered as a white solid: 91.4 mg (99% yield).



¹H NMR (400 MHz, CDCl₃): δ = 7.33-7.26 (m, 2H), 7.15 (d, *J* = 8.1 Hz, 2H), 7.09-7.03 (m, 4H), 6.94 (tt, *J* = 7.8, 1.0 Hz, 1H), 5.63 (br, s, 1H), 2.37 (s, 3H). ¹³C{¹H} NMR (101 MHz, CDCl₃): δ = 144.1, 140.4, 131.0, 130.0, 129.4, 120.5, 119.1, 117.0, 20.8.

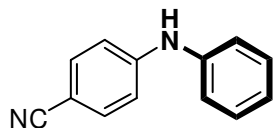
diphenylamine (2.21c): After flash chromatography on silica gel (Pentane/Ethyl Acetate:



95/5), the title compound was recovered as a white solid: 80.0 mg (95% yield).

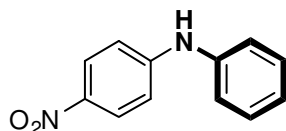
¹H NMR (400 MHz, CDCl₃): δ = 7.31 (t, *J* = 7.9 Hz, 4H), 7.11 (d, *J* = 8.4 Hz, 4H), 6.98 (t, *J* = 7.3 Hz, 2H), 5.73 (br, s, 1H). **¹³C{¹H} NMR (101 MHz, CDCl₃):** δ = 143.2, 129.5, 121.1, 117.9.

4-(phenylamino)benzonitrile (2.21d): After flash chromatography on silica gel (Hexane/Ethyl Acetate: 4/1), the title compound was recovered as a beige solid: 93.4 mg (96% yield).



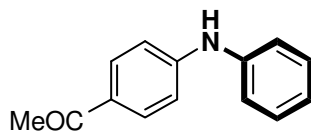
¹H NMR (400 MHz, CDCl₃): δ = 7.50 (d, *J* = 8.6 Hz, 2H), 7.43-7.32 (m, 2H), 7.23-7.17 (m, 2H), 7.17-7.10 (m, 1H), 7.04-6.94 (m, 2H), 6.13 (br, s, 1H). **¹³C{¹H} NMR (101 MHz, CDCl₃):** δ = 148.1, 140.1, 133.9, 129.8, 124.1, 121.4, 120.0, 115.0, 101.6.

N-phenyl-4-nitroaniline (2.21e): After flash chromatography on silica gel (Pentane/Diethyl Ether: 7/3), the title compound was recovered as a yellow solid: 104.2 mg (97% yield).



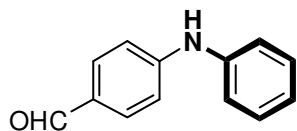
¹H NMR (400 MHz, CDCl₃): δ = 8.15-8.06 (m, 2H), 7.44-7.35 (m, 2H), 7.24-7.12 (m, 3H), 6.97-6.87 (m, 2H), 6.30 (br, s, 1H). **¹³C{¹H} NMR (101 MHz, CDCl₃):** δ = 150.3, 139.9, 139.6, 129.9, 126.4, 124.8, 122.1, 113.8.

N-(4-acetylphenyl)aniline (2.21f): After flash chromatography on silica gel (Hexane/Ethyl Acetate: 7/3), the title compound was recovered as a yellow solid: 99.7 mg (94% yield).



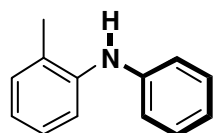
¹H NMR (400 MHz, CDCl₃): δ = 7.91-7.82 (m, 2H), 7.39-7.30 (m, 2H), 7.22-7.14 (m, 2H), 7.13-7.04 (m, 1H), 7.03-6.94 (m, 2H), 2.53 (s, 3H). **¹³C{¹H} NMR (101 MHz, CDCl₃):** δ = 196.5, 148.5, 140.7, 130.7, 129.7, 129.2, 123.5, 120.8, 114.6, 26.3.

4-(phenylamino)benzaldehyde (2.21g): After flash chromatography on silica gel (Pentane/Diethyl Ether: 8/1), the title compound was recovered as a yellow solid: 88.1 mg (89% yield).



¹H NMR (400 MHz, CDCl₃): δ = 9.79 (s, 1H), 7.81-7.68 (m, 2H), 7.43-7.30 (m, 2H), 7.23-7.18 (m, 2H), 7.16-7.08 (m, 1H), 7.06-6.99 (m, 2H), 6.40 (br, s, 1H). **¹³C{¹H} NMR (101 MHz, CDCl₃):** δ = 190.5, 150.0, 140.2, 132.2, 129.7, 128.6, 124.0, 121.4, 114.6.

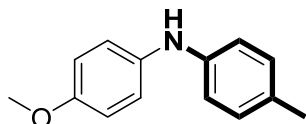
N-phenyl-2-methylaniline (2.21h): After flash chromatography on silica gel (hexane/ethyl



acetate: 20/1), the title compound was recovered as a colorless oil: 91.0 mg (99% yield).

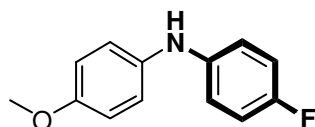
¹H NMR (400 MHz, CDCl₃): δ = 7.37-7.26 (m, 4H), 7.22 (td, J = 7.8, 1.4 Hz, 1H), 7.06-6.95 (m, 4H), 5.43 (br, s, 1H), 2.33 (s, 3H). **¹³C{¹H} NMR (101 MHz, CDCl₃):** δ = 144.1, 141.3, 131.0, 129.4, 128.4, 126.8, 122.1, 120.5, 118.9, 117.5, 18.0.

***N*-(4-methylphenyl)-4-methoxyaniline (2.21i):** After flash chromatography on silica gel (Hexane/EtOAc: 8/1), the title compound was recovered as a white solid: 97.4 mg (91% yield).



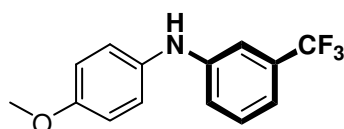
¹H NMR (300 MHz, CDCl₃): δ = 7.06-7.01 (m, 4H), 6.88-6.83 (m, 4H), 5.42 (br, s, 1H), 3.80 (s, 3H), 2.2 (s, 3H). **¹³C{¹H} NMR (75 MHz, CDCl₃):** δ = 154.9, 142.5, 136.7, 129.9, 129.5, 121.2, 116.7, 114.8, 55.7, 20.7.

***N*-(4-methoxyphenyl)-4-fluoroaniline (2.21j):** After flash chromatography on silica gel (Pentane/Et₂O: 9/1), the title compound was recovered as a grey solid: 105.5 mg (97% yield).



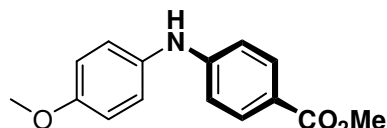
¹H NMR (400 MHz, CDCl₃): δ = 7.05-6.98 (m, 2H), 6.97-6.81 (m, 6H), 5.39 (br, s, 1H), 3.80 (s, 3H). **¹³C{¹H} NMR (101 MHz, CDCl₃):** δ = 157.3 (d, J = 238 Hz), 155.1, 141.2 (d, J = 2 Hz), 136.6, 121.3, 117.9 (d, J = 7 Hz), 115.9 (d, J = 22 Hz), 114.9, 55.7.

***N*-(4-methoxyphenyl)-3-(trifluoromethyl)aniline (2.21k):** After flash chromatography on silica gel (Pentane/Et₂O: 7/1), the title compound was recovered as a beige solid: 90.3 mg (68% yield).



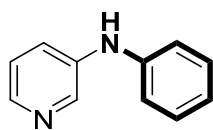
¹H NMR (400 MHz, CDCl₃): δ = 7.28 (t, J = 8.2 Hz, 1H), 7.14-7.06 (m, 3H), 7.06-6.96 (m, 2H), 6.95-6.85 (m, 2H), 5.62 (br, s, 1H), 3.82 (s, 3H). **¹³C{¹H} NMR (101 MHz, CDCl₃):** δ = 156.3, 146.1, 134.4, 131.8 (q, J = 32 Hz), 129.9, 124.3 (q, J = 273 Hz), 123.6, 118.0, 115.7 (q, J = 4 Hz), 115.0, 111.4 (q, J = 4 Hz), 55.7.

Methyl 4-(4-methoxyphenylamino)benzoate (2.21l): After flash chromatography on silica gel (Pentane/Et₂O: 7/1), the title compound was recovered as a beige solid: 67.2 mg (52% yield).



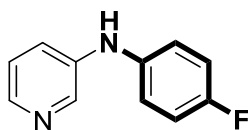
¹H NMR (400 MHz, CDCl₃): δ = 7.87 (d, J = 8.4 Hz, 2H), 7.12 (d, J = 8.5 Hz, 2H), 6.90 (d, J = 8.6 Hz, 2H), 6.81 (d, J = 8.5 Hz, 2H), 5.99 (s, 1H), 3.85 (s, 3H), 3.81 (s, 3H). **¹³C{¹H} NMR (101 MHz, CDCl₃):** δ = 167.2, 156.5, 150.0, 133.5, 131.6, 124.4, 119.9, 114.8, 113.3, 55.6, 51.7.

N-phenylpyridin-3-amine (2.21m): After flash chromatography on silica gel (Hexane/Ethyl Acetate: 1/4), the title compound was recovered as a white solid: 70.6 mg (83% yield).



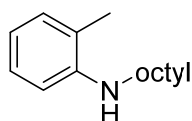
¹H NMR (400 MHz, CDCl₃): δ = 8.39 (s, 1H), 8.16 (d, *J* = 3.9 Hz, 1H), 7.41 (ddd, *J* = 8.2, 2.5, 1.2 Hz, 1H), 7.30 (t, *J* = 7.9 Hz, 2H), 7.17 (dd, *J* = 8.2, 4.7 Hz, 1H), 7.08 (d, *J* = 7.6 Hz, 2H), 6.99 (t, *J* = 7.4 Hz, 1H), 5.89 (d, *J* = 14.3 Hz, 1H). ¹³C{¹H} NMR (101 MHz, CDCl₃): δ = 142.1, 142.0, 140.3, 140.0, 129.7, 123.8, 123.5, 122.1, 118.4.

N-(4-fluorophenyl)pyridin-3-amine (2.21n): After flash chromatography on silica gel (100% Ethyl Acetate), the title compound was recovered as a white solid: 82.3 mg (88% yield).



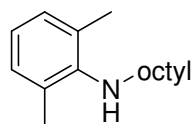
¹H NMR (400 MHz, CDCl₃): δ = 8.31 (d, *J* = 2.7 Hz, 1H), 8.13 (d, *J* = 4.6 Hz, 1H), 7.28 (ddd, *J* = 8.3, 2.8, 1.4 Hz, 1H), 7.14 (dd, *J* = 8.3, 4.7 Hz, 1H), 7.10-6.95 (m, 4H), 5.81 (d, *J* = 38.2 Hz, 1H). ¹³C{¹H} NMR (101 MHz, CDCl₃): δ = 158.7 (d, *J* = 242 Hz), 141.7 (d, *J* = 3 Hz), 140.7, 139.4, 123.9, 122.5, 121.4 (d, *J* = 8 Hz), 116.3 (d, *J* = 22 Hz).

N-octyl-2-methylaniline (2.22a): After flash chromatography on silica gel (Hexane/Ethyl Acetate: 20/1), the title compound was recovered as a colorless oil: 109.6 mg (94% yield).



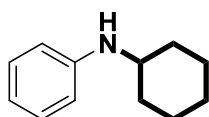
¹H NMR (400 MHz, CDCl₃): δ = 7.23 (td, *J* = 7.6, 1.2 Hz, 1H), 7.15 (d, *J* = 7.7 Hz, 1H), 6.79-6.64 (m, 2H), 3.52 (br, s, 1H), 3.24 (t, *J* = 7.1 Hz, 2H), 2.23 (s, 3H), 1.76 (p, *J* = 7.1 Hz, 2H), 1.57-1.33 (m, 10H), 1.06-0.95 (m, 3H). ¹³C{¹H} NMR (101 MHz, CDCl₃): δ = 146.5, 130.1, 127.2, 121.7, 116.7, 109.7, 44.1, 32.0, 29.7, 29.6, 29.4, 27.4, 22.8, 17.5, 14.2.

N-octyl-2,6-dimethylaniline (2.22b): After flash chromatography on silica gel (Pentane/Ethyl Acetate: 20/1), the title compound was recovered as a colorless oil: 109.6 mg (94% yield).



¹H NMR (400 MHz, CDCl₃): δ = 7.00 (d, *J* = 7.4 Hz, 2H), 6.81 (t, *J* = 7.4 Hz, 1H), 3.07-2.90 (m, 3H), 2.30 (s, 6H), 1.64-1.52 (m, 2H), 1.46-1.24 (m, 10H), 0.95-0.84 (m, 3H). ¹³C{¹H} NMR (101 MHz, CDCl₃): δ = 146.6, 129.2, 128.9, 121.6, 48.8, 32.0, 31.4, 29.7, 29.4, 27.3, 22.8, 18.7, 14.2.

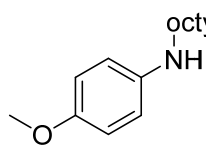
N-cyclohexylaniline (2.22c): After flash chromatography on silica gel (Hexane/Ethyl



Acetate: 10/1), the title compound was recovered as a colorless oil: 64.5 mg (74% yield).

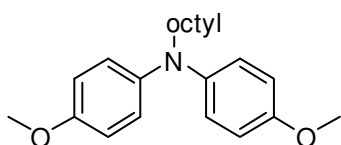
¹H NMR (400 MHz, CDCl₃): δ = 7.23- 7.13 (m, 2H), 6.73-6.65 (m, 1H), 6.65-6.55 (m, 2H), 3.53 (br, s, 1H), 3.35-3.22 (m, 1H), 2.08 (d, J = 12.6 Hz, 2H), 1.86-1.73 (m, 2H), 1.74-1.61 (m, 1H), 1.48-1.33 (m, 2H), 1.32-1.10 (m, 3H). **¹³C{¹H} NMR (101 MHz, CDCl₃):** δ = 147.5, 129.4, 116.9, 113.2, 51.8, 33.6, 26.1, 25.2.

***N*-octyl-4-methoxy-aniline (2.22d):** After flash chromatography on silica gel (Hexane/Ethyl Acetate: 20/1), the title compound was recovered as a white solid: 51.6 mg.



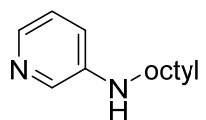
¹H NMR (400 MHz, CDCl₃): δ = 6.82-6.76 (m, 2H), 6.62-6.55 (m, 2H), 3.75 (s, 3H), 3.12 (s, br, 1H), 3.06 (t, J = 7.1 Hz, 2H), 1.61 (p, J = 7.0 Hz, 2H), 1.44-1.23 (m, 10H), 0.90 (t, J = 6.7 Hz, 3H). **¹³C{¹H} NMR (101 MHz, CDCl₃):** δ = 152.1, 143.0, 115.0, 114.1, 56.0, 45.2, 32.0, 29.8, 29.6, 29.4, 27.4, 22.8, 14.2.

***N,N*-bis(4-methoxyphenyl)octylamine (2.22d'):** After flash chromatography on silica gel (Hexane/Ethyl Acetate: 20/1), the title compound was recovered as a white solid: 48.6 mg.



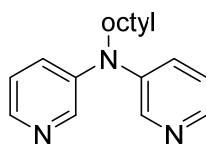
¹H NMR (400 MHz, CDCl₃): δ = 6.92-6.86 (m, 4H), 6.86-6.80 (m, 4H), 3.79 (s, 6H), 3.60-3.52 (m, 2H), 1.62 (p, J = 7.6 Hz, 2H), 1.35-1.23 (m, 10H), 0.89 (t, J = 6.6 Hz, 3H). **¹³C{¹H} NMR (101 MHz, CDCl₃):** δ = 154.3, 142.7, 122.2, 114.7, 55.7, 53.0, 32.0, 29.6, 29.5, 27.7, 27.3, 22.8, 14.2.

***N*-octyl-pyridin-3-amine (2.22f):** After flash chromatography on silica gel (Pure Ethyl Acetate), the title compound was recovered as a white solid: 72 mg.



¹H NMR (400 MHz, CDCl₃): δ = 8.01 (d, J = 2.8 Hz, 1H), 7.93 (dd, J = 4.7, 1.2 Hz, 1H), 7.10-7.01 (m, 1H), 6.84 (ddd, J = 8.3, 2.9, 1.4 Hz, 1H), 3.66 (br, s, 1H), 3.10 (t, J = 7.0 Hz, 2H), 1.62 (p, J = 7.1 Hz, 2H), 1.44-1.22 (m, 10H), 0.93-0.82 (m, 3H). **¹³C{¹H} NMR (101 MHz, CDCl₃):** δ = 144.5, 138.6, 136.2, 123.8, 118.4, 43.7, 31.9, 29.6, 29.5, 29.4, 27.2, 22.8, 14.2.

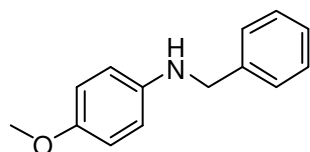
***N,N*-bis(pyridin-3-yl)octylamine (2.22f'):** After flash chromatography on silica gel (Pure Ethyl Acetate), the title compound was recovered as a white solid: 14 mg.



¹H NMR (400 MHz, CDCl₃): δ = 8.35 (d, J = 2.4 Hz, 2H), 8.23 (d, J = 3.8 Hz, 2H), 7.30-7.25 (m, 2H), 7.19 (dd, J = 8.3, 4.6 Hz, 2H), 3.70 (t, J = 7.7 Hz, 2H), 1.66 (p, J = 7.6 Hz, 2H), 1.33-1.21 (m, 10H), 0.86 (t, J = 6.9 Hz, 3H). **¹³C{¹H} NMR**

(101 MHz, CDCl₃): δ = 143.6, 143.1, 127.7, 124.0, 52.4, 31.9, 29.5, 29.4, 27.4, 27.1, 22.7, 14.2.

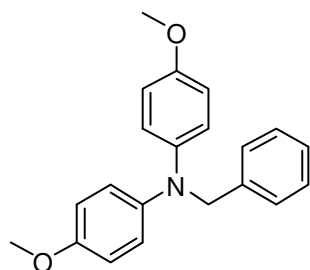
***N*-benzyl-4-methoxyaniline (2.22g):** After flash chromatography on silica gel (Hexane/Ethyl



Acetate: 20/1), the title compound was recovered as a white solid: 52.4 mg.

¹H NMR (400 MHz, CDCl₃): δ = 7.40-7.27 (m, 4H), 7.31-7.27 (m, 1H), 6.82-6.78 (m, 2H), 6.64-6.60 (m, 2H), 4.30 (s, 2H), 3.79 (s, br, 1H), 3.76 (s, 3H).
¹³C{¹H} NMR (101 MHz, CDCl₃): δ = 152.3, 142.6, 139.8, 128.7, 127.7, 127.3, 115.0, 114.2, 55.9, 49.4.

***N,N*-bis(4-methoxyphenyl)benzylamine (2.22g')**: After flash chromatography on silica gel (Hexane/Ethyl Acetate: 20/1), the title compound was recovered as a white solid: 35.1 mg.



¹H NMR (400 MHz, CDCl₃): δ = 7.40-7.27 (m, 4H), 7.22 (t, *J* = 7.1 Hz, 1H), 7.00-6.91 (m, 4H), 6.84-6.75 (m, 4H), 4.89 (s, 2H), 3.77 (s, 6H). **¹³C{¹H} NMR (101 MHz, CDCl₃):** δ = 154.4, 142.6, 139.7, 128.6, 126.8, 126.8, 121.9, 114.7, 57.2, 55.7.

4 Chapter 3

4.1 Palladium-Catalyzed Buchwald-Hartwig amination reaction with aryl tosylates

General procedure for the optimization of the Pd-PEPPSI pre-catalyst (Table 3.2.1)

4-toluenyl tosylate **3.1a** (131 mg, 0.5 mmol, 1.0 eq) or 4-methoxyphenyl tosylate **3.2a** (139 mg, 0.5 mmol, 1.0 eq.), K₃PO₄ (318 mg, 1.5 mmol, 3.0 eq) and Pd catalyst (0.01 mmol, 2 mol%) were charged under air into a Schlenk tube (15 mL volume) that was sealed with a septum, and the tube was evacuated and flushed with nitrogen for three times. Morpholine (66 μ L, 0.75 mmol, 1.5 eq) and *t*AmOH (1.5 mL) were subsequently added via syringe at room temperature. The mixture was stirred for about one minute at room temperature and was then placed into a pre-heated oil bath at 120°C. The reaction was allowed to stir for 18 h. The reaction mixture was cooled, diluted with 10 mL ethyl acetate and dodecane was added (112 μ L, 0.5 mmol) as internal standard. Yields were measured by passing an aliquot of the

solution through a plug of silica gel using ethyl acetate as eluant and monitoring the relative areas of the peaks compared to that of dodecane in the GC chromatogram.

General procedure for screening of aryl tosylates (Table 3.2.3)

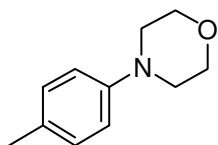
Aryl tosylate (0.5 mmol, 1.0 eq), K_3PO_4 (318 mg, 1.5 mmol, 3.0 eq) and complex **2.17** (7.7 mg, 0.01 mmol, 2 mol%) were charged under air into a Schlenk tube (15 mL volume) that was sealed with a septum, and the tube was evacuated and flushed with nitrogen for three times. Morpholine **3.2a** (66 μ L, 0.75 mmol, 1.5 eq) and *t*AmOH (1.5 mL) were subsequently added via syringe at room temperature. The mixture was stirred for about one minute at room temperature and then transferred to a preheated oil bath at 120 °C and the reaction was stirred for 18 h. At that point, the reaction mixture was cooled down to room temperature and diluted with EtOAc (10 mL), filtered through a small plug of Silica gel and washed with ethyl acetate. The filtrate was concentrated under reduced pressure and purified via silica gel flash chromatography.

General procedure for the screening of the amine partner (Table 3.2.4)

4-toluenyl tosylate **3.1a** (131 mg, 0.5 mmol, 1.0 eq), K_3PO_4 (318 mg, 1.5 mmol, 3.0 eq) and complex **2.17** (7.7 mg, 0.01 mmol, 2 mol%) were charged under air into a Schlenk tube (15 mL volume) that was sealed with a septum, and the tube was evacuated and flushed with nitrogen for three times. The amine (0.75 mmol, 1.5 eq) and *t*AmOH (1.5 mL) were subsequently added via syringe at room temperature. In case of diphenylamine, which is solid at room temperature, it was introduced into the tube prior to purging with nitrogen. The mixture was stirred for about one minute at room temperature and then transferred to a preheated oil bath at 120 °C and the reaction was stirred for 18 h. At this point, the reaction mixture was cooled down to room temperature and diluted with EtOAc (10 mL), filtered through a small plug of Silica gel and washed with ethyl acetate. The filtrate was concentrated under reduced pressure and purified via silica gel flash chromatography

4.2 Catalytic products

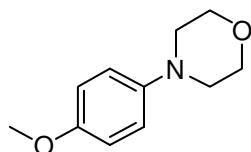
4-(4-methylphenyl)morpholine (3.3a): After flash chromatography on silica gel (Hexane/EtOAc: 20/1), the title compound was recovered as a white solid: 85.2 mg (96 % yield).



1H NMR (400 MHz, $CDCl_3$): δ = 7.10 (d, J = 8.4 Hz, 2H), 6.85 (d, J =

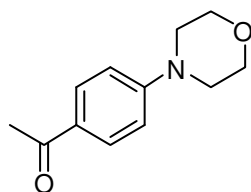
8.5 Hz, 2H), 3.90-3.83 (m, 4H), 3.15-3.08 (m, 4H), 2.29 (s, 3H). $^{13}\text{C}\{^1\text{H}\}$ NMR (101 MHz, CDCl_3): δ = 149.3, 129.9, 129.7, 116.2, 67.1, 50.1, 20.6.

4-(4-methoxyphenyl)morpholine (3.3b): After flash chromatography on silica gel (Hexane/EtOAc: 4/1), the title compound was recovered as a white solid: 70.0 mg (73 % yield).



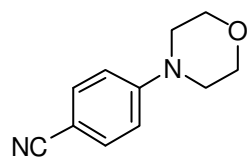
^1H NMR (400 MHz, CDCl_3): δ = 6.94-6.80 (m, 4H), 3.91-3.83 (m, 4H), 3.77 (s, 3H), 3.09-3.02 (m, 4H). $^{13}\text{C}\{^1\text{H}\}$ NMR (101 MHz, CDCl_3): δ = 154.1, 145.8, 118.0, 114.7, 67.2, 55.7, 51.0.

4-(4-acetylphenyl)morpholine (3.3c): After flash chromatography on silica gel (Hexane/EtOAc: 2/1), the title compound was recovered as a yellow solid: 89.0 mg (87 % yield).



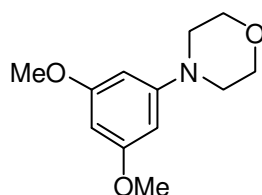
^1H NMR (300 MHz, CDCl_3): δ = 7.88 (d, J = 8.9 Hz, 2H), 6.86 (d, J = 8.9 Hz, 2H), 3.93-3.76 (m, 4H), 3.36-3.23 (m, 4H), 2.52 (s, 3H). $^{13}\text{C}\{^1\text{H}\}$ NMR (75 MHz, CDCl_3): δ = 196.6, 154.3, 130.5, 128.3, 113.4, 66.7, 47.7, 26.3.

4-morpholinophenyl nitrile (3.3d): After flash chromatography on silica gel (Pentane/Et₂O: 3/2), the title compound was recovered as a white solid: 75.0 mg (80 % yield).



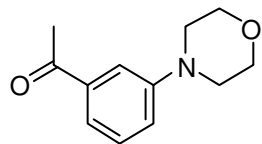
^1H NMR (300 MHz, CDCl_3): δ = 7.56-7.43 (m, 2H), 6.85 (d, J = 9.0 Hz, 2H), 3.92-3.74 (m, 4H), 3.38-3.15 (m, 4H). $^{13}\text{C}\{^1\text{H}\}$ NMR (75 MHz, CDCl_3): δ = 153.6, 133.6, 120.0, 114.2, 101.0, 66.5, 47.4.

4-(3,5-dimethoxyphenyl)morpholine (3.3e): After flash chromatography on silica gel (Hexane/EtOAc: 8/1), the title compound was recovered as a white solid: 102 mg (91 % yield).



^1H NMR (400 MHz, CDCl_3): δ = 6.09 (d, J = 2.0 Hz, 2H), 6.05 (t, J = 2.1 Hz, 1H), 3.84 (t, J = 5.2 Hz, 4H), 3.78 (s, 6H), 3.14 (t, J = 4.9 Hz, 4H). $^{13}\text{C}\{^1\text{H}\}$ NMR (101 MHz, CDCl_3): δ = 161.7, 153.2, 95.0, 92.2, 66.9, 55.4, 49.6.

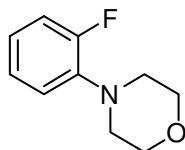
4-(3-acetylphenyl)morpholine (3.3f): After flash chromatography on silica gel (Hexane/EtOAc: 2/1), the title compound was recovered as a yellow oil: 78.8 mg (77 % yield).



^1H NMR (400 MHz, CDCl_3): δ = 7.49 (s, 1H), 7.42 (d, J = 7.5 Hz, 1H), 7.34 (t, J = 7.9 Hz, 1H), 7.10 (dd, J = 8.3, 1.9 Hz, 1H), 3.85 (t, J = 4.5 Hz, 4H), 3.19 (t, J

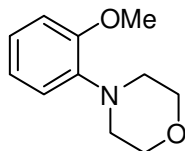
= 4.7 Hz, 4H), 2.57 (s, 3H). $^{13}\text{C}\{^1\text{H}\}$ NMR (101 MHz, CDCl_3): δ = 198.5, 151.5, 138.1, 129.4, 120.3, 114.5, 66.8, 49.1, 26.8.

4-(2-fluorophenyl)morpholine (3.3g): After flash chromatography on silica gel (Hexane/EtOAc: 10/1), the title compound was recovered as a colorless oil: 60 mg (66 % yield).

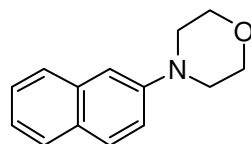


^1H NMR (300 MHz, CDCl_3): δ = 7.12-6.89 (m, 4H), 3.93-3.84 (m, 4H), 3.13-3.04 (m, 4H). $^{13}\text{C}\{^1\text{H}\}$ NMR (75 MHz, CDCl_3): δ = 155.8 (d, J = 244 Hz), 140.1 (d, J = 9 Hz), 124.6 (d, J = 4 Hz), 122.8 (d, J = 8 Hz), 118.8 (d, J = 3 Hz), 116.3 (d, J = 19 Hz), 67.1, 51.0 (d, J = 4 Hz).

4-(2-methoxyphenyl)morpholine (3.3h): After flash chromatography on silica gel (Hexane/EtOAc: 10/1), the title compound was recovered as a colorless oil: 85 mg (88 % yield).



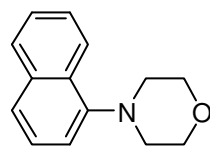
^1H NMR (400 MHz, CDCl_3): δ = 7.05-6.98 (m, 1H), 6.95-6.91 (m, 2H), 6.87 (d, J = 7.9 Hz, 1H), 3.92-3.87 (m, 4H), 3.86 (s, 3H), 3.20-2.97 (m, 4H). $^{13}\text{C}\{^1\text{H}\}$ NMR (101 MHz, CDCl_3): δ = 152.3, 141.2, 123.2, 121.1, 118.1, 111.4, 67.3, 55.4, 51.2.



4-(2-naphthyl)morpholine (3.3j): After flash chromatography on silica gel (Hexane/EtOAc: 8/1), the title compound was recovered as a white solid: 89.6 mg (84 % yield).

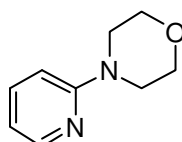
^1H NMR (400 MHz, CDCl_3): δ = 7.85-7.60 (m, 3H), 7.46-7.39 (m, 1H), 7.35-7.29 (m, 1H), 7.26 (dd, J = 9.0, 2.5 Hz, 1H), 7.13 (d, J = 1.9 Hz, 1H), 3.93 (t, J = 4.7 Hz, 4H), 3.27 (t, J = 4.9 Hz, 4H). $^{13}\text{C}\{^1\text{H}\}$ NMR (101 MHz, CDCl_3): δ = 149.1, 134.6, 129.0, 128.9, 127.6, 126.9, 126.5, 123.7, 119.0, 110.3, 67.0, 50.0.

4-(1-naphthyl)morpholine (3.3k): After flash chromatography on silica gel (Hexane/EtOAc: 10/1), the title compound was recovered as a yellowish solid: 104.5 mg (98 % yield).



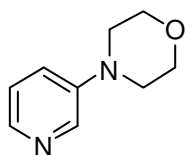
^1H NMR (400 MHz, CDCl_3): δ = 8.30-8.21 (m, 1H), 7.91-7.82 (m, 1H), 7.61 (d, J = 8.2 Hz, 1H), 7.56-7.48 (m, 2H), 7.43 (t, J = 7.5 Hz, 1H), 7.12 (dd, J = 7.4, 1.1 Hz, 1H), 4.01 (t, J = 4.5 Hz, 4H), 3.19 (t, J = 4.5 Hz, 4H). $^{13}\text{C}\{^1\text{H}\}$ NMR (101 MHz, CDCl_3): δ = 149.5, 134.9, 128.9, 128.6, 126.0, 125.5, 123.9, 123.5, 114.8, 67.5, 53.6.

4-(pyridin-2-yl)morpholine (3.3l): After flash chromatography on silica gel (Pentane/Et₂O: 5/1), the title compound was recovered as a colorless oil: 56 mg (68% yield).



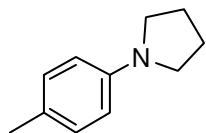
¹H NMR (400 MHz, CDCl₃): δ = 8.22-8.15 (m, 1H), 7.53-7.43 (m, 1H), 6.68-6.58 (m, 2H), 3.84-3.77 (m, 4H), 3.51-3.44 (m, 4H). **¹³C{¹H} NMR (101 MHz, CDCl₃):** δ = 159.7, 148.0, 137.6, 113.9, 107.0, 66.9, 45.7.

4-(pyridin-3-yl)morpholine (3.3m): After flash chromatography on silica gel (Hexane/EtOAc: 1/1), the title compound was recovered as a yellow oil: 71 mg (87% yield).



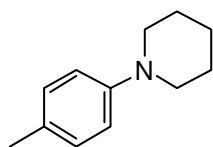
¹H NMR (300 MHz, CDCl₃): δ = 8.32-8.27 (m, 1H), 8.15-8.08 (m, 1H), 7.19-7.12 (m, 2H), 3.95-3.76 (m, 4H), 3.28-3.08 (m, 4H). **¹³C{¹H} NMR (75 MHz, CDCl₃):** δ = 147.0, 141.3, 138.5, 123.6, 122.2, 66.8, 48.7.

1-(4-methylphenyl)pyrrolidine (3.4b): After flash chromatography on silica gel (Pentane/Et₂O: 10/1), the title compound was recovered as a white solid: 73.7 mg (91 % yield).



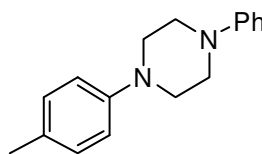
¹H NMR (400 MHz, CDCl₃): δ = 7.06 (d, J = 8.4 Hz, 2H), 6.53 (d, J = 8.5 Hz, 2H), 3.28 (t, J = 6.5 Hz, 4H), 2.28 (s, 3H), 2.15-1.88 (m, 4H). **¹³C{¹H} NMR (101 MHz, CDCl₃):** δ = 146.2, 129.8, 124.7, 112.0, 48.0, 25.5, 20.4. Spectral data were in accordance with those reported in literature.¹

1-(4-methylphenyl)piperidine (3.4c): After flash chromatography on silica gel (Hexane/EtOAc: 50/1), the title compound was recovered as a colorless oil: 70.2 mg (80 % yield).



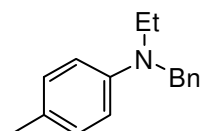
¹H NMR (400 MHz, CDCl₃): δ = 7.13-7.06 (m, 2H), 6.95-6.85 (m, 2H), 3.12 (t, J = 5.4 Hz, 4H), 2.30 (s, 3H), 1.75 (p, J = 5.6 Hz, 4H), 1.64-1.55 (m, 2H). **¹³C{¹H} NMR (101 MHz, CDCl₃):** δ = 150.3, 129.6, 128.9, 117.1, 51.5, 26.1, 24.4, 20.5.

1-(4-methylphenyl)-4-phenylpiperazine (3.4d): After flash chromatography on silica gel (Hexane/EtOAc: 10/1), the title compound was recovered as white shining crystals: 121 mg (96 % yield).



¹H NMR (400 MHz, CDCl₃): δ = 7.31 (t, J = 7.9 Hz, 2H), 7.12 (d, J = 8.1 Hz, 2H), 7.00 (d, J = 8.1 Hz, 2H), 6.97-6.86 (m, 3H), 3.40-3.25 (m, 8H), 2.30 (s, 3H). **¹³C{¹H} NMR (101 MHz, CDCl₃):** δ = 151.4, 149.2, 129.8, 129.3, 120.2, 116.9, 116.5, 50.2, 49.6, 20.6.

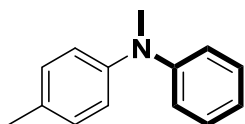
4-methyl-N-ethyl-N-phenylaniline (3.4e): After flash chromatography on silica gel



(Hexane/EtOAc: 95/5), the title compound was recovered as a colorless oil: 102.9 mg (91 % yield).

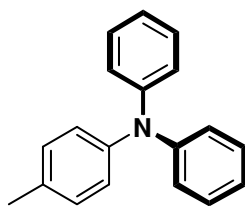
¹H NMR (400 MHz, CDCl₃): δ = 7.40-7.26 (m, 5H), 7.12-7.02 (m, 2H), 6.82-6.58 (m, 2H), 4.55 (s, 2H), 3.51 (q, J = 7.0 Hz, 2H), 2.31 (s, 3H), 1.25 (t, J = 7.0 Hz, 3H). **¹³C{¹H} NMR (101 MHz, CDCl₃):** δ = 146.5, 139.7, 129.8, 128.6, 126.8, 126.7, 125.3, 112.6, 54.3, 45.4, 20.3, 12.2.

4-methyl-*N*-methyl-*N*-phenylaniline (3.4f): After flash chromatography on silica gel (Hexane/EtOAc: 20/1), the title compound was recovered as a yellowish oil: 89.5 mg (91 % yield).



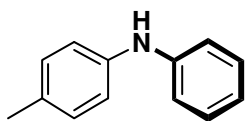
¹H NMR (300 MHz, CDCl₃): δ = 7.48-7.38 (m, 2H), 7.31 (d, J = 8.2 Hz, 2H), 7.24-7.17 (m, 2H), 7.18-7.11 (m, 2H), 7.11-7.03 (m, 1H), 3.47 (s, 3H), 2.52 (s, 3H). **¹³C{¹H} NMR (75 MHz, CDCl₃):** δ = 149.4, 146.7, 132.0, 130.0, 129.1, 122.6, 119.9, 118.3, 40.3, 20.8.

***N,N*-diphenyl-4-methylaniline (3.4g):** After flash chromatography on silica gel (Hexane/DCM: 10/1), the title compound was recovered as a white solid: 122.4 mg (94 % yield).



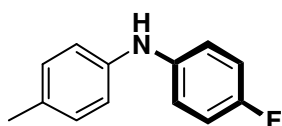
¹H NMR (300 MHz, CDCl₃): δ = 7.36-7.22 (m, 4H), 7.20-6.96 (m, 10H), 2.39 (s, 3H). **¹³C{¹H} NMR (75 MHz, CDCl₃):** δ = 148.2, 145.4, 132.8, 130.0, 129.2, 125.1, 123.7, 122.3, 21.0.

4-methyl-*N*-phenylaniline (3.4h): After flash chromatography on silica gel (Hexane/ EtOAc: 95/5), the title compound was recovered as a white solid: 80.0 mg (87% yield).



¹H NMR (400 MHz, CDCl₃): δ = 7.37-7.25 (m, 2H), 7.16 (d, J = 8.3 Hz, 2H), 7.11-7.02 (m, 4H), 6.95 (t, J = 7.3 Hz, 1H), 5.64 (br, s, 1H), 2.38 (s, 3H). **¹³C{¹H} NMR (101 MHz, CDCl₃):** δ = 144.1, 140.4, 131.0, 130.0, 129.4, 120.4, 119.0, 117.0, 20.8.

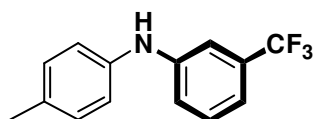
4-fluoro-*N*-(*p*-tolyl)aniline (3.4i): After flash chromatography on silica gel (Hexane/EtOAc: 20/1), the title compound was recovered as a white solid: 96.5 mg (96% yield).



¹H NMR (300 MHz, CDCl₃): δ = 7.16-7.07 (m, 2H), 7.06-6.88 (m,

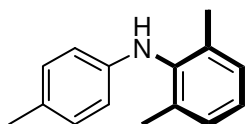
6H), 5.49 (br, s, 1H), 2.34 (s, 3H). $^{13}\text{C}\{^1\text{H}\}$ NMR (75 MHz, CDCl_3): δ = 157.7 (d, J = 238 Hz), 141.23, 139.9 (d, J = 2 Hz), 130.6, 130.0, 119.5 (d, J = 7 Hz), 118.0, 116.0 (d, J = 22 Hz), 20.7.

3-trifluoromethyl-*N*-(*p*-tolyl)aniline (3.4j): After flash chromatography on silica gel (Hexane/EtOAc: 20/1), the title compound was recovered as a white solid: 115 mg (92% yield).



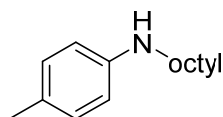
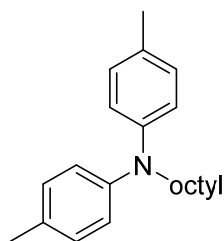
^1H NMR (300 MHz, CDCl_3): δ = 7.31 (t, J = 7.9 Hz, 1H), 7.23-6.98 (m, 7H), 5.73 (br, s, 1H), 2.34 (s, 3H). $^{13}\text{C}\{^1\text{H}\}$ NMR (75 MHz, CDCl_3): δ = 145.0, 139.1, 132.6, 131.8 (q, J = 32 Hz), 130.2, 129.9, 124.3 (q, J = 271 Hz), 120.3, 119.0, 116.4 (q, J = 4 Hz), 112.5 (q, J = 4 Hz), 20.9.

2,6-dimethyl-*N*-(4-methylphenyl)aniline (3.4k): After flash chromatography on silica gel (Pentane/Et₂O: 9/1), the title compound was recovered as a white solid: 90.0 mg (85 % yield).



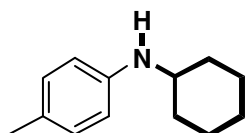
^1H NMR (400 MHz, CDCl_3): δ = 7.23-7.12 (m, 3H), 7.06 (d, J = 8.0 Hz, 2H), 6.60-6.47 (m, 2H), 5.14 (br, s, 1H), 2.34 (s, 3H), 2.30 (s, 6H). $^{13}\text{C}\{^1\text{H}\}$ NMR (101 MHz, CDCl_3): δ = 143.9, 138.8, 135.6, 129.8, 128.6, 127.5, 125.5, 113.9, 20.6, 18.5.

4-methyl-*N*-(oct-1-yl)-aniline (3.4n) and *N,N*-bis(4-methylphenyl)octyl-1-amine (3.4n'):



Hexane/EtOAc = 98/2; a first crop of pure was collected as the first fraction (29.4 mg) but, due to coelution of the two products, the second fraction consisted of a mixture of **3.4n** and **3.4n'** in a 2/1 ratio determined by integration of the ^1H NMR spectrum (41.1 mg). **3.4n** 0.11 mmol (22%); ^1H NMR (400 MHz, CDCl_3): δ = 7.01 (d, J = 8.1 Hz, 2H), 6.56 (d, J = 8.4 Hz, 2H), 3.46 (br s, 1H), 3.11 (t, J = 7.1 Hz, 2H), 2.27 (s, 3H), 1.73-1.53 (m, 2H), 1.48-1.20 (m, 10H), 1.01-0.82 (m, 3H). $^{13}\text{C}\{^1\text{H}\}$ NMR (101 MHz, CDCl_3): δ = 146.4, 129.8, 126.4, 113.1, 44.6, 32.0, 29.8, 29.6, 29.4, 27.3, 22.8, 20.5, 14.2. **3.4n'**: colorless oil, 0.15 mmol (60%); ^1H NMR (400 MHz, CDCl_3): δ = 7.06 (d, J = 8.2 Hz, 4H), 6.87 (d, J = 8.0 Hz, 4H), 3.62 (t, J = 7.0 Hz, 2H), 2.30 (s, 6H), 1.64 (p, J = 7.6 Hz, 2H), 1.39-1.19 (m, 10H), 0.88 (t, J = 6.8 Hz, 3H). $^{13}\text{C}\{^1\text{H}\}$ NMR (101 MHz, CDCl_3): δ = 146.0, 130.2, 129.7, 120.8, 52.5, 31.8, 29.4, 29.3, 27.5, 27.1, 22.7, 20.6, 14.1.

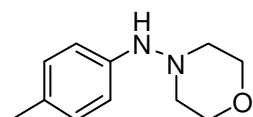
4-methyl-*N*-cyclohexylaniline (3.4o): After flash chromatography on silica gel (Hexane/



EtOAc: 95/5), the title compound was recovered as a white solid: 88 mg (93% yield).

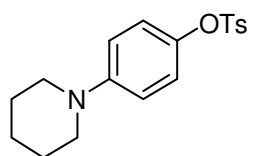
¹H NMR (400 MHz, CDCl₃): δ = 6.97 (d, J = 8.1 Hz, 2H), 6.55 (d, J = 8.4 Hz, 2H), 3.58 (br, s, 1H), 3.22 (tt, J = 10.1, 3.7 Hz, 1H), 2.23 (s, 3H), 2.11-2.00 (m, 2H), 1.75 (dt, J = 12.9, 3.6 Hz, 2H), 1.65 (dt, J = 12.6, 3.7 Hz, 1H), 1.42-1.29 (m, 2H), 1.27-1.08 (m, 3H). **¹³C{¹H} NMR (101 MHz, CDCl₃):** δ = 144.9, 129.9, 126.5, 113.9, 52.4, 33.6, 26.1, 25.2, 20.5.

4-methyl-*N*-morpholinylaniline (3.4p): After flash chromatography on silica gel (Hexane/EtOAc: 4/1), the title compound was recovered as a yellowish oil: 80 mg (83% yield).



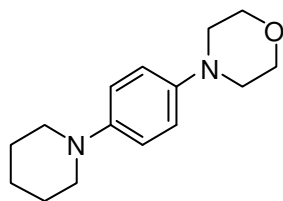
¹H NMR (400 MHz, CDCl₃): δ = 7.03 (d, J = 9.1 Hz, 2H), 6.88-6.81 (m, 2H), 4.32 (br, s, 1H), 3.81 (t, J = 4.6 Hz, 4H), 2.75 (s, 4H), 2.27 (s, 3H). **¹³C{¹H} NMR (101 MHz, CDCl₃):** δ = 144.8, 129.8, 129.1, 114.1, 67.2, 56.5, 20.6.

4-piperidinyphenyl tosylate (3.3n) : 4-chlorophenyl tosylate **3.1m** (141.4 mg, 0.5 mmol, 1.0 eq), K₃PO₄ (265 mg, 1.25 mmol, 2.5 eq) and pre-catalyst **2.17** (7.7 mg, 0.01 mmol, 2 mol%) were charged under air into a Schlenk tube (15 mL volume) that was sealed with a septum, and the tube was evacuated and flushed with nitrogen for three times. Piperidine (59 μ L, 0.6 mmol, 1.2 eq) and *t*AmOH (1.5 mL) were subsequently added via syringe at room temperature. The mixture was stirred for about one minute at room temperature and then transferred to a preheated oil bath (90 °C). The reaction was stirred for another 18 h. The reaction mixture was diluted with 10 mL ethyl acetate, filtered through a small plug of Silica gel and washed with ethyl acetate. The filtrate was concentrated under reduced pressure and purified via silica gel flash chromatography (SiO₂, Hexane/EtOAc: 2/1) to afford compound **3.3n** as a white solid: 158.3 mg (96% yield).



m.p. = 123-124°C; **¹H NMR (300 MHz, CDCl₃):** δ = 7.75-7.64 (m, 2H), 7.33-7.24 (m, 2H), 6.90-6.67 (m, 4H), 3.14-3.05 (m, 4H), 2.44 (s, 3H), 1.73-1.62 (m, 4H), 1.60-1.52 (m, 2H). **¹³C{¹H} NMR (75 MHz, CDCl₃):** δ = 151.0, 145.1, 142.0, 132.7, 129.8, 128.7, 122.9, 116.8, 50.7, 25.9, 24.2, 21.8. **IR (ATR):** ν = 2936, 2854, 2815, 1595, 1508, 1450, 1372, 1246, 1188, 1176, 1157, 1124, 1092, 1019, 1007, 915, 859, 809, 754, 693, 656 cm⁻¹; **MS (ESI):** m/z (%): 332 (100) [M + H]⁺; **HRMS (ESI):** m/z calcd. for C₁₈H₂₂NO₃S: 332.1320; found: 332.1321, ϵ_r = 0.3 ppm; **elemental analysis calcd (%)** for C₁₈H₂₁NO₃S (MW = 331.43): C 65.23, H 6.39, N 4.23, *found*: C 64.98, H 6.42, N 4.19.

4-(4-piperidinylphenyl)morpholine (3.5): 4-piperidinylphenyl tosylate **3.3n** (165.7 mg,



0.5mmol, 1.0 eq), K_3PO_4 (318 mg, 1.5 mmol, 2.5 eq) and complex **2.17** (15.4 mg, 0.02 mmol, 4 mol%) were charged under air into a Schlenk tube (15 mL volume) that was sealed with a septum, and the tube was evacuated and flushed with nitrogen for three times.

Morpholine (66 μ L, 0.75 mmol, 1.5 eq) and *t*AmOH (1.5 mL) were subsequently added via syringe at room temperature. The mixture was stirred for about one minute at room temperature and then transferred to a preheated oil bath (120 °C). The reaction was stirred for another 18 h. The reaction mixture was diluted with 10 mL ethyl acetate, filtered through a small plug of Silica gel and washed with ethyl acetate. The filtrate was concentrated under reduced pressure and purified via silica gel flash chromatography (SiO_2 , Hexane/EtOAc: 2/1) to afford the title compound as a white solid: 74.2 mg (60% yield).

1H NMR (300 MHz, $CDCl_3$): δ = 7.00-6.78 (m, 4H), 3.97-3.74 (m, 4H), 3.13-2.98 (m, 8H), 1.82-1.60 (m, 4H), 1.63-1.45 (m, 2H). **$^{13}C\{^1H\}$ NMR (75 MHz, $CDCl_3$):** δ = 146.9, 145.1, 118.4, 117.4, 67.2, 52.0, 50.7, 26.2, 24.3.

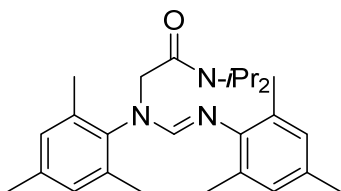
4-(4-piperidinylphenyl)morpholine (3.5): one-pot procedure

4-chlorophenyl tosylate **3.1m** (141.4 mg, 0.5 mmol, 1.0 eq), K_3PO_4 (265 mg, 1.25 mmol, 2.5 eq) and pre-catalyst **2.17** (7.7 mg, 0.01 mmol, 2 mol%) were charged under air into a Schlenk tube (15 mL volume) that was sealed with a septum, and the tube was evacuated and flushed with nitrogen for three times. Piperidine (59 μ L, 0.6 mmol, 1.2 eq) and *t*AmOH (1.5 mL) were subsequently added via syringe at room temperature. The mixture was stirred for about one minute at room temperature and then transferred to a preheated oil bath at 90 °C for 6 h to observe the full conversion (checked by TLC). After cooling down to the room temperature, K_3PO_4 (318 mg, 1.5 mmol, 3.0 eq), pre-catalyst **2.17** (15.4 mg, 0.02 mmol, 4.0 mol%) and morpholine (66 μ L, 0.75 mmol, 1.5 eq) were subsequently added to the solution upon a flow of N_2 . The mixture was heated at 120 °C for another 18 h. The reaction mixture was diluted with 10 mL ethyl acetate, filtered through a small plug of Silica gel and washed with ethyl acetate. The filtrate was concentrated under reduced pressure and purified via silica gel flash chromatography (SiO_2 , Hexane/EtOAc: 2/1) to afford compound **3.5** as a white solid: 70.0 mg (57% yield).

5 Chapter 4

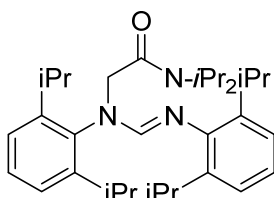
5.1 Synthetic methods

N-(N'',N''-diisopropylcarbamoylmethyl)-N,N'-dimesitylformamidinium (4.1a)



To a solution of N,N'-dimesitylformamidinium (1.4 g, 5.0 mmol) and KI (0.080 g, 0.5 mmol, 0.1 eq) in DMF (15 mL), 2-chloro-N,N-diisopropylacetamide (1.06 g, 6.0 mmol, 1.2 eq.) and triethylamine (1.1 mL, 7.5 mmol, 1.5 eq.) were added respectively at room temperature. The resulting mixture was stirred at 100°C overnight. After cooling down to room temperature, the reaction mixture was diluted with Et₂O (150 mL) and the organic phase was washed with water (50 mL). The aqueous phase was then extracted with ether (3×30 mL) and the organic layers were combined and washed again with water (30 mL) and brine (30 mL). After drying over Na₂SO₄, the solution was filtered and evaporated under reduced pressure. The crude residue was purified by flash chromatography (SiO₂, Hexane/EtOAc : 2/1 then 1/1) to afford a colorless, sticky foam (1.9 g, 90%). **¹H NMR (400 MHz, CDCl₃):** δ = 7.22 (s, 1H, N₂CH), 6.91 (s, 2H, CH_{Mes}), 6.83 (s, 2H, CH_{Mes}), 4.42 (s, 2H, CH₂), 4.25 (br, s, 1H, CH_{iPr}), 3.59 (br, s, 1H, CH_{iPr}), 2.40 (s, 6H, CH_{3 ortho}), 2.28 (s, 3H, CH_{3 para}), 2.24 (s, 3H, CH_{3 para}), 2.16 (s, 6H, CH_{3 ortho}), 1.44-1.18 (m, 12H, CH_{3 iPr}). **¹³C{¹H} NMR (101 MHz, CDCl₃):** δ = 166.9 (C=O), 152.0 (N₂CH), 147.4, 140.0, 137.1, 137.0, 131.1 (C_{q Mes}), 129.6 (CH_{Mes}), 129.4 (C_{q Mes}), 128.4 (CH_{Mes}), 51.0 (CH₂), 48.1, 45.9 (N-CH_{iPr}), 21.3 (CH_{3 iPr}), 21.0, 20.8 (CH_{3 Mes}), 20.7 (CH_{3 iPr}), 18.8, 18.7 (CH_{3 Mes}). **HRMS:** Calcd. for C₂₇H₃₉N₃O, [M + H]⁺: 422.3171; found: 422.3163, ε_r = 1.9 ppm.

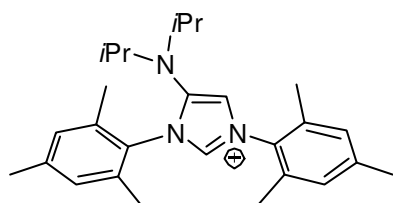
N-(N'',N''-diisopropylcarbamoylmethyl)-N',N'-di(2,6-diisopropylphenyl)formamidinium (4.1b)



To a solution of N,N'-bis(2,6-diisopropylphenyl)formamidinium (3.64 g, 10.0 mmol) and KI (0.16 g, 1.0 mmol, 0.1 eq) in DMF (30 mL), 2-chloro-N,N-diisopropylacetamide (2.12 g, 12.0 mmol, 1.2 eq.) and triethylamine (2.2 mL, 15.0 mmol, 1.5 eq) were added respectively at room temperature. The resulting mixture was stirred at 100°C overnight. After cooling down to room temperature, water (100 mL) was added to the solution and the mixture was extracted with ether (3×60 mL) and the organic layers were combined and washed again with water (60 mL) and brine (60 mL). After drying over Na₂SO₄, the solution was filtered and evaporated under reduced

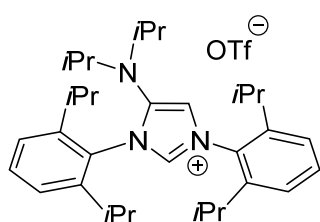
pressure. The crude residue was purified by flash chromatography (SiO₂, Hexane/EtOAc : 10/1) to afford a white solid (5.0 g, 99%). **¹H NMR (300 MHz, CDCl₃):** δ = 7.31 (t, *J* = 7.6 Hz, 1H, CH_{Dipp}), 7.23 (s, 1H, N₂CH), 7.21-7.13 (m, 2H, CH_{Dipp}), 7.08 (d, *J* = 7.4 Hz, 2H, CH_{Dipp}), 6.98 (t, *J* = 7.6 Hz, 1H, CH_{Dipp}), 4.41 (s, 2H, CH₂), 4.24-3.98 (m, 1H, CH_{iPr}), 3.80-3.39 (m, 3H, CH_{iPr}), 3.38-3.22 (m, 2H, CH_{iPr}), 1.40-1.09 (m, 36H). **¹³C{¹H} NMR (75 MHz, CDCl₃):** δ = 166.2 (C=O), 151.1 (N₂CH), 148.6, 147.4, 140.2, 139.8 (*Cq*_{Ar}), 128.7, 124.5, 122.7, 122.6 (CH_{Dipp}), 52.9 (CH₂), 47.5, 46.0 (N-CH_{iPr}), 28.0, 27.6 (CH_{iPr}), 25.3, 24.6, 23.9, 21.4, 20.8 (CH₃_{iPr}). **HRMS:** *Calcd.* for C₃₃H₅₁N₃O, [M + H]⁺: 506.4115; *found*: 506.4115, ϵ_r = 0.0 ppm.

1,3-dimesityl-4-(diisopropylamino)imidazolium triflate (4.2a)



2,6-lutidine (0.78 mL, 6.77 mmol, 1.5 eq) was added to a solution of compound **4.1a** (1.9 g, 4.51 mmol) in CH₂Cl₂ (35 mL) at -78°C. Triflic anhydride (0.83 mL, 4.95 mmol, 1.1 eq) was then added dropwise. The solution became brown and the mixture was stirred for another 2.5 h in the cooling bath and then allowed to warm to room temperature. A saturated solution of NaHCO₃ (60 mL) was added to the resulting solution and the biphasic mixture was stirred for another 30 minutes. The organic phase was separated and washed again with NaHCO₃ (2 × 60 mL), dried over Na₂SO₄ and evaporated under reduced pressure. The crude product was washed with Et₂O and dried to get a white powder (1.3 g, 52%). **¹H NMR (400 MHz, CDCl₃)** δ = 9.14 (d, *J* = 1.7 Hz, 1H, N₂CH), 7.04 (s, 4H, CH_{Mes}), 6.82 (d, *J* = 1.7 Hz, 1H, CH_{Im}), 3.39 (hept, *J* = 6.8 Hz, 2H, CH_{iPr}), 2.35 (s, 6H, CH₃_{para}), 2.18 (s, 6H, CH₃_{ortho}), 2.16 (s, 6H, CH₃_{ortho}), 1.07 (d, *J* = 6.8 Hz, 12H, CH₃_{iPr}). **¹³C{¹H} NMR (101 MHz, CDCl₃)** δ = 141.4, 141.3, 141.3 (*Cq*_{Ar}), 135.5 (N₂CH), 134.9, 134.2 (*Cq*_{Ar}), 131.0, (*Cq*_{Ar}) 130.2, 129.9 (CH_{Mes}), 129.2 (*Cq*_{Ar}), 120.6 (q, *J*_{CF} = 322 Hz, CF₃SO₃⁻), 110.9 (C_{Im}), 50.2 (N-CH_{iPr}), 21.8 (CH₃_{iPr}), 21.3, 18.1, 17.4 (CH₃_{Mes}). **Elemental analysis** *calcd* (%) for C₂₈H₃₈F₃N₃O₃S (MW = 553.69): C 60.74, H 6.92, N 7.59; *found*: C 60.53, H 6.65, N 7.51.

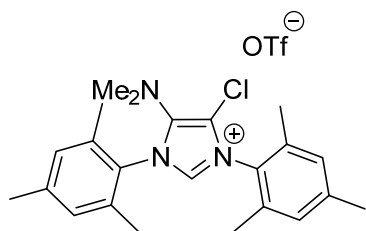
1,3-bis(2,6-diisopropylphenyl)-4-(dimethylamino)imidazolium triflate (4.2b)



2,6-lutidine (0.347 mL, 3.0 mmol, 1.5 eq) was added to a solution of compound **4.1b** (1.011 g, 2.0 mmol, 1.0 eq) in CH₂Cl₂ (15 mL) at -78°C. Triflic anhydride (0.37 mL, 2.2 mmol, 1.1 eq) was then

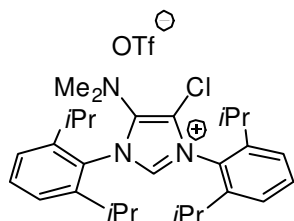
added dropwise. The solution became brown and the mixture was stirred for another 2.5 h in the cooling bath and then allowed to warm to room temperature. A saturated solution of NaHCO₃ (20 mL) was added to the resulting solution and the biphasic mixture was stirred for another 30 minutes. The organic phase was separated and washed again with NaHCO₃ (2 × 20 mL), dried over Na₂SO₄ and evaporated under reduced pressure. The crude product was washed with Et₂O and dried to get a white powder (0.50 g, 39%). **¹H NMR (400 MHz, CDCl₃)** δ = 9.15 (d, *J* = 9.1 Hz, 1H, N₂CH), 7.56 (dt, *J* = 10.7, 7.8 Hz, 2H, CH_{Dipp}), 7.35 (d, *J* = 7.9 Hz, 2H, CH_{Dipp}), 7.32 (d, *J* = 7.9 Hz, 2H, CH_{Dipp}), 6.90 (d, *J* = 1.6 Hz, 1H, CH_{Im}), 3.50-3.35 (m, 2H, CH_{iPr}), 2.54-2.38 (m, 4H, CH_{iPr}), 1.32 (d, *J* = 6.8 Hz, 6H, CH_{3 iPr}), 1.28 (d, *J* = 6.9 Hz, 6H, CH_{3 iPr}), 1.26 (d, *J* = 6.8 Hz, 6H, CH_{3 iPr}), 1.19 (d, *J* = 6.8 Hz, 6H, CH_{3 iPr}), 1.07 (d, *J* = 6.7 Hz, 12H, CH_{3 iPr}). **¹³C{¹H} NMR (101 MHz, CDCl₃)** δ = 145.5, 145.0, 141.2 (*Cq*_{Ar}), 135.4 (N₂CH), 132.4, 132.0 (CH_{Ar}), 130.3, 128.7 (*Cq*_{Ar}), 125.1, 124.8 (CH_{Ar}), 120.6 (q, *J*_{CF} = 322 Hz, CF₃SO₃[−]), 111.1 (CH_{Im}), 49.9 (N-CH_{iPr}), 29.5, 29.3 (CH_{iPr}), 25.6, 24.5, 24.2, 22.6, 21.4 (CH_{3 iPr}). **HRMS**: Calcd. for C₃₃H₅₁N₃O, [M – OTf]⁺: 488.4005; found: 488.4007, ε_r = 0.4 ppm

1,3-dimesityl-4-(dimethylamino)-5-chloroimidazolium triflate(4.3a)



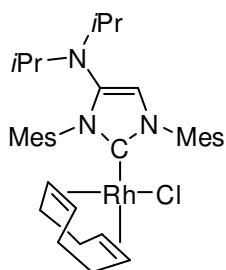
2.2a (200.0 mg, 0.4 mmol, 1.0 eq) and *N*-chlorosuccinimide (80 mg, 0.6 mmol, 1.5 eq) were placed in a vial and dissolved in CHCl₃ (6.0 mL), and the mixture was stirred for 2 h at room temperature. The resulting solution was concentrated under reduced pressure leading to a crude residue which was purified by flash chromatography (SiO₂, pure ethyl acetate) to afford a white powder (100 mg, 47%). **¹H NMR (400 MHz, CDCl₃)** δ = 9.41 (s, 1H, N₂CH), 7.06 (s, 4H, CH_{Mes}), 2.76 (s, 6H, N-(CH₃)₂), 2.36 (s, 3H, CH_{3 para}), 2.36 (s, 3H, CH_{3 para}), 2.16 (s, 6H, CH_{3 ortho}), 2.13 (s, 6H, CH_{3 ortho}). **¹³C{¹H} NMR (101 MHz, CDCl₃)** δ = 142.1, 141.8, 139.1 (*Cq*_{Ar}), 135.2 (N₂CH), 135.1, 134.6 (*Cq*_{Ar}), 130.3, 130.0 (CH_{Mes}), 128.5, 127.9 (*Cq*_{Ar}), 120.5 (q, *J*_{CF} = 323 Hz, CF₃SO₃[−]), 111.0 (C_{Im}), 42.0 (N-CH₃), 21.4, 21.3 (CH_{3 para}), 17.8, 17.5 (CH_{3 ortho}). **MS (ESI)**: *m/z* (%): 382 (100) [M – OTf]⁺; **HRMS (ESI)**: *m/z* calcd. for C₂₃H₂₉ClN₃: 382.2050; found: 382.2050, ε_r = 0 ppm.

1,3-bis(2,6-diisopropylphenyl)-4-(dimethylamino)-5-chloroimidazolium triflate (4.3b)



2.2b (232.8 mg, 0.4 mmol, 1.0 ea) and *N*-chlorosuccinimide (64 mg, 0.48 mmol, 1.2 eq), were placed in a small vial and dissolved by CHCl_3 (6.0 mL), and the mixture was stirred for 2 h at room temperature. The resulting solution was concentrated under reduced pressure leading to a crude residue which was recrystallized by a mixture solvent of hexane and ethyl acetate (2/1) to afford a white powder (160 mg, 65%). Single crystals suitable for an X-Ray diffraction experiment were grown by diffusion of pentane to a solution of **4.3b** in CH_2Cl_2 . ^1H NMR (400 MHz, CDCl_3) δ = 9.66 (s, 1H, N_2CH), 7.59 (t, J = 7.8 Hz, 2H, CH_{Dipp}), 7.35 (d, J = 7.8 Hz, 4H, CH_{Dipp}), 2.77 (s, 6H, $\text{N}-(\text{CH}_3)_2$), 2.40-2.29 (m, 4H, $\text{CH}_{i\text{Pr}}$), 1.32 (d, J = 6.8 Hz, 6H, $\text{CH}_3_{i\text{Pr}}$), 1.28 (d, J = 6.8 Hz, 6H, $\text{CH}_3_{i\text{Pr}}$), 1.26-1.19 (m, 12H, $\text{CH}_3_{i\text{Pr}}$). $^{13}\text{C}\{^1\text{H}\}$ NMR (101 MHz, CDCl_3) δ = 145.7, 145.4, 139.6, 135.8 ($\text{C}_{\text{q Ar}}$), 135.7 (N_2CH), 132.6, 132.5 (CH_{Ar}), 127.7, 127.1 ($\text{C}_{\text{q Ar}}$), 125.1, 124.9 (CH_{Ar}), 120.5 (q, $J_{\text{CF}} = 322$ Hz, CF_3SO_3^-), 112.3 (C_{Im}), 42.2 ($\text{N}-\text{CH}_3$), 29.7, 29.6 ($\text{CH}_{i\text{Pr}}$), 25.3, 24.4, 23.5, 23.0 ($\text{CH}_3_{i\text{Pr}}$). **Elemental analysis calcd (%)** for $\text{C}_{30}\text{H}_{41}\text{ClF}_3\text{N}_3\text{O}_3\text{S}$ (MW = 616.18): C 58.48, H 6.71, N 6.82; **found**: C 58.0, H 6.22, N 6.62.

Chloro-(η^4 -cycloocta-1,5-diene)-(1,3-dimesityl-4-(diisopropylamino)imidazol-2-ylidene)rhodium(I) (**4.4**)

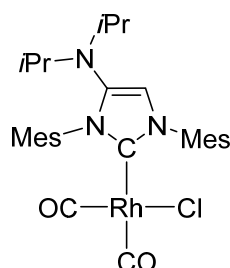


A solution of KHMDS (0.5 M in toluene, 600 μL , 0.298 mmol, 1.1 eq.) was added dropwise to a solution of **4.2a** (150 mg, 0.271 mmol, 1.0 eq) in THF (10 mL) at 0°C. After 30 min, solid $[\text{RhCl}(\text{1,5-cod})]_2$ (67 mg, 0.136 mmol, 0.5 eq.) was added as a solid and the ice-water bath was removed. After 2 h, all volatiles were removed *in vacuo* and the crude residue was purified by flash chromatography (SiO_2 , CH_2Cl_2) to give a yellow powder (147 mg, 84%). **NMR (400 MHz, CDCl_3)** δ = 7.04 (s, 2H, CH_{Mes}), 7.00 (s, 1H, CH_{Mes}), 6.95 (s, 1H, CH_{Mes}), 6.57 (s, 1H, CH_{Im}), 4.45 (s, 2H, CH_{COD}), 3.37-3.28 (m, 1H, CH_{COD}), 3.23 (hept, J = 6.8 Hz, 2H, $\text{CH}_{i\text{Pr}}$), 3.14-3.05 (m, 1H, CH_{COD}), 2.45 (d, J = 14.9 Hz, 6H, CH_3_{Mes}), 2.37 (d, J = 4.3 Hz, 6H, CH_3_{Mes}), 2.18 (s, 3H, CH_3_{Mes}), 2.06 (s, 3H, CH_3_{Mes}), 1.91-1.76 (m, 3H, CH_2_{COD}), 1.76-1.63 (m, 1H, CH_2_{COD}), 1.55-1.40 (m, 4H, CH_2_{COD}), 0.96 (d, J = 6.8 Hz, 6H, $\text{CH}_3_{i\text{Pr}}$), 0.93 (d, J = 6.7 Hz, 6H, $\text{CH}_3_{i\text{Pr}}$). $^{13}\text{C}\{^1\text{H}\}$ NMR (101 MHz, CDCl_3) δ = 179.9 (d, $J_{\text{RhC}} = 53$ Hz, $\text{N}_2\text{C}_{\text{carb}}$), 142.1, 142.1, 138.5, 138.3, 138.2, 137.9, 137.0 ($\text{C}_{\text{q Ar}}$), 129.8, 129.7, 128.1, 128.0 (CH_{Mes}), 113.7 (CH_{Im}), 95.6 (d, $J_{\text{CRh}} = 7$ Hz, CH_{COD}), 95.3 (d, $J_{\text{CRh}} = 8$ Hz, CH_{COD}), 68.1 (d, $J_{\text{CRh}} = 15$ Hz, CH_{COD}), 67.4 (d, $J_{\text{CRh}} = 15$ Hz, CH_{COD}), 49.9 ($\text{N}-\text{CH}_{i\text{Pr}}$), 32.9, 28.57,

28.43, 22.24 (CH_2 COD), 21.7 (CH $i\text{Pr}$), 21.3, 21.2 (CH_3 para), 20.1, 19.2, 18.4 (CH_3 ortho).

Elemental analysis calcd (%) for $\text{C}_{35}\text{H}_{49}\text{ClN}_3\text{Rh}$ (MW = 650.15): C 64.66, H 7.60, N 6.46; *found*: C 64.25, H 7.46, N 6.22.

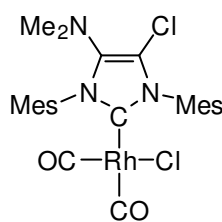
Chloro-dicarbonyl-(1,3-dimesityl-4-(diisopropylamino)imidazol-2-ylidene) rhodium(I)



(4.5)

CO gas was bubbled into a solution of **4.4** (100.0 mg, 0.154 mmol) in CH_2Cl_2 (5 mL) for 10 min during which the color changed from bright yellow to very pale yellow. After 30 minutes, all volatiles were removed under vacuum and the residue was washed with pentane (3×5 mL) to yield after drying a pale yellow powder (80 mg, 87%). **^1H NMR (400 MHz, CDCl_3)** δ = 7.00 (s, 2H, CH_{Mes}), 6.97 (s, 2H, CH_{Mes}), 6.70 (s, 1H, CH_{Im}), 3.28 (hept, J = 6.8 Hz, 2H, $\text{CH}_{i\text{Pr}}$), 2.36 (s, 3H, CH_3_{Mes}), 2.34 (s, 3H, CH_3_{Mes}), 2.26 (s, 6H, CH_3_{Mes}), 2.23 (s, 6H, CH_3_{Mes}), 0.98 (d, J = 6.7 Hz, 12H, $\text{CH}_3_{i\text{Pr}}$). **$^{13}\text{C}\{^1\text{H}\}$ NMR (101 MHz, CDCl_3)** δ = 185.3 (d, J_{RhC} = 54 Hz, Rh-CO), 183.1 (d, J_{RhC} = 76 Hz, Rh-CO), 173.9 (d, J_{RhC} = 44 Hz, $\text{N}_2\text{C}_{\text{carb}}$), 142.1, 139.1, 138.8, 136.1, 135.9, 135.5, 133.9 (C_q_{Ar}), 129.3, 129.3 (CH_{Mes}), 113.7 (CH_{Im}), 49.9 (N- $\text{CH}_{i\text{Pr}}$), 22.0 ($\text{CH}_{i\text{Pr}}$), 21.3, 19.7, 18.7 (CH_3). **IR (CH_2Cl_2):** ν_{CO} = 2076.4, 1993.5 cm^{-1} ; **Elemental analysis calcd (%)** for $\text{C}_{29}\text{H}_{36}\text{ClN}_3\text{O}_2\text{Rh}$ (MW = 597.99): C 58.25, H 6.24, N 7.03; *found*: C 58.22, H 6.19, N 6.63.

Chloro-dicarbonyl-(1,3-dimesityl-4-(dimethylamino)-5-chloroimidazol-2-ylidene) rhodium(I) (4.6)

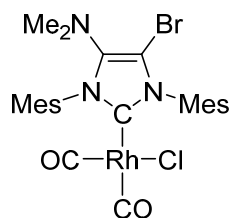


rhodium(I) (4.6)

2.10 (20.0 mg, 0.037 mmol, 1.0 eq) and *N*-chlorosuccinimide (6.0 mg, 0.044 mmol, 1.2 eq), were placed in a small vial and dissolved in CHCl_3 (0.6 mL), and the mixture was stirred for 2 h at room temperature. The resulting solution was concentrated under reduced pressure leading to a crude residue which was diluted by CH_2Cl_2 and filtered through a plug of silica to get a yellow solution. Evaporating the filtration to afford a yellow solid (15 mg, 71 %). **^1H NMR (400 MHz, CDCl_3)** δ = 7.02 (s, 2H, CH_{Mes}), 7.00 (s, 2H, CH_{Mes}), 2.67 (s, 6H, N- $(\text{CH}_3)_2$), 2.37 (s, 3H, $\text{CH}_3_{\text{para}}$), 2.36 (s, 3H, $\text{CH}_3_{\text{para}}$), 2.22 (s, 6H, $\text{CH}_3_{\text{ortho}}$), 2.21 (s, 6H, $\text{CH}_3_{\text{ortho}}$). **$^{13}\text{C}\{^1\text{H}\}$ NMR (101 MHz, CDCl_3)** δ = 185.0 (d, J_{RhC} = 55 Hz, Rh-CO), 182.9 (d, J_{RhC} = 75 Hz, Rh-CO), 174.5 (d, J_{RhC} = 46 Hz, $\text{N}_2\text{C}_{\text{carb}}$), 139.5, 139.8, 139.4, 136.3, 135.8, 133.2, 132.6 (C_q_{Ar}), 129.5, 129.4 (CH_{Mes}), 111.8 (C_{Im}), 42.6 (N- CH_3), 21.4, 21.4 ($\text{CH}_3_{\text{para}}$), 19.0, 18.6. ($\text{CH}_3_{\text{ortho}}$).

IR (CH₂Cl₂): ν_{CO} = 2079.6, 1996.4 cm⁻¹. **HRMS (ESI):** m/z *calcd* (%). for [Rh(NHC)(CO)(CH₃CN)]⁺: 553.1241; *found*: 553.1248, ϵ_r = 1.3 ppm.

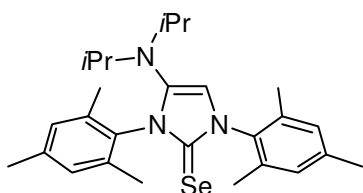
Chloro-dicarbonyl-(1,3-dimesityl-4-(dimethylamino)-5-bromoimidazol-2-ylidene)



rhodium(I) (4.7)

2.10 (30.0 mg, 0.055 mmol, 1.0 eq) and *N*-bromosuccinimide (11.0 mg, 0.06 mmol, 1.1 eq), were placed in a small vial and dissolved by CHCl₃ (0.6 mL), and the mixture was stirred for 2 h at room temperature. The resulting solution was concentrated under reduced pressure leading to a crude residue which was diluted by CH₂Cl₂ and filtered through a plug of silica to get a yellow solution. Evaporating the filtration affords a yellow solid (28 mg, 71 %). **¹H NMR (400 MHz, CDCl₃)** δ = 7.01 (s, 2H, *CH*_{Mes}), 7.00 (s, 2H, *CH*_{Mes}), 2.68 (s, 6H, N-(CH₃)₂), 2.37 (s, 3H, *CH*_{3 para}), 2.36 (s, 3H, *CH*_{3 para}), 2.22 (s, 6H, *CH*_{3 ortho}), 2.19 (s, 6H, *CH*_{3 ortho}). **¹³C{¹H} NMR (101 MHz, CDCl₃)** δ = 184.9 (d, J_{RhC} = 54 Hz, Rh-CO), 183.0 (d, J_{RhC} = 74 Hz, Rh-CO), 174.7 (d, J_{RhC} = 45 Hz, N₂C_{carb}), 142.5, 139.9, 139.3, 136.3, 135.8, 133.7, 132.3 (*Cq*_{Ar}), 129.5, 129.4 (*CH*_{Mes}), 98.0 (*C*_{Im}), 42.7 (N-CH₃), 21.5, 21.4 (*CH*_{3 para}), 19.0, 18.6 (*CH*_{3 ortho}). **IR (CH₂Cl₂):** ν_{CO} = 2079.0, 1996.2 cm⁻¹. **HRMS (ESI):** m/z *calcd* (%). for [Rh(NHC)(CO)(CH₃CN)]⁺: 597.0736; *found*: 597.0725, ϵ_r = - 1.8 ppm.

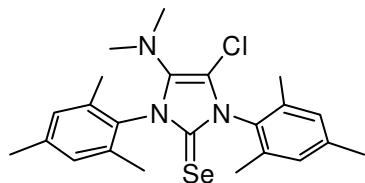
1,3-dimesityl-4-(diisopropylamino)imidazolin-2-selenone (4.8)



A solution of KHMDS (0.5 M in toluene, 880 μ L, mmol, 1.1 eq.) was added dropwise to a solution of **4.2a** (221.2 mg, 0.4 mmol, 1.0 eq) in THF (10 mL) at 0°C. After 30 min, selenium element (excess, *ca.* 75 mg) was added as a solid and the ice-water bath was then removed. After 2 h, the solution was filtered by celite and silica and rinsed by CH₂Cl₂ until the solution was colorless. Evaporated the solvent under reduced pressure and the residue was washed by pentane to get a grey powder (196 mg, 99%). **¹H NMR (400 MHz, CDCl₃)** δ = 7.00 (s, 2H, *CH*_{Mes}), 6.98 (s, 2H, *CH*_{Mes}), 6.56 (s, 1H, *CH*_{Im}), 3.28 (hept, J = 6.7 Hz, 2H, *CH*_{iPr}), 2.34 (s, 3H, *CH*_{3 ortho}), 2.33 (s, 3H, *CH*_{3 ortho}), 2.18 (s, 6H, *CH*_{3 para}), 2.16 (s, 6H, *CH*_{3 para}), 1.00 (d, J = 6.8 Hz, 12H, *CH*_{3 iPr}). **¹³C{¹H} NMR (101 MHz, CDCl₃)** δ = 154.2 (NCN), 139.1, 138.8, 136.3, 135.5, 134.7, 133.1 (*Cq*_{Ar}), 129.3 (*CH*_{Ar}), 110.2 (*CH*_{Im-5}), 49.7 (N-CH *iPr*), 22.1 (*CH*_{3 iPr}), 21.3, 21.3, 18.7, 18.2 (*CH*_{3, Mes}). **⁷⁷Se{¹H}**

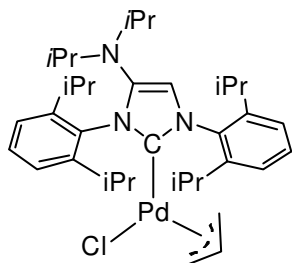
NMR (95 MHz, CDCl₃) δ = 35.8. Elemental analysis calcd (%) for C₂₇H₃₇N₃Se (MW = 482.57): C 67.20, H 7.73, N 8.71; *found*: C 67.25, H 7.71, N 8.63.

1,3-dimesityl-4-(dimethylamino)-5-chloroimidazolin-2-selenone (4.9)

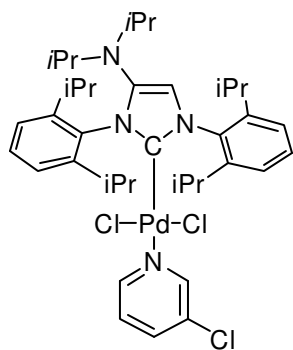


2.12 (43 mg, 0.1 mmol, 1.0 eq) and *N*-chlorosuccinimide (15 mg, 0.11 mmol, 1.1 eq), were placed in a small vial and dissolved in CHCl₃ (1.0 mL), and the mixture was stirred for 1 h at room temperature. All volatiles were evaporated and the crude product was filtered through a small plug of silica and evaporated to yield a green-yellow powder (20.0 mg, 44%). **¹H NMR (400 MHz, CDCl₃) δ = 7.03 (s, 2H, *CH*_{Mes}), 7.01 (s, 2H, *CH*_{Mes}), 2.68 (s, 6H, N-CH₃), 2.35 (s, 3H, *CH*_{3 para}), 2.35 (s, 3H, *CH*_{3 para}), 2.16 (s, 6H, *CH*_{3 ortho}), 2.15 (s, 6H, *CH*_{3 ortho}). **¹³C{¹H} NMR (101 MHz, CDCl₃) δ = 154.5 (NCN), 139.9, 139.4, 137.0, 136.2, 135.9, 132.3, 131.7 (*Cq*_{Ar}), 129.5, 129.4 (*CH*_{Ar}), 107.5 (*CH*_{Im-5}), 42.8 (N-CH₃), 21.5, 21.4, 18.4, 18.0 (*CH*_{3 Mes}). **⁷⁷Se{¹H} NMR (95 MHz, CDCl₃) δ = 67.8.******

Chloro-(η^3 -allyl)-(1,3-bis(2,6-diisopropylphenyl)-4-diisopropylaminoimidazol-2-ylidene)palladium(II) (4.10)

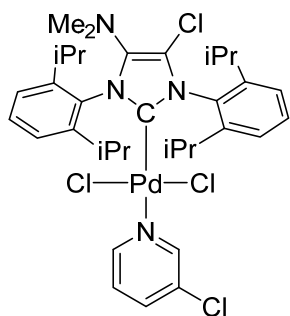


4.2b (191.4 mg, 0.3 mmol, 1.0 eq) was dissolved in dry THF (10 mL) and the solution was cooled to 0 °C. KHMDS (solution at 0.5 M in toluene, 0.66 mL, 0.33 mmol, 1.1 eq) was added dropwise and the solution became light yellow. After 30 min reacting at 0°C, [Pd(allyl)Cl]₂ (55.0 mg, 0.15 mmol, 0.5 eq) was added as a solid and the mixture was warmed to room temperature and allowed to stir for another 3 h. Volatiles were evaporated under vacuum and the crude residue was purified through flash chromatography (Al₂O₃, CH₂Cl₂) to get a light yellow powder which was further purified by recrystallization in CH₂Cl₂/Pentane to give a yellow powder (130 mg, 65 %). **¹H NMR (400 MHz, CDCl₃) δ = 7.39 (q, *J* = 7.9 Hz, 2H, *CH*_{Dipp-p}), 7.16-7.30 (m, 4H, *CH*_{Dipp-o}), 6.65 (s, 1H, *CH*_{Im}), 4.80-4.63 (m, 1H, *CH*_{allyl}), 3.87 (d, *J* = 7.5 Hz, 1H, *CH*_{2 allyl}), 3.40 (hept, *J* = 6.7 Hz, 2H, *CH*_{iPr}), 3.12 (br, s, 2H, *CH*_{iPr}), 3.02 (br, s, 1H, *CH*_{iPr}), 2.91-2.61 (m, 3H, (2H, *CH*_{allyl} + 1H, *CH*_{iPr})), 1.48-0.98 (m, 36H, *CH*_{3 iPr}). **¹³C{¹H} NMR (101 MHz, CDCl₃) δ = 181.5 (N₂C_{carb}), 146.0, 141.5, 137.0, 135.6 (*Cq*_{Ar}), 129.6, 129.5, 124.8, 123.9 (*CH*_{Ar}), 114.0 (*CH*_{allyl}), 112.6 (*C*_{Im}), 72.6 (*CH*_{2 allyl}), 50.0 (*CH*_{2 allyl}), 49.9 (N-CH_{iPr}), 28.8, 28.5 (*CH*_{iPr}), 26.4, 26.1, 25.8, 24.9, 23.3, 23.1, 21.0 (*CH*_{3 iPr}). **Elemental analysis calcd (%) for C₃₅H₅₃ClN₃Pd (MW = 657.70): C 63.92, H 8.12, N 6.39; *found*: C 64.32, H 8.56, N 6.09.******

Dichloro-(3-chloropyridine)(1,3-bis(2,6-diisopropylphenyl)-4-**(diisopropylamino)imidazol-2-ylidene)palladium(II) (4.11)**

A solution of HCl (2M in Et₂O, 2.0 mL) was added to solid **4.10** (91 mg, 0.25 mmol, 1.0 eq), at room temperature. The color of the solution changed from light yellow to orange and soon after an orange solid began to precipitate. After 2 h, the volatiles were evaporated under vacuum and the solid was dissolved in CH₂Cl₂ (5.0 mL). Further addition of 3-chloropyridine (100 μL, excess) led to a

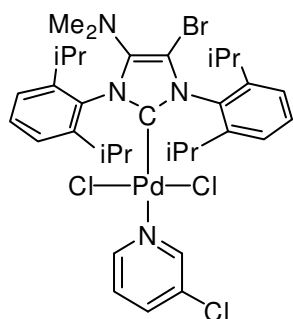
color change from orange to bright yellow. The reaction mixture was stirred for another 1 h and filtered through a plug of silica gel. The solvent was removed under vacuum to leave a yellow solid which was washed with pentane and dried under vacuum to afford yellow powder (140 mg, 72%). Single crystals suitable for an X-Ray diffraction experiment were grown by diffusion of pentane to a solution of **4.11** in CH₂Cl₂. ¹H NMR (400 MHz, CDCl₃) δ = 8.63 (d, *J* = 2.3 Hz, 1H, CH_{Py}), 8.54 (dd, *J* = 5.6, 1.3 Hz, 1H, CH_{Py}), 7.53 (ddd, *J* = 8.3, 2.4, 1.3 Hz, 1H, CH_{Py}), 7.50-7.42 (m, 2H, CH_{Dipp}), 7.34 (t, *J* = 7.4 Hz, 4H, CH_{Dipp}), 7.04 (dd, *J* = 8.2, 5.5 Hz, 1H, CH_{Py}), 6.64 (s, 1H, CH_{Im}), 3.46-3.31 (m, 4H, CH_{iPr}), 2.99 (hept, *J* = 6.6 Hz, 2H, CH_{iPr}), 1.72 (d, *J* = 6.5 Hz, 6H, CH_{3 iPr}), 1.49 (d, *J* = 6.6 Hz, 6H, CH_{3 iPr}), 1.28 (d, *J* = 6.6 Hz, 6H, CH_{3 iPr}), 1.15 (d, *J* = 6.8 Hz, 6H, CH_{3 iPr}), 1.07 (d, *J* = 6.7 Hz, 12H, CH_{3 iPr}). ¹³C{¹H} NMR (101 MHz, CDCl₃) δ = 150.6, 149.6 (CH_{Py}), 147.6 (N₂C_{carb}), 147.0, 146.6, 143.2 (*Cq*_{Ar}), 137.4 (CH_{Py}), 136.4, 133.5, 132.0 (*Cq*_{Ar}), 130.0, 129.8, 125.1, 124.4, 124.2 (CH_{Ar}), 113.8 (C_{Im}), 50.3 (N-CH_{iPr}), 28.9, 28.7 (CH_{iPr}), 26.9, 26.4, 26.0, 23.4, 20.9 (CH_{3 iPr}). **Elemental analysis calcd (%)** for C₃₈H₅₃Cl₃N₄Pd (MW = 778.64): C 58.62, H 6.86, N 7.20; **found:** C 58.42, H 6.53, N 7.07.

Dichloro-(3-chloropyridine)(1,3-bis(2,6-diisopropylphenyl)-4-(dimethylamino)-5-**chloroimidazol-2-ylidene)palladium(II) (4.12)**

2.14 (182.0 mg, 0.252 mmol, 1.0 eq) and *N*-chlorosuccinimide (40.1 mg, 0.3 mmol, 1.2 eq), were placed in a small vial and dissolved by CHCl₃ (4.0 mL), and the mixture was stirred for 2 h at room temperature. All volatiles were evaporated and the crude product was purified by flash column chromatography (SiO₂, CH₂Cl₂) to yield a yellow powder (162 mg, 85 %). ¹H NMR (400 MHz, CDCl₃) δ = 8.58 (d, *J* = 2.2 Hz, 1H, CH_{Py}), 8.51 (dd, *J* = 5.5, 1.0 Hz, 2H, CH_{Py}), 7.60-7.46 (m, 3H, CH_{Py} + CH_{Dipp}), 7.37 (d, *J* =

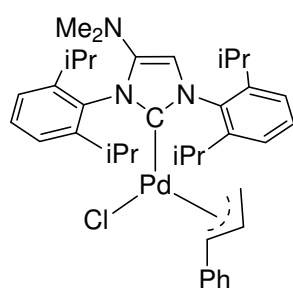
7.8 Hz, 4H, CH_{Dipp}), 7.05 (dd, $J = 8.2, 5.6$ Hz, 1H, CH_{Py}), 3.18-2.99 (m, 4H, CH_{iPr}), 2.62 (s, 6H, N- CH_3), 1.58 (d, $J = 6.5$ Hz, 6H, CH_3_{iPr}), 1.50 (d, $J = 6.5$ Hz, 6H, CH_3_{iPr}), 1.22 (d, $J = 4.4$ Hz, 6H, CH_3_{iPr}), 1.21 (d, $J = 4.5$ Hz, 6H, CH_3_{iPr}). $^{13}C\{^1H\}$ NMR (101 MHz, $CDCl_3$) δ = 152.0 (N_2C_{carb}), 150.6, (CH_{py}), 149.6 (CH_{py}), 148.0, 147.3, 140.7 (Cq_{Ar}), 137.5 (CH_{py}), 132.8, 132.0 (Cq_{Ar}), 130.8, 130.2 (CH_{Dipp}), 125.1 (CH_{Dipp}), 124.6 (CH_{Dipp}), 124.4 (CH_{py}), 112.2 (CH_{Im-5}), 43.1 (N- CH_3), 29.0 (CH_{iPr}), 26.2, 25.7, 25.5, 24.9 (CH_3_{iPr}). **Elemental analysis calcd (%)** for $C_{34}H_{44}Cl_4N_4Pd$ (MW = 756.97): C, 53.95; H, 5.86; N, 7.40. *found*: C, 53.82; H, 5.57; N, 7.29.

Dichloro-(3-chloropyridine)(1,3-bis(2,6-diisopropylphenyl)-4-(dimethylamino)-5-bromo(imidazol-2-ylidene)palladium(II) (4.13)



2.14 (144.0 mg, 0.2 mmol, 1.0 eq) and *N*-bromosuccinimide (43.0 mg, 0.24 mmol, 1.2 eq) were placed in a small vial and dissolved by $CHCl_3$ (4.0 mL), and the mixture was stirred for 1.5 h at room temperature. All volatiles were evaporated and the crude product was purified by flash column chromatography (SiO_2 , CH_2Cl_2) to yield a yellow powder (153 mg, 95 %). 1H NMR (400 MHz, $CDCl_3$) δ = 8.59 (dd, $J = 2.3, 0.6$ Hz, 1H, CH_{Py}), 8.51 (dd, $J = 5.6, 1.3$ Hz, 1H, CH_{Py}), 7.59-7.45 (m, 3H, $CH_{Py} + CH_{Dipp}$), 7.39-7.34 (m, 4H, CH_{Dipp}), 7.06 (ddd, $J = 8.2, 5.6, 0.6$ Hz, 1H, CH_{Py}), 3.13 (hept, $J = 6.6$ Hz, 2H, CH_{iPr}), 3.03 (hept, $J = 6.7$ Hz, 2H, CH_{iPr}), 2.63 (s, 6H, N- CH_3), 1.56 (d, $J = 6.5$ Hz, 6H, CH_3_{iPr}), 1.51 (d, $J = 6.6$ Hz, 6H, CH_3_{iPr}), 1.26 (d, $J = 6.8$ Hz, 6H, CH_3_{iPr}), 1.21 (d, $J = 6.7$ Hz, 6H, CH_3_{iPr}). $^{13}C\{^1H\}$ NMR (101 MHz, $CDCl_3$) δ = 153.2 (N_2C_{carb}), 150.6 (CH_{py}), 149.6 (CH_{py}), 147.9, 147.4, 143.4 (Cq_{Ar}), 137.5 (CH_{py}), 134.1, 132.9, 132.0, (Cq_{Ar}), 130.7, 130.2, 125.1, 124.7, 124.4 (CH_{Ar}), 99.0 (CH_{Im-5}), 43.4 (N- CH_3), 29.1, 29.0 (CH_{iPr}), 26.1, 25.8, 25.7, 25.4 (CH_3_{iPr}). **Elemental analysis calcd (%)** for $C_{34}H_{44}BrCl_3N_4Pd$ (MW = 801.4): C 50.96, H 5.53, N 6.99; *found*: C 50.53, H 5.35, N 6.79.

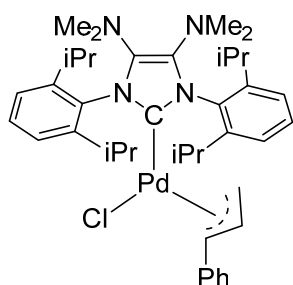
Chloro-(η^3 -2-cinnam-1-yl)-(1,3-bis(2,6-diisopropylphenyl)-4-(dimethylamino)imidazol-2-ylidene)palladium(II) (4.14)



2.2b (116 mg, 0.2 mmol, 1.0 eq) was dissolved in dry THF (10 mL) and the solution was cooled to 0 °C. KHMDS (solution at 0.5 M in toluene, 0.44 mL, 0.22 mmol, 1.1 eq) was added dropwise and the solution became light yellow. After 40 min reacting at 0°C,

[Pd(cinnamyl)Cl]₂ (51.6 mg, 0.1 mmol, 0.5 eq) was added as a solid and the mixture was warmed to room temperature and allowed to stir for another 3 h. Volatiles were evaporated under vacuum and the crude residue was purified through flash chromatography (Al₂O₃, CH₂Cl₂) to get a light yellow powder which was further purified by recrystallization in CH₂Cl₂/Pentane to give a yellow powder (113 mg, 82 %). **¹H NMR (300 MHz, CDCl₃):** δ = 7.56-7.34 (m, 2H, CH_{Dipp}), 7.34-7.22 (m, 4H, CH_{Dipp}), 7.20-7.05 (m, 5H, CH_{Ph}), 6.47 (s, 1H, CH_{Im-5}), 5.06 (dt, *J* = 12.9, 9.2 Hz, 1H, CH_{cinnamyl}), 4.35 (d, *J* = 12.9 Hz, 1H, CH_{cinnamyl}), 3.09 (hept, *J* = 6.6 Hz, 2H, CH_{iPr}), 2.91 (br, 2H, CH_{iPr}), 2.66 (s, 1H, CH_{cinnamyl}), 2.46 (s, 6H, N-CH₃), 1.43 (d, *J* = 6.7 Hz, 6H, CH_{3 iPr}), 1.38 (d, *J* = 6.7 Hz, 6H, CH_{3 iPr}), 1.23 (d, *J* = 6.7 Hz, 6H, CH_{3 iPr}), 1.14 (d, *J* = 6.8 Hz, 6H, CH_{3 iPr}). **¹³C{¹H} NMR (75 MHz, CDCl₃):** δ = 181.4 (NCN), 146.8 (Cq_{Im-4}), 146.7 (Cq_{Ar}), 137.9, 136.9, 134.5 (Cq_{Ar}), 129.7, 129.7, 128.4, 127.5, 126.8, 124.7, 123.9 (CH_{Ar}), 109.5 (CH_{Im-5}), 108.8 (CH_{cinnamyl}), 91.0 (CH_{cinnamyl}), 45.9 (CH_{2 cinnamyl}), 43.0 (N-CH₃), 28.8, 28.7 (CH_{iPr}), 26.4, 25.4, 24.8, 23.2 (CH_{3 iPr}); **IR (ATR):** ν = 2958, 2931, 2868, 1621, 1451, 1382, 1360, 1318, 1057, 931, 801, 758, 692, 675 (cm⁻¹). **MS (ESI, positive mode):** *m/z* (%): 654 (100) [M - Cl]⁺.

Chloro-(η³-2-cinnam-1-yl)-(1,3-bis(2,6-diisopropylphenyl)-4,5-bis(dimethylamino)imidazol-2-ylidene)palladium(II) (4.15)

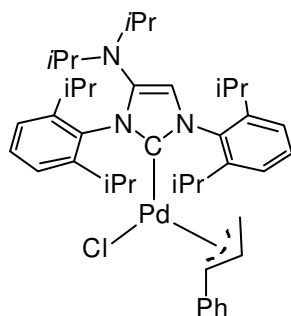


2.6b (400 mg, 0.64 mmol, 1.0 eq) was dissolved in dry THF (15 mL) and the solution was cooled to -78°C. nBuLi (solution at 1.6 M in Hexane, 440 μL, 0.704 mmol, 1.1 eq) was added dropwise and the solution became light yellow. The reaction was continued for another 40 min at low temperature. [Pd(cinnamyl)Cl]₂ (166 mg, 0.32 mmol, 0.5 eq) was added as a solid and the mixture was warmed to room

temperature and allowed to stir for another 2 h. Volatiles were evaporated under vacuum and the crude residue was purified through flash chromatography (Al₂O₃, CH₂Cl₂) to get a yellow powder (360 mg, 77 %). **¹H NMR (400 MHz, CDCl₃):** δ = 7.41 (t, *J* = 7.7 Hz, 2H, CH_{Dipp}), 7.24 (d, *J* = 7.7 Hz, 4H, CH_{Dipp}), 7.17-7.09 (m, 5H, CH_{phenyl}), 5.02 (dt, *J* = 12.8, 9.3 Hz, 1H, CH_{cinnamyl}), 4.31 (d, *J* = 12.8 Hz, 1H, CH_{cinnamyl}), 2.85 (hept, *J* = 6.7 Hz, 4H, CH_{iPr}), 2.60 (s, 12H, N-CH₃), 2.60-2.55 (m, 1H, CH_{cinnamyl}), 1.46 (d, *J* = 6.7 Hz, 12H, CH_{3 iPr}), 1.21 (d, *J* = 6.8 Hz, 12H, CH_{3 iPr}); **¹³C{¹H} NMR (101 MHz, CDCl₃):** δ = 174.2 (NCN), 146.7 (Cq_{Im-4,5}), 138.0, 135.1 (Cq_{Ar}), 129.3, 128.4, 127.6, 126.7, 124.2 (CH_{Ar}), 108.4 (CH_{cinnamyl}), 90.8 (CH_{cinnamyl}), 47.7 (CH_{cinnamyl}), 43.8 (N-CH₃), 28.9 (CH_{iPr}), 25.3, 25.3 (CH_{3 iPr}); **IR (ATR):** ν =

2957, 2928, 2864, 1636, 1456, 1381, 1361, 1291, 1140, 1058, 990, 952, 933, 801, 779, 762, 755, 689 (cm^{-1}); **MS (ESI, positive mode):** m/z (%): 697 (100) $[\text{M} - \text{Cl}]^+$. **Elemental analysis** *calcd* (%) for $\text{C}_{40}\text{H}_{55}\text{ClN}_4\text{Pd}$ (MW = 732.32): C 65.47, H 7.56, N 7.64; *found*: C 65.20, H 7.74, N 7.74.

Chloro-(η^3 -2-cinnam-1-yl)-(1,3-bis(2,6-diisopropylphenyl)-4-



(diisopropylamino)imidazol-2-ylidene)palladium(II) (4.16)

4.2b (500 mg, 0.784 mmol, 1.0 eq) was dissolved in dry THF (20 mL) and the solution was cooled to 0 °C. KHMDS (solution at 0.5 M in toluene, 1.72 mL, 0.862 mmol, 1.1 eq) was added dropwise and the solution became light yellow. After 40 min reacting at 0 °C, $[\text{Pd}(\text{cinnamyl})\text{Cl}]_2$ (203 mg, 0.392 mmol, 0.5 eq) was added as a solid and the mixture was warmed to room temperature and allowed to stir for another 3 h. Volatiles were evaporated under vacuum and the crude residue was purified through flash chromatography (Al_2O_3 , CH_2Cl_2) to get a yellow powder which was further washed with pentane to give a pale-yellow powder (385 mg, 66 %). **^1H NMR (400 MHz, CDCl_3)** δ = 7.51-7.34 (m, 2H, CH_{Dipp}), 7.34-7.20 (m, 4H, CH_{Dipp}), 7.20-7.08 (m, 5H, CH_{Ph}), 6.67 (s, 1H, CH_{Im}), 5.04 (dt, J = 13.1, 9.3 Hz, 1H, $\text{CH}_{\text{cinnamyl}}$), 4.34 (d, J = 12.8 Hz, 1H, $\text{CH}_{\text{cinnamyl}}$), 3.48-3.28 (m, 2H, CH_{iPr}), 3.15 (m, 2H, CH_{iPr}), 3.02-2.76 (m, 2H, CH_{iPr}), 1.45 (d, J = 6.7 Hz, 6H, CH_3_{iPr}), 1.40 (d, J = 6.8 Hz, 6H, CH_3_{iPr}), 1.24 (d, J = 6.6 Hz, 6H, CH_3_{iPr}), 1.15 (d, J = 6.8 Hz, 6H, CH_3_{iPr}), 1.07 (d, J = 6.8 Hz, 12H, CH_3_{iPr}). **$^{13}\text{C}\{^1\text{H}\}$ NMR (101 MHz, CDCl_3)** δ = 179.5 (NCN), 146.5 ($\text{Cq}_{\text{Im-4}}$), 145.7, 141.3, 137.8, 137.0, 135.6 (Cq_{Ar}), 129.4, 129.4, 128.3, 127.3, 126.6, 124.6, 123.7 (CH_{Ar}), 112.8 ($\text{CH}_{\text{Im-5}}$), 108.7 ($\text{CH}_{\text{cinnamyl}}$), 90.6 ($\text{CH}_{\text{cinnamyl}}$), 49.7 ($\text{CH}_2_{\text{cinnamyl}}$), 46.4 (N- CH_3), 28.6, 28.4 (CH_{iPr}), 25.9, 25.7, 25.1, 23.2, 20.9 (CH_3_{iPr}). **Elemental analysis** *calcd* (%) for $\text{C}_{42}\text{H}_{58}\text{ClN}_3\text{Pd}$ (MW = 746.82): C 67.55, H 7.83, N 5.63; *found*: C 67.86, H 7.90, N 5.59.

5.2 Palladium-Catalyzed Buchwald-Hartwig amination reaction

Kinetic studies on the amination of 4-chloroanisole with morpholine

Pre-catalysts **2.14**, **2.17**, **1.1**, **1.2**, **1.11**, **4.11**, **4.12** and **4.13** (0.02 mmol, 0.5 mol%) and were placed in eight separate Schlenk tubes which were then transferred to the glove box to weight KO t Bu (128 mg, 1.1 mmol, 1.1 eq). The tubes were closed with a septum, taken out of the glove box and placed in a thermostatic bath at 25 °C. Dodecane (224 μL , 1.0 mmol, internal

standard), morpholine (106 μ L, 1.1 mmol), 4-chloroanisole (122 μ L, 1.0 mmol) and DME (1.0 mL) were then injected via syringe respectively and the time was started at this point. Conversions were measured by passing an aliquot of the solution through a plug of silica gel using EtOAc as eluant and monitoring the relative areas of the peaks compared to that of dodecane in the GC chromatography.

Kinetic studies on the amination of 2-chloroanisole with morpholine

Pre-catalysts **2.14**, **2.17**, **1.1**, **1.2**, **1.11**, **4.11**, and **4.12** (0.02 mmol, 0.5 mol%) and were placed in eight separate Schlenk tubes which were then transferred to the glove box to weight KO t Bu (128 mg, 1.1 mmol, 1.1 eq). The tubes were closed with a septum, taken out of the glove box and placed in a thermostatic bath at 25°C. Dodecane (224 μ L, 1.0 mmol, internal standard), morpholine (106 μ L, 1.1 mmol, 1.1 eq), 2-chloroanisole (126 μ L, 1.0 mmol, 1.0 eq) and DME (1.0 mL) were then injected via syringe respectively and the time was started at this point. Conversions were measured by passing an aliquot of the solution through a plug of silica gel using EtOAc as eluant and monitoring the relative areas of the peaks compared to that of dodecane in the GC chromatography.

General procedure for the optimization of the Pd-catalyzed amination reaction (Table 4.6.1)

The palladium pre-catalyst (0.005 mmol, 0.5 mol%) was placed in a Schlenk tube which was then transferred into the glove box to weight KO t Bu (128 mg, 1.1 mmol, 1.1 eq). The tube was closed with a septum, taken out of the glove box. Under N₂, DME (1.0 mL), 2-chloroanisole (126 μ L, 1.0 mmol, 1.0 eq), *tert*-butyl amine (116 μ L, 1.1 mmol, 1.1 eq) were subsequently injected via syringe at room temperature. Then, the mixture was put into a preheated oil bath (40-80 °C), and was allowed to stir for intended time. Conversions were measured by passing an aliquot of the solution through a plug of silica gel using EtOAc as eluant and monitoring the relative areas of the peaks compared to that of dodecane in the GC chromatography.

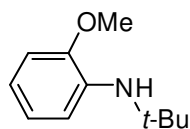
Palladium-catalyzed amination with bulky primary amines (Table 4.6.2)

4.15 or **4.16** (0.005 mmol, 0.5 mol%) was placed in Schlenk tube which was then transferred into the glove box to weight KO t Bu (128 mg, 1.1 mmol, 1.1 eq). After then, the tube was closed with a septum, taken out of the glove box. Under N₂, DME (1.0 mL), aryl chlorides (1.0 mmol, 1.0 eq), amine (1.1 mmol, 1.1 eq) were subsequently injected via syringe at room

temperature. Then the mixture was put into a preheated oil bath (40-80 °C), and was allowed to stir for intended time checked by GC. The reaction mixture was diluted with EtOAc (10 mL), filtered through a small plug of silica gel and washed with ethyl acetate. The filtrate was concentrated under reduced pressure and purified via silica gel flash chromatography.

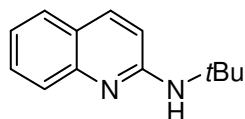
5.3 Catalytic products (Table 4.6.2)

2-methoxy-N-*tert*-butylaniline (4.18a): Following the general procedure using 0.5 mol% of pre-catalyst **4.15**, the reaction was stirred for 3h at 40 °C. After flash chromatography on silica gel (Hexane/EtOAc: 10/1), the title compound was recovered as a light yellow oil: 146 mg (82 % yield).



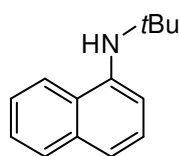
¹H NMR (300 MHz, CDCl₃): δ = 6.91 (dd, *J* = 7.9, 1.6 Hz, 1H), 6.88-6.74 (m, 2H), 6.68 (ddd, *J* = 8.0, 7.2, 1.7 Hz, 1H), 4.24 (br, s, 1H), 3.83 (s, 3H), 1.38 (s, 9H). ¹³C{¹H} NMR (75 MHz, CDCl₃): δ = 148.2, 136.8, 120.9, 116.9, 114.5, 109.8, 55.6, 51.0, 30.1.

2-(N-*tert*-butylamino)quinoline (4.18b): Following the general procedure using 0.5 mol% of pre-catalyst **4.15**, the reaction was stirred for 4h at 40°C. After flash chromatography on silica gel (Hexane/EtOAc: 10/1), the title compound was recovered as a yellow oil: 151 mg (75%).



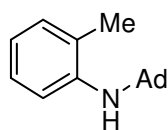
¹H NMR (400 MHz, CDCl₃): δ = 7.75 (d, *J* = 8.9 Hz, 1H), 7.68 (d, *J* = 8.4 Hz, 1H), 7.56 (d, *J* = 8.0 Hz, 1H), 7.54-7.48 (m, 1H), 7.22-7.15 (m, 1H), 6.59 (d, *J* = 8.9 Hz, 1H), 4.62 (br, s, 1H), 1.55 (s, 9H). ¹³C{¹H} NMR (101 MHz, CDCl₃): δ = 156.6, 148.2, 136.6, 129.3, 127.4, 126.7, 123.0, 121.9, 113.1, 51.6, 29.6.

1-(N-*tert*-butyl)aminonaphthalene (4.18c): Following the general procedure using 0.5 mol% of pre-catalyst **4.15**, the reaction was stirred for 3h at 40°C. After flash chromatography on silica gel (Hexane/EtOAc: 20/1), the title compound was recovered as a yellow oil: 165 mg (83%).



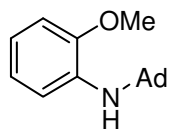
¹H NMR (400 MHz, CDCl₃): δ = 7.80 (m, 2H), 7.48-7.39 (m, 2H), 7.34 (t, *J* = 7.8 Hz, 1H), 7.28 (s, 1H), 6.99-6.92 (m, 1H), 4.25 (br, s, 1H), 1.49 (s, 9H). ¹³C{¹H} NMR (101 MHz, CDCl₃) δ = 141.9, 134.8, 128.9, 126.3, 125.6, 125.6, 124.8, 120.5, 118.0, 110.1, 51.8, 30.1.

2-methyl-N-adamantylaniline (4.18d): Following the general procedure using 0.5 mol% of pre-catalyst **4.15**, the reaction was stirred for 3h at 40°C. After flash chromatography on silica gel (Hexane/EtOAc: 20/1), the title compound was recovered as a white solid: 234 mg (97 % yield).



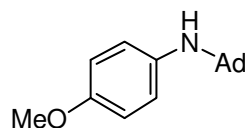
¹H NMR (400 MHz, CDCl₃): δ = 7.13-7.03 (m, 2H), 6.99 (d, J = 8.5 Hz, 1H), 6.69 (t, J = 7.3 Hz, 1H), 3.31 (s, 1H), 2.16 (s, 3H), 2.15-2.09 (m, 3H), 1.97 (d, J = 3.0 Hz, 6H), 1.78-1.66 (m, 6H). **¹³C{¹H} NMR (101 MHz, CDCl₃):** δ = 144.6, 130.6, 126.5, 124.6, 117.8, 116.5, 52.3, 43.7, 36.7, 29.9, 18.4. **HRMS:** *Calcd.* for C₁₇H₂₃N, [M+H]⁺: 242.1909, Found: [M+H]⁺: 242.1908. ϵ_r = -0.4 ppm.

2-methoxy-*N*-adamantylaniline (4.18e): Following the general procedure using 0.5 mol% of pre-catalyst **4.15**, the reaction was stirred for 4h at 40°C. After flash chromatography on silica gel (Hexane/EtOAc: 10/1), the title compound was recovered as a white solid: 209 mg (81 % yield).



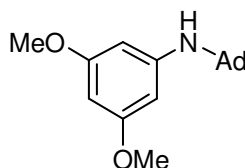
¹H NMR (300 MHz, CDCl₃): δ = 6.98 (dd, J = 7.8, 1.6 Hz, 1H), 6.86-6.75 (m, 2H), 6.75-6.66 (m, 1H), 4.10 (s, 1H), 3.83 (s, 3H), 2.19-2.05 (m, 3H), 1.94 (d, J = 3.0 Hz, 6H), 1.76-1.62 (m, 6H). **¹³C{¹H} NMR (75 MHz, CDCl₃):** δ = 148.8, 136.1, 120.7, 117.6, 116.6, 110.0, 55.6, 51.9, 43.3, 36.7, 29.9. **HRMS:** *Calcd.* for C₁₇H₂₃NO, [M+H]⁺: 258.1858, Found: [M+H]⁺: 258.1865. ϵ_r = 2.7 ppm.

4-methoxy-*N*-adamantylaniline (4.18f): Following the general procedure using 0.5 mol% of pre-catalyst **4.15**, the reaction was stirred for 3h at 60°C. After flash chromatography on silica gel (Hexane/EtOAc: 4/1), the title compound was recovered as a white solid: 240 mg (93 % yield).



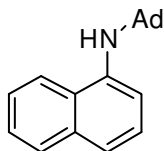
¹H NMR (400 MHz, CDCl₃): δ = 6.86-6.78 (m, 2H), 6.79-6.71 (m, 2H), 3.75 (s, 3H), 2.86 (br, s, 1H), 2.07 (s, 3H), 1.74 (d, J = 2.4 Hz, 6H), 1.63 (q, J = 12.1 Hz, 6H). **¹³C{¹H} NMR (101 MHz, CDCl₃):** δ = 154.9, 138.4, 124.3, 113.9, 55.5, 52.7, 43.8, 36.6, 29.8.

3,5-dimethoxy-*N*-adamantylaniline (4.18g): Following the general procedure using 0.5 mol% of pre-catalyst, the reaction was stirred for 3h at 60°C. After flash chromatography on silica gel (Hexane/EtOAc: 10/1-4/1), the title compound was recovered as a white solid: 241 mg (91%).



¹H NMR (400 MHz, CDCl₃): δ = 5.96 (d, J = 2.2 Hz, 2H), 5.93 (t, J = 2.2 Hz, 1H), 3.75 (s, 6H), 3.38 (br, s, 1H), 2.10 (s, 3H), 1.91 (d, J = 2.8 Hz, 6H), 1.74-1.61 (m, 6H). **¹³C{¹H} NMR (101 MHz, CDCl₃):** δ = 161.2, 148.1, 96.8, 90.6, 55.2, 52.2, 43.4, 36.6, 29.8.

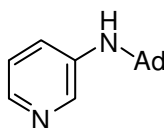
1-(*N*-adamantyl)aminonaphthalene (4.18h): Following the general procedure using 0.5 mol% of pre-catalyst **4.15**, the reaction was stirred for 4h at 40°C. After flash chromatography



on silica gel (Hexane/EtOAc: 20/1), the title compound was recovered as a white solid: 179 mg (65%).

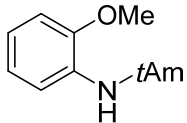
¹H NMR (400 MHz, CDCl₃): δ = 7.94-7.84 (m, 1H), 7.83-7.75 (m, 1H), 7.47-7.39 (m, 2H), 7.34-7.30 (m, 2H), 7.10-7.02 (m, 1H), 4.02 (br, s, 1H), 2.15 (s, 3H), 2.03 (d, J = 2.8 Hz, 6H), 1.77-1.65 (m, 6H). **¹³C{¹H} NMR (101 MHz, CDCl₃)** δ = 141.3, 134.8, 128.9, 126.8, 126.0, 125.5, 124.9, 121.1, 119.2, 113.4, 53.0, 43.5, 36.7, 30.0.

3-(1-adamantylamino)pyridine (4.18i): Following the general procedure using 0.5 mol% of pre-catalyst **4.15**, the reaction was stirred for 3h at 60°C. After flash chromatography on silica gel (EtOAc), the title compound was recovered as a white solid: 185 mg (81%).



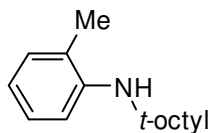
¹H NMR (300 MHz, CDCl₃): δ = 8.11 (d, J = 2.2 Hz, 1H), 8.04-7.95 (m, 1H), 7.16-6.94 (m, 2H), 3.36 (br, s, 1H), 2.11 (s, 3H), 1.86 (d, J = 2.6 Hz, 6H), 1.74-1.56 (m, 6H). **¹³C{¹H} NMR (75 MHz, CDCl₃):** δ = 142.4, 140.8, 140.1, 124.4, 123.3, 52.4, 43.3, 36.5, 29.7.

2-methoxy-*N*-tert-amylaniline (4.18j): Following the general procedure using 0.5 mol% of pre-catalyst **4.16**, the reaction was stirred for 3h at 60°C. After flash chromatography on silica gel (Hexane/EtOAc: 20/1), the title compound was recovered as a light yellow oil: 185 mg (96 % yield).



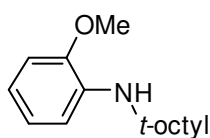
¹H NMR (300 MHz, CDCl₃): δ = 6.90-6.74 (m, 3H), 6.69-6.61 (m, 1H), 4.23 (br, s, 1H), 3.84 (s, 3H), 1.72 (q, J = 7.5 Hz, 2H), 1.32 (s, 6H), 0.89 (t, J = 7.5 Hz, 3H). **¹³C NMR (75 MHz, CDCl₃)** δ = 147.9, 136.9, 120.9, 116.5, 113.8, 109.8, 55.6, 53.5, 33.9, 27.9, 8.6. **HRMS:** *Calcd.* for C₁₂H₁₉NO, [M+H]: 194.1545, *Found:* [M+H]: 194.1545. ϵ_r = 0.0 ppm

2-methyl-*N*-tert-octylaniline (4.18k): Following the general procedure using 0.5 mol% of pre-catalyst **4.16**, the reaction was stirred for 3h at 60°C. After flash chromatography on silica gel (Hexane/EtOAc: 20/1), the title compound was recovered as a light yellow oil: 180mg (82% yield).



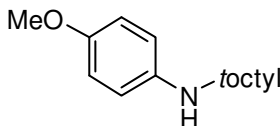
¹H NMR (400 MHz, CDCl₃): δ = 7.13-7.01 (m, 2H), 6.86 (d, J = 8.1 Hz, 1H), 6.61 (t, J = 7.3 Hz, 1H), 3.50 (br, s, 1H), 2.12 (s, 3H), 1.77 (s, 2H), 1.46 (s, 6H), 1.04 (s, 9H). **¹³C{¹H} NMR (101 MHz, CDCl₃):** δ = 145.1, 130.5, 126.7, 122.9, 116.3, 113.4, 55.1, 53.3, 32.0, 31.8, 30.6, 18.5. **HRMS:** *Calcd.* for C₁₅H₂₅N, [M+H]: 220.2065, *Found:* [M+H]: 220.2061. ϵ_r = -1.8 ppm.

2-methoxy-*N*-*tert*-octylaniline (4.18l): Following the general procedure using 1.0 mol% of pre-catalyst, the reaction was stirred for 4h at 60°C. After flash chromatography on silica gel (Hexane/EtOAc: 10/1), the title compound was recovered as a light yellow oil: 224mg (93% yield).



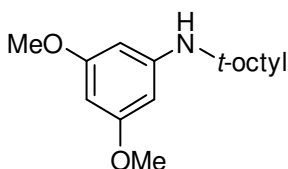
¹H NMR (400 MHz, CDCl₃): δ = 6.89-6.80 (m, 2H), 6.77 (dd, *J* = 8.0, 1.4 Hz, 1H), 6.63 (ddd, *J* = 7.9, 7.0, 1.9 Hz, 1H), 4.38 (br, s, 1H), 3.83 (s, 3H), 1.75 (s, 2H), 1.44 (s, 6H), 1.03 (s, 9H). **¹³C{¹H} NMR (101 MHz, CDCl₃):** δ = 147.7, 137.0, 120.9, 115.9, 113.5, 109.8, 55.7, 54.7, 53.1, 31.9, 31.7, 30.4. **HRMS:** *Calcd.* for C₁₅H₂₅NO, [M+H]: 236.2014, *Found:* [M+H]: 236.2020. ε_r = 2.5 ppm.

4-methoxy-*N*-*tert*-octylaniline (4.18m): Following the general procedure using 0.5 mol% of pre-catalyst **4.16**, the reaction was stirred for 4h at 60°C. After flash chromatography on silica gel (Hexane/EtOAc: 8/1), the title compound was recovered as a yellow oil: 188 mg (80%).



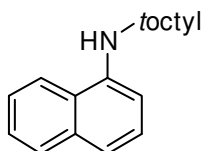
¹H NMR (300 MHz, CDCl₃): δ = 6.80-6.65 (m, 4H), 3.76 (s, 3H), 3.13 (br, s, 1H), 1.61 (s, 2H), 1.29 (s, 6H), 1.04 (s, 9H). **¹³C{¹H} NMR (75 MHz, CDCl₃):** δ = 153.5, 140.3, 121.3, 114.3, 55.9, 55.7, 54.5, 31.9, 30.3.

3,5-dimethoxy-*N*-*tert*-octylaniline (4.18n): Following the general procedure using 0.5 mol% of pre-catalyst **4.16**, the reaction was stirred for 4h at 60°C. After flash chromatography on silica gel (Hexane/EtOAc: 10/1), the title compound was recovered as a white solid: 241 mg (91%).



¹H NMR (300 MHz, CDCl₃): δ = 5.92-5.79 (m, 3H), 3.75 (s, 6H), 3.61 (s, 1H), 1.70 (s, 2H), 1.40 (s, 6H), 1.03 (s, 9H). **¹³C{¹H} NMR (75 MHz, CDCl₃):** δ = 161.4, 148.8, 94.9, 89.4, 55.3, 55.2, 53.0, 31.9, 31.8, 30.7. **HRMS:** *Calcd.* for C₁₆H₂₇NO₂, [M+H]: 266.2120, *Found:* [M+H]: 266.2124. ε_r = 1.5 ppm.

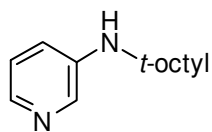
1-(*N*-*tert*-octyl)aminonaphthalene (4.18o): Following the general procedure using 0.5 mol% of pre-catalyst **4.16**, the reaction was stirred for 4h at 40°C. After flash chromatography on silica gel (Hexane/EtOAc: 95/5), the title compound was recovered as a colorless oil: 211 mg (83%).



¹H NMR (400 MHz, CDCl₃): δ = 7.82-7.74 (m, 2H), 7.47-7.38 (m, 2H), 7.33 (t, *J* = 7.9 Hz, 1H), 7.21 (d, *J* = 8.1 Hz, 1H), 6.89 (dd, *J* = 7.7, 0.8 Hz, 1H), 4.38 (br, s, 1H), 1.89 (s, 2H), 1.55 (s, 6H), 1.08 (s, 9H). **¹³C{¹H} NMR (101 MHz, CDCl₃):** δ = 141.8, 134.9, 129.0, 126.3,

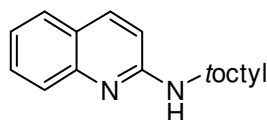
125.5, 124.8, 124.7, 120.2, 116.9, 108.5, 55.5, 53.0, 32.0, 31.8, 30.4. **HRMS:** *Calcd.* for $C_{16}H_{27}N$, $[M+H]^+$: 256.2065, *Found:* $[M+H]^+$: 256.2068. $\epsilon_r = 1.2$ ppm.

3-(1-octylamino)pyridine (4.18p): Following the general procedure using 1.0 mol% of pre-catalyst **4.16**, the reaction was stirred for 18h at 60°C. After flash chromatography on silica gel (EtOAc), the title compound was recovered as a yellow solid: 208 mg (99%).



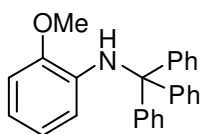
1H NMR (300 MHz, $CDCl_3$): δ = 8.04 (dd, J = 2.8, 0.8 Hz, 1H), 7.92 (dd, J = 4.5, 1.5 Hz, 1H), 7.03 (ddd, J = 8.3, 4.5, 0.8 Hz, 1H), 6.97 (ddd, J = 8.3, 2.8, 1.6 Hz, 1H), 3.59 (br, s, 1H), 1.68 (s, 2H), 1.39 (s, 6H), 1.01 (s, 9H). **$^{13}C\{^1H\}$ NMR (75 MHz, $CDCl_3$):** δ = 143.1, 139.0, 138.7, 123.4, 121.8, 55.4, 52.8, 31.9, 31.7, 30.5. **HRMS:** *Calcd.* for $C_{13}H_{22}N_2$, $[M+H]^+$: 207.1861, *Found:* $[M+H]^+$: 207.1860. $\epsilon_r = -0.5$ ppm

2-(*N*-tertoctylamino)quinoline (4.18q): Following the general procedure using 0.5 mol% of pre-catalyst **4.16**, the reaction was stirred for 4h at 60°C. After flash chromatography on silica gel (Hexane/EtOAc: 10/1), the title compound was recovered as a yellow solid: 155 mg (61%).



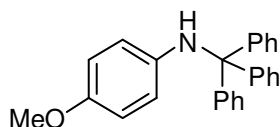
1H NMR (300 MHz, $CDCl_3$): δ = 7.73 (d, J = 8.9 Hz, 1H), 7.67 (d, J = 8.4 Hz, 1H), 7.58-7.45 (m, 2H), 7.21 – 7.13 (m, 1H), 6.54 (d, J = 8.9 Hz, 1H), 4.57 (br, s, 1H), 2.01 (s, 2H), 1.59 (s, 6H), 1.01 (s, 9H). **$^{13}C\{^1H\}$ NMR (75 MHz, $CDCl_3$):** δ = 156.5, 148.3, 136.5, 129.2, 127.4, 126.7, 122.9, 121.7, 113.3, 55.5, 51.5, 32.0, 31.8, 30.3. **HRMS:** *Calcd.* for $C_{17}H_{24}N_2$, $[M+H]^+$: 257.2018, *Found:* $[M+H]^+$: 257.2020. $\epsilon_r = 0.8$ ppm.

2-methoxy-*N*-tritylaniline (4.18r): Following the general procedure using 1.0 mol% of pre-catalyst **4.15**, the reaction was stirred for 18h at 60°C. After flash chromatography on silica gel (Hexane/EtOAc: 10/1), the title compound was recovered as a white solid: 302 mg (83%).



1H NMR (400 MHz, $CDCl_3$): δ = 7.55-7.37 (m, 6H), 7.38-7.15 (m, 9H), 6.85-6.70 (m, 1H), 6.65-6.51 (m, 1H), 6.51-6.37 (m, 1H), 6.17-6.04 (m, 1H), 5.91-5.70 (m, 1H), 3.90 (br, s, 3H). **$^{13}C\{^1H\}$ NMR (101 MHz, $CDCl_3$):** δ = 147.4, 145.7, 136.0, 129.3, 128.0, 126.8, 120.1, 116.6, 115.5, 109.1, 71.2, 55.7. **HRMS:** *Calcd.* for $C_{26}H_{23}NO$, $[M+H]^+$: 366.1852, *Found:* $[M+H]^+$: 366.1858. $\epsilon_r = 1.2$ ppm

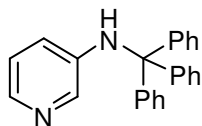
4-methoxy-*N*-tritylaniline (4.18s): Following the general procedure using 1.0 mol% of pre-catalyst **4.15**, the reaction was stirred for 18h at 60°C. After flash



chromatography on silica gel (Hexane/EtOAc: 10/1), the title compound was recovered as a white solid: 301 mg (82%).

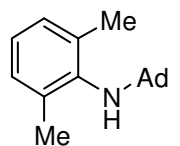
¹H NMR (400 MHz, CDCl₃): δ = 7.47-7.37 (m, 6H), 7.38-7.19 (m, 9H), 6.59-6.49 (m, 2H), 6.40-6.28 (m, 2H), 4.78 (br, s, 1H), 3.66 (s, 3H). **¹³C{¹H} NMR (101 MHz, CDCl₃)** δ = 151.9, 145.7, 140.4, 129.4, 128.0, 126.8, 117.4, 113.9, 71.8, 55.6.

3-(tritylamino)pyridine (4.18t): Following the general procedure using 1.0 mol% of pre-catalyst **4.15**, the reaction was stirred for 18h at 60°C. After flash chromatography on silica gel (Hexane/EtOAc: 4/1-100% EtOAc), the title compound was recovered as a yellow solid: 180 mg (54%).

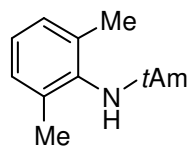


¹H NMR (400 MHz, CDCl₃): δ = 7.93 (d, J = 2.8 Hz, 1H), 7.82 (dd, J = 4.7, 1.3 Hz, 1H), 7.40-7.20 (m, 15H), 6.75 (dd, J = 8.4, 4.7 Hz, 1H), 6.48 (ddd, J = 8.1, 2.6, 1.2 Hz, 2H), 5.10 (br, s, 1H). **¹³C{¹H} NMR (101 MHz, CDCl₃)** δ = 144.7, 142.6, 138.9, 138.8, 129.2, 128.2, 127.2, 122.7, 121.9, 71.6.

1,3-dimethyl-*N*-adamantylaniline (4.18u): Following the general procedure using 1.0 mol% of pre-catalyst **4.15**, the reaction was stirred for 14h at 60°C. After flash chromatography on silica gel (Hexane/EtOAc: 10/1), the title compound was recovered as a light yellow solid: 222 mg (87%). **¹H NMR (400 MHz, CDCl₃):** δ = 7.02 (d, J = 7.4 Hz, 2H), 6.89 (t, J = 7.4 Hz, 1H), 2.65 (br, s, 1H), 2.37 (s, 6H), 2.06 (s, 3H), 1.79 (s, 6H), 1.69-1.55 (m, 6H). **¹³C{¹H} NMR (101 MHz, CDCl₃)** δ = 143.2, 134.9, 128.5, 123.1, 55.7, 44.5, 36.6, 30.3, 20.8.

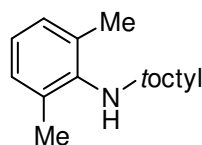


1,3-dimethyl-*N*-tert-amtylaniline (4.18v): Following the general procedure using 1.0 mol% of pre-catalyst **4.15**, the reaction was stirred for 18h at 60°C. After flash chromatography on silica gel (Hexane/EtOAc: 20/1), the title compound was recovered as a light yellow oil: 130 mg (68%).



¹H NMR (400 MHz, CDCl₃): δ = 7.01 (d, J = 7.4 Hz, 18H), 6.88 (t, J = 7.4 Hz, 1H), 2.60 (br, s, 1H), 2.33 (s, 6H), 1.61 (q, J = 7.5 Hz, 2H), 1.09 (s, 6H), 1.01 (t, J = 7.5 Hz, 3H). **¹³C NMR (101 MHz, CDCl₃)** δ = 144.2, 134.9, 128.6, 123.1, 57.6, 37.3, 27.7, 20.5, 9.1. HRMS: Calcd. for C₁₃H₂₁N, [M+H]: 192.1752, Found: [M+H]: 192.1758. ϵ_f = 3.1 ppm

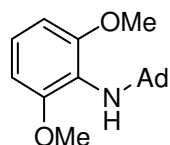
1,3-dimethyl-*N*-tert-octylaniline (4.18w): Following the general procedure using 2.0 mol%



of pre-catalyst **4.15**, the reaction was stirred for 18h at 60°C. After flash chromatography on silica gel (Hexane/EtOAc: 20/1), the title compound was recovered as a yellow oil: 160 mg (69%).

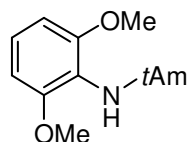
¹H NMR (400 MHz, CDCl₃): δ = 7.02 (d, J = 7.5 Hz, 2H), 6.88 (t, J = 7.4 Hz, 1H), 2.71 (br, s, 1H), 2.34 (s, 6H), 1.69 (s, 2H), 1.16 (s, 6H), 1.12 (s, 9H). **¹³C{¹H} NMR (101 MHz, CDCl₃)** δ = 144.1, 135.2, 128.6, 123.1, 59.7, 58.0, 32.2, 32.1, 30.0, 20.8. **HRMS:** *Calcd.* for C₁₆H₂₇N, [M+H]: 234.2222, *Found:* [M+H]: 234.2226. ϵ_r = 1.7 ppm.

1,3-dimethoxy-*N*-adamantylaniline (4.18x): Following the general procedure using 1.0 mol% of pre-catalyst **4.15**, the reaction was stirred for 14h at 60°C. After flash chromatography on silica gel (Hexane/EtOAc: 4/1), the title compound was recovered as a white solid: 220 mg (77%).



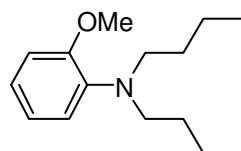
¹H NMR (400 MHz, CDCl₃): δ = 6.95 (t, J = 8.3 Hz, 1H), 6.53 (d, J = 8.3 Hz, 2H), 3.79 (s, 6H), 3.19 (br, s, 1H), 2.07-1.97 (m, 3H), 1.76 (d, J = 3.1 Hz, 6H), 1.65-1.54 (m, 6H). **¹³C{¹H} NMR (101 MHz, CDCl₃)** δ = 155.6, 123.5, 123.2, 103.9, 55.6, 54.9, 43.5, 36.7, 30.2. **HRMS:** *Calcd.* for C₁₈H₂₆NO₂, [M+H]: 288.1964, *Found:* [M+H]: 288.1968. ϵ_r = 1.4 ppm.

1,3-dimethoxy-*N*-tert-amylaniline (4.18y): Following the general procedure using 1.0 mol% of pre-catalyst **4.15**, the reaction was stirred for 6h at 60°C. After flash chromatography on silica gel (Hexane/EtOAc: 4/1), the title compound was recovered as a white solid: 205 mg (93%).



¹H NMR (300 MHz, CDCl₃): δ = 6.93 (t, J = 8.3 Hz, 1H), 6.53 (d, J = 8.3 Hz, 2H), 3.79 (s, 6H), 3.25 (br, s, 1H), 1.56 (q, J = 7.5 Hz, 2H), 1.09 (s, 6H), 0.94 (t, J = 7.5 Hz, 3H). **¹³C{¹H} NMR (75 MHz, CDCl₃)** δ = 155.2, 124.8, 122.9, 104.1, 57.0, 55.5, 36.1, 27.0, 9.2.

2-methoxy-*N*, *N'*-dibutylaniline (4.18z): Following the general procedure using 0.5 mol% of pre-catalyst **4.16**, the reaction was stirred for 2h at 60°C. After flash chromatography on silica gel (Hexane/EtOAc: 6/1), the title compound was recovered as a colorless oil: 201 mg (86 % yield).



¹H NMR (400 MHz, CDCl₃): δ = 7.00-6.93 (m, 2H), 6.91-6.83 (m, 2H), 3.84 (s, 3H), 3.13-3.01 (m, 4H), 1.49-1.37 (m, 4H), 1.34-1.21 (m, 4H), 0.87 (t, J = 7.3 Hz, 6H). **¹³C{¹H} NMR (101 MHz, CDCl₃):** δ = 153.9, 140.1, 122.5, 121.7, 120.6, 111.9, 55.6, 52.9, 29.3, 20.7, 14.2. **HRMS:** *Calcd.* for C₁₅H₂₅NO, [M+H]: 236.2014, *Found:* [M+H]: 236.2010. ϵ_r = -1.7 ppm.

6 X-Ray experimental data

X-Ray experimental data for compounds **2.2a**, **2.2b**, **2.6a**, **2.6b**, **2.7**, **2.9**, **2.14**, **2.17**, **4.3b** and **4.11**.

	2.2a	2.2b	2.6a	2.6b
Formula	C ₂₄ H ₃₀ F ₃ N ₃ O ₃ S	C ₃₀ H ₄₂ F ₃ N ₃ O ₃ S	C ₂₆ H ₃₅ F ₃ N ₄ O ₃ S	C ₃₁ H ₄₇ F ₃ N ₄ O ₃ S
Molecular weight	497.57	581.73	540.65	624.8
Crystal system	orthorhombic	orthorhombic	monoclinic	orthorhombic
Space group	P 21	P 21	P 21/c	P 21
a (Å)	8.4439(3)	10.4485(3)	11.679(2)	9.6304(3)
b (Å)	15.4854(4)	15.7243(5)	16.176(2)	17.9708(5)
c (Å)	19.7230(7)	19.4279(6)	30.263(6)	19.6340(5)
α (deg)	90	90	90	90
β (deg)	90	90	91.278(2)	90
γ (deg)	90	90	90	90
V (Å ³)	2578.92(15)	3191.91(17)	5715.8(17)	3397.98(17)
Z	4	4	8	4
color	colorless	colorless	colorless	colorless
Crystal dimm (mm)	0.25* 0.05* 0.05	0.5* 0.5* 0.3	0.5* 0.5* 0.3	0.5* 0.3* 0.2
ρ _{calc} (g.cm ⁻³)	1.282	1.211	1.257	1.221
F000	1048	1240	2288	1336
μ (mm ⁻¹)	0.176	0.152	0.166	0.148
Temperature (K)	173	180	173	173
Wavelength (Å)	0.71073	0.71073	0.71073	0.71073
Radiation	MoKα	MoKα	MoKα	MoKα
Number of data meas.	4811	6522	11660	6911
Number of data with I > 2 σ(I)	4336	6102	10013	6334
Number of variables	315	371	687	400
R	0.0342	0.0322	0.0518	0.0321
wR	0.0849	0.0833	0.135	0.0783
Goodness-of-fit on F ²	1.002	1.037	1.023	1.022
Largest peak in final difference (eÅ ⁻³)	0.295 and -0.301	0.222 and -0.232	0.56 and -0.544	0.163 and - 0.215

	2.7	2.9	2.14
Formula	C ₃₁ H ₄₇ F ₃ N ₄ O ₃ S	C ₃₃ H ₄₆ ClN ₄ Rh·CH ₂ Cl ₂	C ₃₄ H ₄₅ Cl ₃ N ₄ Pd
Molecular weight	624.8	875.83	722.49
Crystal system	monoclinic	Monoclinic	monoclinic
Space group	P 21/n	P 21/n	P 21/n
a (Å)	10.56470(10)	10.8560(2)	10.8335(5)
b (Å)	15.9641(2)	11.6010(2)	14.8687(7)
c (Å)	20.0193(3)	32.1170(5)	21.5220(10)
α (deg)	90	90	90
β (deg)	91.1500(10)	99.3550(10)	91.9340(10)
γ (deg)	90	90	90
V (Å ³)	3375.69(7)	3991.03(12)	3464.8(3)
Z	4	4	4
color	colorless	yellow	yellow
Crystal dimm (mm)	0.4* 0.4* 0.2	0.5* 0.25* 0.1	0.5* 0.2* 0.2
ρ _{calc} (g.cm ⁻³)	1.229	1.456	1.385
F000	1336	1796	1496
μ (mm ⁻¹)	0.149	0.927	0.796
Temperature (K)	100	173	173
Wavelength (Å)	0.71073	0.71073	0.71073
Radiation	MoKα	MoKα	MoKα
Number of data meas.	6872	7923	7079
Number of data with I > 2 σ(I)	5969	6191	6446
Number of variables	394	474	389
R	0.0407	0.0389	0.0203
wR	0.0407	0.0888	0.0501
Goodness-of-fit on F ²	1.067	1.034	1.077
Largest peak in final difference (eÅ ⁻³)	0.571 and -0.422	0. 875 and -0. 467	0.533 and -0.441

	2.17	4.3b	4.11
Formula	2 C ₃₆ H ₅₀ Cl ₃ N ₃ Pd, 3 CH ₂ Cl ₂	C ₃₀ H ₄₁ ClF ₃ N ₃ O ₃ S	C ₃₈ H ₅₃ Cl ₃ N ₄ Pd
Molecular weight	1785.89	616.17	778.59
Crystal system	monoclinic	monoclinic	monoclinic
Space group	P 21/c	P 21/n	P 21/c
a (Å)	19.9816(8)	10.7745(18)	16.0431(5)
b (Å)	22.9101(8)	19.824(3)	13.2272(5)
c (Å)	19.6911(7)	14.780(2)	19.1066(6)
α (deg)	90	90	90
β (deg)	111.965(2)	93.837(5)	106.6440(10)
γ (deg)	90	90	90
V (Å ³)	8359.9(5)	3149.7(9)	3884.6(2)
Z	4	4	4
color	yellow	yellow	yellow
Crystal dimm (mm)	0.30*0.25*0.15	0.25* 0.15* 0.15	0.15* 0.15* 0.15
ρ _{calc} (g.cm ⁻³)	1.419	1.289	1.333
F000	3688	1304	1624
μ (mm ⁻¹)	0.860	0.238	0.715
Temperature (K)	173	100	173
Wavelength (Å)	0.71073	0.71073	0.71073
Radiation	MoKα	MoKα	MoKα
Number of data meas.	17081	6424	7932
Number of data with I > 2 σ(I)	14689	6035	7121
Number of variables	916	380	427
R	0.039	0.069	0.0235
wR	0.0953	0.1846	0.0543
Goodness-of-fit on F ²	1.058	1.193	1.05
Largest peak in final difference (eÅ ⁻³)	0.092 and -1.56	0.861 and -0.522	0.665 and - 0.446

Résumé

Ce travail s'inscrit dans le cadre de la chimie des carbènes N-hétérocycliques (NHC) et s'articule autour de la fonctionnalisation directe de l'hétérocycle des l'imidazol-2-ylidènes par substitution formelle d'un ou deux groupements diméthylamino. Deux nouvelles catégories de NHCs ont d'abord été obtenues par cette stratégie, dénommées 4-(diméthylamino)imidazol-2-ylidène $\text{IAr}^{\text{NMe}_2}$ et 4,5-bis(diméthylamino)imidazol-2-ylidène $\text{IAr}^{(\text{NMe}_2)_2}$.

Les sels d'imidazolium précurseurs de ces NHCs, à savoir le triflate de 4-(diméthylamino)imidazolium ($\text{IAr}^{\text{NMe}_2}$)-HOTf et le triflate de 4,5-bis(diméthylamino)imidazolium ($\text{IAr}^{(\text{NMe}_2)_2}$)-HOTf, ont été synthétisés en couplant la formamidine disubstituée correspondante avec le *N,N*-diméthyl-chloroacétamide et le 1,2-dichloro-1,2-bis(diméthylamino)éthylène généré in situ respectivement.

La quantification des propriétés électroniques des deux nouveaux NHCs a été réalisée à l'aide des complexes de type $[\text{Rh}(\text{IMes}^{(\text{NMe}_2)_2}\text{Cl}(\text{CO})_2)]$, montrant que la donation électronique des ligands NHCs augmente séquentiellement par la décoration avec un ou deux groupements diméthylamino, tandis que les propriétés de π -rétrodonation des NHCs ne sont que légèrement influencées. Par la suite, les complexes de palladium Pd-PEPPSI- $\text{IPr}^{\text{NMe}_2}$ et Pd-PEPPSI- $\text{IPr}^{(\text{NMe}_2)_2}$ (PEPPSI : Pyridine Enhanced Preparation Purification Stabilization and Initiation) ont été préparés par des voies de complexation classiques. Les propriétés stériques des ligands a été évaluée par la mesure du pourcentage de volume occupé ($\%V_{\text{bur}}$), et il est apparu que les propriétés stériques de ces deux nouveaux ligands NHCs sont également accrues. Les activités catalytiques des deux pré-catalyseurs ont été évaluées en amination de type Buchwald-Hartwig et comparées avec celle de la référence Pd-PEPPSI-IPr. Le pré-catalyseur Pd-PEPPSI- $\text{IPr}^{(\text{NMe}_2)_2}$ s'est révélé le plus actif en amination des chlorures d'aryle à température ambiante. Il constitue également le catalyseur Pd-NHC le plus efficace et le plus général connu à ce jour en permettant de réaliser l'amination des chlorures d'aryle avec une charge de catalyseur très faible (jusqu'à 50 ppm), ou à l'aide d'une base faible telle que le carbonate de césium, et même d'activer les tosylates d'aryle, substrats beaucoup plus difficiles que les chlorures d'aryle.

Afin de rationaliser au mieux les effets observés en catalyse en termes de propriétés stéréoelectroniques des ligands NHCs, le squelette arrière aminé des imidazol-2-ylidènes a été dérivatisé plus avant, soit en augmentant la contrainte stérique du groupe NMe_2 dans $\text{IAr}^{(\text{NMe}_2)_2}$ en ciblant le ligand $\text{IAr}^{(\text{N}^i\text{Pr}_2)}$, soit en remplaçant formellement un des groupes amino par un groupe électro-attracteur tel un halogène dans le ligand $\text{IAr}^{(\text{NMe}_2)_2}$. Alors que le sel d'imidazolium ($\text{IAr}^{\text{N}^i\text{Pr}_2}$)-HOTf a été synthétisé suivant la même méthode que ($\text{IAr}^{\text{NMe}_2}$)-HOTf, l'halogénéation oxydante du squelette d'arrière de ($\text{IAr}^{\text{NMe}_2}$)-HOTf par du NCS ou du NBS a donné les sels ($\text{IAr}^{\text{NMe}_2, \text{X}}$)-HOTf avec de très bons rendements dans des conditions très douces. Il convient de noter que cette réactivité originale a été également observée sur les complexes de rhodium(I) et le palladium(II) du ligand $\text{IAr}^{(\text{NMe}_2)}$. Les influences électroniques et catalytiques de ces modifications ont été étudiées de la même façon. Les résultats des tests d'activité catalytique dans la réaction d'amination arylique ont permis de conclure que les facteurs stériques jouent le rôle le plus important pour l'efficacité des catalyseurs dans cette série et dans cette réaction, mais la donation électronique a également un impact important principalement en terme de stabilité du catalyseur. Dans tous les cas, le carbène $\text{IPr}^{(\text{NMe}_2)_2}$ reste le plus efficace, car il combine un grand encombrement stérique avec la donation électronique la plus forte de la série. Dans une dernière partie, nous avons mis à profit cette grande palette de ligands pour optimiser l'amination des chlorures d'aryle avec les amines primaires très encombrées. Dans cette réaction, il a été nécessaire de modifier les pré-catalyseurs puisque les complexes PEPPSI n'ont montré que des activités très faibles. Ainsi, les pré-catalyseurs $[\text{Pd}(\text{NHC})(\text{cin})\text{Cl}]$ (cin = η^3 -cinnamyl) portant les ligands $\text{IPr}^{(\text{NMe}_2)_2}$ ou $\text{IPr}^{\text{N}^i\text{Pr}_2}$ ont montré les meilleures activités catalytiques, en permettant le couplage d'amines très encombrées ($t\text{BuNH}_2$, $t\text{AmNH}_2$, Ph_3CNH_2 ...) avec une grande variété de chlorures d'(hétéro)aryles dans des conditions douces. Ces derniers résultats concurrencent voire surpassent les meilleurs résultats obtenus jusqu'alors.

Abstract

This work is incorporated within the framework of the chemistry of N-Heterocyclic Carbenes (NHCs) and aims at functionalizing the skeleton of imidazol-2-ylidenes by attachment of one or two amino groups. Two new NHC classes were first obtained by this strategy, namely the 4-(dimethylamino)imidazol-2-ylidene $\text{IAr}^{\text{NMe}_2}$ and the 4,5-bis(dimethylamino)imidazol-2-ylidene $\text{IAr}^{(\text{NMe}_2)_2}$.

The synthesis of the precursors of these NHCs, the 4-(dimethylamino)imidazolium triflates ($\text{IAr}^{\text{NMe}_2}$)-HOTf and the 4,5-bis(dimethylamino)imidazolium triflates ($\text{IAr}^{(\text{NMe}_2)_2}$)-HOTf is based on the coupling between the corresponding disubstituted formamidine and either an α -chloroacetamide for the mono-amino derivative or a reactive dichlorodiaminoethene for the bis-amino analogue.

The electronic properties of the resulting new NHCs ligands have been studied by measurement of their Tolman Electronic Parameter (TEP) values obtained from the IR spectra of the complexes $[\text{Rh}(\text{IMes}^{\text{XY}})\text{Cl}(\text{CO})_2]$ and by ^{77}Se NMR spectroscopy of their corresponding selenoureas $[(\text{IMes}^{\text{XY}})=\text{Se}]$. It was shown that the electronic donation of the carbenic carbon sequentially increases by decoration with one or two amino groups respectively whereas the π -accepting properties of the NHC are only slightly or even not affected by the adjunction of the NMe_2 groups on the imidazolyl backbone. Later, the synthesis of the two new PEPPSI-type palladium pre-catalysts PEPPSI-Pd- $\text{IPr}^{\text{NMe}_2}$ and Pd-PEPPSI- $\text{IPr}^{(\text{NMe}_2)_2}$ were successfully achieved. From the calculated the percent buried volume $\%V_{\text{bur}}$ which is related to the steric properties of the two supporting NHC ligands, it appeared that grafting one amino group onto the backbone already leads to significant improvement of steric congestion while the second amino only results in a slight increase of the steric issue. The catalytic efficiencies of both pre-catalysts were evaluated in the benchmark Buchwald-Hartwig amination and compared with this of the reference PEPPSI-Pd-IPr. The bis-aminated pre-catalyst Pd-PEPPSI- $\text{IPr}^{(\text{NMe}_2)_2}$ was shown to be the most active and stable pre-catalyst, and it was shown to be also highly efficient in more challenging amination reaction. It indeed allows to carry out the amination of aryl chlorides at low catalyst loadings or by using a mild base such as cesium carbonate, and even to activate the aryl tosylates, which are more difficult substrates than aryl chlorides.

In order to study the critical stereoelectronic properties of the NHC ligands for the efficiency of the corresponding catalysts, further derivatization of the heterocyclic backbone was carried out, either by increasing the bulkiness of the mono-amino group from dimethylamino to diisopropylamino group to generate the carbene $\text{IAr}^{\text{NIPr}_2}$, or by formally replacing one dimethylamino group by an halogen X in the bis-aminoimidazo-2-ylidene to give the carbenes $\text{IAr}^{\text{NMe}_2, \text{X}}$. While the imidazolium salts ($\text{IAr}^{\text{NIPr}_2}$)-HOTf was synthesized following the same method as ($\text{IAr}^{\text{NMe}_2}$)-HOTf, the oxidative halogenation of the backbone of ($\text{IAr}^{\text{NMe}_2}$)-HOTf with a N-halosuccinimide afforded ($\text{IAr}^{\text{NMe}_2, \text{X}}$)-HOTf in good yields under very mild conditions. Noteworthy, this original reactivity was also observed on the rhodium and palladium complexes of this ligand. The electronic and catalytic influences of these modifications were studied in the same manner. From the kinetic studies in arylative amination, it could be concluded that the steric factors play the most important role for the efficiency of the catalysts in this series and in this reaction, but the electronic donicity also has a significant impact mainly in terms of catalyst stability. In all cases, the $\text{IPr}^{(\text{NMe}_2)_2}$ carbene revealed to be the most efficient ancillary ligand, since it combines a great steric hindrance with the strongest electron donation of the series. In a last part, we took advantage of this large palette of ligands to optimize the arylative amination of bulky primary amines with aryl chlorides. The pre-catalysts $[\text{Pd}(\text{NHC})(\text{cin})\text{Cl}]$ (cin = η^3 -cinnamyl) bearing the $\text{IPr}^{(\text{NMe}_2)_2}$ or $\text{IPr}^{\text{NIPr}_2}$ ligands showed the best catalytic activities and displayed a large substrate scope under unprecedentedly mild conditions.